Preclinical development of ACT-1004-1239, a potent and selective CXCR7/ACKR3 antagonist in multiple sclerosis treatment

Laetitia Pouzol

université PARIS-SACLAY

Preclinical development of ACT-1004-1239, a potent and selective CXCR7/ACKR3 antagonist in multiple sclerosis treatment

Développement préclinique d'ACT-1004-1239, un antagoniste puissant et sélectif du récepteur CXCR7/ACKR3 pour le traitement de la sclérose en plaques

Thèse de doctorat de l'université Paris-Saclay

École doctorale n° 569, Innovation thérapeutique : du fondamental à l'appliqué (ITFA)
Spécialité de doctorat : Immunologie
Graduate School : Santé et médicaments. Référent : Faculté de Pharmacie

Thèse préparée dans l'unité de recherche **Inflammation microbiome immunosurveillance (Université Paris-Saclay, Inserm)**, sous la direction de **Géraldine SCHLECHT-LOUF**, professeure

Thèse soutenue à Paris-Saclay, le 20 mai 2022, par

Laetitia POUZOL

Composition du Jury

Bernard MAILLERE Directeur de Recherche, CEA- Univ. Paris-Saclay	Président
Isabelle LARTAUD Professeure, Univ. De Lorraine	Rapporteur & Examinatrice
Jean Luc GALZI Directeur de Recherche, Univ. De Strasbourg (UMR-7242)	Rapporteur & Examinateur
Françoise BACHELERIE Directrice de Recherche, Univ. Paris-Saclay (UMR-S996)	Examinatrice
Fréderic PENE PU-PH, INSERM, Univ. Paris-Cité	Examinateur
Jerôme DE SEZE PU-PH, CHU Strasbourg	Examinateur
Angélique LEVOYE Maître de conférences, Univ. Sorbonne Paris Nord	Examinatrice
Géraldine SCHLECHT-LOUF Professeure, Univ. Paris-Saclay	Directrice de thèse

THESE DE DOCTORAT

NNT : 2022UPASQ021

ACKNOWLEDGMENTS

First, I would like to thank all the members of my jury for kindly having accepted my invitation to review my PhD manuscript. I am very grateful to Isabelle Lartaud who inspired me during my pharmacy studies to study pharmacology and for having accepted to review my manuscript. Thank you to Jean Luc Galzi for having accepted to review my manuscript. I would like to thank Françoise Bachelerie, Angélique Levoye, Fréderic Pene, and Jerôme De Seze for kindly having accepted to examine my thesis. I would like to thank Bernard Maillère for having accepted to examine my thesis and to take the lead of the thesis defense as the committee's president.

I would like to express my gratitude to Géraldine Schlecht-Louf for having accepted to supervise my work. A big thank you to you and to Françoise Bachelerie, for pushing me and for motivating me in doing this validation of experience work.

I would like to acknowledge the work of my mentor, the biologist of the project, François Lehembre, who was the first to trust my abilities to work on a research project, and without whom I would not have made it through my PhD degree. Thank you for providing me feedback throughout this project, for always guiding me so positively and for helping me feeling confident in my abilities to do my work even without the PhD degree, it was a real pleasure to work together with you. I would also like to thank all the other initial core team members of the project, especially Carmela Gnerre, Philippe Guerry, Eleanor Lindenberg, and Martin Holdener, without whom ACT-1004-1239 would not have been discovered and selected.

I would like to thank my dream boss, Marianne Martinic, who is simply leading by example, who is inspiring me in my daily work. Thank you for always guiding me so positively, for your consistent support, for all our conversations, for the stimulating questions, for making my professional life so much easier since you've joined our company. Without your help and wise guidance this project would not have been the same!

I would like to thank my laboratory team members without whom I would not have done anything: Anna Sassi, Nadège Baumlin, Mélanie Tunis you are simply the best people I would have ever dreamt to work with. Thank you for being always so positive, so motivated, so flexible, so proactive and thank you for also being my friends.

I would like to say a special thank you to Sylvie Froidevaux and Jérémy Scherer, who simply taught me all the basis of my work and without whom I would not be where I am now in the company. Thanks also to Anaïs Zurbach for being always flexible and for providing help each time we necessitated, and for now willing to join my laboratory.

I am also grateful to Martine Clozel and Ulrich Mentzel for providing me with such an amazing job opportunity.

Thank you to all my friends for your emotional support and for keeping my mental health in check.

Thank you to my parents, who set me off on the road to research a long time ago, who inspired me and gave me the chance to study. Thank you to my parents in law, for always being supportive and proud of my achievements and for doing so many things for our family.

This thesis is dedicated to my son Evan Riboulet, to my husband Julien Grimont and his children Eléa and Louis Grimont. Thank you so much for your unconditional love, your emotional support, and for supporting me during the compilation of this manuscript.

Résumé en français

La sclérose en plaques (SEP), initialement décrite en 1868 par Jean-Martin Charcot, est une maladie auto-immune chronique qui affecte le système nerveux central (SNC). Elle atteint plus de 2.8 millions de personnes à travers le monde et est la première cause de handicap sévère non traumatique chez le sujet jeune. Dans 70% des cas, la SEP est diagnostiquée entre 20 et 40 ans, avec une prédominance féminine. La cause de la maladie reste mal connue mais plusieurs facteurs de risques, génétiques et environnementaux, ont pu être associés à son développement.

La SEP est caractérisée par une inflammation qui attaque la gaine de myéline autour des axones, qui permet de les protéger et d'accélérer la vitesse de propagation de l'influx nerveux. Ce phénomène inflammatoire entraîne des plaques de démyélinisation dans le SNC, responsable d'une altération de la conduction nerveuse et, souvent, d'une dégénérescence axonale. Ces plaques de démyélinisation sont responsables de divers symptômes, en fonction de la localisation des lésions au niveau du SNC. La SEP est très hétérogène d'un patient à l'autre et se présente sous différentes formes cliniques avec le plus souvent lors du diagnostic une forme dite récurrente-rémittente, caractérisée par des poussées suivies de périodes de rémissions de la maladie. La physiopathologie de la SEP fait intervenir de nombreux acteurs cellulaires de l'inflammation tels que les lymphocytes T et B, les macrophages ainsi que les cellules résidentes du SNC.

Des avancées considérables ont été réalisées ces dernières années et les traitements actuels permettent de réduire le nombre de poussées et permettent d'améliorer la qualité de vie des patients en agissant principalement sur le système immunitaire. Cependant, ces nouveaux traitements n'empêchent pas la progression de la maladie et aucun traitement ne répare les gaines de myéline endommagées. Ainsi, la recherche de nouvelles stratégies thérapeutiques visant à stimuler la régénération de la myéline afin de réduire la dégénérescence axonale et le handicap, constitue un espoir important pour les patients atteints de SEP.

Le développement d'un médicament est un processus complexe nécessitant une approche pluridisciplinaire, incluant la pharmacologie. Avant de pouvoir tester une molécule candidate chez l'être humain, un médicament doit passer par le développement préclinique. Cette première étape débute avec l'identification et la validation d'une cible thérapeutique, puis l'identification et l'optimisation de molécules candidates. Dans ce processus, les données visant à étudier la pharmacocinétique (PK), la pharmacodynamique (PD), le mécanisme d'action et l'efficacité de la molécule au sein d'organismes animaux vivants sont essentielles et sont nécessaires à la constitution du dossier réglementaire permettant d'entrer chez l'Homme.

Les chimiokines sont de petites protéines sécrétées dont la fonction initialement décrite est le contrôle de la migration leucocytaire. Elles se fixent à deux familles de récepteurs à sept domaines transmembranaires couplés aux protéines G : les récepteurs conventionnels et les récepteurs atypiques, qui ne parviennent pas à activer les protéines G lorsqu'ils se lient à leurs ligands. Le récepteur atypique des chimiokines ACKR3 (précédemment nommé CXCR7) a été proposé comme étant une cible thérapeutique potentielle pour le traitement de la SEP. ACKR3 se lie aux chimiokines CXCL11 et CXCL12 et les dégradent, contribuant ainsi à la régulation de leurs concentrations. Ces deux chimiokines, CXCL11 et CXCL12, se lient également aux récepteurs conventionnels des chimiokines CXCR3 et CXCR4, respectivement. Aussi, ACKR3 module de nombreux processus biologiques, notamment via les axes de signalisation CXCL12/CXCR4 et CXCL11/CXCR3.
Il est exprimé au niveau du SNC, particulièrement sur les cellules endothéliales et les cellules résidentes telles que les astrocytes et les cellules précurseurs des oligodendrocytes (CPOs). Il joue un rôle clé dans des processus biologiques impliqués dans la physiopathologie de la SEP : ACKR3 faciliterait l'infiltration des cellules inflammatoires dans le SNC et aurait un effet controversé sur la différenciation des CPOs en oligodendrocytes matures, capable de remyéliniser les axones. Cependant, les mécanismes de signalisation cellulaire à l'origine des effets physiopathologiques d'ACKR3 sont mal connus, et aucun antagoniste au récepteur

ACKR3 inhibant le recrutement de β-arrestine à la suite de la liaison d'ACKR3 avec ses agonistes, n'a été testé dans des modèles animaux.

Cette thèse de doctorat décrit la découverte et le développement préclinique, d'un point de vue pharmacologique, d'ACT-1004-1239, le premier antagoniste au récepteur ACKR3, puissant, sélectif et insurmontable qui peut être donné par voie orale. Après avoir caractérisé les propriétés PK/PD d'ACT-1004-1239, en mesurant l'augmentation de CXCL12 dans le plasma comme biomarqueur de PD, le mécanisme d'action de l'antagoniste a été évalué dans un modèle d'inflammation du poumon, induit par l'inhalation de lipopolysaccharide nébulisé. Suite à la caractérisation du modèle chez la souris DBA/1, l'efficacité de l'antagoniste, administré de manière préventive ou thérapeutique, fut évaluée sur l'infiltration de leucocytes dans le lavage bronchoalvéolaire. Ces expériences ont mis en évidence le rôle d'ACKR3 dans la migration des cellules immunitaires, notamment celles exprimant les récepteurs CXCR3 et CXCR4, vers le site de l'inflammation, supportant l'hypothèse qu'ACKR3 contribue à la mise en place de gradients de migration en modulant la concentration de ses ligands. De plus, l'administration d'ACT-1004-1239 a permis de diminuer la perméabilité alvéolocapillaire, une des caractéristiques pathologiques de l'inflammation aigue du poumon.

Enfin, le principal but de ce travail de thèse était d'évaluer l'efficacité d'ACT-1004-1239 dans des modèles animaux de la SEP, notamment les modèles d'encéphalomyélite auto-immune expérimentale (EAE) et de démyélinisation induite par l'ingestion de cuprizone chez la souris.
Dans un modèle murin d'EAE induit par l'injection d'un peptide de la myéline, nommé myelin oligodendrocyte glycoprotein (MOG_{35-55}), l'administration préventive d'ACT-1004-1239 a réduit de manière dose-dépendante la sévérité de la maladie. Cette efficacité sur les scores cliniques de paralysie corrèle avec l'augmentation dose-dépendante du biomarqueur plasmatique, CXCL12. De plus, cet effet est associé à une réduction de l'infiltration leucocytaire dans le SNC des souris EAE.

Ces résultats ont confirmé l'effet immunomodulateur d'ACT-1004-1239 sur l'infiltration des cellules inflammatoires dans le SNC.

Ensuite, l'évaluation d'ACT-1004-1239 *in vitro* dans des co-cultures de CPOs et de neurones a permis de démontrer que l'antagoniste d'ACKR3 augmente le nombre d'oligodendrocytes matures, probablement via l'augmentation de CXCL12 dans le surnageant des co-cultures qui entraîne la maturation des CPOs. Ces résultats ont été confirmés *in vivo*, dans un modèle murin de démyélinisation non-autoimmune, dans lequel, l'administration d'ACT-1004-1239 de manière préventive ou thérapeutique a réduit significativement la démyélinisation induite par l'ingestion de cuprizone et a augmenté le nombre d'oligodendrocytes matures, produisant de la myéline.

Les résultats exposés dans cette thèse démontrent qu'antagoniser le récepteur ACKR3 avec ACT-1004-1239 réduit à la fois la neuro-inflammation et améliore la myélinisation, ce qui supporte le développement clinique de ce composé pour le traitement des patients ayant une SEP.

TABLE OF CONTENTS

LIST OF TABLES

LIST OF FIGURES

LIST OF ABBREVIATIONS AND ACRONYMS

ACKR3	Atypical chemokine receptor 3
ADME	Absorption, distribution, metabolism, and excretion
ALI	Acute lung injury
APC	Antigen presenting cell
API	Active pharmaceutical ingredient
ARDS	Acute respiratory distress syndrome
ARR	Annualized relapse rate
BAFF	B cell activating factor
BBB	Blood brain barrier
BDNF	brain-derived neurotrophic factor
CC	Corpus callosum
CCKR	Conventional chemokine receptor
CCR5	CC motif chemokine receptor 5
CIS	Clinically isolated syndrome
CNS	Central nervous system
CSF	Cerebrospinal fluid
CXCL11	C-X-C motif chemokine ligand 11
CXCL12	C-X-C motif chemokine ligand 12
CXCR3	C-X-C motif chemokine receptor 3
CXCR4	C-X-C motif chemokine receptor 4
CXCR7	C-X-C motif-chemokine receptor 7
Cx43	Connexin 43
DC	Dendritic cell
DIT	Disseminated in time
DMF	Dimethyl fumarate
DMT	Disease modifying therapy
EBV	Epstein-Barr virus
ECG	Electrocardiogram
EDSS	Expanded disability disease scale

EMA	European medicines agency
FDA	Food and drug administration
FIH	First in human
FoxP3	Factor forkhead box P3
GA	Glatiramer acetate
GAG	Glycosaminoglycan
GLP	Good laboratory practice
GM-CSF	Granulocyte-macrophage colony-stimulating factor
GPCR	G-protein-coupled receptor
GRK	GPCR kinase
GWAS	Genome wide association studies
HTS	High throughput screening
HSC	Hematopoietic stem cell
IFNb	Interferon beta
IFN-γ	Interferon gamma
IGF-1	Insulin-like growth factor-1
IL	Interleukin
IMPD	Investigational medicinal product dossier
IND	Investigational new drug
ITAC	Interferon-inducible T cell a chemoattractant
JCV	John Cunningham virus
LFA-1	Lymphocyte function-associated antigen 1
LINGO1	Leucine-rich repeat and Ig-domain containing 1
LPS	Lipopolysaccharide
MBP	Myelin basic protein
MDCK	Madin-Darby canine kidney
MHC	Major histocompatibility complex
MOG	Myelin oligodendrocyte glycoprotein
MRI	Magnetic resonance image
MS	Multiple sclerosis
MSFC	Multiple sclerosis functional composite

NF	Neurofilament proteins
NFL	Neurofilament light chain
NO	Nitric oxide
Nrf2	Nuclear factor (erythroid-Derived 2)-Like 2
OCB	Oligoclonal bands
OL	Oligodendrocyte
OPC	Oligodendrocyte progenitor cell
PCC	Preclinical candidate
PD	Pharmacodynamic
PDGF	Platelet-derived growth factor
P-gp	P-glycoprotein
PK	Pharmacokinetic
PLP	Proteolipid protein
PML	Progressive multifocal leukoencephalopathy
POE	Proof of efficacy
POM	Proof of mechanism
PPMS	Primary progressive MS
RIS	Radiologically isolated syndrome
ROS	Reactive oxygen specie
RRMS	Relapsing-remitting MS
SDF-1	Stromal derived factor-1
SEMA 3F	Semaphorin 3F
SEMA 3A	Semaphorin 3A
SAR	Structure activity relationship
S1P	Sphingosine 1 phosphate
S1PR	Sphingosine 1 phosphate receptor
SPMS	Secondary progressive MS
TGF-β	Transforming growth factor
Th cell	T helper cell
TNF	Tumor necrosis factor
VLA-4	Very late antigen 4 (a4b1 integrin)

INTRODUCTION

1 Multiple sclerosis

Multiple sclerosis (MS) is a chronic inflammatory demyelinating disease of the central nervous system (CNS). In 1868, the French neurologist Jean-Martin Charcot recognized MS as a novel disease by connecting the appearance of multiple neurological symptoms to pathological findings throughout the CNS. He named it "Sclérose en plaques" based on the presence of numerous and disseminated lesions or "plaques" within the CNS [1] [Figure 1]. These plaques are found both in white and grey matter regions and are characterized by demyelinated nervous tissue, with variable degrees of inflammation, gliosis, and axonal loss [2]. These lesions interfere with the transmission of nerve signals between the CNS and the rest of the body, which cause multiple neurological symptoms. MS is one of the most common causes for disability in young adults.

Figure 1: Original color drawing from Dr. Jean-Martin Charcot's notebook illustrating the center of a lesion in a patient with MS.

In the center of the lesion, the drawing depicts a blood vessel covered with carmine dye positive nuclei and on each side demyelinated axons with different diameters. On the right is the legend handwritten by Dr. Charcot indicating patient's name (Mr. Vulpian), the date and the sample: spinal cord without preparation. The original document belongs to the Département de Neuropathologie, Groupe Hospitalier Pitié-Salpêtrière-Charles Foix, Musée de l'assistance publique-Hôpitaux de Paris [1].

1.1 Epidemiology of MS

The global prevalence of MS is rising with an estimated 2.8 million people affected by MS worldwide in 2020 [3]. Prevalence of the disease is variable depending on geography and ethnicity, from high levels in America and Europe (>100 per 100 000 population) to low rates in Southeast Asia and Africa (<10 per 100 000 population) [3]. Globally, females are more affected than men with a gender ratio for MS incidence (women/men) of 2:1 [4].

1.2 Etiology of MS

MS is a complex disease in which the etiology is still incompletely understood. Both environmental and genetic risk factors have been associated with the development of MS disease.

1.2.1 Environmental risk factors

Several environmental risk factors have been proposed and studied in relation to onset of MS [5]. Among them, only infection with Epstein-Barr virus (EBV) in adolescents and young adults, which often manifests as infectious mononucleosis, and cigarette smoking were confirmed as consistent risk factors for developing MS [4,5]. Recently, Bjornevik et al, confirmed in a large cohort that risk of developing MS increased 32-fold after EBV infection and that it preceded the development of the disease [6]. In addition, high levels of serum vitamin D, which is produced by the skin following sun exposure, were associated with lower MS activity, slower progression, and lower risk of developing MS [7,8]. A meta-analysis refuted the association of a variety of factors, including several vaccines, stress, presence of allergies, and traumatic events with MS [5].

1.2.2 Genetic risk factors

MS susceptibility is known to be partially heritable. Familial studies reported increased risk for relatives of patients with MS [9]. A meta-analysis of twin studies with MS concluded that genetic variation was responsible for about half of the individual differences in susceptibility to MS [10]. The first and the strongest identified genetic risk factor is an allele from the HLA-DRB1 gene in the major histocompatibility complex (MHC) class II region, the variant HLA-DRB1*15:01. This genetic variant increases the risk by 3-fold, while the other variants confer an increased risk less than 1.2-fold [11-13]. In the past decade, genome wide association studies (GWAS) in MS identified more than 200 associated risk genetic variants outside the MHC region, that independently contribute to disease susceptibility. These MS risk variants genes are dominantly expressed in the immune system and a large proportion of them is shared with other autoimmune diseases [14].

1.3 MS clinical presentation

MS onset usually occurs in young adults with ages between 20 and 40 years. MS takes a variety of forms, distinguished by the clinical pattern of disease activity [15]. At onset, 85% of the patients present a relapsing-remitting course, characterized by periods of neurological dysfunction, called relapses followed by complete or incomplete remissions [Figure 2]. Relapses are associated with focal inflammatory and demyelinated lesions in the CNS, especially in the white matter. The first clinical presentation of an inflammatory demyelinating episode with no previous attack is called clinically isolated syndrome (CIS). Over time, usually 10-15 years after disease onset, around 80% of the patients diagnosed with relapsing-remitting MS (RRMS) accumulate progressively disabilities and the disease transitions to secondary progressive MS (SPMS). The progressive neurological decline is associated with reduced brain volume and increased axonal loss [16]. In approximately 15% of the patients, the accumulation of neurological disabilities without periods of recovery occurs from disease onset and is known as primary progressive MS (PPMS) [15] [Figure 2]. Recently, the description of disease course has been refined, including description of activity (showing evidence of new relapses)

and progression (evidence of disease worsening confirmed over a specified time period) [17].

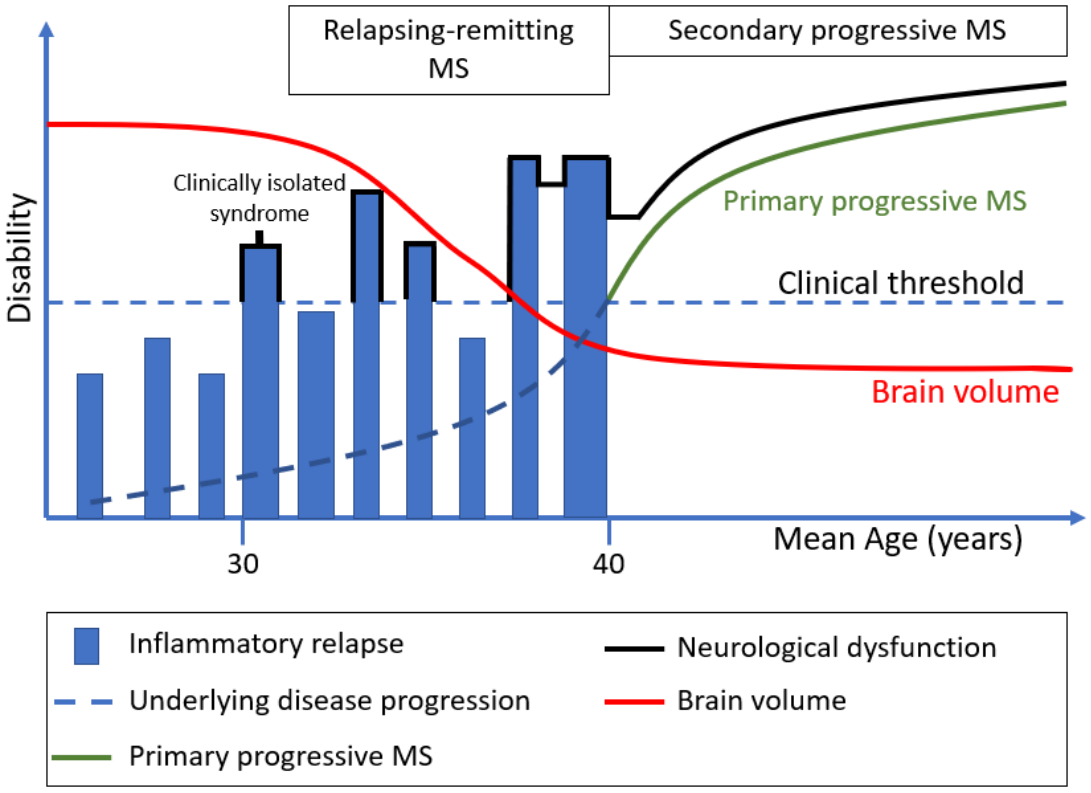

Figure 2: Multiple sclerosis disease courses.
The first episode of inflammatory demyelination in the central nervous system which is clinically visible is called clinically isolated syndrome. Relapsing remitting multiple sclerosis (RRMS) is characterized by episodes of acute worsening of neurologic disability with total or partial recovery and no apparent progression of disease. Progressive disease is defined by steadily increasing neurological dysfunction without recovery, starting either from onset of symptoms (primary progressive MS, green line) or following an initial RRMS course (secondary progressive MS). The progressive disability accumulation is associated with brain volume loss. Designed from Dendrou *et al* [16].

MS symptoms can differ widely from patient to patient and can fluctuate throughout the disease course. They depend on the spatial location of the CNS lesions. A clinical attack also called relapse, must last at least one day in the absence of fever or infection. In PPMS, clinical signs should gradually worsen over at least

one year after disease onset [18]. Symptoms often affect several domains, such as mobility, vision, sensory function, bowel/bladder function, cognitive function [19] [Figure 3]. Certain symptoms seem to be particularly early in the disease course, such as sensory disturbances, while other symptoms such as difficulties in walking which relate to spasticity, balance problems, weakness and tremor, are progressively more common with disease duration [20,21].

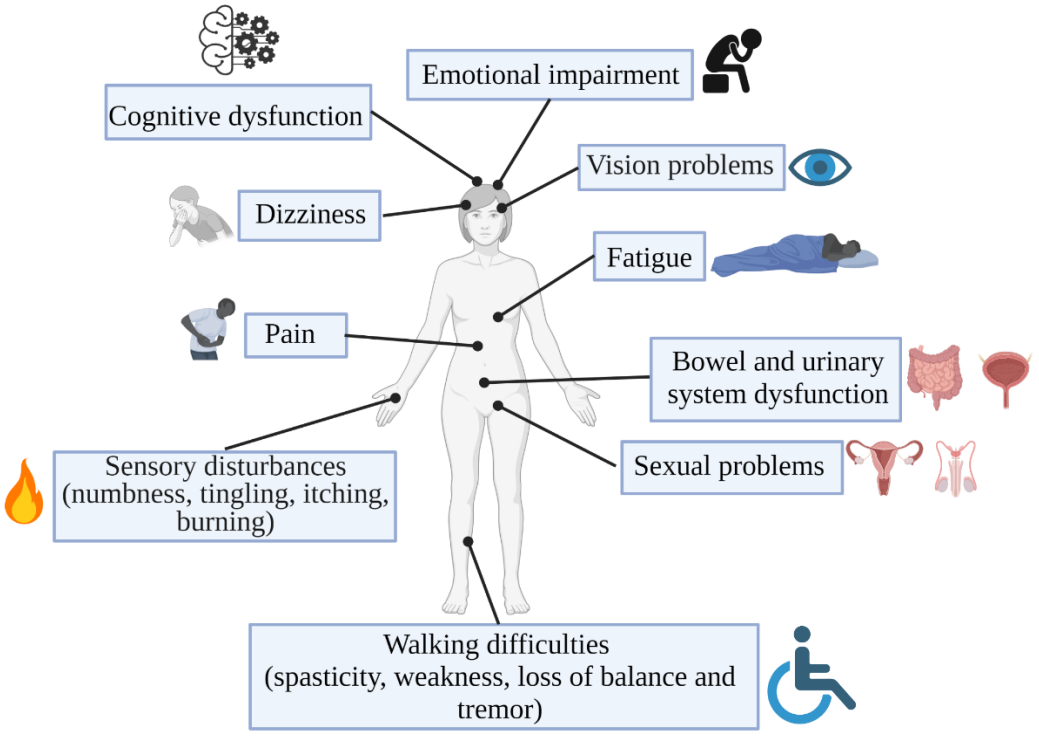

Figure 3: Most common symptoms of multiple sclerosis.
Figure adapted from Ghasemi *et al.* [22] and made with Biorender.com

1.4 MS diagnosis

The diagnosis of MS is based on the medical history and clinical presentation of the attacks. There are no symptoms, or laboratory findings that can by themselves define MS [21]. An expert consensus has defined the 2010 McDonald criteria for MS diagnosis which requires evidence of CNS lesions disseminated in space (at least two separate areas of the CNS are damaged) and in time (dissemination in time

(DIT), lesions have occurred at different times), with exclusion of other possible causes either clinically or radiologically. These criteria were revised in 2017 to allow an earlier diagnosis of MS after a demyelinating episode, using magnetic resonance imaging (MRI) and laboratory cerebrospinal fluid (CSF) analysis to search for the presence of oligoclonal bands (OCBs), indicating local CNS production of immunoglobulin G, to complement the clinical observation of an attack [18]. MRI findings with T1-weighted and T2-weighted images help in replacing or explaining some clinical criteria in some patients [Figure 4]. T1-weighted images (high fat content tissue appears bright) without contrast show lesions as hypointense signal compared to normal white matter and are commonly known as "black holes" [Figure 4B]. T1-weighted images with contrast agent such as gadolinium, injected few minutes before MRI, show active inflammatory lesions; when the lesion is active, gadolinium will cross the blood brain barrier (BBB) and reveal areas of inflammation, which will appear brighter (enhancing lesions) [Figure 4C]. T2-weighted images (water within the tissue appears bright, such as CSF) show the total amount of scar from MS, showing both old and new lesions, thus, helping to meet the DIT criteria [Figure 4A] [23]. Of note, most of damaged tissues tend to develop edema. A large clinical study showed that the number of MRI T2 lesions in patients with CIS was associated with conversion to MS, and with disability accumulation [24].

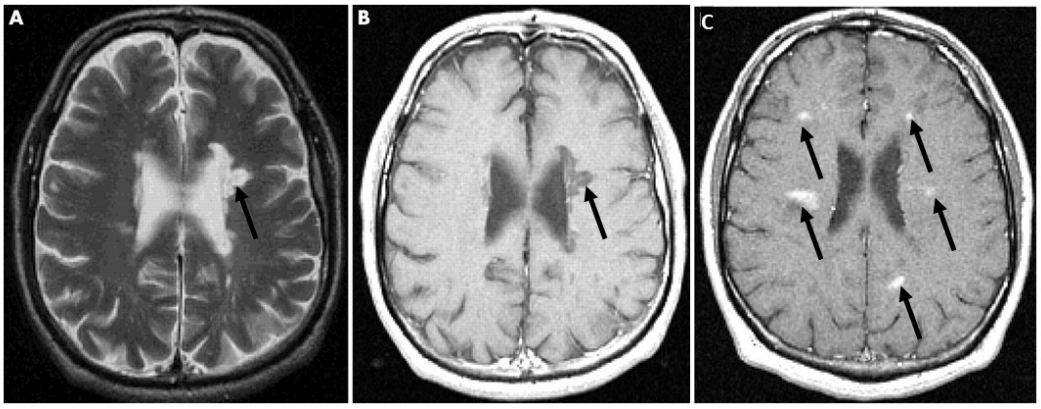

Figure 4: Examples of axial magnetic resonance imaging (MRI) images from patients with MS.

MRI images from a man with SPMS showing a large periventricular lesion (black arrow) which appears brighter in the T2-weighted image (A) and hypointense in the T1-weighted image (B). MRI image of a man with RRMS showing multiple lesions (black arrows) which appear enhanced in the T1-weighted image following administration of gadolinium (C). Pictures from Trip *et al.* [25]

1.5 Pathology of MS and classification of MS lesions

It is still debated whether the initial event leading to MS is the inflammation, or whether inflammation is secondary to the action of unknown intrinsic events in the CNS. However, the pathologic features of MS lesions strongly support the notion that myelin destruction and subsequent axonal loss are driven by a complex progression of inflammation within the CNS [26]. MS plaques pathology features vary across patients and disease stage and are characterized by confluent demyelinated areas which include variable levels of inflammation, axonal injury, and reactive gliosis [27]. They are found in both white and grey matter regions of the brain and spinal cord [2].

In early stages of MS, inflammation is more pronounced with increased permeability of the BBB and infiltration of peripheral immune cells. Active MS lesions contain mainly activated macrophages, microglia and $CD8^+$ T cells, with smaller numbers of $CD4^+$ T cells, B cells and plasma cells [16] [28]. There is still little damage to the CNS outside the plaques. As the disease advances, the relative proportion of B cells and plasma cells increases together with diffuse demyelination and axonal injury [26] [Figure 5]. Microglia and macrophages remain increased and activated over the disease course [29]. This results in diffuse grey and white matter atrophy. Eventually, during progression, the inflammation becomes compartmentalized inside the CNS, with fewer infiltrating cells inside the lesions and increased axonal loss [Figure 5]. In progressive forms of the disease, B cells, along with T cells aggregate in the meninges and perivascular cuffs, forming meningeal follicles with features of tertiary lymphoid tissue, associated with extensive demyelination, increased cortical lesions and axonal injury [16].

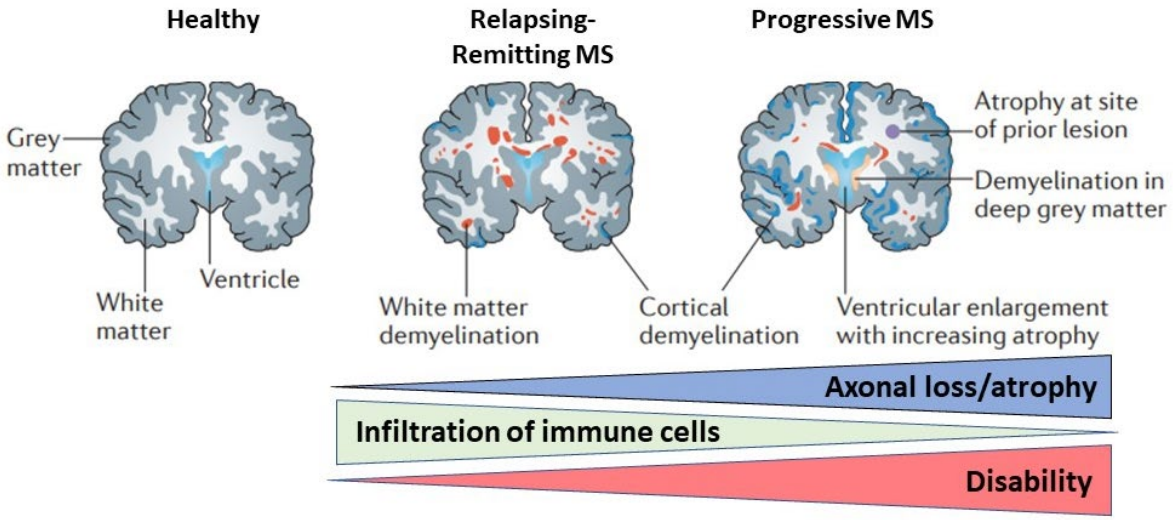

Figure 5: Pathology of multiple sclerosis.
Multiple sclerosis pathology is characterized by demyelinated lesions both in the withe and grey matter of the CNS. Accumulation of disability during the disease correlates with increased axonal loss and brain atrophy. Inflammation becomes compartmentalized inside the CNS with fewer infiltrating immune cells observed in the lesions during progression. Figure adapted from Dendrou *et al.* [16]

Active lesions have been subdivided into four distinct patterns, termed pattern I, II, III and IV based on histological features in biopsy tissue from patients with MS [2,30] [Table 1]. Pattern I lesions, found in 15% of patients with MS, show active demyelination on a T cell and activated macrophage/microglia inflammatory background and are perivascular. Pattern II lesions, found in approximately 58% of MS biopsies, are characterized by additional immunoglobulin and complement deposition. Pattern III lesions, found in 26% of biopsied patients with MS, are distinguished by oligodendrocytes apoptosis and dysregulated myelin protein expression, but still on an inflammatory background. No evidence of antibody or complement deposition has been reported [2]. Lastly, pattern IV lesions, found in only 1% of MS biopsies, were exclusively observed in PPMS patients and present with non-apoptotic loss of oligodendrocytes [30]. Some lesions with evidence of remyelination, defined by the presence of thin myelin sheaths can be observed

alongside active lesions, especially in pattern I and II lesions, and are named "shadow plaques" [2]. Chronic active lesions, also called smoldering plaques, are slowly expanding lesions characterized by a hypocellular center surrounded by a rim of activated microglia and/or macrophages with altered morphology, and ongoing demyelination and axonal loss. These types of lesions are a hallmark of chronic inflammation in MS and their proportion correlates with greater severity of the disease [31,32]. They are more often seen than active lesions in patients with progressive MS. Inactive lesions are sharply demarcated with very few macrophages/microglia and lymphocytes, demyelination, and loss of oligodendrocytes and axons throughout the lesion [33].

Table 1: Criteria for lesion types in MS

Lesion type	Histological features
Active	**Pattern I:** activated macrophages/ microglia, T cells, variable loss of oligodendrocytes at the lesion border **Pattern II:** activated macrophages/ microglia, T cells, antibody and complement deposition, variable loss of oligodendrocytes at the lesion border **Pattern III:** activated macrophages/ microglia, T cells, preferential loss of the peri-axonal myelin proteins, apoptotic oligodendrocytes **Pattern IV:** activated macrophages/ microglia, T cells, non-apoptotic loss of oligodendrocytes, no remyelinated lesions
Chronic active	Hypocellular center surrounded with rim of activated macrophages/ microglia, axonal loss
Shadow plaque	Presence of thin myelin sheaths alongside pattern I and II active lesions
Inactive	Hypocellular, oligodendrocytes and axonal loss

Table adapted from Guerrero *et al.* [34]

1.6 Immunopathology of MS

The pathogenesis of MS involves a complex multicellular pathophysiological process that evolves along the disease course.

1.6.1 Autoreactive T cells

The presence of lymphocytes within MS lesions suggests that CNS damage in MS could be driven by myelin-reactive T cells. Several studies have shown the presence of activated myelin-reactive T cells, with high avidity in MS patients [35]. However, how these T cells get abnormally activated toward CNS antigens and which antigens specifically activate them, remain unclear. These antigens could be self CNS antigens or cross-reactive antigens, such as viral antigens. One hypothesis is that antigens derived from some infectious agents, such as EBV share structural similarities with self-myelin antigens causing activation of autoreactive T cells through molecular mimicry [36]. This is consistent with the method employed to induce MS-like disease in animals where autoreactive T cells against myelin peptides are activated at peripheral sites, before crossing the BBB to penetrate the CNS.

1.6.1.1 $CD4^+$ T cells

Susceptibility to MS has been linked to genetic risk factors within the MHC class II region. The encoded MHC class II protein molecules are expressed mainly on antigen-presenting cells (APCs) and can present processed antigens to $CD4^+$ T cells, initiating the antigen-specific adaptative immune response [Figure 6]. In MS, the major proinflammatory $CD4^+$ T cells found to be increased in CNS lesions, CSF, and in the blood are T helper (Th) 1 and Th17 cells, producing interferon-g (IFN-g) and interleukin (IL)-17, respectively [37]. The levels of both cytokines have been associated with MS disease activity. In the CNS, both IFN-g and IL-17 are known to exacerbate immune activation by inducing the release of proinflammatory mediators, increasing antigen presentation, or by affecting the viability or function of CNS resident cells [38] [Figure 6]. The pathogenic role of IFN-g in MS has been confirmed from the results of a clinical trial where this cytokine was administered

to patients and which markedly exacerbated the disease [39]. In addition, more recently, a proof-of concept clinical trial using a monoclonal antibody against IL-17A provided first evidence that blocking IL-17 might be beneficial in patients with MS [40]. Th17 cells are also able to produce IFN-g under certain conditions and are called Th17.1, emphasizing the plasticity of Th cells. Th cells can switch from one class to another depending on the surrounding inflammatory environment. Th17.1 cells have cytotoxic properties and are involved in the disruption of BBB permeability in MS [41]. Also, untreated patients with MS present high numbers of $CD4^+$ T cells secreting granulocyte-macrophage colony-stimulating factor (GM-CSF), a pro-inflammatory cytokine found elevated in the CSF from patients with active MS [42,43]. GM-CSF efficiently activates and polarizes myeloid cells toward a pro-inflammatory phenotype [44] [Figure 6]. Recently, Galli et al. identified a specific Th cell signature in the blood and CSF from patients with RRMS, characterized by the expression of GM-CSF, tumor necrosis factor (TNF), IFN-g, interleukin-2 (IL-2) and C-X-C motif chemokine receptor type 4 (CXCR4). This Th cell population was also found within the inflamed CNS tissue in samples of untreated patients with MS, suggesting its involvement in the pathogenesis of MS [45].

1.6.1.2 $CD8^+$ T cells

While $CD8^+$ T cells show clonal expansion, indicating antigen-specificity, and are more abundant in MS lesions than $CD4^+$ T cells, their involvement in the pathogenesis of MS has been less well studied. A positive correlation between the number of $CD8^+$ T cells and axonal damage was found in MS lesions [46]. In addition, increased frequency of C-C motif chemokine receptor type 5 $(CCR5)^+$ and C-X-C motif chemokine receptor type 3 $(CXCR3)^+$ $CD8^+$ T cells in blood from patients with MS correlates with increased annualized MS lesion load [47]. Expression of MHC class I is necessary to present antigens to $CD8^+$ T cells, inducing their cytotoxic functions [Figure 6]. Interestingly, under inflammatory conditions such as MS, all CNS-resident cells including astrocytes, oligodendrocytes, and axons gradually upregulate MHC class I molecules expression, making these cells targets for $CD8^+$ T cells [38]. Upon recognition of cognate MHC class I- peptide complexes, $CD8^+$ T cells release granules containing perforin and/or granzyme B which destabilize the

cell membrane and induce apoptosis of the targeted cell. In human brains from MS patients, $CD8^+$ T cells releasing granzyme B cytotoxic granules were found in close contact to demyelinated axons [48] [Figure 6]. Genetic studies also demonstrated an association of MS with some alleles from the MHC class I region, further advocating a role of $CD8^+$ T cells in this disease. In addition, CNS infiltrating $CD8^+$ T cells can also express IFN-g, GM-CSF, and IL-17, emphasizing their ability to worsen inflammation and mediate CNS damage [42,49]. However, some regulatory $CD8^+$ T cells may have beneficial functions in MS pathogenesis.

1.6.1.3 Regulatory T cells

In physiological conditions, regulatory T (T_{reg}) cells maintain homeostasis and prevent excessive inflammation and autoimmunity. T_{reg} cells suppress different immune cell types by direct or indirect mechanisms, including the release of anti-inflammatory cytokines such as IL-10, IL-35 and transforming growth factor (TGF-β) and the release of perforin and granzyme [50]. They are characterized by several cell surface markers, including CD25, the transcription factor forkhead box P3 (FoxP3), which is necessary to maintain suppressive function, and low expression of CD127. Disruption of the balance between inflammatory and T_{reg} cells may be involved in the pathogenesis of MS [51]. Several studies have found that $CD25^+Foxp3^+$ T_{reg} cells were reduced in patients with MS compared with healthy controls and their frequency was further reduced in patients in relapse compared to patients in remission phase [51,52]. In addition, T_{reg} populations in patients with MS produced more IFN-g and less IL-10 compared with healthy controls [53] [Figure 6]. These Th1-like T_{reg} cells have defective suppressive activity *in vitro* [Figure 6]. In addition, genetic studies demonstrated an association of MS with some genetic variants of the CD25 and CD127, further advocating a defect of T_{reg} cells in this disease [51]. There are also other regulatory T-cell populations besides FoxP3 T_{reg} cells, including Tr1 cells which suppress autoreactive cells by secreting IL-10 independently of FoxP3 expression [51,54].

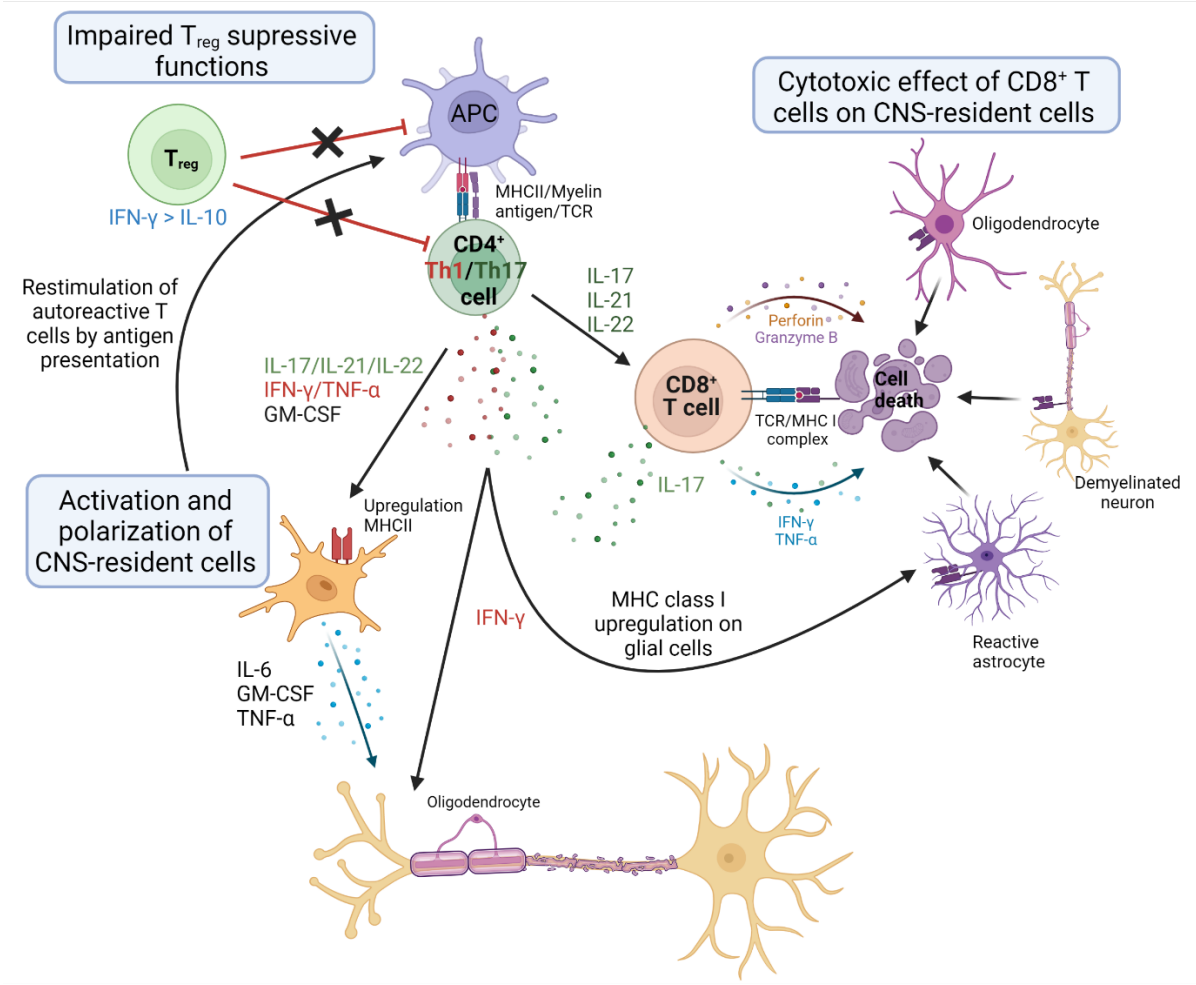

Figure 6: Proposed T cell functions in MS.
Upon entry into the CNS, both Th1 and Th17 cells release proinflammatory cytokines, activating and polarizing CNS-resident glial cells and antigen presenting cells (APCs). These cells upregulate major histocompatibility complex (MHC) molecules, resulting in the restimulation of myelin-autoreactive T cells at local sites and amplification of the inflammation. The pro-inflammatory milieu leads to the upregulation of MHC class I molecules on CNS-resident cells such as oligodendrocytes, reactive astrocytes and neurons which become the target for the cytotoxic activity of $CD8^+$ T cells. $CD8^+$ T cells release cytolytic granules containing perforin and granzyme B molecules, directed against CNS-resident cells expressing the self-antigen on MHC class I molecules. $CD8^+$ T cells can also secrete IL-17, which further amplifies the inflammation and CNS damage. IFN-g secreted by Th1 cells can directly kill oligodendrocytes, further contributing to the demyelination process. In addition, regulatory T cells (T_{reg}) display defective suppressive

activity towards autoreactive immune cells and secrete more IFN-g than IL-10. Figure adapted from Kaskow *et al.* [38] and made with Biorender.com.

1.6.2 Autoreactive B cells

The approval of anti-CD20 antibodies in the treatment of MS has revealed the importance of B cells in MS pathogenesis. In MS, the crosstalk between B and T cells, which normally occurs in secondary lymphoid organs to generate an optimal immune response against a pathogen, is likely disturbed. Peripheral B cell tolerance checkpoints are defective in MS, leading to increased frequency of polyreactive B cells in the blood [55]. Although the cause of this tolerance defect is not known, one hypothesis is that this may be due to chronic T cell stimulation and T cell intrinsic defects, such as impaired T regulatory cell function. B cells are potent APCs, recognizing low concentrations of antigens and constitutively expressing MHC class II and co-stimulatory molecules, which are increased in patients with active MS [Figure 7]. Therefore, after their escape from peripheral tolerance, autoreactive B cells likely activate CNS-infiltrating T cells via presentation of self-antigen on MHC class II molecules and develop into memory B cells and antibody-producing plasma cells [41]. The presence of oligoclonal immunoglobulin production in the CSF of most patients with MS highlight the pathogenic involvement of B cells in MS. While antibody-secreting plasma cells accumulate in the CNS and are increased with age in patients with MS, suggesting their contribution to disease progression, their role is still not well understood. Like in other chronic inflammatory diseases, the meninges of patients with secondary progressive MS often contain tertiary lymphoid structures with aggregated plasma cells, B cells, T cells, and follicular dendritic cells (FDCs) [16] [Figure 7]. Besides acting as potent APCs and differentiating into antibody-secreting plasma cells, B cells modulate T cell activation trough cytokines production, with pro- but also anti-inflammatory properties [Figure 7]. As an example, IL-6 production by B cells induces the differentiation of Th17 cells and prevents the differentiation into Treg cells. In patients with MS, B cells isolated from the blood exhibit an abnormal pro-inflammatory cytokine profile compared to heathy controls [56]. However, some B-cell subsets may also exert regulatory properties via secretion of anti-inflammatory cytokines, such as IL-10 or IL-35

[Figure 7]. Low serum IL-10 and IL-35 levels have been associated with the risk of disease progression [57,58].

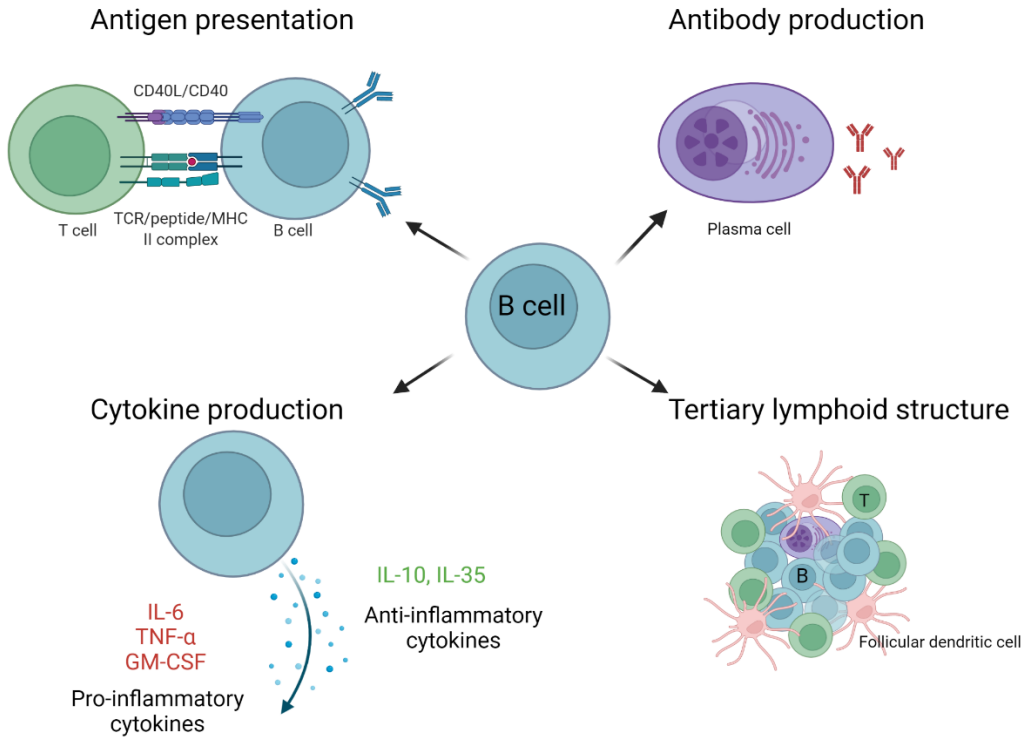

Figure 7: Proposed B cell functions in MS.
B cells impact the pathophysiology of multiple sclerosis through several functions, such as the presentation of self-antigen to T cells, autoantibody production, cytokines production and the formation of tertiary lymphoid structures into the CNS. Figure adapted from Baker *et al.* [59] and made with Biorender.com

1.6.3 Myeloid cells in MS

Myeloid cells such as macrophages, dendritic cells (DCs) and microglia constitute a significant proportion of cells found in active MS lesions with ongoing demyelination and axonal injury. Myeloid cells can present antigens via MHC molecules and consequently activate T cells. Cytokines such as IL-1b, IL-12, and IL-23 produced by myeloid cells will polarize T cells to pro-inflammatory T cells, which in turn produce cytokines leading to a vicious cycle that facilitates leukocytes

infiltration into the CNS and propagation of neural injury [60] [Figure 8]. Myeloid cells can act as phagocytes and are the main producers of cytotoxic factors and reactive oxygen species, suggesting their role in CNS damage [61] [Figure 8]. However, certain aspects of myeloid cells can also be beneficial and could promote recovery by enhancing remyelination [62], removing myelin debris, and producing neuroprotective factors [63] [Figure 8]. Thus, their role in pathological mechanisms of MS is complex and remains to be better elucidated.

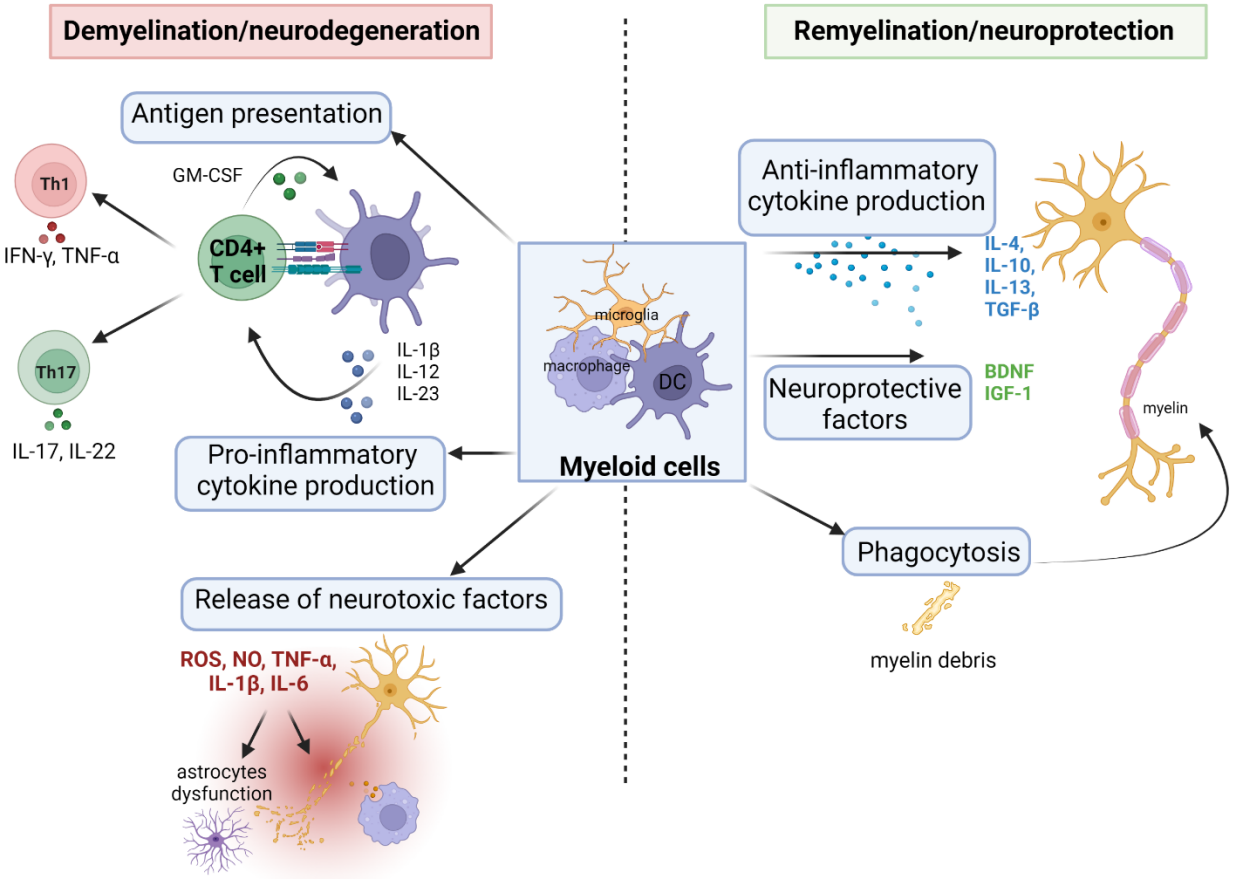

Figure 8: Proposed functions of myeloid cells in MS.
Cytokine secretion and self-antigen presentation by myeloid cells to T cells are critical to shape the anti-myelin and hence, pathological T cell response. These interactions take place both in the periphery and in the CNS leading to T cell priming and reactivation, respectively. Myeloid cells can also act as phagocytes and thus directly induce tissue damage within the CNS. In addition, infiltrating myeloid cells generate oxidative stress and release neurotoxic factors, further damaging CNS-resident cells. At the same time, myeloid

cells can also exert beneficial effects in the CNS. For example, the removal of myelin debris by resident myeloid cells, such as microglia, and the production of anti-inflammatory cytokines and some neuroprotective factors may have beneficial functions in MS pathology. Figure made with Biorender.com.
BDNF: brain-derived neurotrophic factor; IGF-1: insulin-like growth factor-1; NO: nitric oxide; ROS: reactive oxygen species.

1.6.3.1 Circulating monocytes and monocyte-derived macrophages in MS

Monocytes arise from hematopoietic stem cells and progenitor cells located in the bone marrow. In the periphery, monocytes are divided into different subsets based on their function and surface expression of CD14 and CD16. Higher levels of non-classical monocytes ($CD14^{+}CD16^{++}$) secreting IL-6 and IL-12 were found in untreated patients with MS compared to healthy controls [64,65]. Monocytes infiltrate the inflamed CNS and differentiate into macrophages expressing MHC class II and costimulatory molecules, and act as potent APCs. They also produce pro-inflammatory cytokines such as IL-1b, IL-6, IL-12, IL-23, TNF-a and chemokines. Macrophage accumulation in MS lesion correlates positively with demyelination [33]. However, macrophages can also facilitate resolution of inflammation and repair by producing anti-inflammatory cytokines such as IL-10, IL-13, TGF-β and neurotrophic factors including insulin-like growth factor-1 (IGF-1) and brain-derived neurotrophic factor (BDNF) [Figure 8]. Macrophages are plastic and change from an inflammatory to an anti-inflammatory phenotype depending on the microenvironment [61].

1.6.3.2 Microglia in MS

Microglia are CNS-resident macrophages that represent 10-20% of glial cells and that are involved in the development of neuronal circuits, maintenance of synapses, and neurogenesis. They are derived from myeloid precursors in the yolk sac and actively survey the CNS environment. Upon neuroinflammation, microglia undergo morphological changes. Activation of microglia in the CNS of patients with MS occurs already in "preactive" lesions, before BBB disruption, leukocyte infiltration, or demyelination [66]. Neuroinflammatory microglia secrete pro-inflammatory cytokines such as TNF-α, IL-1β, reactive oxygen species and, induce astrocyte

dysfunction, leading to the dysfunction of oligodendrocytes and neurons [Figure 8]. Microglia are also critical for phagocytosis of myelin and antigen presentation to T cells in active lesions [34]. In addition, the level of microglial activity in the cortical grey matter shows a relationship to progression of disability in patients with MS and they might be particularly relevant in the progressive forms of MS [67]. However, microglia are also beneficial trough phagocytosis of myelin debris, production of growth factors, and enabling successful remyelination [68] [Figure 8]. Interestingly, MS susceptibility genes were found to be more associated with microglia functions than neurons or astrocytes, suggesting a central but complex role of microglia in MS pathogenesis [69].

1.6.4 Astrocytes in MS

Astrocytes represent approximately 30% of the CNS-resident cells and are characterized by star-shaped processes. They form the glia limitans which contributes to the maintenance of the BBB integrity and are involved in several processes such as energy supply to neurons and oligodendrocytes, ion homeostasis, and synaptic plasticity [70]. They are connected to other glial cells using gap junctions made up connexin 30 and/or 43, which are lost in active and chronic lesions in patients with MS [71]. Astrocytes are considered as early active players in the pathology of MS, and hypertrophic astrocytes containing myelin debris are found at the edge of active demyelinating lesions [72] [Figure 9]. They express chemokines and cell adhesion molecules associated with leukocytes recruitment into the CNS parenchyma. In addition, reactive astrocytes produce B cell activating factor (BAFF), which promotes B cell survival and proliferation within the CNS [73]. They also produce pro-inflammatory chemokines such as CXCL10 and CCL20 which attract Th1 and Th17, respectively. In MS, astrocytes are also involved in the formation of the lesion scar which prevents the spread of the inflammatory processes and thus CNS damage, but also prevents neural repair [Figure 9]. Indeed, astrocytes present in the lesion create a physical and molecular barrier by upregulating some inhibitor factors such as hyaluronan, which restrict the remyelination process and thus severely limit axonal repair [74]. Astrocytes may also dampen inflammation and promote repair by producing neuroprotective agents

such as BDNF [70] or chemokine C-X-C motif chemokine ligand 12 (CXCL12) [75] [Figure 9]. Therefore, astrocytes have multiple functions and play dichotomous roles in MS pathogenesis.

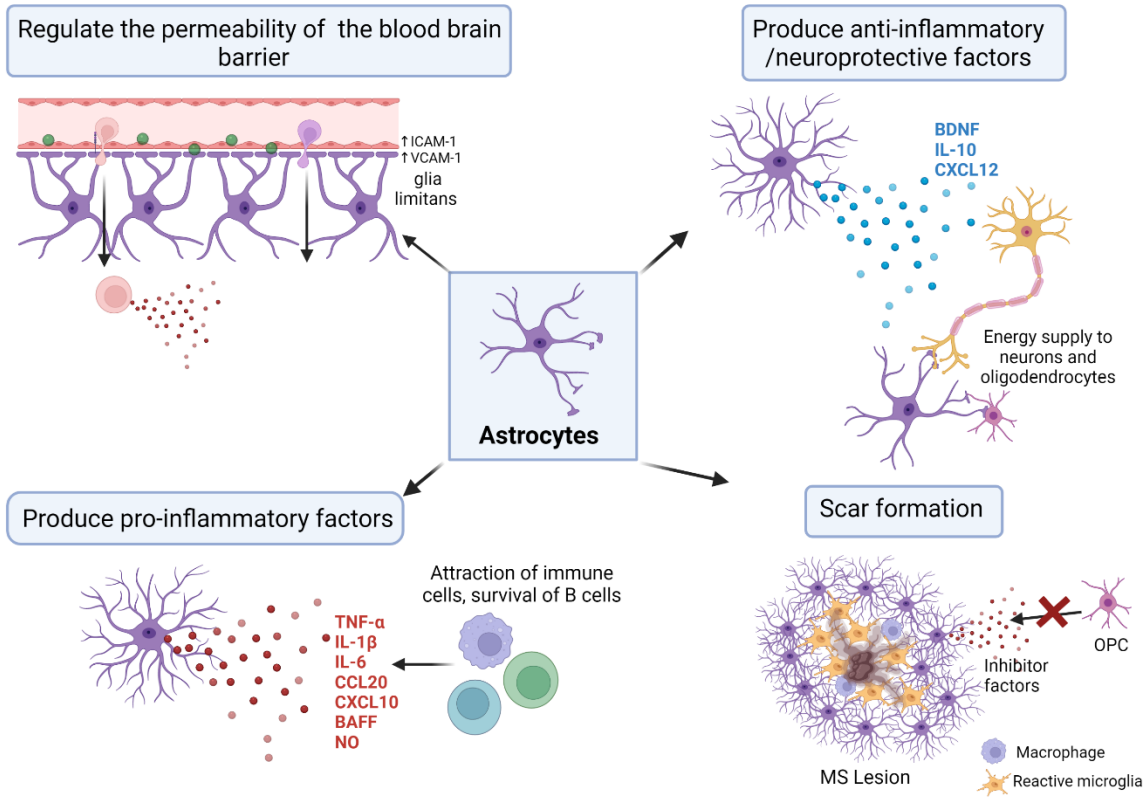

Figure 9: Proposed astrocyte functions in MS.
The distal end feet of astrocytes form the glia limitans that contribute to the maintenance of the blood brain barrier integrity, restricting the entry of peripheral immune cells into the CNS. Upon inflammation, however, astrocytes express cell adhesion molecules and chemokines, facilitating the entry of immune cells into the CNS. Reactive astrocytes produce pro-inflammatory factors such as proinflammatory cytokines and chemokines, and B cell activating factor (BAFF), which attract leukocytes into the CNS and promote the survival and proliferation of B cells within the CNS, further contributing to CNS damage. Following demyelination, hypertrophic astrocytes form a dense wall of filamentous processes around the lesion penumbra, named a glial scar. While it serves to confine the inflammation to the center of the lesion, this glial scar is a major barrier for regenerating axons. Reactive astrocytes may also produce anti-inflammatory cytokines such as IL-10

and neuroprotective factors such as CXCL12 and BDNF. Further, astrocytes are functionally connected to neurons and oligodendrocytes and provide energy supply. Figure made with Biorender.com.

1.7 Remyelination failure and axonal loss in MS

Demyelination resulting from the autoimmune damage to myelin and neurodegeneration are key hallmarks of all forms of MS.

1.7.1 Benefits of oligodendrocytes and myelin

Oligodendrocytes (OLs) are CNS resident cells that are primarily responsible for generating myelin sheaths and providing metabolic support to neurons via channels within the myelin [76]. Myelin is the spiral extension of the OL's plasma membrane, rich in lipids and proteins and wrapped around the axons of neurons. The ensheathment of axons by myelin provides electrical insulation and trophic support. Myelinated axons have multiple short segments of myelin, called internodes that are separated by short unmyelinated gaps, the nodes of Ranvier, where voltage-gated sodium and potassium channels are concentrated [Figure 10]. It allows action potentials to propagate in a saltatory fashion, which accelerates information conduction compared with unmyelinated axons of the same diameter [77].

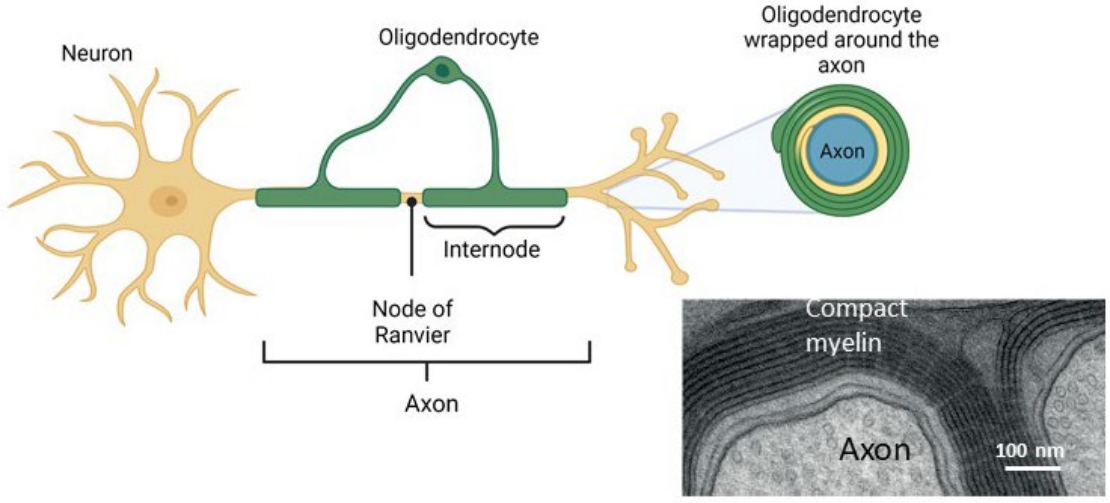

Figure 10: Myelinated axon in the central nervous system.

Schematic model of a myelinated neuron depicting an oligodendrocyte which extends its membranous sheath in a concentric movement around the axon. In the lower right part of the figure, the ultrastructure of the myelin is observed with electron microscopy and shows the multiple membrane layers compacted around the axon. Adapted from Nave *et al* [77] and made with Biorender.com.

1.7.2 Consequences of demyelination

Demyelination resulting from the autoimmune damage to OLs and myelin sheaths, leads to both reduced information conductance velocity, resulting in neurological disability, and reduced axonal resistance due to lack of physical and metabolic support. Several studies have demonstrated enhanced mitochondrial activity and density in demyelinated axons, suggesting higher metabolic request. In addition, sodium channels which generate the action potential, no longer cluster to nodes of Ranvier and therefore conduction is less efficient, probably explaining why demyelinated axons need more energy [78]. This increase in metabolic demand disrupts the neuro-axonal homeostasis, leading first to an increase in oxidative stress and, second to intra-axonal mitochondrial damage, resulting in energy failure that further compromises axonal integrity [79,80]. In patients with MS, axonal injury and loss represent key factors associated with neurological deficits and disability accumulation [18,29,81].

1.7.3 Myelination process

During development, oligodendrocyte progenitor cells (OPCs) originate in the ventricular zones of the CNS and migrate throughout the developing CNS parenchyma before differentiating into myelinating OLs. In adulthood, OPCs remain abundant representing 5–8% of the total cell population of the adult brain and are found distributed widely throughout the CNS [82]. They continually repel adjacent OPC processes via contact-mediated inhibition and are maintained during adult CNS homeostasis by local proliferation [83]. In the uninjured adult human brain, new myelin is continually generated [84]. Myelination in the CNS involves sequential processes in which OPCs migrate, proliferate, and differentiate into newly formed OLs, before maturing into myelinating OLs [Figure 11]. This process is tightly

controlled by positive and negative factors [85,82] [Figure 11]. As an example, axonal activity can increase myelination and new myelin formation can also occur as part of the acquisition of some cognitive functions, in the healthy adult CNS and referred to as adaptive myelination [86]. Other promoting factors, such as CXCL12 [87,88,89], the neuropeptide dynorphin [90], BDNF [91], Insulin-like growth factor-1 (IGF-1) [92], semaphorin 3F (SEMA3F) [93], and autotaxin [94] have also been described to promote one or several key steps of the myelination process [Figure 11]. On the other side, myelination is also controlled by negative regulators, such as the neuronal surface molecule leucine-rich repeat and Ig-domain containing 1 (LINGO1) [95], myelin debris [96], SEMA3A [97] as well as by extracellular matrix components, aggregated fibronectin [98], and hyaluronan [99] [Figure 11]. Myelination process is also known to be modulated by non-disease related factors such as age and sex. However, the cellular basis of myelination in the human CNS remains challenging to assess due to the lack of appropriate tools [100].

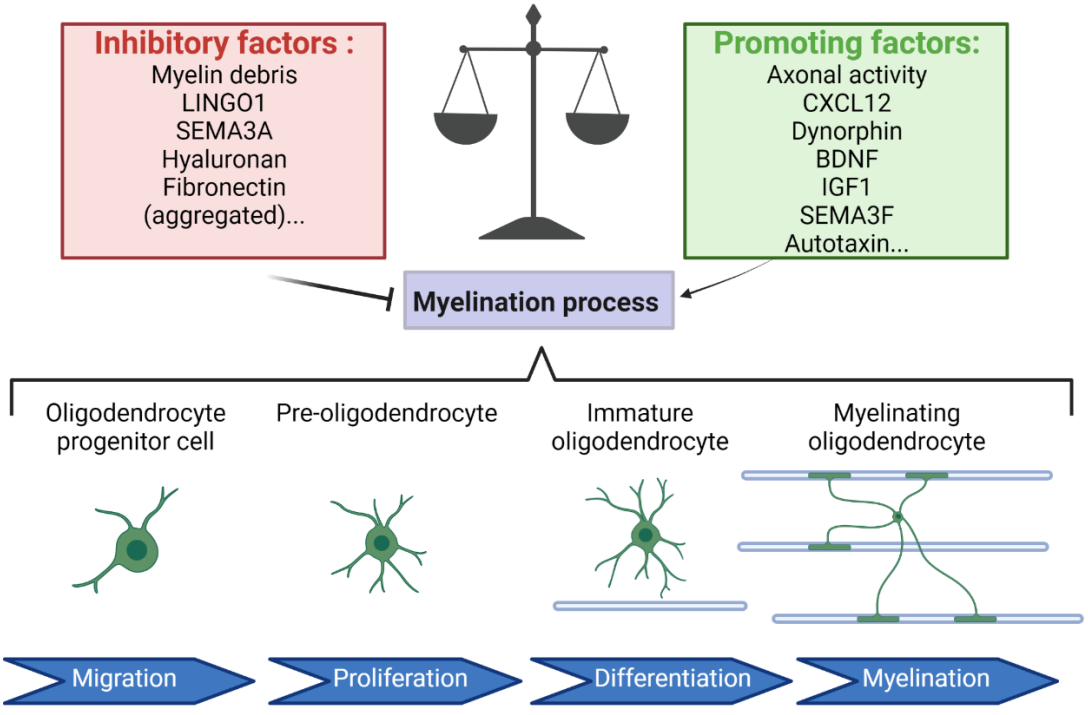

Figure 11: Regulation of the myelination process.

Oligodendrocyte development and myelination is tightly regulated by inhibitory and promoting factors that orchestrate the migration, proliferation, and maturation of oligodendrocyte progenitor cells into myelinating oligodendrocytes. Many of these factors can be differentially expressed at distinct stages of oligodendrocyte development. Adapted from Munzel *et al* [85] and Plemel *et al* [76] and made with Biorender.com.

1.7.4 Remyelination to mediate neuroprotection

In various experimental animal models, CNS remyelination is associated with restoration of saltatory conduction and even functional recovery [101] [102]. Therefore, remyelination might be important to reverse or prevent some of the structural and metabolic changes observed in axons, and thus provide neuroprotection. In line with this hypothesis, signs of axonal injury are less frequent in remyelinated shadow plaques than in active and inactive demyelinated plaques in brain tissue from patients with MS [103]. In addition, positron emission tomography (PET) studies using a myelin tracer demonstrated that dynamic remyelination inversely correlates with clinical disability in patients with MS, suggesting neuroaxonal preservation [104]. Furthermore, certain axonal structural changes observed in demyelinated areas are restored in remyelinated lesions in human and rodent tissues, such as aggregation of sodium channels in nodes of Ranvier and amelioration in mitochondria pathology [105] [106]. However, remyelination capacity in people with MS is highly variable and can be extensive in some individuals [107], while very low in a significant proportion of patients. In brain tissue sections, it has been shown that the myelin formed during remyelination is thinner than during normal myelination [76].

1.7.5 Inadequate remyelination in MS patients

There are differences in remyelination capacity both between individual lesions and patients, indicating heterogeneity within the mechanisms underlying inadequate remyelination in patients with MS [108]. Recent publications emphasized the existing heterogeneity among the oligodendroglia cell population based on localization, origin, and lineage alterations upon demyelination [109,110], which may explain the variability observed in response to demyelination. Based on data generated in

rodents, remyelination was thought to depend only on newly formed OLs arising from OPCs. However, it has recently been shown that mature OLs that survived the demyelination event were also able to participate in remyelination [100,111]. About a quarter of patients with MS exhibit an increase in the generation of new OLs in normal appearing white matter, demonstrating the potential to increase OL generation in the adult human MS brain [112]. Taken together, deficient remyelination can occur through a failure at any of the steps necessary to generate myelinating OLs, including migration to the lesion site, differentiation and wrapping of the axons [Figure 11]. As an example, differentiation blockade is known to occur because chronically demyelinated MS lesions are depleted of mature OLs, whereas OPCs, while reduced, can still be detected [113]. In addition, some demyelinated lesions in individuals with MS contain few OPCs, probably due to reduced recruitment of these cells to the lesion [114]. Also, OPCs differentiation can be stopped just before forming compact myelin around axons [115]. It also appears that remyelination failure correlates with age and disease duration [116], which could be related to reduced myelin debris clearance and decrease in extrinsic factors promoting differentiation of OPCs, or accumulation of inhibitory factors [117] [Figure 12]. Lastly, failure in remyelination in patients with MS could be related to the presence of inflammatory cells that can directly damage OPCs and OLs through the release of free radicals and inflammatory cytokines. On the other hand, the clearance of myelin debris by myeloid cells is crucial to facilitate remyelination and the number of activated macrophages or microglia correlates with the number of OPCs in MS lesions. Therefore, the complex relationship between the immune response and remyelination in MS are important to elucidate [76] [Figure 12].

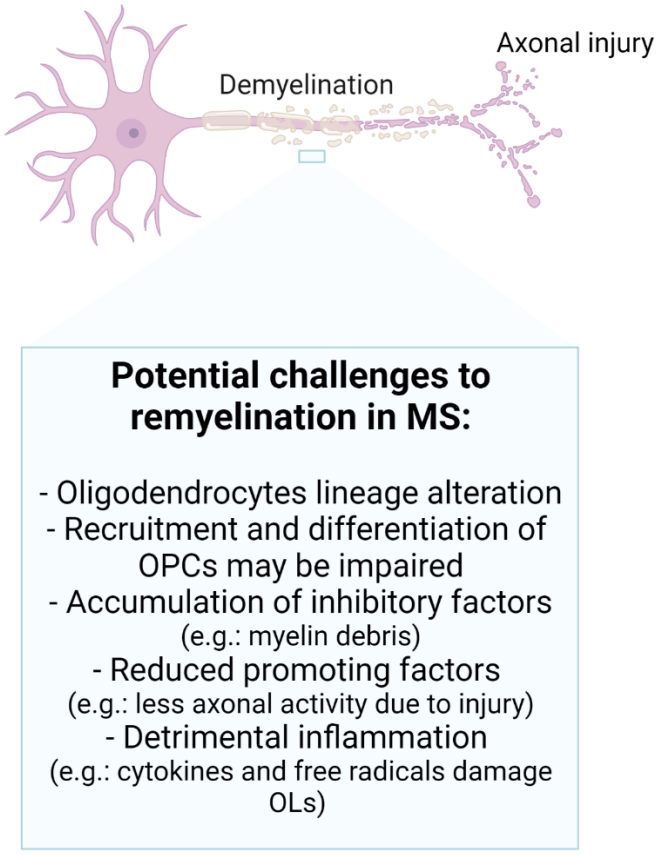

Figure 12: Potential causes for remyelination failure in patients with multiple sclerosis.
Figure adapted from Plemel *et al.* [76] and made with Biorender.com

1.8 Existing treatments for MS

Unfortunately, there is currently no cure for MS. Remarkable advances in treatment have been done in the recent years with 19 food and drug administration (FDA)-approved disease-modifying therapies (DMTs) that can help modifying the disease course, managing relapses, and providing a better quality of life, especially for patients with RRMS. Treatment of MS consists of a multidisciplinary approach including DMTs, symptomatic treatment, physical therapy, psychological support, and lifestyle modifications [118].

1.8.1 Disease modifying therapy

As of October 2021, there were 9 classes of DMTs approved for the treatment of MS with different mechanisms of action and routes of administration.

1.8.1.1 Injectable treatment

Injectable medications reduce the relapse rate by approximately 30% compared with placebo [119] and are considered safer than alternative therapies. However, they need to be frequently injected and can lead to flu-like symptoms and adverse effects at the site of injection.

1.8.1.1.1 Interferon beta

Interferon beta (IFNb) is the first DMT approved by the FDA in 1993 for the treatment of RRMS. IFNb is a cytokine belonging to the type I IFN family, involved in anti-viral responses. Although its mechanism of action in MS has not been fully elucidated, it is proposed that IFNb inhibits T-cell activation and proliferation, leads to the apoptosis of autoreactive T cells, modifies the cytokine milieu and, reduces migration of leukocytes across the BBB [120]. Recombinant forms of IFNb are the most widely used DMT for MS, reducing MRI disease activity and the annualized relapse rate (ARR) by 30%. Although, IFNb preparations are administrated either intramuscularly or subcutaneously, their favorable safety profile and minimal monitoring requirements, allow them to be used as first line therapies for RRMS [119]. However, they have no effect on disability progression and do not improve established progressive forms of MS [121,122].

1.8.1.1.2 Glatiramer acetate

Glatiramer acetate (GA) is a synthetic peptide that shares similarities with the sequence of the myelin basic protein (MBP). Several potential mechanisms of action have been suggested, including molecular mimicry. GA may compete with the binding of myelin antigens to MHC class II, leading to reduced activation of effector $CD4^+$ T cells. In addition, the GA-MHC class II complex binds to the T cell receptor and induces tolerance, shifting the immune response from a pro-

inflammatory state to an anti-inflammatory response [123]. Phase III clinical trials conducted in patients with RRMS demonstrated a 29% reduction in ARR and reduction of enhancing MRI lesions [124].

1.8.1.2 Oral treatment

Over the past decade, the availability of orally administered drugs has changed considerably the therapeutic landscape of MS, increasing treatment compliance.

1.8.1.2.1 Sphingosine 1 phosphate (S1P) receptor modulators

Fingolimod, a non-selective S1P receptor modulator (S1PRM), was the first oral drug approved by the FDA for RRMS treatment in 2010. S1PRMs are structural analogues of sphingosine and bind to the S1P receptor subtype 1 (S1PR1) on lymphocytes. S1PRMs lead to the internalization and degradation of S1PR1 which results in loss of responsiveness to the S1P gradient that drives lymphocyte egress from lymphoid tissues into the circulation, thus reducing peripheral lymphocytes in a dose-dependent manner [125,126]. Consequently, upon treatment with S1PRMs, pathogenic lymphocytes are sequestered in peripheral lymphoid organs, thus, preventing their egress into the circulation and infiltration into the CNS [127]. However, this mechanism of action does not directly affect other white blood cell types nor impact antigen-dependent T cell activation, expansion, and survival [128]. Besides the effect on lymphocyte trafficking, preclinical data suggests that S1PRMs may have a direct beneficial effect on CNS resident cells such as astrocytes, oligodendrocytes, and neurons [129,130]. The relevance of targeting S1P receptors in MS has been well established with fingolimod, which reduced the ARR by 48-55%, the rate of disability progression, and MRI lesions compared to placebo [131]. However, fingolimod did not show benefit on disability progression in a phase III trial in patients with PPMS [132]. Although fingolimod was demonstrated to be superior to IFNb, it was mainly used as a second-line agent in patients with highly active disease due to its adverse effects. These adverse effects included first dose bradycardia or atrioventricular block, macular edema, headache, dyspnea, cough, influenza, and diarrhea. Many of these side effects were attributed to fingolimod's

nonselective S1PR modulation, such as its binding to S1PR subtypes 3, 4 and 5. The favorable efficacy profile of fingolimod has led to an interest in developing improved S1PRMs with higher S1PR1 selectivity [133]. As of October 2021, there are three additional S1PRMs approved for the treatment of relapsing forms of MS, which all exhibit an improved selectivity profile: siponimod, ozanimod, and ponesimod [133]. Siponimod, a selective modulator of S1PR1 and S1PR5, was the first treatment to be approved for the treatment of patients with SPMS with active disease. In those patients, siponimod has demonstrated a significant benefit on disability worsening, along with reduction in MRI lesions [134]. In contrast to fingolimod, which requires a first dose observation of all patients due to a transient agonistic effect on S1PR1 leading to cardiac effects, dose up-titration of siponimod, ozanimod, and ponesimod over the first days of treatment attenuates the initial cardiac effects, avoiding the requirement for first dose observation in the absence of cardiac history [133].

1.8.1.2.2 Teriflunomide

Teriflunomide, the active metabolite of leflunomide, used in the treatment of rheumatoid arthritis since 1998 [135], has been the second oral DMT approved for adults with RRMS. The primary mechanism of action of teriflunomide relates to its inhibitory effects on the mitochondrial enzyme dihydroorotate-dehydrogenase, required for the de novo pyrimidine synthesis. Blockade of this pathway rapidly reduces DNA and RNA synthesis and consequently the proliferation of dividing cells such as T and B lymphocytes. In contrast, resting cells or slowly proliferating cells are not affected by teriflunomide as they rely on an alternate pathway [136-138]. In addition to its effect on the proliferation of auto-reactive lymphocytes, teriflunomide impairs several cellular functions such as integrin activation [139], cytokine production, and cellular migration [140,141]. Its clinical efficacy on ARR is comparable with IFNb [142]. The most common side effects include diarrhea, abnormal liver tests, nausea, flu, and hair thinning.

1.8.1.2.3 Dimethyl fumarate (DMF)

DMF is an oral fumaric acid ester approved since 2013 for the treatment of relapsing forms of MS, including CIS, RRMS, and active SPMS. Phase III clinical trials with DMF demonstrated a significant reduction of MRI disease activity and relapse rate compared to placebo [143]. While fumarates have been investigated as possible anti-inflammatory substances since the 1950s [144], the underlying mechanism for the therapeutic effect of DMF in MS is not fully understood. DMF has demonstrated antioxidant properties [145] and its metabolite, monomethyl fumarate (MMF) [146], is able to cross the BBB, supporting a direct effect on CNS-resident cells [147]. The neuroprotective effect of DMF appears to be mediated by two different pathways. First, by activating the nuclear factor (Erythroid-Derived 2)-Like 2 (Nrf-2) [148], DMF upregulates cytoprotective genes, involved in the cell-defense antioxidant response [148-151]. Next, DMF is a ligand for the G-protein-coupled receptor (GPCR) GPR109A (also known as hydrocarboxylic acid receptor or the niacin receptor), which modulates microglial and astrocytes activation, thereby indirectly affecting neuronal survival and function [152-155].
Preclinical studies have also demonstrated that DMF exhibits anti-inflammatory properties by inhibiting the translocation of the transcription-factor NF-κB [156-159], a key inducer of pro-inflammatory cytokines and inhibitor of T cell apoptosis. Other studies have described the alteration of dendritic cell polarization resulting in a shift in the polarization of Th cells towards a Th2 rather than a Th1 or Th17 phenotype [160-163]. Recently, it has been shown that DMF inhibits aerobic glycolysis in activated myeloid and lymphoid cells shifting the immune response from an immunostimulatory to an immunoregulatory environment [164]. Most common side effects of DMF include flushing, redness, itching, nausea, stomach pain.

1.8.1.2.4 Cladribine

Cladribine is a purine nucleoside analog developed initially to treat lymphoid malignancies. This molecule has also been approved since 2019 for the treatment of relapsing forms of MS, including RRMS, and active SPMS. In clinical trials,

cladribine administrated as short-course treatment (8 to 20 days per year), significantly reduced ARR by 55-58%, the risk of disability progression and MRI disease activity versus placebo [165,166]. Cladribine is intracellularly phosphorylated into an active metabolite, the 2-chlorodeoxyadenosine triphosphate. Accumulation of this nucleotide in the cell results in the disruption of cellular metabolism and the inhibition of DNA synthesis and repair, thereby leading to cell death. Cladribine metabolite accumulates preferentially in cell types with high levels of deoxycytidine kinase compared to 5'-deoxynucleotidase activity, such as seen in lymphocytes, resulting in a rapid and long-lasting lymphopenia [167]. Additional immunomodulatory effects of cladribine have been suggested, such as inhibition of proinflammatory cytokines secretion by T cells [168], altered expression of adhesion molecules, and modulation of activation markers on DCs [169]. Most common side effects of cladribine include lymphopenia, opportunistic infections (herpes zoster and tuberculosis), rash, and hair loss.

1.8.1.3 Infused treatment

Monoclonal antibody infusions are highly efficacious in reducing ARR in patients with RRMS. However, all these therapies can cause infusion reactions and some severe adverse effects.

1.8.1.3.1 Natalizumab

Natalizumab is a humanized monoclonal antibody directed against the a4 chain of the a4b1 integrin, also known as the very late antigen 4 (VLA-4). Binding of the antibody to VLA-4 interferes with the adhesion of immune cells to endothelial cells, thus limiting the entry of inflammatory cells into the CNS. This antibody, infused intravenously over one hour, every four weeks, is indicated for the treatment of relapsing forms of MS, including RRMS, and active SPMS. In clinical trials performed in patients with RRMS, natalizumab demonstrated impressive efficacy with significant reduction of the ARR by 68%, the risk of disability worsening by 42%, and gadolinium enhanced MRI lesions by 92% compared to placebo [170]. However, when studied in patients with SPMS, natalizumab failed to show

significant efficacy on disability progression [171]. The main concern associated with the use of natalizumab is the risk of developing an opportunistic and life-threatening viral CNS infection, named progressive multifocal leukoencephalopathy (PML). This infection is caused by reactivation of a common polyomavirus, the John Cunningham virus (JCV) which is present in approximately 50 to 70% of the population. In the general population, the risk of developing PML is rare but this risk increases when a patient is treated with immunosuppressive therapy, likely due to compromised CNS immune surveillance [172]. Retrospective analyses of post marketing data from various sources have estimated the incidence of PML in patients treated with natalizumab for two years and positive for anti-JCV antibodies at 1 per 1000 patients. Because of this risk, natalizumab is available only under a restricted distribution program, named the TOUCH® Prescribing program [173].

1.8.1.3.2 Alemtuzumab

Alemtuzumab is a humanized monoclonal antibody binding to the cell surface protein CD52, which is highly expressed on B and T cells, and at lower levels on natural killer cells, monocytes, and macrophages. Therefore, alemtuzumab leads to the depletion of CD52-expressing cells either by complement-induced or antibody-dependent cell-mediated cytotoxicity, followed by their repopulation in a defined pattern [174]. Overall, alemtuzumab has been proposed to reprogram the immune repertoire, leading to very long duration of action [175]. In clinical trials in patients with RRMS, alemtuzumab reduced ARR by 49.6%, radiological disease activity, and slowed down progression of RRMS to SPMS compared to IFNb-treated patients [176,177]. Based on these results, alemtuzumab has been approved first in Europe, in 2013, for the treatment of patients with RRMS. In the US, the antibody has been approved in 2014 but only as a third-line therapy, namely in patients who did not show appropriate response with two or more DMTs. In 2019, based on pharmacovigilance data, reporting fatal cases, cardiovascular events, and immune-mediated diseases in association with alemtuzumab infusions, the approval label in Europe was updated and has restricted the use of alemtuzumab

to treat RRMS only if the disease is highly active despite treatment with at least one DMT or if the disease is worsening rapidly [178].

1.8.1.3.3 Ocrelizumab

Ocrelizumab is a humanized monoclonal antibody targeting CD20, a cell-surface epitope that is mainly expressed by cells of the B cell lineage, including pre-B cells, mature B cells and memory B cells but not stem cells and plasma cells. Therefore, ocrelizumab selectively binds and depletes CD20-expressing B cells while preserving the preexisting humoral immunity and capacity for B cell reconstitution [179]. In addition, CD20 is also expressed on a subset of T cells, characterized by enhanced production of TNFa, IL-1b, and IL-17. Targeting these CD20-expressing T cells might also contribute to the efficacy of Ocrelizumab [180].

Ocrelizumab which is given twice yearly is the first and only therapy approved for the treatment of adults with relapsing forms of MS and with early PPMS with imaging features demonstrating inflammatory activity. In phase III clinical trials conducted in patients with RRMS, ocrelizumab significantly reduced ARR by 46-47% and MRI lesions as compared to IFNb-treated patients [181]. In a clinical trial in patients with PPMS, treatment with ocrelizumab reduced the risk of confirmed disability progression by 24% relative to placebo [182]. The most frequently reported adverse events were infections and infusion-related reactions including pruritus, rash, throat irritation, and flushing [183].

1.8.2 Relapse treatment

DMTs reduce relapses occurrence but none of them fully suppress all relapses. The most common relapse treatment regimen is a short course of high dose systemic corticosteroids (e.g.: methylprednisolone) or gel of adrenocorticotropic hormone (ACTH) to accelerate recovery. When patients do not respond adequately to these first line treatments, plasmapheresis may be considered for severe exacerbations of the disease [184].

1.8.3 Symptomatic treatment

Management of symptoms such as pain, spasticity, cognitive impairment, bladder, and bowel issues, include a combination of pharmacological and nonpharmacological treatments. For example, fampridine, a potassium channel blocker is used as a symptomatic treatment for walking disability in patients with MS [185].

1.9 Unmet needs of patients with MS

MS is a very complex heterogenous condition and despite an increasing number of approved DMTs, which mainly target peripheral immune cell activation and entry into the CNS, there are still several unmet needs [Figure 13].

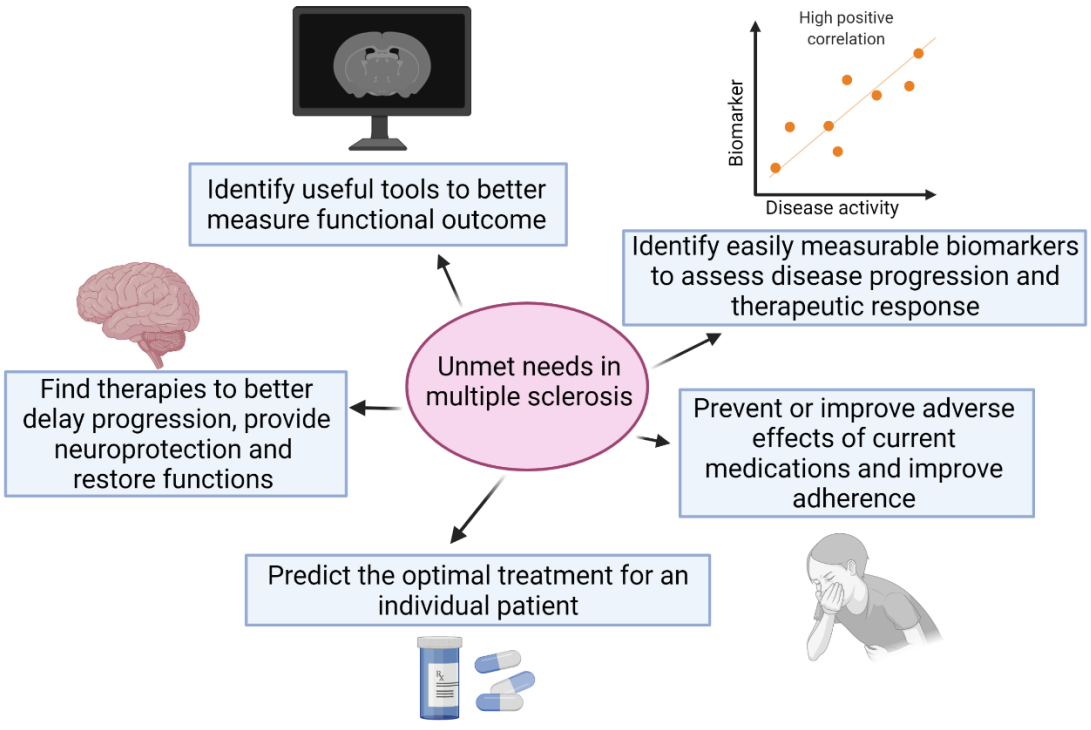

Figure 13: Unmet needs in multiple sclerosis.

1.9.1 Biomarkers for MS prognosis or for monitoring therapy response

MRI remains the most common clinical tool used to diagnose, evaluate disease progression, and therapy response in MS. However, MRI assessments are difficult to standardize and do not allow to track the patient's disease activity and monitor therapy response, in real time [186]. Therefore, there is a need for easier-to-perform and less expansive new molecular biomarkers, suitable for longitudinal monitoring of disease activity and therapeutic response. So far, only few molecular biomarkers have been routinely used in clinical practice, such as the detection of OCBs in CSF, which is associated with a conversion from CIS to MS [187]. The validation process takes several years which slows down the expansion of biomarkers for MS monitoring. Recently, neurofilament proteins (NF) have gained attention to monitor neuro-axonal damage. Indeed, NF, which are neuronal cytoskeletal proteins, consist of 3 subunits (light, intermediate and heavy) that are released both into the CSF and blood if axonal damage occurs. Specifically, neurofilament light chain (NFL) levels measured in blood samples from patients with MS are associated with MRI-related disease activity, degree of disability, and brain atrophy rate, supporting its utility as a molecular biomarker of disease progression and treatment response [188].

1.9.2 Tools to better measure functional outcome

MS is a heterogenous and progressive disease which causes a variety of symptoms that can evolve throughout the disease course. Therefore, assessing the patient's disease status is complex and necessitates multiple outcome measures or tools. The expanded disability status scale (EDSS) has been introduced in 1983 to quantify the patient's neurological impairment. While it has been widely used in clinical trials to assess the efficacy of new drugs, EDSS has some limitations such as a low sensitivity to change and the underrepresentation of fatigue, visual function, and cognitive impairment [189]. Since the introduction of EDSS, new tools have been developed for the assessment of the patient's neurological status such as the multiple sclerosis functional composite (MSFC), a three-component scale including the timed 25-feet walk test for leg function and ambulation, 9-hole peg test for

arm and hand function, and the paced auditory serial addition test for cognitive function [190]. These tools have limitations and additional work is in progress to assess for example wearable biosensors to collect data in real-life on ambulation balance and physical activity or function, allowing clinicians to better understand disease progression. However, none of the techniques introduced so far, provides an ideal outcome measure. In addition, pathologic assessments using MRI techniques, which correlate with disease progression, do not capture the pathophysiologic changes occurring during progression. Indeed, neuronal function could be impaired in the absence of structural and detectable changes and therefore, tools that would measure the neuronal function changes over time, such as evoked potentials, would be beneficial, especially for the progressive forms of the disease [191].

1.9.3 Preventing or ameliorating adverse effects of current medication and improving treatment adherence

Although the current treatments reduce the frequency of relapses, they are also associated with adverse events which can be serious, sometimes life-threatening, and which can contribute to a lack of adherence to the treatment [192]. Some progresses have been done for some treatments such as natalizumab which is associated with PML risk. While this serious adverse event cannot be fully eliminated, the use of the anti-JCV antibody test has mitigated the risk. Due to the lack of long-term safety data, especially for the more recently approved DMTs, post-marketing surveillance activities will have to be conducted to improve their use in clinical practice. In addition, prevent adverse effects of the current DMTs is also an essential strategy to increase treatment adherence in patients with MS [Figure 13] [193]. Other barriers to treatment adherence are the difficulties linked with the administration route, especially injections, which have already been improved by the introduction of oral treatments.

1.9.4 Restorative therapies

Despite the arrival of new DMTs, MS progression is not halted and there is currently no drug approved to repair the damaged myelin and provide neuroprotection.

Only one DMT, ocrelizumab, is approved for PPMS and its effects remain modest with only 24% of reduction in disability progression relative to placebo [182]. MS-related disability can be either physical or psychological, including a decline in cognitive functions. Many targets have been proposed for neuroprotection, however none of them have proven efficacy in phase III clinical trials [76]. The promotion of regeneration of the myelin sheath, which restores the support to axons, or the use of agents to directly protect axons have emerged as the most promising therapy to delay, prevent, or reverse progression. However, the lack of tools to assess properly remyelination and neuroprotection in clinical trials is a huge challenge.

To conclude on this section, there are still many unmet needs for patients with MS, especially for the patients with progressive forms of the disease [192] [Figure 13]. Despite a substantial investment and intensive preclinical research in the field of MS, the proportion of promising compounds that reaches the approval status remains low.

2 Preclinical drug development of small molecules

Developing a novel small molecule drug and introducing it to the market is a complex and interdisciplinary effort involving a project team with various competences including chemists, biologists, pharmacologists, toxicologists, clinicians, statisticians, computer scientists, and regulatory experts. Multiple stages exist for this drug development process including preclinical and clinical drug development [Figure 14]. In average, this process takes up to 12 years and costs more than 1 US $ billion [194]. Preclinical drug development includes all the activities necessary to bring a drug from early discovery to initiation of human clinical trials [Figure 14]. Then, once the drug has reached phase I, the probability of regulatory approval is less than 10% [195].

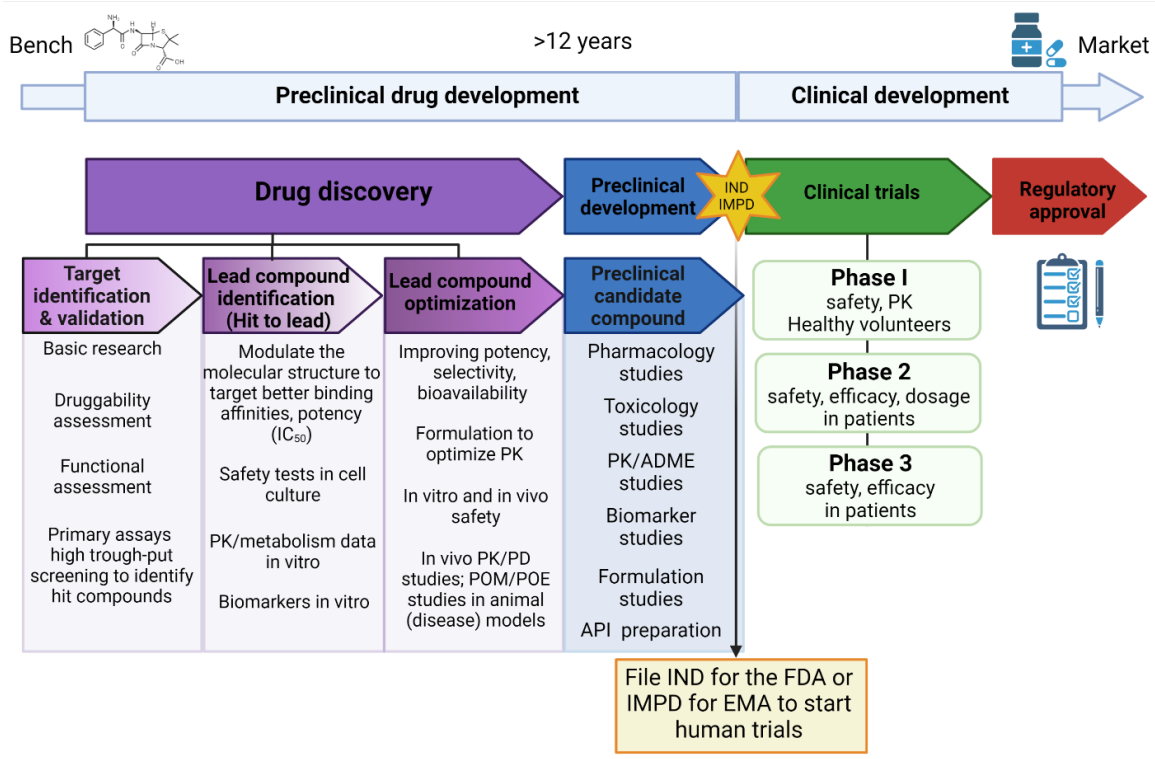

Figure 14: Small molecule drug development process: from basic research to approval of a drug.
Preclinical development encompasses drug discovery and preclinical development processes, meaning all the activities before starting human clinical trials. The boundary between preclinical and clinical development is defined by the approval of an investigational new drug (IND) application or investigational medicinal product dossier (IMPD) which is required to start clinical trials in the US or Europe, respectively.
ADME: absorption, distribution, metabolism, and excretion; API: active pharmaceutical ingredient; EMA: European medicines agency; FDA: food and drug administration; PD: pharmacodynamic; PK: pharmacokinetic; POE: proof of efficacy; POM: proof of mechanism

2.1 Drug discovery for small molecules

2.1.1 Target identification

Identifying the molecular mechanisms of a disease and therefore the potential targets for therapeutic intervention are the first steps in the discovery of a new drug. A target is a broad concept to qualify a biological entity such as a protein

and/or a biological mechanism such as a metabolic pathway, which is believed to play a role in a disease. A target needs to be "druggable", meaning that it should be accessible to the potential new drug and should elicit a biological effect that could be measured both *in vitro* and *in vivo*. Certain target classes such as G protein-coupled receptors (GPCRs) are widely proposed as new targets in small molecule drug discovery as they have druggable sites accessible at the cell surface [196]. In addition, the target should have, based on theoretical assessment, acceptable potential side effects and competition status [197]. There are various strategies to search for a therapeutic target, including the review of previously published data on a disease target pathway or target coming from different sources such as genetic association studies, transgenic organisms, pathway analysis, imaging, biomarkers. An alternative approach is also to use phenotypic screening to identify evidence of new mechanisms that modulate disease relevant pathways. As an example, Mei et al [198] used micropillar arrays to identify compounds that increase differentiation of OPCs into myelinating OLs. Based on this phenotypic screen, the study proposed compounds with antimuscarinic properties as a therapeutic target for repair in MS.

2.1.2 Target validation

Once identified, this new target should be validated experimentally according to the proposed mechanism of action. Functional studies should demonstrate that the target is involved in a disease pathway, and that modulation of the target is likely to have a therapeutic effect [197]. Different validation tools ranging from the analysis of molecular signaling pathways to cell-based and *in vivo* disease models, are available. For example, antibodies with high affinity against the target or tool compounds which are known to modulate the target can be used in cell-based assays or in animal models. In addition, transgenic animals, such as knockout mice for the target are attractive validation tools to assess the functional consequence of gene manipulation [199]. In addition, market potential of the disease (target space) may be considered.

2.1.3 Identification of hit compounds

Following the validation of the proposed target, the hit discovery process starts with the aim of discovering compounds with confirmed purity and identity which have a consistent activity in screening assays. Therefore, the challenge of this drug discovery phase is to develop pharmacologically relevant and reproducible compound screening assays [199]. Such assays often include biochemical assays to measure affinity of the molecule to the target or cell-based assays such as stable mammalian cell lines over-expressing the target of interest which typically generates a functional readout following the activation or inhibition of the target [200]. Different screening strategies can be run to identify active molecules. High throughput screening (HTS) involves the screening of large libraries of compounds in screening assays designed to be run in plates of 384 wells and above [201]. One example of an HTS technology to screen for and profile functional agonists or antagonists of GPCRs is the use of assays measuring β-arrestin recruitment upon activation of GPCRs [202]. The outcome of these HTS campaigns is the identification of compounds displaying activity on the drug target, usually defined by percent activity relative to control compounds. In parallel or after the primary screen, active compounds undergo counter-screens, which are screens developed to identify false positive compounds that have the potential to interfere with the assay used in the primary screen. Counter-screens can also be used to eliminate compounds with undesirable properties, such as cytotoxicity [Figure 14]. Then, the identification of hit compounds need to be confirmed and refined by performing a concentration response curve in the same primary screen. The surviving hit compounds displaying good selectivity index [Figure 14] are tested in secondary assays for specificity, selectivity, and to confirm the mechanism. At this stage, the drug discovery project team, especially the medicinal chemists will cluster hit compounds into groups sharing common chemical structure features [203]. They will start to work on the structure-activity-relationship (SAR), meaning that they will define chemical motifs in common and see whether the addition or removal of different chemical groups to a core structure results in different potencies on the

target. The number of chemical series taken to the hit to lead stage depends on the resources available.

2.1.4 Lead compound identification (Hit to Lead phase)

Chemistry programs are initiated to improve the potency, the selectivity, and physicochemical properties (reactivity, stability, solubility) of the selected hit chemical classes [203]. Intensive work is done to define the SAR around each core compound structure. Usually, the discovery project team designs a screening cascade to test the best representatives of each of these chemical series in key *in vitro* assays, providing information regarding potency on other species, preliminary toxicity, physicochemical properties, pharmacokinetic (PK), and absorption, distribution, metabolism, and excretion (ADME) properties [Table 2]. This cascade helps the team to eliminate compounds prior to initiating *in vivo* studies. As an example, solubility and permeability determination are important to consider with regards to the adsorption in the digestive system. If one compound lacks both these properties, it is unlikely that it will be escalated to the next phase of development no matter how potent it was in primary and secondary screen assays [199]. Also, if the target necessitates the drug to penetrate the brain, the project team will prefer a chemical class of compounds which is likely to pass the BBB based on lipophilicity and efflux ratio [Table 2]. The compounds that meet the criteria fixed by the project team based on the target and the foreseen therapeutic indication, including potency in primary and secondary assays, specificity, and selectivity, as well as most of the physicochemical and PK property targets, are then escalated to be assessed in *in vivo* PK studies.

Table 2: Example of key in vitro assays used to profile hit chemical classes in drug discovery

In vitro assays	Target value	Utility
Aqueous solubility	>100 mM	Determine the solubility in the aqueous medium: important for running *in vitro* assays and to work on formulating the drug to be administered *in vivo*.
Distribution coefficient at pH 7.4 ($LogD_{7.4}$)	0-3 (for BBB penetration)	Measure of lipophilicity: indication for drug movement across membranes.
Microsomal stability Cl_{int}	< 30 mL/min/mg protein	Determine metabolic stability using human liver microsomes (HLM) which contain membrane bound drug metabolizing enzymes. This assay measures compound intrinsic clearance (Cl_{int}) and gives an idea on how fast the compound will be eliminated *in vivo*.
CYP450 inhibition	>10 mM	Determine whether the compound inhibits the cytochrome (CYP) P450 family, the main enzymes metabolizing drugs in human liver. Blocking them can result in toxicity and drug-drug interactions.
Plasma protein binding	Depends on the potency of the drug in relevant functional assays (IC_{50} or EC_{50})	Determine the fraction of the drug bound to proteins in plasma. Usually, only free unbound compounds interact with the therapeutic target and can diffuse and distribute into the tissues. Therefore, this parameter is used to predict the doses which will be needed in *in vivo* efficacy studies, using potency obtained from *in vitro* functional assays.
MDCK- MDR1 permeability	Efflux ratio < 2 (drugs are not	Determine whether a compound undergoes an active efflux across the cell monolayer. MDCK-MDR1 cells originate from Madin-Darby canine kidney (MDCK)

	substrates of P-gp)	cells transfected with the MDR1 gene, which encodes the efflux protein, P-glycoprotein (P-gp). This protein is expressed in many tissues including intestine and brain and can therefore be used to predict intestinal and BBB permeability.
HepG2	No effect at 50 times IC_{50} or EC_{50}	Determine whether a compound has toxic effects on human liver, using the human liver cancer cell line HepG2.
hERG IC_{50}	>10 mM	Patch clamp, an electrophysiology technique, to study drug effects on hERG potassium current in human cells. This assay is a standard component of cardiac safety evaluation and is considered a surrogate of proarrhythmic risk liability.

Adapted from [199,204,205]; IC_{50}: half maximal inhibitory concentration; EC_{50}: half maximal efficacy concentration; Cl_{int}: intrinsic clearance; CYP: cytochrome; Madin-Darby canine kidney (MDCK); P-gp: P-glycoprotein

2.1.5 Lead optimization phase

The aim of this phase is to conserve the favorable properties of the lead compounds while improving their potential liabilities to be able to select one preclinical candidate [Figure 14]. Different activities in different areas, including chemistry, biology, drug metabolism and PK, pharmacology, toxicology, pre-formulation and preclinical galenic are conducted in parallel to characterize the lead compounds. These activities vary from company to company and are established by the project team to fulfill the requirements of the research project [199]. As an example, in pharmacology, the compounds displaying favorable PK properties *in vivo*, are further investigated in tolerability studies and target engagement assays, in which dose-response studies are performed to characterize the PK/ pharmacodynamic (PD) relationship of the compound. The compounds demonstrating a favorable PK/PD profile are further tested in target-relevant proof of mechanism/proof of efficacy disease models to estimate the compound

efficacious concentration [Figure 15]. Toxicology assays are run *in vitro* to determine potential mutagenicity, phototoxicity, hepatotoxicity, and cytotoxicity. With the most promising compounds, pilot toxicity studies can also be conducted to assess the maximal tolerated doses in rodents and determine therapeutic index in animals, describing the ratio of the compound concentration causing toxicity and the concentration eliciting the therapeutic effect [203] [Figure 15]. The patent situation is considered, and process chemists assess whether the chemical synthesis of the most promising compounds are scalable. The physicochemical properties, the chemical stability and polymorphism of the selected molecules are studied in the context of pharmaceutical development. The compounds are also characterized for their selectivity against closely related targets and against a wide range of other targets (off-target screen), based on the input from the toxicology data. Other tests including safety pharmacology studies to assess any potential liability of a compound can be performed [206]. For example, if a compound inhibits hERG with an IC_{50} below 10mM, it is worth to characterize it further in additional assays such as isolated heart vessels or performing electrocardiogram (ECG) in guinea pigs or dogs. All the information accumulated about the molecules at this stage will enable the drug discovery project team to select a preclinical candidate (PCC) compound.

In parallel the team continues to explore potential follow-up or back-up molecules that could replace the PCC if required or be considered when targeting additional indications. For example, ponesimod, a selective S1P1RM, has been recently approved to treat adults with MS [207], while the follow-up molecule, cenerimod, is being developed for the treatment of patients with systemic lupus erythematosus [208].

2.2 Preclinical development

A PCC is a compound that will be fully characterized to allow first-in-human (FIH) clinical trials. Therefore, the primary goal of this stage is to provide enough information regarding the safety of the compound and to demonstrate that the PCC exhibits pharmacological activity that justifies its development. The

therapeutic index or safety margin of the PCC should be assessed based on the targeted indication (risk-benefit ratio), the nature of toxicities observed in animals, the duration of the intended clinical trial, and the human PK predicted properties of the drug (inter and intra variability of exposure) [Figure 15]. The international conference of harmonization (ICH) guideline M3(R2) provides recommendations of what authorities expect as nonclinical safety evaluation prior a FIH trial [209]. The main goals for the toxicologists together with the project team are to define the target organ toxicities in relationship with the drug exposure, identify whether toxicities are due to on- or off-target effects and if they are relevant to humans [210]. Rodent and non-rodent mammalian species are used, and studies must comply with good laboratory practices (GLP) to delineate the PK profile and to generate the safety and toxicity profile of the drug. The frequency, the route of administration, and the duration of those studies should conform to the proposed clinical dosing protocol. All these activities help to determine the dose range, including the initial starting dose that mitigates the risk of toxicity and further escalation steps [210]. FIH studies are always preceded by submission of an investigational new drug (IND) application to the FDA or investigational medicinal product dossier (IMPD) to the European medicines agency (EMA). These documents must include summaries of information accumulated during the preclinical development stage, including manufacturing information, data from animal pharmacology and toxicology studies, clinical protocols, and investigator information. Often a meeting to prepare the IND submission is requested to ensure

that the FDA will approve the preclinical package and support the planned phase I clinical trial.

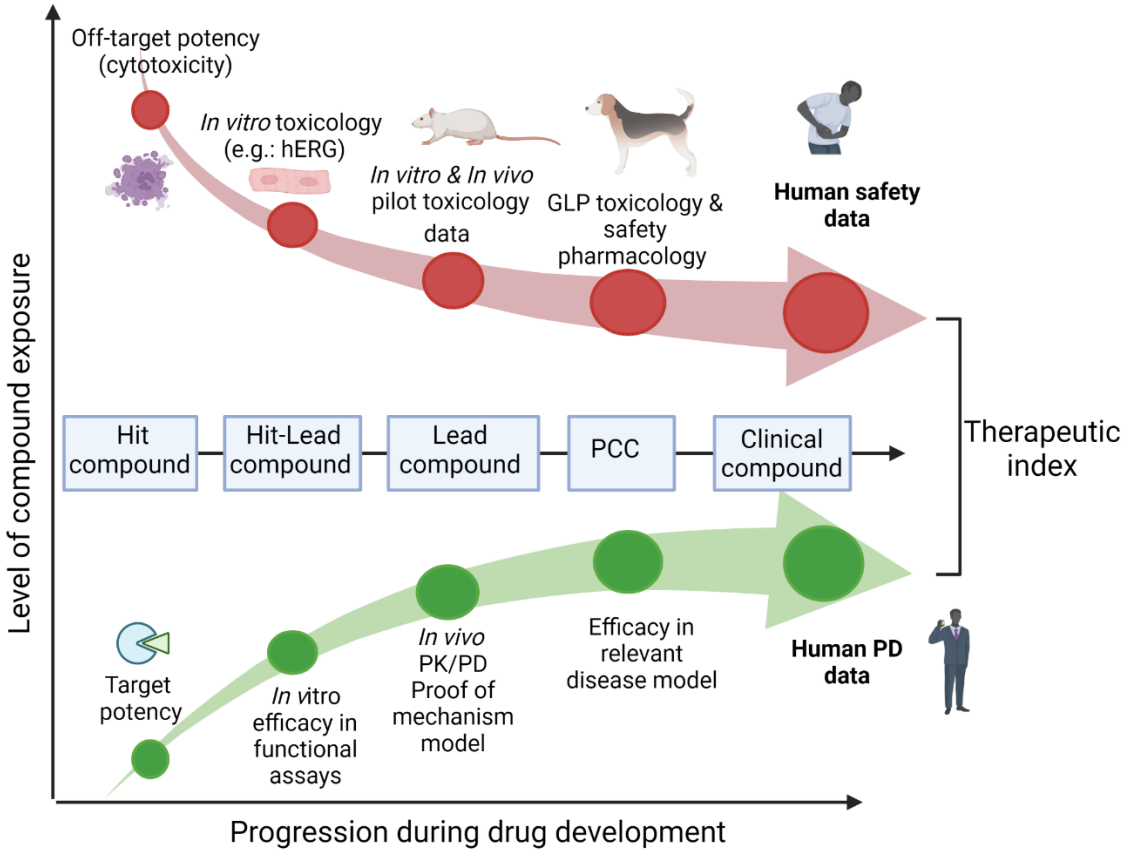

Figure 15: Refinement of the therapeutic index through the small molecule drug development process.
Adapted from Muller *et al.* [211]; GLP: good laboratory practice; PCC: preclinical candidate compound; PD: pharmacodynamic; PK: pharmacokinetic

2.3 Role of animal models in MS drug discovery

The reasons for clinical failure are mostly attributable to lack of safety or efficacy, and unfortunately nervous system disorders are among the areas with the lowest probability of success [195]. The study of drug-target interactions and drug effects *in*

vivo, in an intact organism, is central in the process of drug discovery and development. Selecting the appropriate animal models to establish relationship between drug potency, dose, plasma and/or tissue exposure and efficacy, is a strategically important decision and requires good knowledge of species-specific physiology, differences in immune response, and drug metabolism [212]. Typically, *in vivo* efficacy studies are performed in rodents, such as mice and rats, especially during early phase of preclinical drug development where only small amount of drug are available. As in other diseases areas, the use of animals in MS research has enabled invaluable mechanistic understanding of the complex pathophysiology of this disease. Although no single experimental model can reproduce all the complexity of MS, many different models are available for studying different relevant aspects of the pathogenesis of the disease, such as inflammation, demyelination, remyelination and neurodegeneration [213]. The most used models are experimental autoimmune encephalomyelitis (EAE) and toxin-induced demyelination models.

2.3.1 Experimental autoimmune encephalomyelitis (EAE) models

EAE is a wide spectrum of autoimmune neurological diseases, characterized by paralysis due to CNS inflammation, demyelination, and axonal damage in susceptible animals, such as rodents and non-human primates. EAE is induced in animal trough either active immunization with CNS-derived peptides or proteins emulsified in an adjuvant, or by passive transfer of autoreactive T cells. The first unintentional EAE model was observed as a side effect of anti-rabies vaccination in the 1880's. Indeed, the vaccine preparation was insufficiently purified and contaminated by CNS antigens, which in some patients led to paralysis associated with neuroinflammation, a condition resembling the acute phase of MS [214]. In 1949, EAE was for the first time induced in mice by active immunization with spinal cord homogenates [215]. Since then, numerous encephalitogenic peptides have been discovered and several EAE models with distinct features are now available and can be used for specific research questions [216]. The clinical course and pathological features of EAE depend on the CNS autoantigen and the adjuvant used, as well as the species, strain, gender, and age of the animals used [Table 3]. In the most

frequently used models, EAE is induced in mice by subcutaneous immunization with myelin peptides such as myelin oligodendrocyte glycoprotein (MOG), myelin basic protein (MBP) or proteolipid protein (PLP), emulsified with complete Freund's adjuvant (CFA), containing heat-inactivated *Mycobacterium tuberculosis*. In addition, pertussis toxin injections the same day and 2 days later, may be required to boost the immunological response, by expanding the autoreactive T cells and by opening the BBB. The disease follows a predictable clinical course, characterized by an induction phase and an effector phase with the appearance of ascending paralysis starting around 10 to 15 days after immunization [216]. Depending on the strain of mice used, the disease can follow a chronic progressive course, a relapsing-remitting disease course or a secondary chronic progressive disease course [Table 3]. Clinical signs are usually assessed using a scale from 0-5 to score the paralysis, where 5 corresponds to the death of the mouse [217].

Table 3: Example of the most frequently used active EAE models

Species	EAE disease course	Model	Model features
Mouse	Chronic progressive	MOG_{35-55} emulsified in CFA in C57BL/6 mice Reviewed in [218]	Shortest and very robust model Demyelination starts 10-14 days after the induction: secondary irreversible axonal damage Chronic disease with no remission $CD4^+$ T cell-mediated model in which B cells are not activated by the autoantigen MOG-reactive antibodies are not encephalitogenic
		Human MOG protein (MOG_{1-125}) emulsified in CFA in C57BL/6 mice [219-221]	B cell APC function is required for induction of the disease

			MOG-reactive antibodies are encephalitogenic
	Relapsing-remitting	$PLP_{139-151}$ emulsified in CFA in SJL mice Reviewed in [217]	Demyelination starts 3 weeks after induction Epitope spreading of the immune response, allows the study of mechanisms leading to relapses and remissions $CD4^+$ T cell-mediated model Complex and 6-8 weeks long
	Relapsing and secondary progressive	MOG_{35-55} emulsified in CFA in NOD mice Reviewed in [222,223]	RR-EAE with progressive worsening appearing 20-30 days post-induction with extensive demyelination and axonal damage Both $CD4^+$ and $CD8^+$ T cells play a role
Rat	Relapsing-remitting	MOG protein (MOG_{1-125}) emulsified in CFA in Brown Norway rats [224]	RR disease course Dependent on autoantibody response
	Hyperacute	MBP emulsified in CFA in Lewis rats Reviewed in [225]	Limited demyelination Paralysis is thought to be the result of BBB permeability, inflammation, and edema $CD4^+$ T cell-mediated model Monophasic with resolution in 5 to 7 days
Common marmoset	Chronic	Human MOG_{1-125} emulsified in CFA Reviewed in [226]	Variable disease onset due to the outbred nature of the marmosets. 5 to 39 days after immunization, first lesion can be detected by MRI Lesions resemble the MS pattern II lesions with complement and antibody deposition

Adapated from Bjelobaba *et al.* [227]; CFA: complete Freund's adjuvant; MBP: myelin basic protein; MOG: myelin oligodendrocyte glycoprotein; NOD: non obese diabetic; PLP: proteolipid protein; RR: relapsing-remitting; SJL: Swiss Jim Lambert

In the most commonly used EAE models, myelin peptides are presented to MHC class II-restricted $CD4^+$ Th cells in peripheral lymphoid tissues. Activated T cells proliferate and differentiate into effector myelin-specific $CD4^+$ T cells which egress from secondary lymphoid organs and pass into the blood circulation before migrating to the CNS [Figure 16]. By expressing adhesion molecules, cytokines, and chemokines, together with their receptors, autoreactive T cells infiltrate the CNS and initiate the pathology leading to the destruction of the myelin sheath [Figure 16]. In the CNS, T cells produce cytokines which induce infiltration of peripheral myeloid cells into the CNS parenchyma. Auto-reactive T cells are reactivated after recognition of their antigens on APCs, such as microglia, macrophages, DCs and B cells, which further amplify and sustain the inflammatory response leading to demyelination and subsequent axonal damage. The degree of damaged CNS tissue correlates with the clinical signs observed in animals. At the onset of disease, astrocytes proliferate and express chemokines which can promote T cell migration through the damaged BBB. They also form scar tissue around the injured area, which affects the normal interaction between glial cells in a cytokines and chemokines milieu-dependent manner [227] [Figure 16].

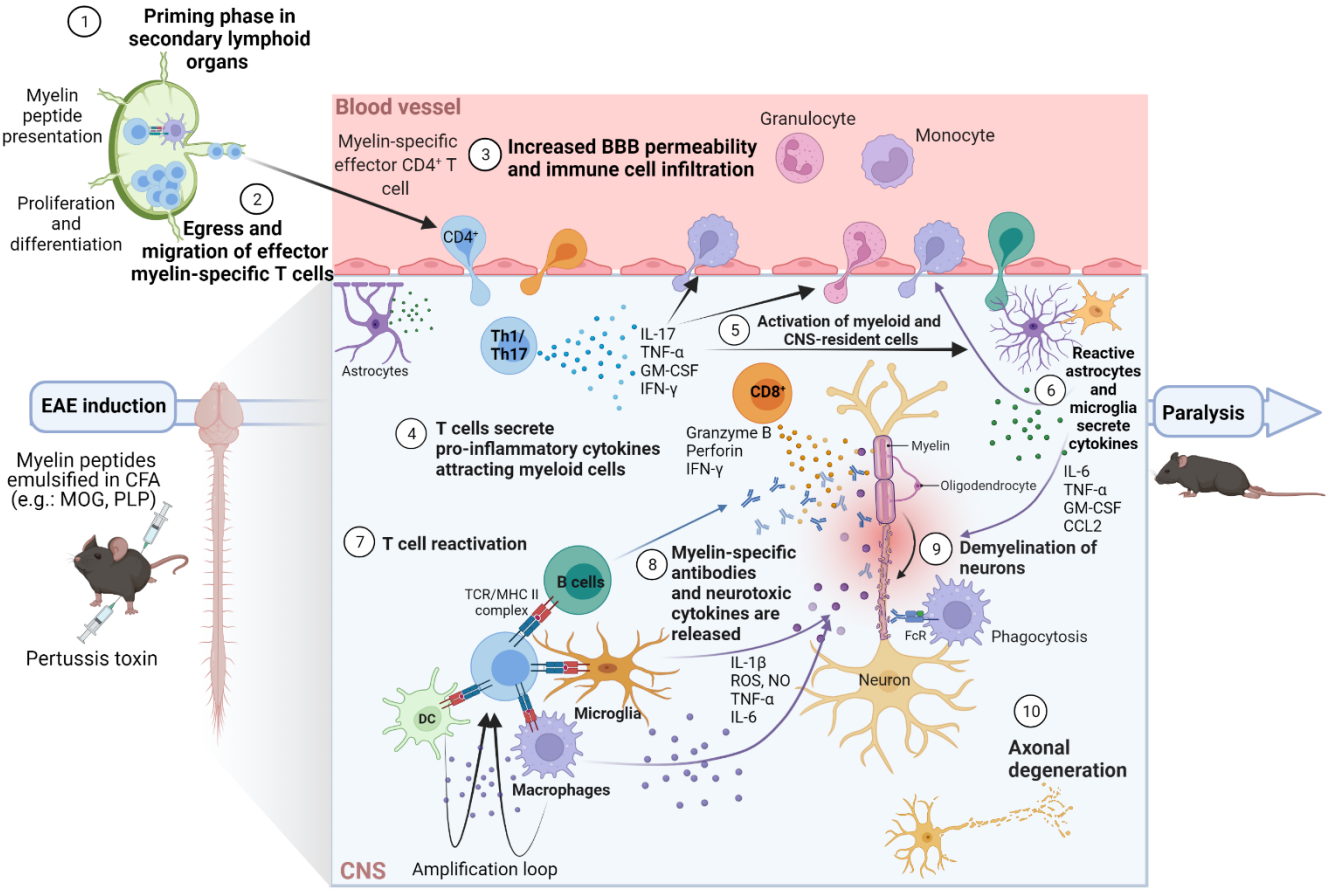

Figure 16: Immunopathology of the most-commonly used active EAE models
In active EAE models, subcutaneous immunization of mice with myelin antigens, emulsified in complete Freund's adjuvant (CFA) leads to the priming of myelin-specific $CD4^+$ T cells in secondary lymphoid organs (1). The effector myelin-specific T cells egress the secondary lymphoid organs and migrate into the blood (2). In postcapillary venules, autoreactive T cells cross the BBB and penetrate the CNS (3). Th1 and Th17 cells in the CNS secrete cytokines and chemokines (4), which attract myeloid cells into and activate myeloid cells and CNS-resident cells in the CNS parenchyma (5). Reactive astrocytes and microglia release cytokines contributing to further recruitment and activation of effector cells (6). In addition, T cells are reactivated by macrophages, dendritic cells, microglia, and B cells through presentation of myelin autoantigens via MHC class II (7). This leads to sustained inflammation with the release of inflammatory cytokines, reactive oxygen species (ROS), nitric oxide (NO), and myelin-specific antibodies (8). All these events result in demyelination (9) and subsequent axonal degeneration (10), resulting in functional deficits

visible in the animal. Figure made with Biorender.com. BBB: blood brain barrier; CNS: central nervous system; MOG: Myelin oligodendrocyte glycoprotein; PLP: proteolipid protein.

Even though all the current FDA-approved drugs have demonstrated a certain degree of efficacy in EAE models, other drug candidates, which were promising in these models, failed in patients with MS, indicating a translational gap. In addition, major unknowns still exist about the mechanism leading to the development of MS and the autoimmune etiology of MS is still debated [228]. The immune-mediated damage has been suggested to be secondary to a primary degenerative scenario which is supported by the fact that current DMTs fail to halt progression in MS, therefore toxin-induced demyelination models, which are not driven by peripheral autoimmunity, are also useful for studying brain-intrinsic inflammatory responses associated with demyelination and remyelination processes.

2.3.2 Cuprizone model

Cuprizone (bis-cyclohexanone-oxaldihydrazone) is a chopper-chelating compound which triggers the death of OLs with subsequent gliosis and demyelination. This toxic agent was first used to assess copper content in biological samples, such as serum and plasma [229]. In 1966, Carlton reported that cuprizone intoxication in rodents leads to edema and noninflammatory demyelination throughout the brain [230]. Later, administration of cuprizone in the standard chow to mice was proposed as a preclinical animal model to study demyelination caused by the massive death of OLs and remyelination, which occurred once the cuprizone was removed from the diet [231,232]. The mechanism of action by which cuprizone induces OL death is still not completely understood. However, cuprizone-treated OLs exhibit enlarged mitochondria and big vacuoles, suggesting mitochondrial dysfunctions in the brain of cuprizone-treated mice [231]. Cuprizone causes disturbances in mitochondrial enzymes of the respiratory chain which contain copper as a co-factor, and thus, leads to oxidative and metabolic stress in OLs [223]. Due to the production of myelin, mature OLs display a high cellular metabolism and they also contain the highest amount of iron in comparison to other brain cells,

which might explain why they are preferentially vulnerable to cuprizone. Of note, apoptosis of OLs is also described in active pattern III lesions in patient with MS. Cuprizone-induced demyelination depends on the dosage and duration of the toxic exposure, and on the strain, age, and gender of the animals [227]. Most commonly, demyelination is induced in male C57BL/6 mice by feeding 0.2% cuprizone mixed into the rodent chow for several weeks [Figure 17]. In this strain of mice, mature OLs start to dye as early as 2 days after cuprizone introduction and are almost fully depleted after 3 weeks of cuprizone treatment, when demyelination is already evident, both in the cortex and in the corpus callosum (CC) [233]. The spatiotemporal pattern of the demyelination induced by cuprizone intoxication is brain region dependent. Most studies have investigated the CC where demyelination peaks after 4 to 5 weeks of cuprizone intoxication, while it is delayed in the cortex and reaches its peak between 5 to 6 weeks [233]. Demyelination is associated with microgliosis, astrogliosis, and axonal damage [223,233]. The severe gliosis observed promotes an inflammatory response with the release of proinflammatory cytokines such as IL-1b, IFN-g, TNF-a, and NO, which can further harm the OLs and axons. However, microglia and astrocytes are also required for remyelination by clearing myelin debris or by releasing growth factors to stimulate CNS repair [Figure 17] [234]. Spontaneous remyelination can occur after cessation of cuprizone. These repair mechanisms are initiated very early during the intoxication, even before the demyelination is detectable immunohistochemically. Upon short-term cuprizone exposure (up to 6 weeks), OPCs migrate, proliferate within lesions, differentiate, and restore myelin sheaths [Figure 17] [234]. Upon chronic exposure to cuprizone (12-16 weeks), the newly generated OLs undergo apoptosis and the number of OPCs is reduced, leading to reduced remyelination capacity after withdrawal of the cuprizone [235]. Taken together, this model is useful to assess therapies that promote remyelination or protect OLs, without the interference with the peripheral immune system. Indeed, cuprizone-induced de- and remyelination are not mediated by T or B cells, as demonstrated by studies performed in cuprizone-treated recombinase activating gene-1 knockout (RAG-$1^{-/-}$) mice that lack lymphocytes [236].

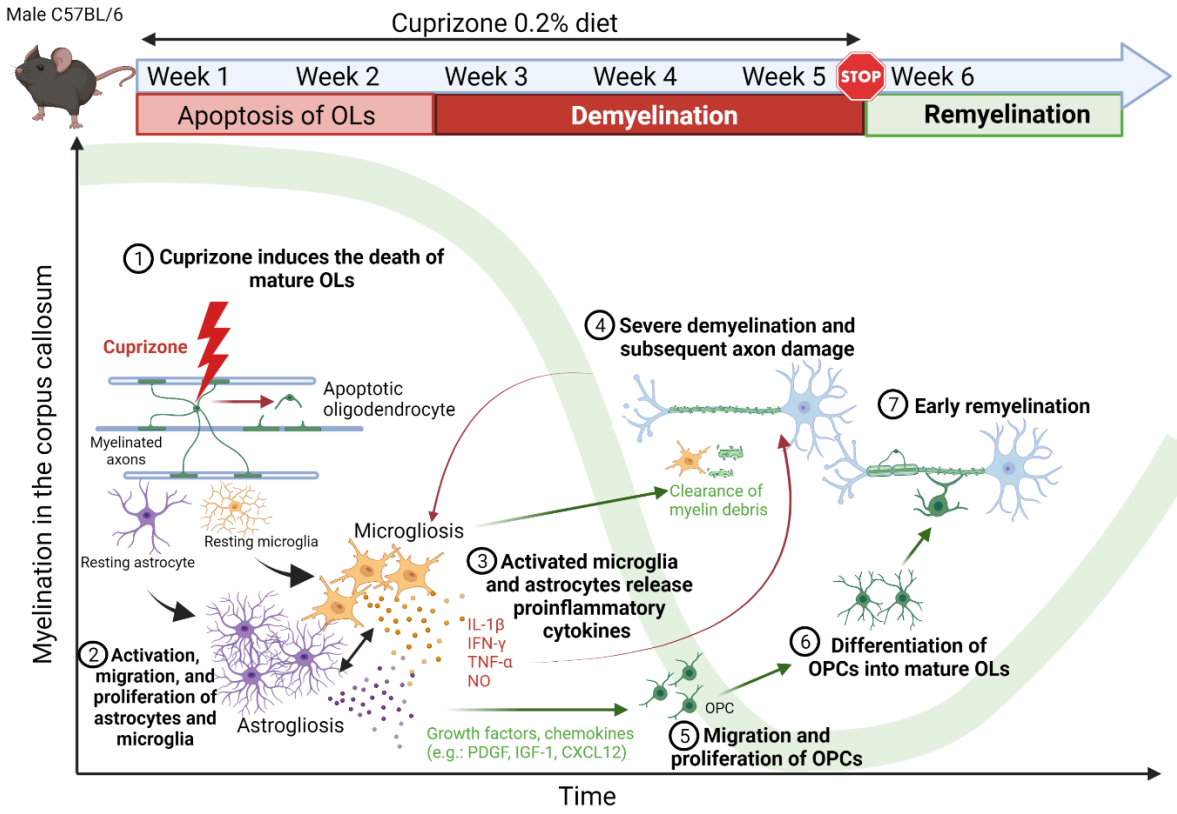

Figure 17: Cuprizone-induced de- and remyelination model in male C57BL/6 mice. Mature OLs start to undergo apoptosis already during the first week of cuprizone exposure (1), leading to the activation, migration, and proliferation of microglia and astrocytes (2). Reactive microglia and astrocytes release pro-inflammatory cytokines (3), which can further harm the OLs and the axon, sustaining an inflammatory cycle. OLs are almost completely depleted at week 3 of cuprizone intoxication and severe demyelination is observed in the corpus callosum at week 4-5 of cuprizone exposure (4). Activated microglia clear the myelin debris and several growth factors and chemokines are produced by activated astrocytes and microglia, supporting the migration and proliferation of OPCs (5). At week 5, nearly all axons in the medial corpus callosum are demyelinated (large green line located at the bottom of the y-axis). After the withdrawal of cuprizone (end of week 5), the amount of activated microglia starts to decrease and astrocytes, which are still activated, continue to produce factors promoting the differentiation of OPCs into mature (6) and then myelinating OLs which remyelinate the axons (7). Figure adapted from Gudi *et al.* [234] and made with Biorender.com.

CXCL12: C-X-C chemokine ligand 12; IFN-γ: Interferon-g; IGF-1: Insulin-like growth factor-1; IL-1b: Interleukin 1b; NO: nitric oxide; OLs: oligodendrocytes; OPC: oligodendrocyte progenitor cell; PDGF: Platelet-derived growth factor; TNF-α: Tumor necrosis factor-α.

All the animal disease models described here are artificially induced and therefore have limitations in reflecting the whole complexity of MS. EAE has the advantage to mimic the autoimmune aspect of MS, while the cuprizone model is useful to study the central effects such as remyelination and the behavior of CNS-resident cells in the absence of peripheral immune cells. The clinical efficacy of a drug has a higher chance of success if the drug demonstrated efficacy in multiple animal models confirming the postulated mechanism(s) of action. However, the only way to be completely certain that the selected compound is indeed efficacious in the selected indication, is to test the compound in clinical trials.

3 ACKR3 as a therapeutic target for neuro-inflammation and demyelinating diseases

3.1 The protein family of chemokines and chemokine receptors

Chemokines form a large family of structurally related, small, and secreted proteins that bind to and signal through seven-transmembrane receptors, mostly cell surface GPCRs. Chemokines selectively coordinate cell trafficking, regulating cellular processes such as leukocyte migration, adhesion, and growth, thereby playing important roles in development and homeostasis processes, in cellular compartmentalization, angiogenesis, and wound healing. However, they also support pathological immune responses observed in chronic inflammation, autoimmunity, and cancer [237]. Based on their expressions and functions, chemokines can be classified as homeostatic or inflammatory chemokines. Inflammatory chemokines are expressed only at low levels at steady-state and induced upon inflammation or injury to guide the leukocytes to sites of inflammation. They display a high degree of sequence diversity probably reflecting the changes in the pathogen environment that occurred along evolution of species.

In contrast, homeostatic chemokines are constitutively produced and are evolutionary highly conserved across species. Homeostatic chemokines are involved in the localization of cells, including immune cells, within tissues and organs under physiological conditions. Some chemokines have a dual function and can exhibit both homeostatic and inflammatory properties such as CXCL12.

Chemokines are split into four subfamilies based on the structural arrangement of the first two cysteine residues closest to the N terminus of the protein. C-X-C motif chemokines have only one amino acid, while C-X3-C motif chemokines have three amino acids between the two cysteines. C-C motif chemokines have adjacent cysteines and XC chemokines lack the first and the third cysteine residues of the motif [238].

Inflammatory chemokines typically bind to more than a single chemokine receptor, which are named according to the main type of chemokine they bind. In contrast, homeostatic chemokines are less promiscuous and typically bind to a single receptor. There are two families of seven transmembrane receptors that bind to chemokines: conventional chemokine receptors (CCKRs) and atypical chemokine receptors (ACKRs) [238]. Binding of ligands to CCKRs typically signals through G proteins and β-arrestin leading to chemotaxis, or other biological functions. In contrast, binding of chemokines to ACKRs, such as ACKR3, does not elicit G protein-dependent signaling but induces β-arrestin recruitment and further internalization of chemokine ligands [239]. Therefore, ACKRs regulate chemokines localization, abundance, and indirectly modulate interactions between chemokines and CCKRs.

During the past six years, I have focused my research on ACKR3 and its potential to be a therapeutic target in inflammatory demyelinating diseases such as MS.

3.2 ACKR3 and its chemokine ligands

ACKR3 was initially known as the orphan receptor named receptor dog cDNA1 (RDC1). In 2005, RDC1 was deorphanized and named chemokine receptor C-X-C chemokine receptor 7 (CXCR7) after the identification of its two chemokine ligands,

namely CXCL11 [240] and CXCL12 [241]. ACKR3 chemokine ligands, CXCL11 and CXCL12, also bind respectively to CXCR3 and CXCR4, but with lower affinity [Figure 18]. It has been postulated that the binding pocket required to activate ACKR3 may be different and less stringent than the one for CXCR3 and CXCR4 [242]. ACKR3 binds CXCL12 with 10- to 20-fold greater affinity than CXCL11 [240]. The mechanisms explaining the functional interaction between ACKR3 and its ligands are still unclear and debated. Binding of its ligands does not elicit G protein-mediated signaling and it is generally accepted that ACKR3 functions primarily as a scavenger receptor for its ligands [243-245]. Binding of either CXCL11 or CXCL12 to ACKR3, leads to the recruitment of β-arrestin, internalization of the ACKR3-ligand complex, and degradation of the ligands in lysosomes [243] [Figure 18]. Consequently, ACKR3 modulates CXCL11 and CXCL12 extracellular concentrations and indirectly impacts the CXCL12/CXCR4-mediated functions [244,246,247] and possibly the CXCL11/CXCR3-mediated functions [Figure 18]. ACKR3 may also have direct functions in response to CXCL11 and CXCL12, through the β-arrestin pathway, although this is still controversial and not yet demonstrated in *in vivo* settings [248-250] [Figure 18]. When co-expressed on the same cell, ACKR3 may heterodimerize with CXCR4 and therefore impact CXCL12-induced CXCR4-mediated signaling [251]. However, the existence of these structures and their functional role still need to be demonstrated and clarified on the native CXCR4 and ACKR3 receptors under *in vivo* settings.

To summarize, ACKR3 (i) tightly regulates its chemokine ligands concentration, (ii) modulates the CXCL12-induced CXCR4 mediated signaling and the CXCL11-induced CXCR3 mediated signaling, and (iii) possibly induces a direct effect through β-arrestin signaling [Figure 18].

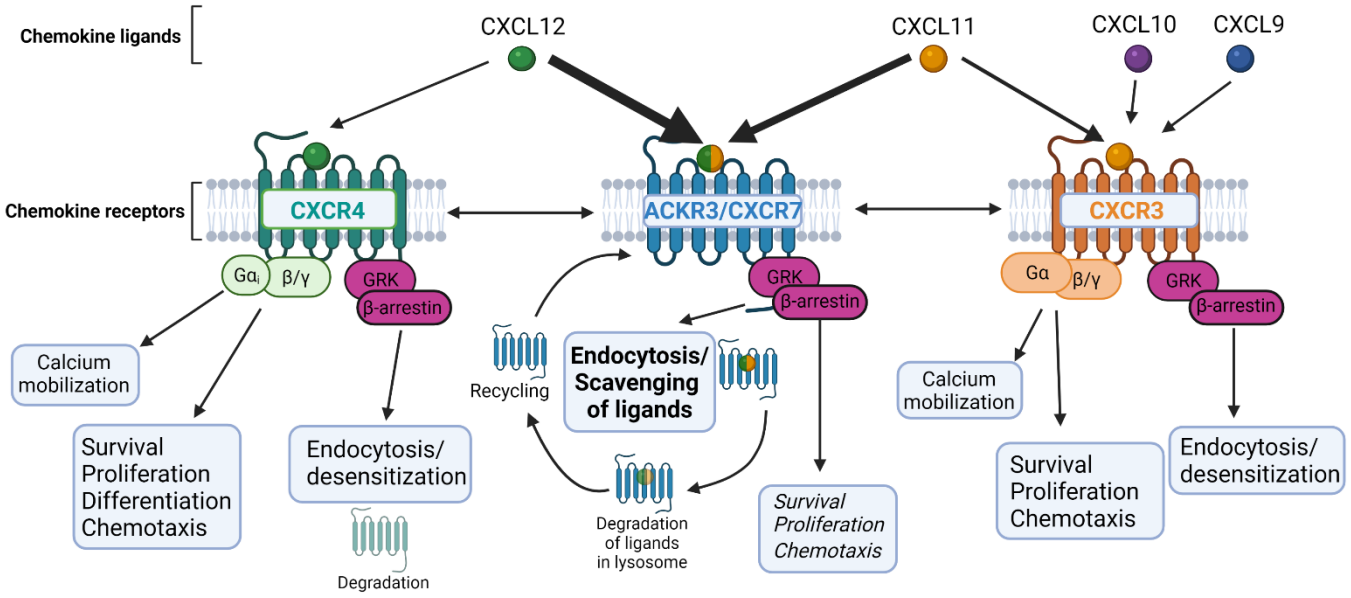

Figure 18: CXCR4, ACKR3 and CXCR3 interactions via their shared chemokine ligands. ACKR3, also named CXCR7, is an atypical chemokine receptor for CXCL11 and CXCL12. CXCL11 and CXCL12 also bind CXCR3 and CXCR4, respectively. Unlike CXCR4 and CXCR3, which signal trough G proteins and β-arrestin pathways, ACKR3/CXCR7 does not elicit G protein-dependent signaling but induces β-arrestin recruitment and functions as a scavenger receptor for its two chemokine ligands. ACKR3 binds CXCL11 and CXCL12 with higher affinity than CXCR3 binds CXCL11 and CXCR4 binds CXCL12 (bold arrows show higher affinity of ligands for the receptor). Therefore, ACKR3 tightly regulates the availability of CXCL11 and CXCL12 in the extracellular medium and indirectly impacts the functions of CXCR3 and CXCR4, respectively. Of note, while CXCR4 only binds CXCL12, CXCR3 has three known ligands, CXCL9, CXCL10, and CXCL11. Italic characters present the debated signaling functions of ACKR3 through β-arrestin pathway. Figure made with Biorender.com.
GRK: GPCR kinase

3.2.1 ACKR3 expression in rodent and human cells

The gene sequence of ACKR3 is highly conserved across species and encodes a protein sharing 95% similarity between human, mouse, and dog [252]. Even in the absence of ligands, ACKR3 is continuously recycling between the membrane and the endosomal compartment [243], which is a limitation for proper identification and validation of ACKR3 expression by antibodies and may explain some discrepancies in studies reporting ACKR3 protein expression [253]. Koenen et al, have recently reviewed the literature regarding ACKR3 expression at both the transcriptional and protein levels in rodent and human tissues [250]. To summarize, ACKR3 was mainly detected in mesenchymal stromal cells [254], in cells of the vascular system, including endothelial and smooth muscle cells [244,255], in brain-resident cells including glial cells, namely astrocytes [256], microglia [257], OPCs [88] and neuronal cells [245,258], and in some immune cell populations such as macrophages [259,260]. This summary of ACKR3 expression is in line with single-cell RNA sequencing data [261], publicly available on the Human Protein Atlas (www.proteinatlas.org), a platform that has the objective to map the expression of all human protein-coding genes across all major human cells and tissues [262]. However, expression of ACKR3 protein on human and mouse leukocytes is widely debated [253] and might depend on the microenvironment and the localization of ACKR3 within the cell, i.e., either at the cell surface or within the endosomal compartment.

3.2.2 ACKR3 endogenous chemokine ligands

3.2.2.1 CXCL12

ACKR3 binds CXCL12, also known as stromal cell-derived factor 1 (SDF-1), a highly evolutionary conserved chemokine, exhibiting both homeostatic and inflammatory properties. CXCL12 was first discovered as a pre-B cell growth stimulating factor and CXCR4 was described as its exclusive receptor. However, while CXCL12 is the only known chemokine ligand for CXCR4, it binds ACKR3 with a 10-fold higher affinity [241] [Figure 18]. CXCL12 is expressed in various organs under steady-state conditions including bone marrow, liver, thymus, lymph nodes, and brain [238,263]. CXCL12 is also induced upon pathological conditions such as inflammation,

hypoxia, tumor, and autoimmune diseases [263,264]. CXCL12, both at the genomic and protein level, shows more than 90% of homology between humans and mice. Mice lacking CXCL12, CXCR4, or ACKR3 demonstrated a lethal phenotype [252,265], stressing the importance of this chemokine axis in development and homeostasis.

CXCL12 displays six isoforms in humans (a, b, g, d, e, f) and only three in mice and rats (a, b, g) due to alternative splicing of a common mRNA precursor [266]. These isoforms are processed post-translationally in the microenvironment, such as by proteolysis in a splicing-variant dependent way, which results in different binding affinity and signaling properties on CXCR4 and ACKR3 [267]. In addition, the expression pattern of CXCL12 isoforms is different depending on cells, tissues, and organs. As an example, CXCL12a is the most studied and the most abundantly splice variant in organs and tissues, while CXCL12b is less abundant and is mainly present in endothelial cells. The distribution of CXCL12 isoforms can also be different between species. For example, the predominant isoform in the adult rat brain is CXCL12g, while it is mainly detected in the heart of humans and mice [266]. The functional role of each of these variants is not well understood, especially under *in vivo* settings where the interaction with glycosaminoglycans (GAGs) contributes to the formation of chemokine gradients [268] and protects CXCL12 from inactivation [269]. As an example, while CXCL12g is less potent than CXCL12a to induce chemotaxis *in vitro*, it is the most active isoform *in vivo* likely due to its high affinity for GAGs which confers protection from proteolysis [270]. Overall, binding of CXCL12 to CXCR4 leads to multiple downstream signaling events trough activation of G-proteins, leading to cell survival, proliferation, differentiation, and migration [Figure 18]. CXCR4 is expressed on multiple cell types, including immune cells such as lymphocytes, DCs, and macrophages, hematopoietic stem cells (HSCs), endothelial and epithelial cells, glial cells, and cancer cells. The CXCL12/CXCR4 axis is involved in diverse biological functions, such as organogenesis, angiogenesis, homing and regulation of HSCs, metastasis, and immune cell chemotaxis in various organs [264].

3.2.2.2 CXCL11

ACKR3 also binds CXCL11, also known as interferon-inducible T cell alpha chemoattractant (I-TAC), an inducible chemokine. CXCL11 is one of the three known inflammatory chemokine ligands for CXCR3, together with CXCL9 and CXCL10 [Figure 18]. The CXCR3 ligands share low sequence homology (around 40%) and exhibit unique temporal and spatial expression patterns, suggesting that they have non-redundant functions *in vivo* [271]. CXCL11 displays the highest affinity for CXCR3 in comparison to CXCL9 and CXCL10 and is also more potent in inducing chemotaxis, stimulating calcium flux, and inducing receptor desensitization [272]. Binding of CXCL11 to CXCR3 leads to downstream signaling leading to migration, differentiation, and activation of immune cells including T helper type 1 cells and macrophages [273] [274]. However, CXCL11 has been investigated to a lesser extent *in vivo* than CXCL9 and CXCL10. This chemokine is secreted at very low concentrations and one of the most used mouse strains for animal models, the C57BL/6 strain, does not express endogenous CXCL11 due to a codon stop in the gene [252]. CXCL11 is induced upon stimulation with IFN-γ in leukocytes, glial cells, fibroblasts, and endothelial cells [271,275]. Like for other chemokines, the CXCL11-directed CXCR3-expressing cell migration *in vivo* requires interaction of CXCL11 with GAGs [276]. In addition, GAGs protect human CXCL11 against proteolytic processing by CD26, which results in a truncated CXCL11 isoform with loss of chemotactic activity, and which may act as a CXCR3 antagonist [277]. In contrast to human CXCL11 that demonstrates a short half-life *in vitro* due to proteolysis and subsequent modification of its biological activity, murine CXCL11 may not be a substrate for CD26, which adds even more complexity to study the biological functions of the CXCL11/CXCR3 axis *in vivo* in animal models [277]. CXCR3 is predominantly expressed on immune cells from the lymphoid lineage, including T cells, plasmacytoid DCs, B cells, NK cells, and on non-immune cells such as endothelial cells [238,278]. In humans, CXCL11 binds three CXCR3 isoforms, resulting from alternative splicing of the Cxcr3 mRNA, namely CXCR3-A, CXCR3-B and CXCR3-alt [279,280]. These CXCR3 splice variants display a cell-dependent expression pattern and have different downstream signaling profiles in response to different

ligands, which may lead to different functions *in vivo* [281]. As an example, leukocytes predominantly express CXCR3-A, which mediates chemotaxis, proliferation, and calcium release, while endothelial cells express exclusively CXCR3-B, which demonstrates opposite effects [279]. However, the relevance of these CXCR3 variants in health and disease remains largely unknown, likely because they don't exist in mice and because variant-specific antibodies remain unavailable. Taken together, while CXCL11 might be one of the most relevant members of the CXCR3 ligands, the current available *in vivo* studies assessing the role of CXCL11/CXCR3 axis are limited.

Thus, with ACKR3 identified as a receptor for both CXCL12 and CXCL11, the roles of the CXCL12/CXCR4 and CXCL11/CXCR3 axis in regulating several biological processes are highly complex. Another level of complexity is added by the microenvironment having an impact on the biological functions exerted by all three chemokine receptors [Figure 19].

3.3 Physiological roles of ACKR3

Similarly to mice lacking CXCR4 or CXCL12, most of *Ackr3*$^{-/-}$ mice die in late development stages or just after birth due to cardiovascular complications, demonstrating an essential role of ACKR3 during development, especially in the cardiovascular system [252,265,282]. However, the lethal phenotype observed in C57BL/6 mice, which do not express endogenous CXCL11 [252], was less severe on a mixed genetic background, reaching a survival rate of 30% [282], suggesting that this could be linked to CXCL11-mediated functions. In addition, during brain development, constitutive and conditional loss of ACKR3 in neurons led to an abnormal distribution of interneurons in the cortex from rodents, suggesting a role for ACKR3 in neuronal migration [283] either via a direct modulation of β-arrestin-mediated downstream signaling of ACKR3 [284] or via an indirect effect through its scavenging activity. Indeed, it was shown that *Ackr3* deletion led to a severe decrease of CXCR4 protein in interneurons that was prevented by concomitant deletion of Cxcl12. This observation suggested that ACKR3, by sequestering CXCL12, prevented excessive CXCL12-mediated CXCR4 endocytosis and

subsequent desensitization in migrating cortical interneurons [285]. Interneuron layering defects were similar in *Cxcr4*$^{-/-}$, *Ackr3*$^{-/-}$ and *Cxcl12*$^{-/-}$ mice, suggesting the requirement of ACKR3 for CXCL12/CXCR4 signaling-dependent neuronal migration [285]. Taken together, these findings support that the most plausible biological function for ACKR3 in the brain is the regulation of chemokine gradients through scavenging activity [245]. ACKR3 controls the amount of ligand and therefore indirectly regulates the amount and the sensitivity of CCKRs made available for signaling at the cell surface. Of note, in contrast to mice deficient for *Cxcr4* or *Cxcl12*, no obvious defects in hematopoiesis were observed in *Ackr3*-deficient mice [252].

ACKR3 biological functions may depend on the microenvironment, including the presence or absence of cells secreting ACKR3 ligands, the chemokine ligand isoforms being secreted, the chemokine receptors expressed, the presence of enzymes processing the ligands, the presence of GAGs [250] [Figure 19]. This microenvironment changes during disease conditions; for example, while CXCL11 is hardly detectable in physiological conditions in the blood, it is induced upon inflammation. Therefore, ACKR3 functions may vary under physiological versus disease conditions, especially because expression of ACKR3 can be induced on different cell types during pathological processes, such as during hypoxia and inflammation. In addition, ACKR3-dependent functions likely depend on the presence of other non-chemokine ligands of ACKR3, including the opioid peptides [286], which add another layer of complexity to the whole CXCR3/CXCR4/ACKR3 axis.

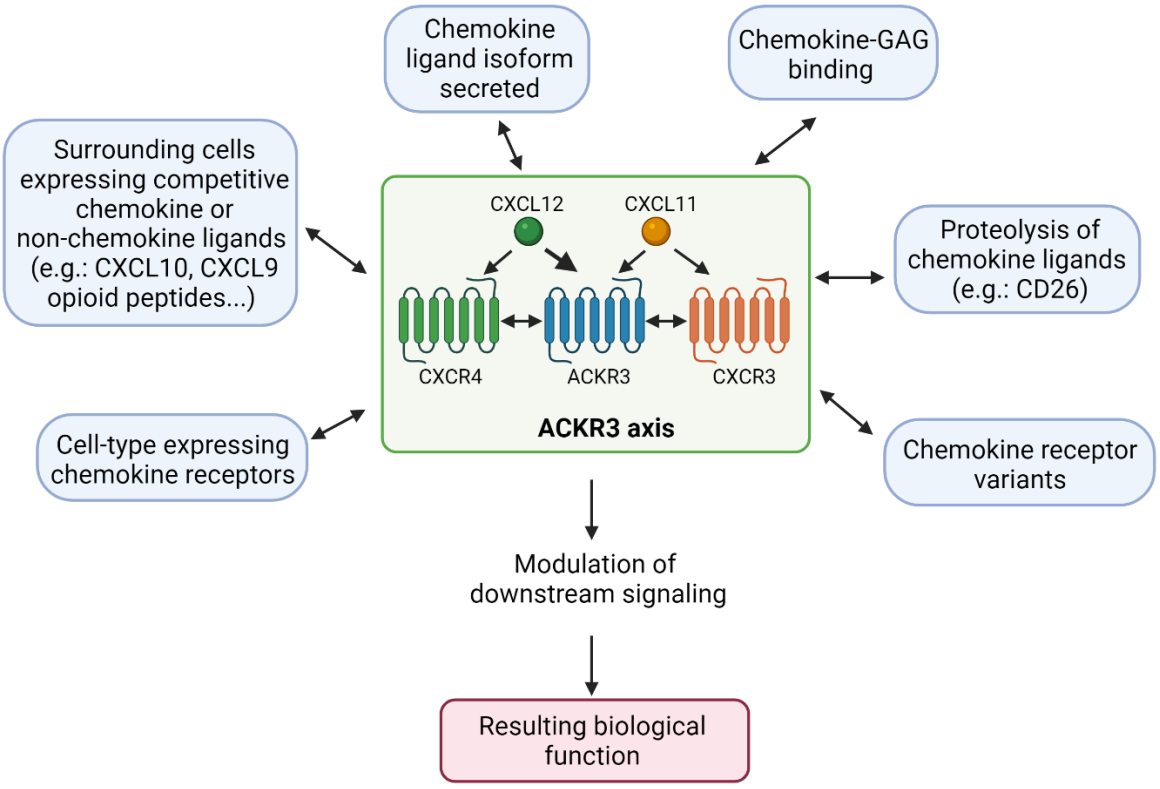

Figure 19: Overview of the mechanisms that may contribute to the microenvironment-dependent functions of ACKR3.
Figure made with Biorender.com.

Overall, controversial results regarding signaling or biological functions of ACKR3 found in the literature are likely due to the complexity of the whole system, underscoring the need to evaluate the relevance of targeting ACKR3 in an *in vivo* context.

3.4 The potential pathophysiological roles of ACKR3 in MS

ACKR3 has been implicated directly or indirectly via its scavenging activity as a functional mediator in MS/EAE pathogenesis, facilitating immune cells infiltration, chemotaxis, [287,288] and demyelination [289,290] in the CNS [Figure 20]. Therefore, ACKR3 has been postulated as a potential therapeutic target for the treatment of inflammatory demyelinating diseases such as MS [291,292].

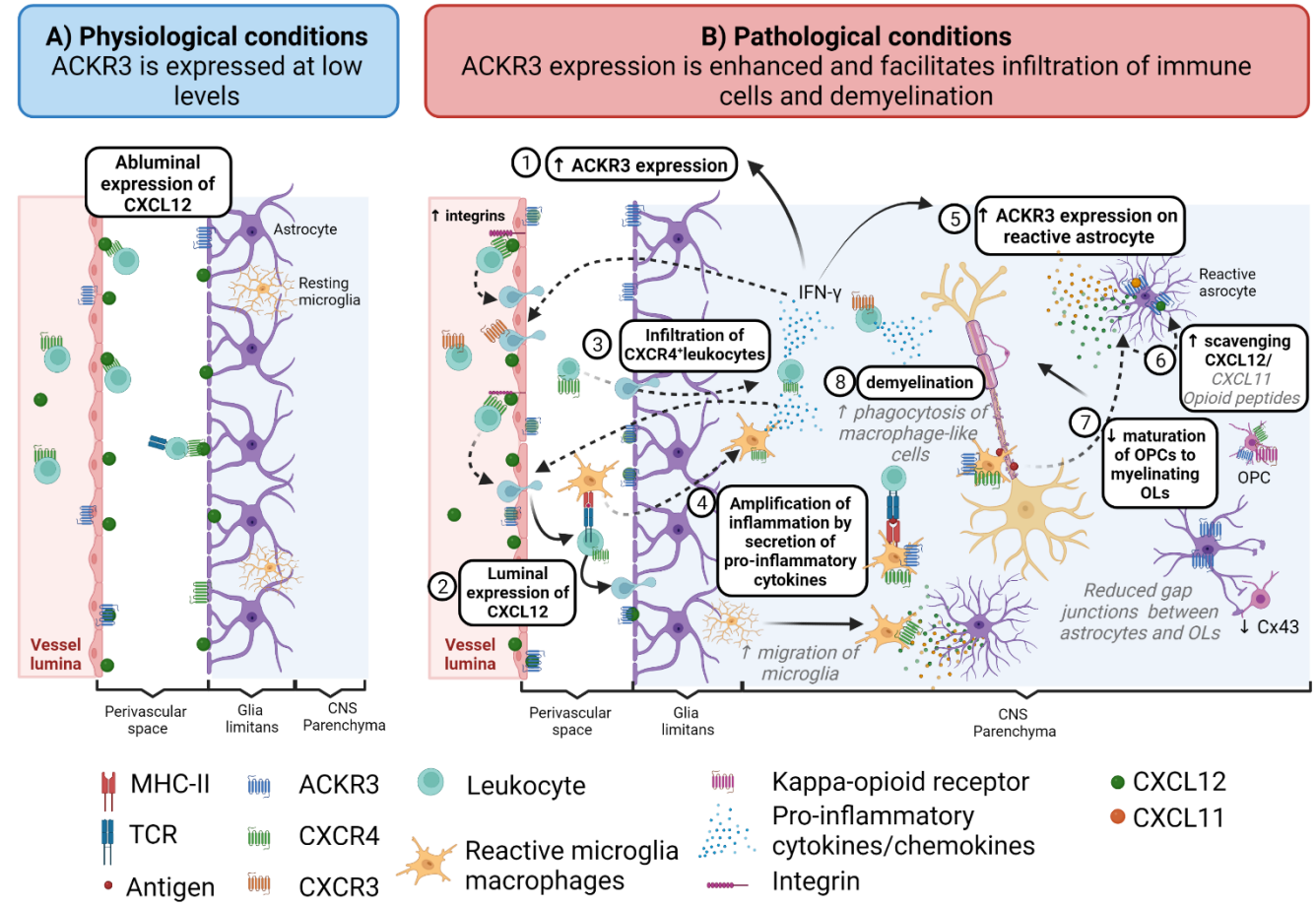

Figure 20: Potential pathophysiological roles of ACKR3 in MS.
Under physiological conditions (A), CXCL12 is expressed along the basolateral surface of the CNS endothelial cells and at the end feet of astrocytes forming the glia limitans. This pattern of CXCL12 expression localizes surveying CXCR4$^+$ leukocytes into the perivascular space, restraining their entry into the CNS parenchyma. Under pathological conditions such as MS/EAE (B), ACKR3 expression is increased on the endothelium (1), which is associated with a change of the spatial distribution of CXCL12 from abluminal to the luminal side of the CNS vessel (2), resulting in increased integrins expression, arrest, and infiltration of CXCR4$^+$ leukocytes. In the perivascular space, CXCR4$^+$ leukocytes get activated by antigen presenting cells such as reactive microglia expressing MHC class II. The loss of CXCL12 on the abluminal surface of the endothelium promotes infiltration of CXCR4$^+$ leukocytes from the perivascular niche to the CNS parenchyma (3). Activated

leukocytes in the parenchyma produce pro-inflammatory cytokines including IFN-γ, leading to an amplification of the neuroinflammation (4), and further increase in ACKR3 expression, especially on reactive astrocytes (5). The up-regulated ACKR3 and its scavenging activity (6), might limit the beneficial effects of CXCL12, secreted by reactive astrocytes, on OPCs maturation (7), exacerbating the differentiation arrest of OPCs within MS lesions and contributing to demyelination (8). In addition, ACKR3 might be directly involved in other pathological processes not confirmed *in vivo* yet (grey and italic characters), such as migration of microglia towards CXCL11 and CXCL12, increased phagocytosis, scavenging of opioid peptides, such as dynorphin, limiting its beneficial effect on OPCs maturation, and decreased Cx43 resulting in reduced gap junctions between astrocytes and OLs. Figure made with Biorender.com.
Cx43: Connexin 43; OLs: Oligodendrocytes; OPCs: oligodendrocyte progenitor cells

3.4.1 ACKR3 contributes to immune cells infiltration and polarization into the CNS

3.4.1.1 Increase in BBB permeability

CXCL12 and its receptors, CXCR4 and ACKR3, are constitutively expressed at low levels in the adult CNS and are upregulated under neuroinflammation [250,292-295] [Figure 20]. Under physiological conditions, CXCL12 protein was detected at the basolateral surface of endothelial cells and this distribution pattern was proposed to participate in the homing of $CXCR4^+$ leukocytes into perivascular spaces, avoiding parenchymal infiltration [293,296,297] [Figure 20A]. In patients with MS, CXCL12 levels were increased in the CSF, and CXCL12 was expressed and significantly increased within reactive astrocytes and endothelial cells in active but also in chronic lesions, suggesting its contribution to leukocytes recruitment to the CNS [293,298-300]. In addition, within active MS lesions, the basolateral expression of CXCL12 was lost and instead, CXCL12 was expressed at the luminal side of brain vessels at the BBB. This abnormal distribution pattern of CXCL12 was associated with an entry of $CXCR4^+$ leukocytes into the brain parenchyma and correlated positively with severity of histological disease in patients with MS [297] [Figure 20B]. CXCR4 expression was detected in most of the cells within perivascular infiltrates of active MS lesions and in some cells within the parenchyma [297], including activated microglia and macrophages expressing MHC-class II [300] and $CD4^+$ T cells producing inflammatory cytokines [45] [Figure 20B]. These pathological changes of

the CXCL12/CXCR4 axis were also confirmed in EAE models, suggesting that the pathological function of this chemokine axis and potential interventional approaches can be studied in these mouse models [288,296]. The mechanism responsible for this altered CXCL12 expression at the BBB observed both in mouse EAE models and in patients with MS, has been proposed to be linked to the scavenging activity of ACKR3, which is also expressed on blood vessels throughout the adult mouse and human brains [288]. Indeed, enhanced expression of ACKR3 on endothelial barriers within the CNS was observed in various EAE models leading to CXCL12 internalization and change in the spatial distribution of CXCL12 at the BBB [288,295] [Figure 20B]. CXCL12 was described to trigger the activation of integrins, inducing the arrest of $CXCR4^+$ leukocytes on endothelial surfaces [301,302]. Interestingly, while antagonizing CXCR4 blocked CXCL12-induced chemotaxis of leukocytes such as T cells and monocytes across *in vitro* BBB model [287], antagonizing CXCR4 or neutralizing CXCL12 *in vivo* worsened CNS cell infiltration and increased EAE severity, suggesting that this chemokine axis is needed for restricting the access of immune cells from the perivascular cuff into the brain parenchyma [54,296] [Figure 20B]. In contrast, maintaining the basolateral expression of CXCL12 at the BBB by treatment with an ACKR3 functional antagonist dose-dependently reduced leukocyte infiltration into the CNS parenchyma, reduced parenchymal adhesion molecule VCAM-1, reduced clinical severity of EAE disease, and axonal injury [288,303]. In addition, blocking ACKR3 with an antibody, attenuated the CXCL12-induced CXCR4-mediated stimulation of integrins, especially the activation of lymphocyte function-associated antigen 1 (LFA-1) and VLA-4 on human T cells [302].

Taken together, these data suggest that ACKR3 might represent a therapeutic target to correct the CXCL12-induced increase of BBB permeability and subsequent $CXCR4^+$ infiltration of immune cells into the CNS parenchyma in patients with MS [Figure 21].

3.4.1.2 Chemotaxis of macrophage-like cells

Macrophage-like cells, including human inflammatory monocytes, inflammatory macrophages and microglia express both ACKR3 and CXCR4 [259,287,304]. CXCR4 levels on the cell surface were inversely correlated with those of ACKR3, suggesting that they may have complementary or opposite functions [259]. The CXCL12/CXCR4/ACKR3 axis has been involved in the transmigration of monocytes across the BBB, inducing monocyte-endothelial cell interactions and facilitating lymphocytes infiltration [287,305]. Some studies suggest that binding of CXCL11 and CXCL12 to ACKR3 led to a direct downstream signaling, independent of CXCR3 and CXCR4, resulting in increased human macrophage chemotaxis and increased phagocytosis [259,306,307] [Figure 20B]. In addition, neutralizing ACKR3 with an antibody, reduced CXCL11- or CXCL12-induced chemotaxis of activated microglia *in vitro,* in contrast to pharmacological CXCR3 and CXCR4 antagonism. Further, anti-ACKR3 treatment dose-dependently reduced clinical scores in a mouse EAE model, and expression of ACKR3 at mRNA level on microglia positively correlated with clinical disease severity of EAE, suggesting its detrimental role in microglia function during neuroinflammation [304] [Figure 21].

3.4.1.3 Polarization of the immune response within the CNS

In vivo administration of ACKR3 ligands, namely CXCL11 and CXCL12 in murine EAE models have both demonstrated efficacy on clinical disease severity. While neutralization of CXCL12 with an antibody started at onset of the disease worsened the clinical course of EAE disease, a chimeric protein of CXCL12 fused to IgG1, which displayed the biological functions of native CXCL12, injected intravenously, reduced ongoing murine EAE disease. CXCL12 treatment was shown to polarize antigen-specific $CD4^+$ T cells into IL-10-secreting T cells. These cells reduced the proliferative response of antigen-specific effector T cells from EAE mice *in vitro* and suppressed EAE clinical scores when transferred in adoptive transfer experiments [54].

In addition, *in vitro*, CXCL11, the second ligand of ACKR3, polarized murine naïve T cells into T cells secreting IL-10 and reduced polarization of Th1 and Th17 $CD4^+$ T

cells, in a CXCR3 dependent manner. *In vivo* administration of a recombinant fusion protein of CXCL11 linked to IgG1 suppressed ongoing EAE clinical disease both in SJL/J and in C57BL/6 mice [273].

Taken together, these data suggest that increasing systemic CXCL12 concentration and possibly CXCL11 concentration by blocking the scavenging activity of ACKR3 on endothelial cells [244], might shift the polarization of T cells towards a regulatory phenotype [Figure 21].

3.4.2 ACKR3 contributes to astrocyte functions

Under physiological conditions, in the postnatal and adult rat brain, ACKR3 and CXCR4 expression are observed on astrocytes forming the glia limitans. However, astrocytic ACKR3 but not CXCR4 expression was increased during neuroinflammation both in rats and human brains, suggesting a crucial role of ACKR3 on reactive astrocytes in various CNS pathologies such as MS [256]. *In vitro*, rodent astrocytic ACKR3 expression was increased by pro-inflammatory conditions, such as IFN-γ and hypoxia, which contributed to leukocyte entry through the BBB [256,308]. In contrast, IFN-b, which is used as a DMT in patient with MS, reduced ACKR3 expression on astrocytes. In line with these data, a recent study reported that ACKR3 mRNA and protein levels were induced by IFN-γ, specifically in primary adult human astrocytes derived from the spinal cord and not the ones derived from the brain stem [309]. These findings were also confirmed in murine astrocytes *in vivo,* by stereotactic injection of the pro-inflammatory cytokine into the brain stem or spinal cord of mice. IFN-γ-induced ACKR3 expression on astrocytes in the spinal cord was associated with a decrease of CXCL12 levels, consistent with the scavenging activity of ACKR3 and its regulation of extracellular levels of CXCL12 [Figure 20B]. These findings were further confirmed in a murine EAE model induced by adoptive transfer of myelin-autoreactive T cells where it was demonstrated that efficacy of treatment with a functional antagonist of ACKR3 on clinical scores was dependent on IFN-γ signaling. Taken together, it suggests that IFN-γ-induced ACKR3 expression on astrocytes is critical for spinal cord inflammation during EAE, promoting entry of T cells into the CNS [309] [Figure 20B].

In addition, ACKR3 was found to interact with the gap junction protein connexin 43 (Cx43), which is mainly expressed in astrocytes [310]. Binding of CXCL11 and CXCL12 to ACKR3 inhibited Cx43-mediated gap junctional intercellular communication in astrocytes trough Cx43 internalization [310]. These gap junctional intercellular communication between astrocytes and for example OLs are crucial as they maintain several physiological processes including glucose diffusion. While astrocytic ACKR3 is upregulated during neuroinflammation, astrocytic Cx43 expression is decreased in MS, especially in active and chronic active lesions and is associated with disease progression and distal oligodendrogliopathy [71]. Taken together, the functional interaction between ACKR3 and Cx43 on astrocytes and its consequences on the gap junction-mediated communication between astrocytes and OLs, might contribute to the pathological role of ACKR3 in MS [Figure 20B].

3.4.3 ACKR3 axis contributes to demyelination/remyelination processes

There are multiple lines of evidence pointing towards a protective function of CXCL12 in CNS pathology [294,311]. Both *in vitro* and *in vivo* studies have demonstrated that activation of CXCL12/CXCR4 signaling promotes neural stem cells (NSCs) and OPCs migration, proliferation, and differentiation, suggesting that CXCL12/CXCR4 axis is involved in neuro/oligodendrogenesis following CNS damage [75,87,289,312-314]. In line with findings in MS lesions showing that CXCL12 is expressed and significantly increased within reactive astrocytes at the lesion edge [293], studies conducted in the mouse cuprizone-induced demyelination model showed that CXCL12 expression was increased by activated astrocytes and microglia within the demyelinating CC [313]. This increase was associated with an increase in the number of OPCs expressing CXCR4. In addition, the number of $CXCR4^{+}/CXCL12^{+}$ OPCs were also increased in the CC in a murine EAE model and was associated with spontaneous recovery [294][Figure 20B]. Pharmacological inhibition of CXCR4 or *in vivo* CXCR4 RNA silencing resulted in detrimental effects on OPC differentiation and prevented remyelination in the murine cuprizone model and in a viral-induced demyelination model [87,290,313], indicating that

activation of CXCL12/CXCR4 signaling may improve remyelination trough enhanced OPCs differentiation into mature OLs.

Interestingly, the expression of ACKR3 was enhanced during demyelination, especially at the peak of the disease in various cells, including astrocytes and OPCs in different murine demyelination models [290,295]. In contrast to CXCL12 and CXCR4, ACKR3 returned to baseline during the remyelination phase following cuprizone-induced demyelination, suggesting its pathological role in demyelination [290]. The co-expression of ACKR3 with CXCR4 in the same cell, such as OPCs, may result in the sequestration of CXCL12 from the microenvironment rather than its binding to CXCR4, thus altering the overall availability of CXCL12 in the OPC's microenvironment. Therefore, ACKR3 may regulate the CXCL12-induced CXCR4 signaling functions in OPCs, namely migration, maturation and thus myelination. In the cuprizone-induced demyelination model, treatment with a functional ACKR3 antagonist resulted in increased OPC proliferation and differentiation leading to an increased number of mature OLs within demyelinated area and increased myelination. The ACKR3 antagonism-mediated increase in myelination was associated with an increase in CXCL12 protein within the demyelinated area and was abrogated by treatment with a CXCR4 antagonist, suggesting that ACKR3 regulates CXCL12/CXCR4-mediated repair effect in the demyelinated adult CNS [290] [Figure 21].

In addition, *in vitro,* ACKR3 was suggested as a scavenger receptor for opioid peptides, including the subfamily of dynorphins which bind preferentially the kappa-opioid receptor (KOR) [286] [Figure 20B]. Interestingly, KOR was found to be expressed on OPCs and KOR agonism has been proposed as a strategy to enhance OPC proliferation, differentiation, and subsequent remyelination *in vivo* [315]. In line with these results, stress-induced dynorphin release has been demonstrated to induce OPC differentiation trough KOR activation [316]. Although it is difficult to judge on the functional relevance of the effects mediated by ACKR3 scavenging activity *in vivo*, the identification of ACKR3 as a negative regulator of opioid peptides availability, including dynorphin, might contribute to the ACKR3

pathological role in limiting remyelination in demyelinating diseases, such as MS [Figure 20B].

In conclusion, inhibiting ACKR3, thus blocking its scavenging activity and potentially also its direct signaling functions, may be beneficial for the treatment of MS [Figure 21].

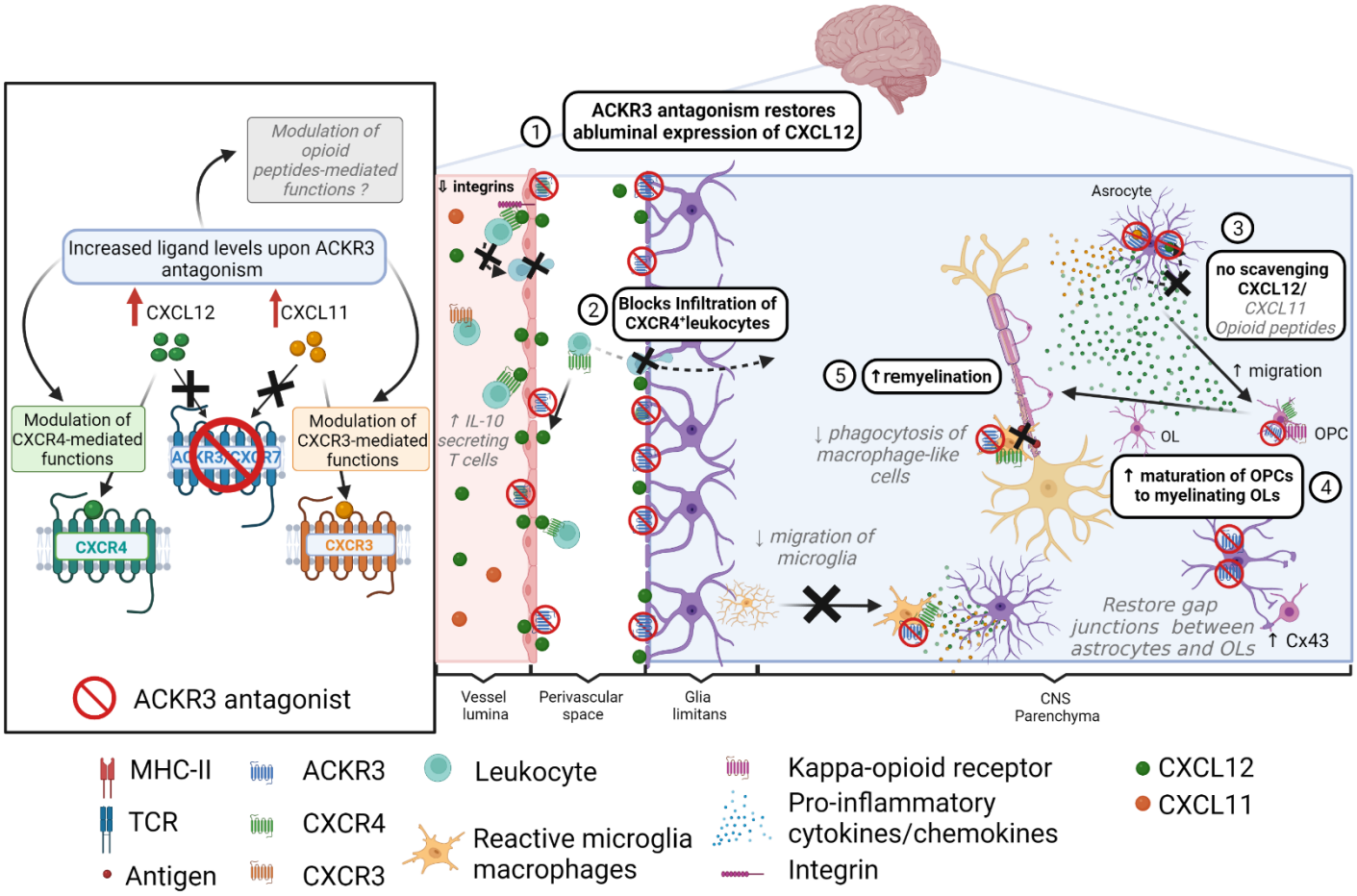

Figure 21: Summary of the potential effects of ACKR3 antagonism in MS.
Blocking ACKR3, thus inhibiting its scavenging activity, will lead to an increase of its ligands' extracellular levels, namely CXCL12 and CXCL11 (left side of the figure). Consequently, depending on the concentration of ligands reached, and the microenvironment, all CXCL12/CXCR4- and CXCL11/CXCR3-mediated functions involved in the pathology of MS might be modulated. In addition, an ACKR3 antagonist should

block the potential direct signaling activites of ACKR3, which are still debated. Recently, ACKR3 has been described as a scavenger receptor for opioid peptides, which needs further confirmation in in vivo settings. ACKR3 antagonism would restore the abluminal distribution of CXCL12 (1), thus preventing infiltration of $CXCR4^+$ leukocytes into the CNS parenchyma (2). Blocking of the scavenging activity of ACKR3 on astrocytes (3) and OPCs would increase the availability of CXCL12 to increase migration and differentiation of OPCs into myelinating OLs, (4), thus enhancing the remyelination process (5). In addition, ACKR3 antagonism might block other pathological processes not confirmed *in vivo* yet (grey and italic characters), such as migration of microglia towards CXCL11 and CXCL12, increased phagocytosis of macrophages-like cells, scavenging of CXCL11 and opioid peptides thus increasing their availability, and decrease in Cx43, thus restoring gap junctions between astrocytes and OLs. Lastly, increasing CXCL11 and CXCL12 levels by blocking ACKR3 might shift the polarization of T cells towards a regulatory phenotype, secreting IL-10 and thus, dampening overall inflammation. Figure made with Biorender.com. Cx43: Connexin 43; OLs: Oligodendrocytes; OPCs: oligodendrocyte progenitor cells

3.5 Existing ACKR3 modulators

Antibodies and/or small interfering RNA (siRNA) have validated the utility of ACKR3 antagonism to treat various disease states such as inflammatory and demyelinating/neurodegenerative conditions [304,317-319]. Several modulators of ACKR3 have been discovered including small molecules and peptide-based modulators and were recently reviewed by Lounsbury *et al* [320]. Although most of them have no reported pharmacological effects in the literature, small molecule compounds discovered by ChemoCentryx, a biopharmaceutical company specialized in the chemokine field, were used in various *in vitro* and animal disease models, including MS models [288,290,303]. These compounds, including CCX771, CCX754, CCX733, were initially reported as ACKR3 antagonists as they displaced CXCL12 from binding to ACKR3 and since they demonstrated the physiological effects observed with anti-ACKR3 antibodies and siRNA [288,304]. However, they have since been described as agonists, recruiting β-arrestin to ACKR3 upon binding to the receptor [320-322]. This contradiction might be linked to the scavenging activity of ACKR3. Indeed, binding of ACKR3 agonists to ACKR3 leads to internalization of the receptor, thus blocking it from binding to its endogenous ligands such as CXCL11 and CXCL12, resulting in functional antagonism and therefore leading to an increase in the extracellular concentration of its ligands [Figure 21]. In line with this

assumption, CCX771 treatment was shown to increase systemic CXCL12 levels in mice [244]. Therefore, functions of ACKR3 might be more related to its ligands-mediated effects rather than its direct effect(s) through β-arrestin signaling. In addition, prolonged CXCL12 stimulation leads to internalization and degradation of CXCR4, which indicates that cells expressing CXCR4 become insensitive to CXCL12 in a very short time [323], which could also explain the results observed with ACKR3 agonists. So far, only one moderately potent ACKR3 antagonist, inhibiting β-arrestin signaling upon CXCL12 stimulation and not orally available, has been reported by the pharmaceutical company Pfizer [324]. So far, no *in vitro* or *in vivo* results have been reported with this compound. Further research is needed to decipher whether disease-ameliorating effects observed with ACKR3 agonists is due to their agonistic activity or their functional antagonism induced by receptor desensitization.

In conclusion, ACKR3 appears as a valuable therapeutic target for the treatment of neuroinflammatory and demyelinating diseases, such as MS. Blocking ACKR3 and thus blocking its scavenging activity and potentially also any direct effector functions, is expected to have a beneficial role through a dual mode of action, immunomodulation and remyelination [Figure 21].

THESIS OBJECTIVES

This doctoral thesis is carried out in the context of a validation of the experience based on my daily work within the company Idorsia Pharmaceuticals Ltd. The general aim of Idorsia pharmaceuticals is to discover, develop, and commercialize innovative small molecules to treat diseases, such as autoimmune diseases. I have joined the company, previously named Actelion, in 2009, in the immunology and pharmacology department and I have started to work on the ACKR3/CXCR7 research project in 2015 (see folder "expérience professionnelle de recherche"). At that time, the project was still in the drug discovery phase [Figure 22]. Large libraries of chemical compounds, composed of more than 300 000 compounds, had already been tested for their ability to antagonize ACKR3, using β-arrestin recruitment as primary screening assays (see Introduction, section 2.1.3). This HTS of the compound collection had led to the identification of a small cluster of antagonists, which were further optimized to increase their potency, their selectivity, their metabolic stability, and their oral bioavailability until the identification of lead compounds (hit to lead phase) [Figure 22].

I joined the project core team, which included a project leader in chemistry, in biology, and in drug metabolism and pharmacokinetics (DMPK) during the lead optimization phase, as the "preclinical pharmacologist project leader" [Figure 22]. My goals were to select and establish *in vivo* assays to evaluate the pharmacological activity of the potential drug candidates and to decipher their mechanisms of action. The compounds that displayed favorable properties *in vitro* and an acceptable *in vivo* PK were further investigated in my laboratory, in tolerability studies and target engagement assays, in which dose-response studies were performed to characterize the PK/ pharmacodynamics (PD) relationship of the compounds [Figure 22]. I was responsible for the conception, design, and execution of these PK/PD animal studies, for the data interpretation, and

presentation to the team project. The compounds demonstrating a favorable PK/PD profile were further tested in target-relevant proof-of-mechanism (POM)/proof-of-efficacy (POE) disease models to estimate the compound efficacious concentration and to help identifying the best drug candidates. I was responsible for proposing, establishing, and validating valuable POM/POE disease models to test ACKR3 antagonists and to propose an indication based on the mechanism of action. Then, I was responsible for the conception, design, and execution of efficacy studies in these models, for data interpretation, and presentation to the team project and high management of Idorsia Pharmaceuticals Ltd. At the end of 2016, the multidisciplinary efforts and the cooperation between all the team members, culminated in the discovery and selection of ACT-1004-1239, a potent, selective, and orally available small molecule ACKR3 antagonist that was disclosed in a patent application, where I am co-inventor [325] [Figure 22]. ACT-1004-1239 insurmountably antagonizes CXCL11- and CXCL12-mediated β-arrestin recruitment to ACKR3 *in vitro,* with a concentration that inhibits the maximal response to these agonists by 50% (IC_{50}) of approximately 1 to 3nM in all species investigated including mouse and human [202].

In this PhD thesis, I will focus on the PCC compound, ACT-1004-1239, and present some of the data, I generated in my laboratory during the preclinical drug development of this first-in-class ACKR3 antagonist, which started with the discovery of this compound up to the FIH study and continues with the preclinical support for the phase 2 study preparations in patients with MS [Figure 22]. My main goal was to support, on the pharmacology side, the generation of a solid preclinical package to allow the submission of regulatory documents to start human trials with ACT-1004-1239 and to support the clinical team with the phase 2 study preparations and indication finding.

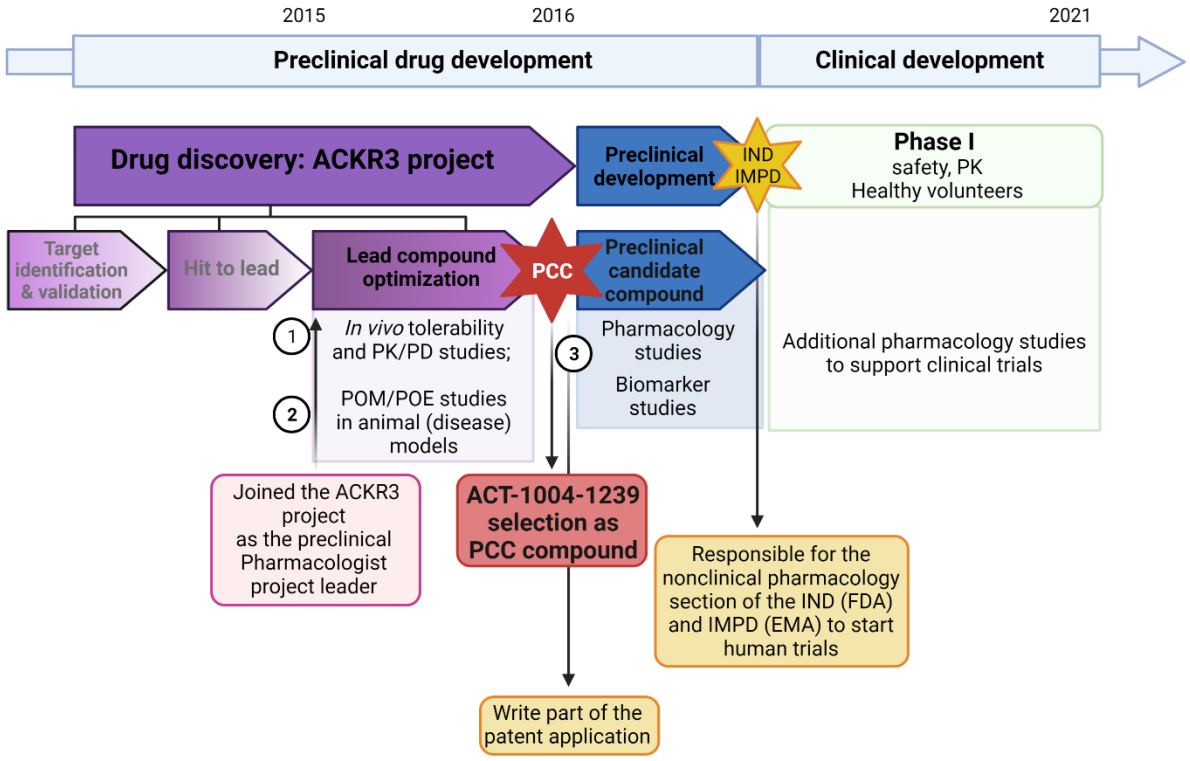

Figure 22: My main goals during the preclinical development of the ACKR3 antagonist ACT-1004-1239.
IMPD: Investigational medicinal product dossier; IND: Investigational new drug; PD: Pharmacodynamics; PK: Pharmacokinetics; PCC: Preclinical candidate; POE: Proof-of-efficacy; POM: Proof-of-mechanism. Figure made with Biorender.com.

In this context I had three main objectives:

1) **To investigate the potential of ACT-1004-1239 to antagonize ACKR3 scavenging activity *in vivo* and evaluate whether CXCL11 and/or CXCL12 plasma levels can be used as biomarkers of target engagement of ACKR3 antagonism [Figure 22; (1)].**

To fulfill this first objective, my laboratory established and validated a target engagement assay to evaluate the PD effect of the ACKR3 antagonist lead compounds, including ACT-1004-1239. We used plasma CXCL12 concentrations as PD biomarker in healthy mice. The PK/PD relationship of the compounds helped

us in defining the dose, route of administration, and treatment regimen (e.g.: once or twice daily administration) to be used in murine disease animal models. These experiments were performed in 2015-2016 with the help of one research associate. I was responsible for the conception, design and execution of the animal studies, data interpretation, and presentation.

My contribution with this target engagement assay was included in two broader articles:

- The first article was co-written with the chemists and core team members and summarizes the hit to lead and lead compound optimization phases, leading to the discovery and the selection of ACT-1004-1239 for further preclinical development [202]. This first article, published in the *Journal of Medicinal Chemistry* in 2020, is attached in Annex 1.
- The second article was co-written with the clinical pharmacologists and summarizes the comparison of PK/PD data obtained in healthy mice following repeated administration of ACT-1004-1239 with PK/PD data from healthy volunteers in the Phase I multiple ascending dose (MAD) phase. This article, published in 2021, in *Biomedicine & Pharmacotherapy* [326], is attached in Annex 2.

2) To select and develop a valuable proof-of-mechanism/proof-of-efficacy disease model to evaluate the potential mechanism(s) of action of ACT-1004-1239, especially its immunomodulatory effects [Figure 22; (2)].

To fulfill this second objective, I proposed to establish, characterize, and validate a suitable model of acute lung injury (ALI) to investigate the effects of ACKR3 antagonists, including ACT-1004-1239, on cell migration towards an inflammation site.

The article describing the specific disease model and the effects of ACT-1004-1239 was published in Frontiers in Pharmacology [327] and will be further presented in the results section (see Article I). I was responsible for the conception, design and execution of the studies, data interpretation, and manuscript drafting.

3) **To assess and confirm whether targeting ACKR3 with ACT-1004-1239 would be beneficial for the treatment of MS using *in vitro* and *in vivo* rodent models [Figure 22; (3)].**

To fulfill this third objective, my laboratory established, characterized, and validated several preclinical MS models which were used to assess the efficacy of ACT-1004-1239. This work was published in the *FASEB journal* [328] and will be further presented in the results section (see Article II). Complementary experimental work performed in my laboratory and further strengthening the rationale to test ACT-1004-1239 in MS was presented as a poster in two different international congresses: ACTRIMS 2021 and AAN 2021. This poster is attached in Annex 3. In addition, my experimental work investigating the potential of combining drugs with different mechanisms of action to improve efficacy in animal models of MS, further allowed to file a patent application on the combination of an ACKR3 antagonist with an $S1P_1$ receptor modulator [329]. For this last goal, I was responsible for the writing of the animal license authorization, the conception, the design and execution of the animal studies, data interpretation, and manuscript drafting.

RESULTS

This section is organized in three parts corresponding to my three main objectives during the preclinical development of ACT-1004-1239:

- To investigate the potential of ACT-1004-1239 to antagonize ACKR3 scavenging activity *in vivo* and evaluate whether CXCL11 and/or CXCL12 plasma levels can be used as biomarkers of target engagement of ACKR3 antagonism. These results are included in two broader articles attached in Annex 1 and Annex 2.
- To select and develop a valuable proof-of-mechanism/proof-of-efficacy disease model to evaluate the potential mechanism(s) of action of ACT-1004-1239, especially its immunomodulatory effects (see Article I).
- To assess and confirm whether targeting ACKR3 with ACT-1004-1239 would be beneficial for the treatment of MS using *in vitro* and *in vivo* rodent models (see Article II).

1 PK/PD properties of ACT-1004-1239

1.1 Preamble

During the lead optimization phase, the ACKR3 antagonists displaying favorable *in vitro* and PK properties (see Introduction, section 2.1.4), were further investigated in a target engagement assay using plasma CXCL12 concentrations as PD biomarker *in vivo*. PK/PD analysis relates drug biological activity to a measure of drug concentration in a given body compartment, such as plasma, rather than to a drug dose.

Based on the competitive binding of the ACKR3 antagonist to ACKR3 vs CXCL11/CXCL12, the concentration of unbound ligand was expected to increase in the presence of ACKR3 antagonists. When I joined the project, the biologic leader

of the project, François Lehembre, had already established an *in vitro* assay with a cell line secreting CXCL12 and endogenously expressing ACKR3 (RXF-393 cells), where he could demonstrate elevation of CXCL12 concentration in the culture supernatants upon ACKR3 antagonist treatment (data not shown). In addition, previous reported findings demonstrated that ACKR3 was highly expressed in vasculature and was suggested to regulate plasma CXCL12 concentrations through its scavenging activity [244]. First, I proposed to measure elevation of CXCL12 as a PD biomarker of ACKR3 antagonism *in vivo* and to investigate the possible elevation of CXCL11 plasma levels in healthy mice. Dose-response studies were performed to characterize the PK/PD relationship of the lead ACKR3 antagonists. We first measured CXCL11 and CXCL12 plasma concentrations over time after a single oral administration of ACKR3 antagonist in healthy mice and linked it with drug exposure. We rapidly noticed that CXCL11 elevation in heathy mice was less robust than that of CXCL12. These initial PK/PD studies provided insight into drug tolerability and dose selection. Antagonists which were well tolerated, and which demonstrated a significant and dose-dependent rise in CXCL12 plasma levels after a single administration were further characterized for PK/PD over time at steady state, after repeated compound administrations.

This target engagement assay guided us to select the best lead compounds, including ACT-1004-1239, to be further investigated in the proof-of-mechanism model described in the following results section. In addition, understanding the PK/PD biomarker profile of ACT-1004-1239 helped us in designing further experiments in diseased mice, to select the dose, the treatment regimen, and the timing of administration depending on the questions to be addressed. In addition, using this assay, the PK/PD data generated with ACT-1004-1239 helped the DMPK department to predict the human PK. Taken together, all this work supported the clinical pharmacologists to select the appropriate human doses and target engagement biomarkers to be investigated in Phase I clinical trials.

1.2 Results

The PK/PD data generated with ACT-1004-1239 in this target engagement assay are reported in two articles attached in Annex 1 and 2:

- Annex 1, Figure 5: Effect of a single oral administration of ascending doses of ACT-1004-1239 on CXCL12 plasma concentration and compound plasma concentration in naïve male DBA/1 mice.
- Annex 2, Figure 1: ACT-1004-1239 and CXCL12 plasma concentration-time profiles and dose-response relationship in mice and Figure 2: PK/PD modeling and simulation results in mice and humans.

1.3 Conclusion

Single and multiple doses of ACT-1004-1239 dose- and time-dependently increased the CXCL12 plasma concentration across the investigated dose range (1-100 mg/kg) in healthy DBA/1 mice, demonstrating target engagement. In contrast, only the highest dose tested (100 mg/kg, twice daily) increased the CXCL11 plasma concentration in healthy mice, albeit with higher variability.

In line with *in vitro* PK data [202], ACT-1004-1239 is a high-clearance drug in mice and only the 100 mg/kg, twice daily oral dosing regimen provided sufficient ACT-1004-1239 plasma exposure to maintain a CXCL12 elevation close to the maximal effect (E_{max}) over 24h. PK/PD modeling of the mouse data indicated that the CXCL12 elevation approached a plateau at doses ≥ 100 mg/kg, twice daily (Annex II, Figure 2). The IC_{50} of ACT-1004-1239, defining the plasma concentration of ACT-1004-1239 leading to a half maximal effect on the CXCL12 increase was estimated at 11.2 ng/mL, representing 21 nM. The obtained results suggested that CXCL12 plasma levels could be used as a PD biomarker of target engagement in healthy volunteers and that CXCL11 needed to be evaluated further under inflammatory conditions.

2 Article I: Effect of ACT-1004-1239 in a POM model

2.1 Preamble

During the lead optimization phase, ACKR3 antagonists that demonstrated valuable PK/PD properties in the target engagement assay described above, were further evaluated in a proof-of-mechanism mouse model that I developed based on the supposed mechanism of action of ACKR3 antagonists. Indeed, the selection of valuable animal models for "screening" the lead compounds during the drug discovery phase, needs to take into consideration the supposed mechanism of action of the drug and the relevance to the human disease but also the practicality of their use, including the length of time for drug testing in the model, the cost, the specie of animal chosen, the technical aspects of generating the data, the animal welfare… In addition, only small amounts of drug are available at this stage of drug discovery, therefore, POM models should ideally be short, robust, and reproducible to be able to assess several compounds in a short period of time, which is not the case of available demyelinating models which are often long and severe for the animals, such as EAE models.

Previous findings with the ACKR3 agonist, CCX771, had demonstrated that endothelial expression of ACKR3 regulated the systemic CXCL12 concentration and thus contributed to the establishment of CXCL12 concentration gradients along which leukocytes could migrate from the blood towards the local source of CXCL12, such as in inflamed tissue [244]. Therefore, we hypothesized that upon inflammation, blocking the 'scavenging' activity of ACKR3 with ACT-1004-1239 should increase plasma levels of both CXCL11 and CXCL12 in the circulation, thereby presumably disrupting CXCL11- and CXCL12-mediated immunological functions, e.g., migration of CXCR3- and CXCR4-positive cells, to the inflammation site.

When I joined the project team (end of 2015) [Figure 22], CXCL11 and CXCL12 gradients had both been described to be involved in the recruitment of immune cells to different lung compartments during acute pulmonary inflammation

induced by lipopolysaccharide (LPS) in mice [330,331]. I proposed to use the LPS-induced pulmonary inflammation model as a POM model to characterize the effect of our lead ACKR3 antagonists, including ACT-1004-1239, on immune cell migration.

First, we established the model in DBA/1 mice, that express both ACKR3 chemokine ligands and we characterized it as a disease model, by showing that this model displayed several pathologic features of ALI and acute respiratory distress syndrome (ARDS). Then, we confirmed that both ACKR3 chemokine ligands were induced during LPS-induced pulmonary inflammation and that $CXCR3^+$ and $CXCR4^+$ leukocytes were recruited into the bronchoalveolar space upon inflammation.

This proof-of-mechanism disease model was used to characterize the dose-dependent effect of ACT-1004-1239 on PK/PD relationship and its broad effect on immune cell migration. In the context of preclinical drug development, this animal disease model helped us to estimate the efficacious concentration of ACKR3 antagonists, including ACT-1004-1239, to block cell migration *in vivo*. Together with the results obtained in pilot toxicity studies, we could define the therapeutic index for each ACKR3 antagonist compound we tested, and the outcome led us to select ACT-1004-1239 for further preclinical development. In the following article, I have only focused on the efficacy results obtained with the antagonist ACT-1004-1239 in this model.

2.2 Manuscript

CXCR7 antagonism reduces acute lung injury pathogenesis

Laetitia Pouzol[1†*], Anna Sassi[1†], Nadège Baumlin[1], Mélanie Tunis[1], Daniel S. Strasser[1], François Lehembre[1], Marianne Martinic[1]

† These authors have contributed equally to this work and share first authorship

[1] Idorsia Pharmaceuticals Ltd, Allschwil, Switzerland

*** Correspondence:**
Laetitia Pouzol
laetitia.pouzol@idorsia.com

Keywords: Acute lung injury, Acute respiratory distress syndrome, immunomodulation, CXCR7, CXCR3, CXCR4, CXCL11, CXCL12

Article Type: Original Research
Word count: 5351
Number of Figures and Tables: 6 figures, 1 table

***Frontiers in Pharmacology*, published online 05 November 2021**
https://doi.org/10.3389/fphar.2021.748740

ABSTRACT

Loss of control in the trafficking of immune cells to the inflamed lung tissue contributes to the pathogenesis of life-threatening acute lung injury (ALI) and its more severe form, acute respiratory distress syndrome (ARDS). Targeting CXCR7 has been proposed as a potential therapeutic approach to reduce pulmonary inflammation, however its role and its crosstalk with the two chemokine receptors CXCR3 and CXCR4 via their shared ligands CXCL11 and CXCL12 is not yet completely understood. The present paper aimed to characterize the pathological role of the CXCR3/CXCR4/CXCR7 axis in a murine model of ALI. Lipopolysaccharide (LPS) inhalation in mice resulted in the development of key pathologic features of ALI/ARDS, including breathing dysfunctions, alteration of the alveolar capillary barrier and lung inflammation. LPS inhalation induced immune cell infiltration into the bronchoalveolar space, including $CXCR3^+$ and $CXCR4^+$ cells, and enhanced the expression of the ligands of these two chemokine receptors. The first-in-class CXCR7 antagonist, ACT-1004-1239, increased levels of CXCL11 and CXCL12 in the plasma without affecting their levels in inflamed lung tissue, and consequently reduced $CXCR3^+$ and $CXCR4^+$ immune cell infiltrates into the bronchoalveolar space. In the early phase of lung inflammation, characterized by a massive influx of

neutrophils, treatment with ACT-1004-1239 significantly reduced the LPS-induced breathing pattern alteration. Both preventive and therapeutic treatment with ACT-1004-1239 reduced lung vascular permeability and decreased inflammatory cell infiltrates. In conclusion, these results demonstrate a key pathological role of CXCR7 in ALI/ARDS and highlight the clinical potential of ACT-1004-1239 in ALI/ARDS pathogenesis.

INTRODUCTION

Acute lung injury (ALI) and its more severe form, acute respiratory distress syndrome (ARDS), are life-threatening lung diseases that can be the result of different indirect or direct insults to the lung, such as sepsis, trauma, gastric acid aspiration, and pneumonia, including viral pneumonia such as SARS-CoV-2-induced pneumonia (1, 2). To date, the pathogenesis of these diseases is still not completely understood and there is no disease-modifying therapy to reduce the high mortality incidence of ARDS (3).

ALI and ARDS are characterized by increased lung vascular permeability, pulmonary edema, diffuse alveolar damage, and recruitment of inflammatory cells to the lung resulting in clinical symptoms such as hypoxemia, dyspnea, and even severe acute respiratory failure (4).

Many chemokines and their receptors, which are key mediators of immune cell trafficking, play a critical role in ALI pathogenesis and in its resolution (5, 6). Following lung injury, chemokine gradients are established and tightly regulated via complex mechanisms to recruit inflammatory cells to the site of inflammation (7).

CXCR3/CXCR4/CXCR7 and their ligands are overexpressed and heavily implicated in the pathology of a number of inflammatory diseases including pulmonary diseases (8-14).

CXCR7, also referred to as ACKR3, is an atypical chemokine receptor which is mainly expressed on endothelial cells (15). CXCR7 does not couple with G proteins but binding of its ligands leads to the recruitment of β-arrestin. CXCR7 functions predominantly as a scavenger receptor for its chemokine ligands CXCL11 and

CXCL12 (16), which bind to and activate the signaling chemokine receptors CXCR3 and CXCR4, respectively. While CXCR7 is not expressed on leukocytes (17), its scavenging activity in endothelial cells contributes to the establishment and maintenance of CXCL11 and CXCL12 concentration gradients along which CXCR3+ and CXCR4+ cells can migrate from the blood towards inflamed tissue (18-20).

CXCR3 is a cell surface receptor expressed on subsets of adaptive and innate immune cells such as lymphocytes, natural killer (NK) cells, dendritic cells (DCs), and can be activated by three interferon-inducible chemokine ligands: CXCL9, CXCL10, and CXCL11 (21). CXCR3-ligand interaction results in various cellular functions including cell migration, proliferation, polarization, and tissue retention (21).

CXCR4 is expressed on various immune cells including lymphoid and myeloid cells, endothelial cells, and hematopoietic stem cells (18). CXCL12-CXCR4 signaling results in pleiotropic cellular functions including cell migration, adhesion, proliferation, differentiation, and survival (19).

Blockade of CXCR7 is expected to increase the systemic CXCL11 and CXCL12 levels, and therefore modulate CXCR3 and CXCR4 signaling activities such as leukocyte chemotaxis and tissue retention (15, 20). In line with this hypothesis, treatment with CCX771, a CXCR7 functional antagonist, which is known to increase plasma CXCL12 levels (15), led to reduced alveolar inflammation and lung microvascular permeability in a murine model of ALI (14, 22). However, this murine model was performed in C57BL/6 mice, which do not express CXCL11 (23). As such, the specific role of CXCR7 in ALI and its indirect effect on CXCR3 and CXCR4 via their shared ligands have not yet been evaluated in an appropriate experimental design. In addition, since so far only CCX771, which recruits β-arrestin upon binding to the receptor, has been used in the ALI model (24), it remains unclear whether the observed efficacy is due to its agonistic activity or its functional antagonism induced by receptor desensitization (25).

To elucidate the role of CXCR7 on pulmonary inflammation, an ALI/ARDS experimental model was established through inhalation of nebulized lipopolysaccharide (LPS) in DBA/1 mice, a strain susceptible to LPS-induced ALI (26) and known to express both CXCL11 and CXCL12 (27). Since the pathological

mechanisms of LPS-induced ALI/ARDS can vary between the early and late phases of the inflammatory response (28), this model was characterized over time for the main features of ALI/ARDS, namely lung dysfunction, vascular permeability, inflammatory cell recruitment, and CXCR3/CXCR4/CXCR7 chemokine ligands release. Furthermore, the mechanistic and functional roles of CXCR7 were evaluated over time using the selective and first-in-class CXCR7 antagonist ACT-1004-1239, that blocks CXCL11- and CXCL12-induced β-arrestin recruitment (27).

MATERIALS AND METHODS

Mice and treatment administration

Male DBA/1 mice were purchased from Janvier Laboratories (Le Genest-Saint-Isle, France) and allowed to acclimatize for at least 7 days before use. The gender of mice was chosen based on previous studies showing that ARDS occurs more commonly in males than females (29). Mice had free access to food and drinking water ad libitum and were group-housed in a light-controlled environment. All animal studies were reviewed and approved by the Basel Cantonal Veterinary Office.

The CXCR7 antagonist ACT-1004-1239 was synthetized as previously described (27). The compound was formulated in 0.5% methylcellulose (Sigma-Aldrich, Schnelldorf, Germany), 0.5% Tween 80 (Sigma-Aldrich) in water. ACT-1004-1239 and vehicle (0.5% methylcellulose, 0.5% Tween 80 in water) were administered orally (p.o.), twice a day (b.i.d) at a volume of 5 mL/kg/administration (10ml/kg/day) at doses and times indicated in the figure legends. The twice daily oral administration regimen was based on the pharmacokinetic properties of this compound, which has been shown to be a high-clearance drug in rodents (27).

Murine model of LPS-induced acute lung injury

LPS challenge was performed as previously described (30). Briefly, mice were exposed to nebulized LPS (Escherichia coli O111:B4, purified by phenol extraction; Sigma-Aldrich) at 0.8 mg/mL diluted in NaCl 0.9% (B Braun Medical, Sempach, Switzerland) in a plexiglas chamber connected to a nebulizer (System assistance

medicale, Ledat, France) for 30 minutes. Control mice inhaled NaCl 0.9% only. Vehicle or ACT-1004-1239 were given p.o., 1h prior (preventive setting) or 3h post inhalation (therapeutic setting).

At different time points indicated in the figure legends (5h, 24h, 48h, 72h) following LPS or NaCl challenge, mice were euthanized with an overdose (150 mg/kg, intraperitoneally) of pentobarbital (esconarkon, Streuli Pharma SA, Uznach, Switzerland) and samples were collected.

In vivo lung function

Lung function was measured in unrestrained, conscious, and spontaneously breathing mice by whole-body plethysmography (Emka technologies, Paris, France) as previously described (31). Briefly, each mouse was placed alone in a calibrated plethysmography chamber and lung function parameters were recorded for 1h for baseline assessment. Right after the baseline, ACT-1004-1239 or vehicle were given orally 1h prior to nebulized LPS or NaCl inhalation. Respiration parameters were measured for 6 hours just after the challenge in the plethysmograph. Enhanced pause, Penh, ((Te/RT)-1)*PEF/PIF, where Te: expiratory time, RT: relaxation time, PEF: peak expiratory flow, PIF: peak inspiratory flow) was used as an index of alterations in respiration (32, 33). Data were analyzed using IOX2 software (Emka) and expressed as area under the curve (AUC), recorded for 30 minutes and averaged at 5-minute intervals. The time indicated in the figure refers to the starting time of the analyzed period (e.g. 60 minutes refers to the AUC calculated for the 60-90 minutes time interval). The mean Penh AUC baseline measurement was set to 100% for each mouse and calculated Penh AUC data was expressed as percentage of this mean baseline measurement.

Bronchoalveolar lavage (BAL) collection

BAL fluid was collected at different time points indicated in the figure legends following LPS or NaCl challenge. BAL was performed by injection of a total volume of 2.25 mL phosphate buffered saline (PBS, Bioconcept, Allschwil, Swizerland) supplemented with EDTA (0.5 mM, Gibco, Thermo Fisher Scientific, Waltham, MA, USA) through the mouse incised trachea. After centrifugation, BAL supernatant was collected and kept at -20°C until use. BAL cells were analyzed by flow cytometry.

Flow cytometry of the BAL cells

BAL cells were stained with the following surface fluorochrome conjugated monoclonal anti-mouse antibodies: APC-Cy7 anti-mouse CD19 (BioLegend, San Diego, CA, USA, Clone 6D5), APC anti-mouse CXCR3 (BioLegend, Clone CXCR3-173), BV510 anti-mouse CD11b (BioLegend, Clone M1/70), BV605 anti-mouse CD4 (BioLegend, Clone GK1.5), FITC anti-mouse B220 (BD, Clone Ra3-6B2), PB anti-mouse CD45 (BioLegend, Clone 30-F11), PECy7 anti-mouse βTCR (BioLegend, Clone H57-597), PE anti-mouse CXCR4 (InVitrogen, Thermo Fisher Scientific, Clone 2B11), BV650 anti-mouse CD8 (BioLegend, Clone 53-6.7), APC-Cy7 anti-mouse Gr-1 (BioLegend, Clone RB6-8C5), AF700 anti-mouse CD3 (BioLegend, Clone 17A2), FITC anti-mouse CD49b (BioLegend, Clone DX5), BV-605 anti-mouse B220 (BioLegend, Clone RA3-6B2), PECy7 anti-mouse CD11c (Biolegend, Clone N418). Staining was performed on ice, in the dark, during 45 minutes after preincubation with Fc receptor blocker (CD16/CD32, BD Biosciences). Dead cells were excluded based on their positive staining with propidium iodide (PI, CAS 25535-16-4, Sigma-Aldrich). Samples were acquired on a CytoFLEX Flow cytometer (Beckman Coulter Life Sciences, Nyon, switzerland) and data were analyzed using Kaluza analysis software version 2.1 (Beckman Coulter). Cells were first gated in forward scatter versus side scatter and doublets were excluded based on forward scatter area-height. From the single cells, dead cells were excluded based on their positive staining with PI. Cell subsets were quantified among viable/CD45+ cells (PI-, CD45+ cells): neutrophils (CD11b+, Gr-1high cells), monocytes/macrophages (CD11b+, Gr-1low cells), alveolar macrophages (CD11bint, SSChigh), B cells (CD11b-, Gr-1-, CD49- , CD3-, B220+ cells), plasmacytoid dendritic cells (pDCs) (CD11b-, Gr-1int, B220+, CD11c+ cells), T cells (CD11b-, B220-, CD49b-, CD3+ cells), natural killer (NK) cells (CD11b-, CD3-, CD49b+), and dendritic cells (DCs) (CD11b-, B220-, CD49b-, CD3-, CD11c+ cells). The CXCR4+ and CXCR3+ leukocytes were identified based on the fluorescence minus one control for CXCR4 and CXCR3, respectively. The gating strategies are illustrated in Figures S1 and S3.

CXCL12 and CXCL11 measurement

Whole blood was collected in EDTA-coated tubes (BD Microtainer, Becton Dickinson, Franklin Lakes, USA) and centrifuged to prepare plasma. After blood and BAL collection, mice were transcardially perfused with PBS/EDTA. Lungs were collected as a whole and kept at -20°C until use. Frozen mouse lungs were homogenized (FastPrep, MP biomedicals, Illkirch, France) in RIPA buffer supplemented with 1% protease inhibitor (Sigma-Aldrich, P8340) and phosphatase inhibitor (PhosSTOP Tablets, Sigma-Aldrich). Plasma samples and lung homogenates were assayed for CXCL12 concentration using the mouse CXCL12/SDF1α Quantikine ELISA (R&D Systems, Minneapolis, MN, USA, catalog no. MCX120) according to the manufacturer's instruction. The method was monitored using quality control samples provided in the assay kit. Mouse CXCL12 levels in BAL supernatant were determined using a commercially available electrochemiluminescence sandwich immunoassay (U-plex mouse CXCL12; Meso Scale Discovery; K152VBK-1). Recombinant human CXCL12 standard duoset kit (RnD Systems; DY350) was used for the standard curve. The assay was performed according to the instruction for use.

Mouse CXCL11 was quantified using an ultrasensitive immunoassay built on the Single Molecule Counting (SMC™) technology (Erenna® immunoassay system, Merck Millipore, Billerica, MA, USA). Paramagnetic microparticles (beads) coated with anti-mouse CXCL11 monoclonal antibody (R&D Systems, MAB572) were used as capturing antibody. Recombinant murine CXCL11 (Peprotech, Cranbury, NJ, USA, 250-29) was used as a standard and Fluor-labeled anti-mouse CXCL11 polyclonal antibody (R&D Systems, AF572) was used as the detection antibody. The number of fluorescently labeled detection antibodies counted with the Erenna® System is directly proportional to the amount of mouse CXCL11 present in the EDTA Plasma.

CXCL9 and CXCL10 measurement

Concentrations of the chemokines CXCL9 and CXCL10 in BAL supernatant were measured using a commercial mouse cytokine magnetic bead multiplex immunoassay kit (#MCYTOMAG-70K, Merck Millipore) according to the manufacturer's instruction. Samples were acquired on a Luminex 200 instrument

system (Thermo Fischer Scientific) and data were analyzed using SoftMaxPro software (Molecular device, San Jose, USA).

BAL supernatant proteins

Protein concentrations in the BAL supernatant were determined using the BCA Protein assay kit (Pierce #23225, Therno Fisher Scientific) according to the manufacturer's instruction.

Statistical analysis

All data were expressed as mean + standard error of the mean (SEM). Statistical analysis was performed using Prism version 8.1.1 (GraphPad software, San Diego, CA, USA) using the tests specified in the figure legends. Briefly, data were evaluated using two-tailed unpaired Student t test, one-way or two-ways analysis of variance (ANOVA) with a post hoc multiple comparison tests as appropriate. Differences were considered significant at p values < 0.05.

RESULTS

LPS-induced ALI/ARDS model in DBA/1 mice

Characterization of the consequences of LPS inhalation in DBA/1 mice was conducted to confirm in this experimental animal model (34) the presence of key features defining human ALI/ARDS, namely breathing dysfunction, increased alveolar capillary barrier permeability and immune cell infiltrates into the airspaces and the lung tissue.

Whole-body plethysmography on conscious, unrestrained mice was performed to monitor the physiological lung dysfunction caused by LPS. Inhalation of nebulized LPS caused a significant increase in enhanced pause (Penh), an index used as a marker of breathing pattern alteration (32, 33), compared to control mice receiving NaCl nebulization (Figure 1A). The increase in Penh peaked between 1.5 and 2 hours after LPS challenge and remained elevated throughout the 6-hour evaluation period.

To assess the effect of LPS on alveolar capillary barrier permeability, total protein concentration was measured in the BAL supernatant up to 72h after LPS challenge. Total BAL protein concentration was significantly increased from 24h up to 72h after LPS challenge, compared to control mice (Figure 1B).

To determine the effect of LPS on inflammatory cell recruitment to the alveolar space, BAL immune cell phenotyping was performed using flow cytometry. LPS inhalation led to a time-dependent infiltration of CD45+ immune cells into the BAL as compared to control mice, peaking 24h after LPS challenge (Figures 1C and Figure S1). In control mice, the main BAL immune cell population was represented by tissue resident alveolar macrophages (Figures 1D and Figure S1). In contrast, in LPS exposed mice, 5h after LPS challenge, neutrophils represented the majority of BAL immune infiltrates (Figure 1D). This early massive influx of neutrophils peaked 24h after the LPS challenge before strongly decreasing 48h and 72h post-LPS challenge (Table 1). Other BAL immune cells such as NK cells, B cells, pDCs and classical CD11b- DCs also peaked 24h after LPS challenge (Table 1) but altogether represented less than 9% of the overall BAL population at any given time point (Figure 1D). In contrast, infiltration of inflammatory macrophages and T cells peaked later, at 48h after LPS challenge (Table 1), and together represented more than 20% of the BAL immune cells (Figure 1D). At 72h post-LPS challenge, BAL immune cell numbers were still significantly increased compared to control mice (Figure 1C, Table 1). Infiltration of neutrophils was also confirmed in the lung tissue by histology, 24h after LPS challenge (Figure S2).

Taken together, these results demonstrate that inhalation of nebulized LPS in DBA/1 mice induced an acute and time-dependent increase in breathing dysfunction, vascular permeability, and infiltration of immune cells into the alveolar space and the lung tissue, and confirm this model as suitable to evaluate these pathogenic features of human ALI/ARDS in DBA/1 mice.

The increase of CXCR3 and CXCR4 ligands in the BAL is associated with an increase of CXCR3+ and CXCR4+ BAL immune cell infiltrates

To confirm that in this strain of mice both the CXCR3/CXCL9/10/11 and CXCR4/CXCL12 axes played a role in the recruitment of immune infiltrates into the

BAL, the expression of CXCR3 and CXCR4 on infiltrating immune cells and the release of their ligands were characterized in the alveolar space following LPS challenge.

In the BAL supernatant, LPS challenge led to a significant increase of the three CXCR3 ligands CXCL9, CXCL10, and CXCL11, compared to control mice (Figure 2A), reaching the highest increase 24h post-LPS challenge. Seventy-two hours after LPS challenge, CXCL11 returned to control levels while CXCL9 and CXCL10 were still significantly elevated compared to control mice (Figure 2A). CXCR3 expression was mainly detected on CD11b- BAL lymphoid cells compared to CD11b+ BAL myeloid cells; in the latter population, CXCR3 was only detected at low levels 48h and 72h post LPS challenge (Figures 2B and 2C and Figure S3). Interestingly, expression of CXCR3 (Figure 2C) and proportion of CXCR3+ BAL lymphoid and myeloid cells (Figure 2D) increased over time following LPS nebulization. At 72h post LPS challenge, almost 60% of BAL lymphoid cells expressed CXCR3 (Figure 2D); in absolute counts, CXCR3+ BAL lymphoid cells were only slightly reduced compared to earlier time points but were still significantly increased compared to control mice (Figure 2E).

LPS inhalation also led to a significant increase of BAL CXCL12 levels compared to control mice, which peaked at 24h and returned to control levels 72h post-LPS challenge (Figure 2F). In the BAL from LPS-challenged mice, CXCR4 expression was detected on the cell surface of most infiltrating leukocytes, with the highest surface expression detected on myeloid cells (Figure 2G and Figure S3). While the expression of CXCR4 on lymphoid cells and the proportion of CXCR4+ BAL lymphoid infiltrates remained stable following LPS nebulization, the expression of CXCR4 on myeloid cells and the proportion of CXCR4+ BAL myeloid infiltrates increased over time, reaching over 80% at the last time point investigated (Figures 2H and 2I). In absolute counts, the highest number of CXCR4+ BAL myeloid cells was reached 24h post-LPS challenge but still remained significantly elevated 72h post-LPS challenge, compared to control mice (Figure 2J).

In conclusion, LPS challenge of DBA/1 mice resulted in a significant increase in CXCR3/CXCR4 ligand levels, including the CXCR7 ligands CXCL11 and CXCL12, in

the BAL supernatant. This increase was associated with a significant increase of predominantly CXCR3+ lymphoid and CXCR4+ myeloid cells in the BAL.

CXCR7 antagonism increases plasma CXCL11 and CXCL12 levels and is associated with a reduction in CXCR3+ and CXCR4+ BAL immune cell infiltrates after LPS challenge

The scavenging activity of CXCR7 expressed on endothelial cells has been proposed to generate CXCL11 and CXCL12 chemokine gradients, thus enabling a directional migration of CXCR3+ and CXCR4+ cells, respectively, from the circulation towards sites of inflammation (15, 20, 35). To evaluate this hypothesis, the impact of CXCR7 antagonism on plasma and lung tissue CXCL11 and CXCL12 levels and BAL immune cell infiltrates was investigated in the ALI/ARDS DBA/1 mouse model following treatment with ACT-1004-1239.

CXCR7 antagonism further increased the LPS-induced elevation of CXCL11 plasma levels at all time points investigated compared to vehicle-treated, LPS-challenged mice (Figure 3A), confirming the proposed scavenging activity of CXCR7. In contrast, in the lung tissue, treatment with ACT-1004-1239 did not further increase CXCL11 concentrations but rather tended to normalize CXCL11 levels from LPS-challenged mice throughout the study period (Figure 3B). In the BAL from LPS-challenged mice, treatment with ACT-1004-1239 significantly reduced LPS-induced CXCR3+ lymphoid cell recruitment (Figure 3C) and showed a trend to decrease the late recruitment of the few CXCR3+ myeloid cells induced by LPS, although this did not reach statistical significance (Figure 3D).

Treatment with ACT-1004-1239 led to a robust and significant increase in plasma CXCL12 concentrations at all time points tested compared to vehicle-treated, LPS-challenged mice (Figure 3E). In contrast to the effect seen in plasma, in the lung tissue, CXCR7 antagonism did not further increase the LPS-induced elevation in CXCL12 levels and even resulted in a slight reduction of CXCL12 levels at 24h post LPS challenge compared to vehicle-treated LPS-challenged mice (Figure 3F). In the BAL from LPS-challenged mice, at all time-points investigated, treatment with ACT-1004-1239 significantly reduced BAL CXCR4+ lymphoid (Figure 3G) and CXCR4+

myeloid cell infiltrates (Figure 3H) compared to vehicle-treated LPS-challenged mice.

To investigate the dose-dependent effect of CXCR7 antagonism on plasma CXCL11 and CXCL12 levels and on immune cell recruitment to the alveolar space, mice were treated with three different doses of ACT-1004-1239 (10, 30, and 100 mg/kg, p.o., twice daily) or vehicle for 3 days, starting one hour prior to LPS challenge. Treatment with ACT-1004-1239 dose-dependently increased plasma CXCL11 and CXCL12 concentrations (Figures 4A and B); this was accompanied by a dose-dependent decrease of the major immune cell infiltrates present in the BAL after 72h (Figure 4D), namely T cells (Figure 4C) and macrophages (Figure 4D).

Taken together, these data demonstrate that CXCR7 antagonism with ACT-1004-1239 significantly increased plasma CXCL11 and CXCL12 levels in a dose-dependent manner and was associated with a reduction of CXCR3+ and CXCR4+ BAL immune infiltrates.

CXCR7 antagonism reduces LPS-induced ALI/ARDS

To monitor whether the CXCR7 antagonist ACT-1004-1239 would affect LPS-induced breathing dysfunction, whole-body plethysmography on conscious, unrestrained DBA/1 mice was performed. As previously reported (36), LPS nebulization caused a significant increase in enhanced pause (Penh) AUC versus vehicle-treated mice challenged with NaCl (Figure 5A). A single oral administration of ACT-1004-1239 (100 mg/kg, p.o.), given one-hour prior to LPS challenge, significantly reduced the LPS-induced elevated Penh AUC, reaching values from control mice at the end of the evaluation period (Figure 5A), indicating a normalization of the breathing pattern. In addition, the effect of CXCR7 antagonism on LPS-induced alveolar capillary barrier permeability increase was assessed 48 hours post-LPS challenge, at the peak of the LPS effect (Figure 1B). Treatment with ACT-1004-1239 (100 mg/kg, p.o., twice daily) was initiated either one-hour prior to LPS challenge (preventive setting) or three-hours after LPS challenge (therapeutic setting), when neutrophil infiltration was already apparent (data not shown). In both settings, treatment with the CXCR7 antagonist significantly reduced the overall protein content in the BAL, compared with vehicle treated, LPS-challenged

mice (Figure 5B). Moreover, treatment with ACT-1004-1239 reduced LPS-induced leukocyte recruitment to the BAL 48h post-LPS challenge. Preventive ACT-1004-1239 treatment significantly reduced all evaluated immune cell subsets present in the BAL (Figure 5C) whereas therapeutic administration of ACT-1004-1239 significantly reduced macrophages and lymphocytes, and showed a trend to reduce all other evaluated cell subtypes without reaching statistical significance (Figure 5C).

In summary, blockade of the CXCR7 axis improved clinical signs of nebulized LPS inhalation as shown by an improvement of the breathing pattern, a reduction of the vascular barrier dysfunction, and a reduction of immune cell infiltrates into the BAL, thus confirming the importance of the CXCR3/CXCR4/CXCR7 axis in ALI/ARDS.

DISCUSSION

Acute lung injury and its more severe form ARDS represent lung disease conditions of multifactorial etiology, associated with diffuse alveolar damage and hypoxemia. Despite better knowledge regarding the pathogenesis of ALI/ARDS, mortality remains high (40%) and current treatment is restricted to supportive care with mechanical ventilation, emphasizing the need to develop and test new therapies for this life-threatening condition (3, 37). The lack of effective therapy has been recently underlined by the coronavirus disease 19 (COVID-19) pandemic which causes ARDS in 3-5% of patients infected with SARS-CoV-2 (38).

The preclinical ALI/ARDS model, induced by LPS inhalation in rodents, is a commonly used model which manifests key features of human ALI/ARDS (34, 39). In the current study, the consequences of LPS inhalation were characterized over time in DBA/1 mice, a strain of mice expressing both CXCR7 ligands (CXCL11 and CXCL12). In line with previous reports in similar models but not expressing CXCL11 (36, 40), inhalation of nebulized LPS in DBA/1 mice induced key parameters recommended by the American Thoracic Society to detect the presence of ARDS in laboratory animals: LPS inhalation caused a rapid and significant recruitment of inflammatory cells to the alveolar space, especially neutrophils at early time points after LPS challenge followed by macrophages and T cells at later time points.

Furthermore, LPS inhalation increased alveolar capillary barrier permeability. The LPS-induced breathing pattern alteration was also observed, which has been shown to be associated with altered lung function (41).

The duration of the pulmonary inflammatory contributes to the pathogenesis of ALI/ARDS and may determine the severity and subsequent mortality in patients (42, 43); however, the mechanisms leading to a persistent inflammation remain unclear. Previous reports have suggested that both the CXCR3 and CXCR4 axis play a pivotal role in the prolonged recruitment, and/or retention of immune cells in ALI/ARDS, exerting a damaging effect in the lung (10, 44, 45).

Consistent with findings from human patients and mouse models of ALI (8-14), in this study using LPS-challenged DBA/1 mice, CXCR3 and CXCR4 ligands were elevated in the BAL, which was associated with increased BAL CXCR3+ and CXCR4+ cell infiltrates. In line with previously reported data (10), the expression of CXCR4 on BAL myeloid cells steadily increased over time following LPS-induced lung injury. Importantly, the same observation was made regarding the expression of CXCR3, especially on lymphoid cells, suggesting a distinct role for CXCR3 and CXCR4 in the recruitment and persistence/retention of BAL infiltrates during ALI/ARDS. Interestingly, a similar observation was made in the BAL from patients with COVID-19, where most BAL infiltrates expressed CXCR3 and/or CXCR4 (11) and the increased presence of activated lung-homing CXCR4+ T cells was associated with fatal COVID-19 (46).

CXCR7 has been reported to scavenge both CXCL11 and CXCL12. Even though CXCL11 was found at lower levels than CXCL9 and CXCL10 in the BAL from LPS challenged mice, this chemokine represents the most potent CXCR3 ligand (47). To date, the role of the CXCR3/CXCR7/CXCL11 axis in preclinical ALI models has not been investigated as previous studies were conducted in C57BL/6 mice, a mouse strain lacking CXCL11 (48). We show here that antagonizing CXCR7 with ACT-1004-1239 not only led to the elevation of CXCL12 in the plasma, confirming previous data (20, 27) but also of the inducible chemokine CXCL11, in a dose-dependent manner, confirming the inhibition of the scavenging activity of CXCR7 in vivo. In contrast, CXCR7 antagonism did not further increase the LPS-induced elevation of CXCL11 and CXCL12 concentrations in the inflamed lung tissue, but rather tended

to normalize them, likely leading to a disruption of the chemokine concentration gradient from the blood to the injured lung tissue. Consequently, a significant reduction of CXCR3+ lymphoid and CXCR4+ myeloid and lymphoid cells in the BAL was observed upon treatment with the CXCR7 antagonist, suggesting an inhibition of directional migration of these cells from the blood to the inflamed tissue and/or a reduction of their retention in the tissue. The immunomodulatory effect of CXCR7 antagonism was consistently shown both in a preventive and therapeutic setting, highlighting its potential clinical impact on acute pulmonary inflammation.

Besides the pivotal role of CXCR7 on immune cells infiltration to the BAL, expression of CXCR7 in the vasculature has been associated with a disruption of the endothelial barrier function (49). CXCR7 antagonism with ACT-1004-1239 both in a preventive and therapeutic setting, successfully reduced alterations of the alveolar capillary barrier function as shown by a reduction of the overall protein content in the BAL following LPS challenge. Furthermore, CXCL12 has been shown to promote endothelial barrier integrity in vivo via CXCR4 (50) and to enhance barrier function in human pulmonary artery endothelial cells following thrombin activation in vitro (51). These data suggest that the reduced vascular permeability seen in the ALI/ARDS model following CXCR7 antagonism could be a result of a direct effect on endothelial cells and/or indirect effect via increased CXCL12 concentration.

An additional interesting finding of this study was the effect of ACT-1004-1239 on breathing pattern alteration following LPS challenge. Endotoxins have been related to pulmonary functional disturbances both in humans (52) and mice (36) and have been shown to exacerbate established emphysema in several experimental models (53, 54). Therefore, this aspect may be relevant to the pathogenesis of ARDS, especially at the late stages where emphysema-like lesions are present (55). In the present study, treatment with ACT-1004-1239 reduced the Penh increase observed within 2 hours following LPS inhalation. Published data in similar models reported that LPS-induced Penh increase was dependent on TNF-a release (56). However, the effect observed with ACT-1004-1239 on this early breathing pattern change could not be explained by a reduction in LPS-induced BAL TNF-a elevation (data

not shown). More studies are needed to unravel the mechanisms that account for this effect.
So far, only CCX771, which recruits β-arrestin upon binding to the CXCR7 receptor, has been evaluated in the context of ALI (14) (24). Our study using ACT-1004-1239, a CXCR7 antagonist of the β-arrestin pathway, provides evidence that the observed efficacy obtained with CCX771 in ALI was likely due to its functional antagonistic effect and not to its agonistic effect.

In conclusion, the presented data provide a characterization of the LPS-induced ALI/ARDS model in DBA/1 mice, demonstrating a key role for CXCR7 on pathological hallmarks of human disease (Figure 6A). The scavenging activity of CXCR7 contributed to the establishment and maintenance of CXCL11 and CXCL12 concentration gradients, thereby allowing the recruitment of CXCR3+ and CXCR4+ leukocytes to the BAL (Figure 6A). Antagonizing CXCR7 with ACT-1004-1239 increased plasma CXCL11 and CXCL12 levels and reduced infiltration of CXCR3+ and CXCR4+ leukocytes to the BAL (Figure 6B). Furthermore, CXCR7 antagonism reduced vascular permeability and breathing dysfunction (Figure 6B). This broad mechanism of action positions ACT-1004-1239 as a potential new therapy to target main pathological features of human ALI/ARDS.

List of non-standard abbreviations

ALI: acute lung injury, ANOVA: analysis of variance, ARDS: acute respiratory distress syndrome, BAL: bronchoalveolar lavage, bid: twice daily, DCs: dendritic cells, LPS: lipopolysaccharide, NK cells: Natural killer cells, pDCs: plasmacytoid dendritic cells, SEM: standard error of the mean.

Acknowledgments

We thank Idorsia's immunology, translational biomarker, DMPK, and formulation and preclinical galenics groups for their continuous support with in vivo experiments. We thank J. Scherer for supporting the evaluation of the lung function. We thank E. Gerossier and A. Zurbach for constant in vivo support. We thank J. Hoerner and H. Farine for the measurement of CXCL11. We thank E. Vezzali

for histology. We thank the core team members of the project, especially P. Guerry, C. Gnerre, E. Lindenberg, M. Holdener, P. Coloma, C. Huynh, S. Schuldes for their careful review of the manuscript.

Contribution to the Field Statement

Acute lung injury is a life-threatening complication that has a high mortality rate. Specific and effective treatment is still lacking, and pathogenesis remains unclear. A better understanding of the mechanisms leading to this life-threatening event may help to find novel therapies. Targeting CXCR7 has been proposed as a potential therapeutic approach to reduce pulmonary inflammation, however its role and its crosstalk in the CXCR7/CXCR3/CXCR4 axis is not yet completely understood. This manuscript describes the pathological role of CXCR7 in one of the most commonly used preclinical models mimicking different features of acute lung injury. Treatment with the CXCR7 antagonist ACT-1004-1239 was associated with a significant increase in plasma CXCR7 ligands leading to the disruption of chemokine gradients, inhibition of pulmonary immune cell infiltration and ultimately in a significant reduction of alveolar capillary barrier dysfunction. Targeting CXCR7 may thus help alleviate inflammation and therefore reduce lung damage in patients with ALI.

Author contributions

L. Pouzol was responsible for the conception, design and execution of the studies, data interpretation, and manuscript drafting. A. Sassi was responsible for the execution of the studies, data interpretation, and manuscript drafting. N. Baumlin, M. Tunis, and D. Strasser carried out the experiments and analyzed the data. F. Lehembre was involved in study concept and design. M. Martinic was involved in the data interpretation and manuscript drafting. All authors helped to critically revise the intellectual content of the manuscript and approved the final submission.

Funding and Conflict of Interest

The authors declared the following potential conflicts of interest with respect to the research, authorship, and/or publication of this article: all authors acknowledge

that the work was performed as employees of Idorsia Pharmaceuticals Ltd, Allschwil, Switzerland. The authors declare no other financial interests and no funding sources.

Data Availability Statement

The raw data supporting the conclusions of this manuscript will be made available by the authors, upon reasonable request.

References

1. Wheeler AP, Bernard GR. Acute lung injury and the acute respiratory distress syndrome: a clinical review. Lancet (2007) 369(9572):1553-64. Epub 2007/05/08. doi: 10.1016/S0140-6736(07)60604-7. PubMed PMID: 17482987.

2. Gibson PG, Qin L, Puah SH. COVID-19 acute respiratory distress syndrome (ARDS): clinical features and differences from typical pre-COVID-19 ARDS. Med J Aust (2020) 213(2):54-6 e1. Epub 2020/06/24. doi: 10.5694/mja2.50674. PubMed PMID: 32572965; PubMed Central PMCID: PMCPMC7361309.

3. Bellani G, Laffey JG, Pham T, Fan E, Brochard L, Esteban A, et al. Epidemiology, Patterns of Care, and Mortality for Patients With Acute Respiratory Distress Syndrome in Intensive Care Units in 50 Countries. JAMA (2016) 315(8):788-800. Epub 2016/02/24. doi: 10.1001/jama.2016.0291. PubMed PMID: 26903337.

4. Ware LB, Matthay MA. The acute respiratory distress syndrome. N Engl J Med (2000) 342(18):1334-49. Epub 2000/05/04. doi: 10.1056/NEJM200005043421806. PubMed PMID: 10793167.

5. Bhatia M, Zemans RL, Jeyaseelan S. Role of chemokines in the pathogenesis of acute lung injury. Am J Respir Cell Mol Biol (2012) 46(5):566-72. Epub 2012/02/11. doi: 10.1165/rcmb.2011-0392TR. PubMed PMID: 22323365; PubMed Central PMCID: PMCPMC3361356.

6. Tomankova T, Kriegova E, Liu M. Chemokine receptors and their therapeutic opportunities in diseased lung: far beyond leukocyte trafficking. Am J Physiol Lung Cell Mol Physiol (2015) 308(7):L603-18. Epub 2015/02/01. doi: 10.1152/ajplung.00203.2014. PubMed PMID: 25637606.

7. Puneet P, Moochhala S, Bhatia M. Chemokines in acute respiratory distress syndrome. Am J Physiol Lung Cell Mol Physiol (2005) 288(1):L3-15. Epub 2004/12/14. doi: 10.1152/ajplung.00405.2003. PubMed PMID: 15591040; PubMed Central PMCID: PMCPMC7191630.

8. Saetta M, Mariani M, Panina-Bordignon P, Turato G, Buonsanti C, Baraldo S, et al. Increased expression of the chemokine receptor CXCR3 and its ligand CXCL10 in peripheral airways of smokers with chronic obstructive pulmonary disease. Am J Respir Crit Care Med (2002) 165(10):1404-9. Epub 2002/05/23. doi: 10.1164/rccm.2107139. PubMed PMID: 12016104.

9. Ichikawa A, Kuba K, Morita M, Chida S, Tezuka H, Hara H, et al. CXCL10-CXCR3 enhances the development of neutrophil-mediated fulminant lung injury of viral and nonviral origin. Am J Respir Crit Care Med (2013) 187(1):65-77. Epub 2012/11/13. doi: 10.1164/rccm.201203-0508OC. PubMed PMID: 23144331; PubMed Central PMCID: PMCPMC3927876.

10. Petty JM, Sueblinvong V, Lenox CC, Jones CC, Cosgrove GP, Cool CD, et al. Pulmonary stromal-derived factor-1 expression and effect on neutrophil recruitment during acute lung injury. J Immunol (2007) 178(12):8148-57. PubMed PMID: 17548653.

11. Liao M, Liu Y, Yuan J, Wen Y, Xu G, Zhao J, et al. Single-cell landscape of bronchoalveolar immune cells in patients with COVID-19. Nat Med (2020) 26(6):842-4. Epub 2020/05/14. doi: 10.1038/s41591-020-0901-9. PubMed PMID: 32398875.

12. Hartl D, Krauss-Etschmann S, Koller B, Hordijk PL, Kuijpers TW, Hoffmann F, et al. Infiltrated neutrophils acquire novel chemokine receptor expression and chemokine responsiveness in chronic inflammatory lung diseases. J Immunol (2008) 181(11):8053-67. Epub 2008/11/20. doi: 10.4049/jimmunol.181.11.8053. PubMed PMID: 19017998.

13. Costello CM, McCullagh B, Howell K, Sands M, Belperio JA, Keane MP, et al. A role for the CXCL12 receptor, CXCR7, in the pathogenesis of human pulmonary vascular disease. Eur Respir J (2012) 39(6):1415-24. Epub 2011/11/18. doi: 10.1183/09031936.00044911. PubMed PMID: 22088972.

14. Ngamsri KC, Muller A, Bosmuller H, Gamper-Tsigaras J, Reutershan J, Konrad FM. The Pivotal Role of CXCR7 in Stabilization of the Pulmonary Epithelial Barrier in Acute Pulmonary Inflammation. J Immunol (2017) 198(6):2403-13. doi: 10.4049/jimmunol.1601682. PubMed PMID: 28188248.

15. Berahovich RD, Zabel BA, Lewen S, Walters MJ, Ebsworth K, Wang Y, et al. Endothelial expression of CXCR7 and the regulation of systemic CXCL12 levels. Immunology (2014) 141(1):111-22. doi: 10.1111/imm.12176. PubMed PMID: 24116850; PubMed Central PMCID: PMCPMC3893854.

16. Naumann U, Cameroni E, Pruenster M, Mahabaleshwar H, Raz E, Zerwes HG, et al. CXCR7 functions as a scavenger for CXCL12 and CXCL11. PLoS One (2010) 5(2):e9175. doi: 10.1371/journal.pone.0009175. PubMed PMID: 20161793; PubMed Central PMCID: PMCPMC2820091.

17. Berahovich RD, Zabel BA, Penfold ME, Lewen S, Wang Y, Miao Z, et al. CXCR7 protein is not expressed on human or mouse leukocytes. J Immunol (2010) 185(9):5130-9. doi: 10.4049/jimmunol.1001660. PubMed PMID: 20889540.

18. Lewellis SW, Knaut H. Attractive guidance: how the chemokine SDF1/CXCL12 guides different cells to different locations. Semin Cell Dev Biol (2012) 23(3):333-40. doi: 10.1016/j.semcdb.2012.03.009. PubMed PMID: 22414535; PubMed Central PMCID: PMCPMC3345092.

19. Quinn KE, Mackie DI, Caron KM. Emerging roles of atypical chemokine receptor 3 (ACKR3) in normal development and physiology. Cytokine (2018) 109:17-23. doi: 10.1016/j.cyto.2018.02.024. PubMed PMID: 29903572; PubMed Central PMCID: PMCPMC6005205.

20. Pouzol L, Baumlin N, Sassi A, Tunis M, Marrie J, Vezzali E, et al. ACT-1004-1239, a first-in-class CXCR7 antagonist with both immunomodulatory and promyelinating effects for the treatment of inflammatory demyelinating diseases. FASEB J (2021) 35(3):e21431. Epub 2021/02/18. doi: 10.1096/fj.202002465R. PubMed PMID: 33595155.

21. Groom JR, Luster AD. CXCR3 in T cell function. Exp Cell Res (2011) 317(5):620-31. Epub 2011/03/08. doi: 10.1016/j.yexcr.2010.12.017
S0014-4827(10)00575-6 [pii]. PubMed PMID: 21376175; PubMed Central PMCID: PMC3065205.

22. Konrad FM, Meichssner N, Bury A, Ngamsri KC, Reutershan J. Inhibition of SDF-1 receptors CXCR4 and CXCR7 attenuates acute pulmonary inflammation via the adenosine A2B-receptor on blood cells. Cell Death Dis (2017) 8(5):e2832. doi: 10.1038/cddis.2016.482. PubMed PMID: 28542132; PubMed Central PMCID: PMCPMC5520683.

23. Sierro F, Biben C, Martinez-Munoz L, Mellado M, Ransohoff RM, Li M, et al. Disrupted cardiac development but normal hematopoiesis in mice deficient in the second CXCL12/SDF-1 receptor, CXCR7. Proc Natl Acad Sci U S A (2007) 104(37):14759-64. doi: 10.1073/pnas.0702229104. PubMed PMID: 17804806; PubMed Central PMCID: PMCPMC1976222.

24. Zabel BA, Wang Y, Lewen S, Berahovich RD, Penfold ME, Zhang P, et al. Elucidation of CXCR7-mediated signaling events and inhibition of CXCR4-mediated tumor cell transendothelial migration by CXCR7 ligands. J Immunol (2009) 183(5):3204-11. doi: 10.4049/jimmunol.0900269. PubMed PMID: 19641136.

25. Menhaji-Klotz E, Ward J, Brown JA, Loria PM, Tan C, Hesp KD, et al. Discovery of Diphenylacetamides as CXCR7 Inhibitors with Novel β-Arrestin Antagonist Activity. ACS Medicinal Chemistry Letters (2020). doi: 10.1021/acsmedchemlett.0c00163.

26. Alm AS, Li K, Chen H, Wang D, Andersson R, Wang X. Variation of lipopolysaccharide-induced acute lung injury in eight strains of mice. Respir Physiol Neurobiol (2010) 171(2):157-64. Epub 2010/03/02. doi: 10.1016/j.resp.2010.02.009. PubMed PMID: 20188866.

27. Richard-Bildstein S, Aissaoui H, Pothier J, Schafer G, Gnerre C, Lindenberg E, et al. Discovery of the Potent, Selective, Orally Available CXCR7 Antagonist ACT-1004-1239. J Med Chem (2020) 63(24):15864-82. Epub 2020/12/15. doi: 10.1021/acs.jmedchem.0c01588. PubMed PMID: 33314938.

28. Domscheit H, Hegeman MA, Carvalho N, Spieth PM. Molecular Dynamics of Lipopolysaccharide-Induced Lung Injury in Rodents. Front Physiol (2020) 11:36. Epub 2020/03/03. doi: 10.3389/fphys.2020.00036. PubMed PMID: 32116752; PubMed Central PMCID: PMCPMC7012903.

29. Lemos-Filho LB, Mikkelsen ME, Martin GS, Dabbagh O, Adesanya A, Gentile N, et al. Sex, race, and the development of acute lung injury. Chest (2013)

143(4):901-9. Epub 2012/11/03. doi: 10.1378/chest.12-1118. PubMed PMID: 23117155; PubMed Central PMCID: PMCPMC3747719.

30. de Souza Xavier Costa N, Ribeiro Junior G, Dos Santos Alemany AA, Belotti L, Zati DH, Frota Cavalcante M, et al. Early and late pulmonary effects of nebulized LPS in mice: An acute lung injury model. PLoS One (2017) 12(9):e0185474. Epub 2017/09/28. doi: 10.1371/journal.pone.0185474. PubMed PMID: 28953963; PubMed Central PMCID: PMCPMC5617199.

31. Piali L, Birker-Robaczewska M, Lescop C, Froidevaux S, Schmitz N, Morrison K, et al. Cenerimod, a novel selective S1P1 receptor modulator with unique signaling properties. Pharmacol Res Perspect (2017) 5(6). Epub 2017/12/12. doi: 10.1002/prp2.370. PubMed PMID: 29226621; PubMed Central PMCID: PMCPMC5723703.

32. Hamelmann E, Schwarze J, Takeda K, Oshiba A, Larsen GL, Irvin CG, et al. Noninvasive measurement of airway responsiveness in allergic mice using barometric plethysmography. Am J Respir Crit Care Med (1997) 156(3 Pt 1):766-75. Epub 1997/10/06. doi: 10.1164/ajrccm.156.3.9606031. PubMed PMID: 9309991.

33. Prada-Dacasa P, Badell AU, Sánchez-Benito L, bianchi p, Quintana A. Measuring Breathing Patterns in Mice Using Whole-body Plethysmography. Bio-protocol (2020) 10(17):e3741. doi: 10.21769/BioProtoc.3741.

34. Matute-Bello G, Frevert CW, Martin TR. Animal models of acute lung injury. Am J Physiol Lung Cell Mol Physiol (2008) 295(3):L379-99. Epub 2008/07/16. doi: 10.1152/ajplung.00010.2008. PubMed PMID: 18621912; PubMed Central PMCID: PMCPMC2536793.

35. Tobia C, Chiodelli P, Barbieri A, Buraschi S, Ferrari E, Mitola S, et al. Atypical Chemokine Receptor 3 Generates Guidance Cues for CXCL12-Mediated Endothelial Cell Migration. Front Immunol (2019) 10:1092. Epub 2019/06/04. doi: 10.3389/fimmu.2019.01092. PubMed PMID: 31156639; PubMed Central PMCID: PMCPMC6529557.

36. Lefort J, Motreff L, Vargaftig BB. Airway administration of Escherichia coli endotoxin to mice induces glucocorticosteroid-resistant bronchoconstriction and vasopermeation. Am J Respir Cell Mol Biol (2001) 24(3):345-51. Epub 2001/03/14. doi: 10.1165/ajrcmb.24.3.4289. PubMed PMID: 11245635.

37. Dushianthan A, Grocott MP, Postle AD, Cusack R. Acute respiratory distress syndrome and acute lung injury. Postgrad Med J (2011) 87(1031):612-22. Epub 2011/06/07. doi: 10.1136/pgmj.2011.118398. PubMed PMID: 21642654.

38. Horie S, McNicholas B, Rezoagli E, Pham T, Curley G, McAuley D, et al. Emerging pharmacological therapies for ARDS: COVID-19 and beyond. Intensive Care Med (2020) 46(12):2265-83. Epub 2020/07/13. doi: 10.1007/s00134-020-06141-z. PubMed PMID: 32654006; PubMed Central PMCID: PMCPMC7352097.

39. Menezes SL, Bozza PT, Neto HC, Laranjeira AP, Negri EM, Capelozzi VL, et al. Pulmonary and extrapulmonary acute lung injury: inflammatory and ultrastructural analyses. J Appl Physiol (1985) (2005) 98(5):1777-83. Epub 2005/01/15. doi: 10.1152/japplphysiol.01182.2004. PubMed PMID: 15649870.

40. Lax S, Wilson MR, Takata M, Thickett DR. Using a non-invasive assessment of lung injury in a murine model of acute lung injury. BMJ Open Respir Res (2014) 1(1):e000014. Epub 2014/12/06. doi: 10.1136/bmjresp-2013-000014. PubMed PMID: 25478170; PubMed Central PMCID: PMCPMC4212707.

41. Hakansson HF, Smailagic A, Brunmark C, Miller-Larsson A, Lal H. Altered lung function relates to inflammation in an acute LPS mouse model. Pulm Pharmacol Ther (2012) 25(5):399-406. Epub 2012/09/15. doi: 10.1016/j.pupt.2012.08.001. PubMed PMID: 22975080.

42. Meduri GU, Headley S, Kohler G, Stentz F, Tolley E, Umberger R, et al. Persistent elevation of inflammatory cytokines predicts a poor outcome in ARDS. Plasma IL-1 beta and IL-6 levels are consistent and efficient predictors of outcome over time. Chest (1995) 107(4):1062-73. Epub 1995/04/01. doi: 10.1378/chest.107.4.1062. PubMed PMID: 7705118.

43. Yang KY, Arcaroli JJ, Abraham E. Early alterations in neutrophil activation are associated with outcome in acute lung injury. Am J Respir Crit Care Med (2003) 167(11):1567-74. Epub 2003/03/11. doi: 10.1164/rccm.200207-664OC. PubMed PMID: 12626346.

44. Kelsen SG, Aksoy MO, Georgy M, Hershman R, Ji R, Li X, et al. Lymphoid follicle cells in chronic obstructive pulmonary disease overexpress the chemokine receptor CXCR3. Am J Respir Crit Care Med (2009) 179(9):799-805. Epub

2009/02/17. doi: 10.1164/rccm.200807-1089OC. PubMed PMID: 19218194; PubMed Central PMCID: PMCPMC5803653.

45. Nie L, Xiang R, Zhou W, Lu B, Cheng D, Gao J. Attenuation of acute lung inflammation induced by cigarette smoke in CXCR3 knockout mice. Respir Res (2008) 9:82. Epub 2008/12/18. doi: 10.1186/1465-9921-9-82. PubMed PMID: 19087279; PubMed Central PMCID: PMCPMC2654035.

46. Neidleman J, Luo X, George AF, McGregor M, Yang J, Yun C, et al. Distinctive features of SARS-CoV-2-specific T cells predict recovery from severe COVID-19. medRxiv (2021). Epub 2021/02/04. doi: 10.1101/2021.01.22.21250054. PubMed PMID: 33532792; PubMed Central PMCID: PMCPMC7852243.

47. Sauty A, Colvin RA, Wagner L, Rochat S, Spertini F, Luster AD. CXCR3 internalization following T cell-endothelial cell contact: preferential role of IFN-inducible T cell alpha chemoattractant (CXCL11). J Immunol (2001) 167(12):7084-93. Epub 2001/12/12. doi: 10.4049/jimmunol.167.12.7084. PubMed PMID: 11739530.

48. Frederic Sierro, Christine Biben, Laura Martı´nez-Munoz, Mario Mellado, Richard M. Ransohoff, Meizhang Li, et al. Disrupted cardiac development but normal hematopoiesis in mice deficient in the second CXCL12/SDF-1 receptor, CXCR7. PNAS (2007) 104:714759–14764.

49. Totonchy JE, Clepper L, Phillips KG, McCarty OJ, Moses AV. CXCR7 expression disrupts endothelial cell homeostasis and causes ligand-dependent invasion. Cell Adh Migr (2014) 8(2):165-76. Epub 2014/04/09. doi: 10.4161/cam.28495. PubMed PMID: 24710021; PubMed Central PMCID: PMCPMC4049862.

50. Kobayashi K, Sato K, Kida T, Omori K, Hori M, Ozaki H, et al. Stromal cell-derived factor-1alpha/C-X-C chemokine receptor type 4 axis promotes endothelial cell barrier integrity via phosphoinositide 3-kinase and Rac1 activation. Arterioscler Thromb Vasc Biol (2014) 34(8):1716-22. Epub 2014/06/14. doi: 10.1161/ATVBAHA.114.303890. PubMed PMID: 24925969.

51. Cheng YH, Eby JM, LaPorte HM, Volkman BF, Majetschak M. Effects of cognate, non-cognate and synthetic CXCR4 and ACKR3 ligands on human lung endothelial cell barrier function. PLoS One (2017) 12(11):e0187949. Epub

2017/11/11. doi: 10.1371/journal.pone.0187949. PubMed PMID: 29125867; PubMed Central PMCID: PMCPMC5681266.
52. Leaker BR, Barnes PJ, O'Connor B. Inhibition of LPS-induced airway neutrophilic inflammation in healthy volunteers with an oral CXCR2 antagonist. Respir Res (2013) 14:137. Epub 2013/12/18. doi: 10.1186/1465-9921-14-137. PubMed PMID: 24341382; PubMed Central PMCID: PMCPMC3867427.
53. Kobayashi S, Fujinawa R, Ota F, Kobayashi S, Angata T, Ueno M, et al. A single dose of lipopolysaccharide into mice with emphysema mimics human chronic obstructive pulmonary disease exacerbation as assessed by micro-computed tomography. Am J Respir Cell Mol Biol (2013) 49(6):971-7. Epub 2013/07/05. doi: 10.1165/rcmb.2013-0074OC. PubMed PMID: 23822858.
54. de Oliveira MV, Rocha NN, Santos RS, Rocco MRM, de Magalhaes RF, Silva JD, et al. Endotoxin-Induced Emphysema Exacerbation: A Novel Model of Chronic Obstructive Pulmonary Disease Exacerbations Causing Cardiopulmonary Impairment and Diaphragm Dysfunction. Front Physiol (2019) 10:664. Epub 2019/06/14. doi: 10.3389/fphys.2019.00664. PubMed PMID: 31191356; PubMed Central PMCID: PMCPMC6546905.
55. Terzi E, Zarogoulidis K, Kougioumtzi I, Dryllis G, Kioumis I, Pitsiou G, et al. Acute respiratory distress syndrome and pneumothorax. J Thorac Dis (2014) 6(Suppl 4):S435-42. Epub 2014/10/23. doi: 10.3978/j.issn.2072-1439.2014.08.34. PubMed PMID: 25337400; PubMed Central PMCID: PMCPMC4203978.
56. Schnyder-Candrian S, Quesniaux VF, Di Padova F, Maillet I, Noulin N, Couillin I, et al. Dual effects of p38 MAPK on TNF-dependent bronchoconstriction and TNF-independent neutrophil recruitment in lipopolysaccharide-induced acute respiratory distress syndrome. J Immunol (2005) 175(1):262-9. Epub 2005/06/24. doi: 10.4049/jimmunol.175.1.262. PubMed PMID: 15972657.

FIGURE LEGENDS

Figure 1: Characterization of the LPS-induced ALI/ARDS model in male DBA/1 mice. LPS inhalation was associated with a significant breathing pattern alteration (**A**), an increase in alveolar-capillary barrier permeability (**B**) and increased immune

cell infiltrates in the bronchoalveolar space (**C-D**) as compared to NaCl exposed mice (control mice). (**A**) Breathing pattern alteration was measured by the change in the calculated enhanced pause (Penh) using whole-body plethysmography in conscious unrestrained mice over a period of 6h following LPS (black triangles) or NaCl inhalation (white circles). Results are expressed as the mean percentage Penh area under the curve (AUC) normalized to the baseline + SEM (n=16 mice per group). ****p<0.0001 paired Student t test. (**B**) Alveolar-capillary barrier permeability was assessed by measuring the total protein concentration in the BAL supernatant at 5h, 24h, 48h, and 72h after LPS challenge (black bars, n=7-16 mice per time point) or NaCl challenge (control mice, white bar, n=20; all time points were pooled). Results are expressed as mean + SEM. *p<0.05, ****p<0.0001 paired Student t test. (**C**) Time course of $CD45^+$ immune cells in the BAL measured by flow cytometry in samples collected at 5h, 24h, 48h, and 72h after LPS challenge (black bars, n=7-16 mice per time point) or NaCl challenge (control mice, white bar, n=20; all time points were pooled). Results are expressed as mean + SEM.***p<0.001, ****p<0.0001 paired Student t test. (**D**) Frequencies of BAL immune cell populations over time. Results are expressed as proportions among total $CD45^+$ cells for each time point.

Figure 2: Kinetics of the expression of CXCR3/CXCR4 and its ligands in the bronchoalveolar lavage of LPS-challenged DBA/1 mice. ALI was induced by nebulized LPS inhalation in male DBA/1 mice. Control mice inhaled NaCl 0.9% (n=12 mice; all time points were pooled). (**A**) LPS inhalation increased protein concentrations of the CXCR3 ligands CXCL9, CXCL10, and CXCL11, measured in the BAL 5h, 24h, 48h, and 72h following LPS challenge, compared to control mice. Results were expressed as mean + SEM (n=8 mice per time point). *p<0.05, **p<0.01, ***p<0.001, ****p<0.0001 versus control mice using Student t test. (**B**) Representative gating strategy for $CXCR3^+$ myeloid and lymphoid cells. (**C**) CXCR3 expression on BAL lymphoid and myeloid infiltrating cells. Results are expressed as mean + SEM of the mean fluorescence intensity (MFI) of CXCR3 obtained for each LPS challenged mouse (n=7-8 mice per time point) corrected by the MFI obtained in the fluorescence minus one (FMO) controls for CXCR3. Negative MFI values were

set to 0. The complete gating strategy for lymphoid and myeloid cells is illustrated in Fig. *S*3. (**D**) Proportion of $CXCR3^+$ lymphoid and myeloid cells expressed as percentages (mean + SEM) of the $CD45^+CD11b^-$ and $CD45^+CD11b^+$ parent population, respectively, in the BAL (see gating strategy in Figure *S*3) (n=7-8 mice per time point). (**E**) Time course of BAL $CXCR3^+$ lymphoid and myeloid cell infiltrates. Results are expressed as absolute counts in the BAL (mean + SEM). **p<0.01, ***p<0.001, ****p<0.0001 using Student t test versus control mice. (**F**) LPS inhalation increased protein concentrations of the CXCR4 ligand CXCL12, measured in the BAL 5h, 24h, 48h, and 72h following LPS nebulization compared to control mice. Results were expressed as mean + SEM (n= 7-8 mice per time point). **p<0.01, ****p<0.0001 versus control mice using Student t test. (**G**) Representative gating strategy for $CXCR4^+$ myeloid and lymphoid cells. (**H**) CXCR4 expression on BAL lymphoid and myeloid infiltrating cells. Results are expressed as mean + SEM of the MFI of CXCR4 obtained for each LPS challenged mouse (n= 7-8 mice per time point) corrected by the MFI obtained in the FMO controls for CXCR4. Negative MFI values were set to 0. The gating strategy for lymphoid and myeloid cells is illustrated in Figure *S*3. (**I**) Proportion of $CXCR4^+$ lymphoid and myeloid cells expressed as percentages (mean + SEM) of the $CD45^+CD11b^-$ and $CD45^+CD11b^+$ parent population, respectively, in the BAL (see gating strategy in Figure *S*3) (n= 7-8 mice per time point). (**H**) Time course of BAL $CXCR4^+$ lymphoid and myeloid cell infiltrates. Results are expressed as absolute counts in the BAL (mean + SEM) (n= 7-8 mice per time point). **p<0.01, ***p<0.001, ****p<0.0001 using Student t test versus control mice.

Figure 3: Antagonism of CXCR7 increases plasma CXCL11 and CXCL12 levels and decreases $CXCR3^+$ and $CXCR4^+$ BAL infiltrates post LPS challenge. ALI was induced by nebulized LPS inhalation and DBA/1 mice were treated with vehicle (LPS-Vehicle, black bars) or ACT-1004-1239 (LPS-ACT-1004-1239, 100mg/kg, red bars) orally, twice daily, 1h prior to LPS challenge. Control mice received vehicle 1h prior NaCl 0.9% inhalation (NaCl-Vehicle, white bars; n=12 mice, pool of all time points). Protein concentrations of CXCL11 and CXCL12 in the plasma and lung tissue and BAL flow cytometry of immune infiltrates were performed 24h, 48h, and

72h after challenge (n=6-8 mice per time point). Time course of CXCL11 protein concentration in the plasma (A) and lung tissue (B). Chemokine concentrations are expressed in pg/ml (plasma) or pg/lung homogenate (mean+SEM). **p<0.01, ***p<0.001 versus LPS-Vehicle treated animals or #p<0.05, ### p<0.001 versus NaCl-Vehicle-treated control mice using Student t tests. Time course of BAL $CXCR3^+$ lymphoid (C) and myeloid (D) infiltrates. Results are expressed as absolute cell counts in the BAL (mean+SEM). *p<0.05, ****p<0.0001 versus LPS-Vehicle-treated animals or ### p<0.001, #### p<0.0001 versus NaCl-Vehicle-treated control mice using Student t tests. Time course of CXCL12 concentration in the plasma (E) and lung tissue (F). Chemokine concentrations are expressed in ng/ml (plasma) or ng/ lung homogenate (mean+SEM). ****p<0.0001 versus LPS-Vehicle-treated animals or #p<0.05, ###p<0.001 versus NaCl-Vehicle-treated control mice using Student t tests. Time course of BAL $CXCR4^+$ lymphoid (G) and BAL $CXCR4^+$ myeloid (H) infiltrates. Results are expressed as absolute counts in the BAL (mean+SEM). *p<0.05, **p<0.01, using Student t test versus LPS-Vehicle-treated animals or ###p<0.001, ####p<0.0001 versus NaCl-Vehicle-treated control mice using Student t tests.

Figure 4: Treatment with ACT-1004-1239 dose-dependently increases plasma CXCL11 and CXCL12 levels and reduces BAL T cell and inflammatory macrophage infiltrates in the LPS-induced ALI/ARDS model. Vehicle (Veh; black bars) or ACT-1004-1239 (10, 30 or 100 mg/kg; bars with different shades of red) was given orally, twice daily, starting 1 h prior LPS nebulization, for a total of 6 administrations. Control mice (white bars) were challenged by NaCl nebulization and received vehicle administrations. Plasma CXCL11 (A) and plasma CXCL12 levels (B) 72h after LPS or NaCl challenge. Results are expressed as mean + SEM (n = 10-25 mice per treatment-LPS groups and n = 4-5 mice for control group). *p<0.05, ****p<0.0001 versus vehicle-treated LPS-challenged mice, using one-way ANOVA test followed by Dunnett's multiple comparisons test. Total BAL T cell (C) and BAL inflammatory macrophage counts (D) 72h after LPS challenge. Results are expressed as mean+SEM with n=11-23 mice per treatment-LPS groups and n=3 for controls. **p<0.01, ***p<0.001, ****p<0.0001 versus vehicle-treated LPS-

challenged mice, using one-way ANOVA test followed by Dunnett's multiple comparisons test.

Figure 5: Antagonism of CXCR7 reduces LPS-induced ALI/ARDS. Treatment with the CXCR7 antagonist ACT-1004-1239 significantly reduced LPS-induced breathing pattern alteration (**A**), alveolar-capillary barrier permeability (**B**) and immune cell infiltrates in the bronchoalveolar space (**C**) as compared to vehicle treated-LPS exposed mice. Mice were treated with vehicle (LPS-Vehicle; black) or ACT-1004-1239 (100mg/kg, LPS-ACT-1004-1239) orally, twice daily, starting 1h prior to LPS challenge (preventive setting; LPS-ACT_{Prev}; red) or 3h after LPS challenge (therapeutic setting; LPS-ACT_{Ther}; hatched bar). Control mice were treated with vehicle and inhaled NaCl 0.9% (NaCl-Vehicle; white). (**A**) Preventive treatment with ACT-1004-1239 reduced the LPS-induced breathing pattern alteration, measured by the calculated enhanced pause (Penh) using whole-body plethysmography in conscious unrestrained mice over a period of 6h following LPS inhalation. Results are expressed as the mean percentage Penh area under the curve (AUC) normalized to the baseline + SEM (n=8 mice per group). ****$p<0.0001$ using two-way ANOVA, followed by Dunnett's multiple comparisons test versus LPS-Vehicle-treated mice. (**B**) Preventive and therapeutic treatment with ACT-1004-1239 reduced alveolar-capillary barrier permeability, measured by a reduction in total protein concentration in BAL supernatant 48h after LPS challenge (n=7-16 mice per LPS-challenged groups; n=6 NaCl-Vehicle control mice). Results are expressed as mean + SEM. *$p<0.05$, **$p<0.01$ versus LPS-Vehicle-treated mice using one-way ANOVA followed by Dunnett's multiple comparisons test. (**C**) Preventive and therapeutic treatment with ACT-1004-1239 reduced immune cell infiltrates in the BAL, measured by flow cytometry 48h after LPS challenge (n=7-16 mice per LPS-challenged groups; n=6 NaCl-Vehicle control mice). Results are expressed as mean + SEM. * $p<0.05$, **$p<0.01$, ***$p<0.001$, ****$p<0.0001$ versus LPS-Vehicle-treated mice using two-way ANOVA followed by Dunnett's multiple comparisons test. The gating strategy for all immune populations is illustrated in Fig S1 A and B.

Figure 6: Summary of pathological role of CXCR7 and potential benefit of CXCR7 antagonism during ALI/ARDS. (**A**) CXCR7 functions predominantly as a scavenger receptor for its two ligands: the interferon-inducible chemokine CXCL11 and the constitutive chemokine CXCL12. Binding of its ligands leads to internalization of the CXCR7-ligand complex and ligand degradation. CXCL11 and CXCL12 also bind and activate the signaling chemokine receptors CXCR3 and CXCR4, respectively. The CXCR3/CXCR4/CXCR7 axes play an important role in lung inflammation. CXCR7 scavenging activity tightly regulates the extracellular levels of its ligands, facilitating the establishment and maintenance of CXCL11/12 chemokine concentration gradients and $CXCR3^+$/$CXCR4^+$ cell migration from the blood to the inflamed lung. In addition, increased CXCR7 expression in the inflamed lung has been reported to be associated with breathing pattern alteration and endothelial barrier dysfunction.
(**B**) CXCR7 antagonism with the CXCR7 antagonist ACT-1004-1239 exhibits immunomodulatory effects: by blocking the scavenging activity of the receptor and consequently increasing CXCL11 and CXCL12 plasma concentrations, chemokine gradients are disrupted, inhibiting $CXCR3^+$ and $CXCR4^+$ cell migration to the inflamed lung. In addition, treatment with ACT-1004-1239, by increasing plasma CXCL12 and/or by direct inhibition of CXCR7 signaling, ameliorates ALI-induced breathing pattern alteration and endothelial barrier dysfunction.

Table 1: **Time course of immune cells present in the BAL following LPS or NaCl challenge in DBA/1 mice.** ALI was induced by LPS nebulization in male DBA/1 mice and flow cytometry analysis of BAL immune infiltrates was performed 5h, 24h, 48h, and 72h after LPS challenge (n=7-16 mice per time point). Control mice received a nebulization of NaCl 0.9% (n=20 mice; all time points were pooled). The gating strategy for all immune populations is illustrated in Figure *S1A*. Results are expressed as mean ± SEM. *p<0.05, **p<0.01, ***p<0.001, ****p<0.0001 versus control mice using Student t test.

Challenge:		**NaCl (control)**	**LPS**			
Time points post challenge		Pool (n=20)	5h (n=8)	24h (n=16)	48h (n=16)	72h (n=7-8)
		Abs number (x10^3 cells/BAL)				
CD11b^{low} FSC^{high}	Alveolar macrophages	19.4 ± 2.9	16.6 ± 2.7	46.3 ± 13.1*	38.7 ± 10.2	40.5 ± 9.6*
CD11b^{+} cells (Myeloid cells)	Neutrophils	0.2 ± 0.0	281.0 ± 61.4****	352.3 ± 29.2****	53.0 ± 8.3****	1.7 ± 0.3****
	Inflammatory Macrophages	1.6 ± 0.3	4.1 ± 0.5***	19.1 ± 3.6****	21.4 ± 3.1****	7.8 ± 1.4****
CD11b^{-} cells (Lymphoid cells)	NK cells	0.1 ± 0.0	0.6 ± 0.1****	9.9 ± 1.6****	6.1 ± 1.1****	1.7 ± 0.4****
	T cells	0.2 ± 0.0	0.6 ± 0.1***	6.2 ± 0.8****	10.7 ± 2.1****	4.3 ± 0.9****
	B cells	0.0 ± 0.0	0.1 ± 0.0	4.6 ± 1.6**	1.8 ± 0.4****	0.2 ± 0.0*
	pDCs	0.0 ± 0.0	0.0 ± 0.0	3.4 ± 0.9***	1.7 ± 0.6**	0.1 ± 0.0****
	DCs	0.9 ± 0.2	0.7 ± 0.0	1.8 ± 0.4*	1.8 ± 0.2**	1.3 ± 0.2

Figure 1: Characterization of the LPS-induced ALI/ARDS model in male DBA/1 mice.

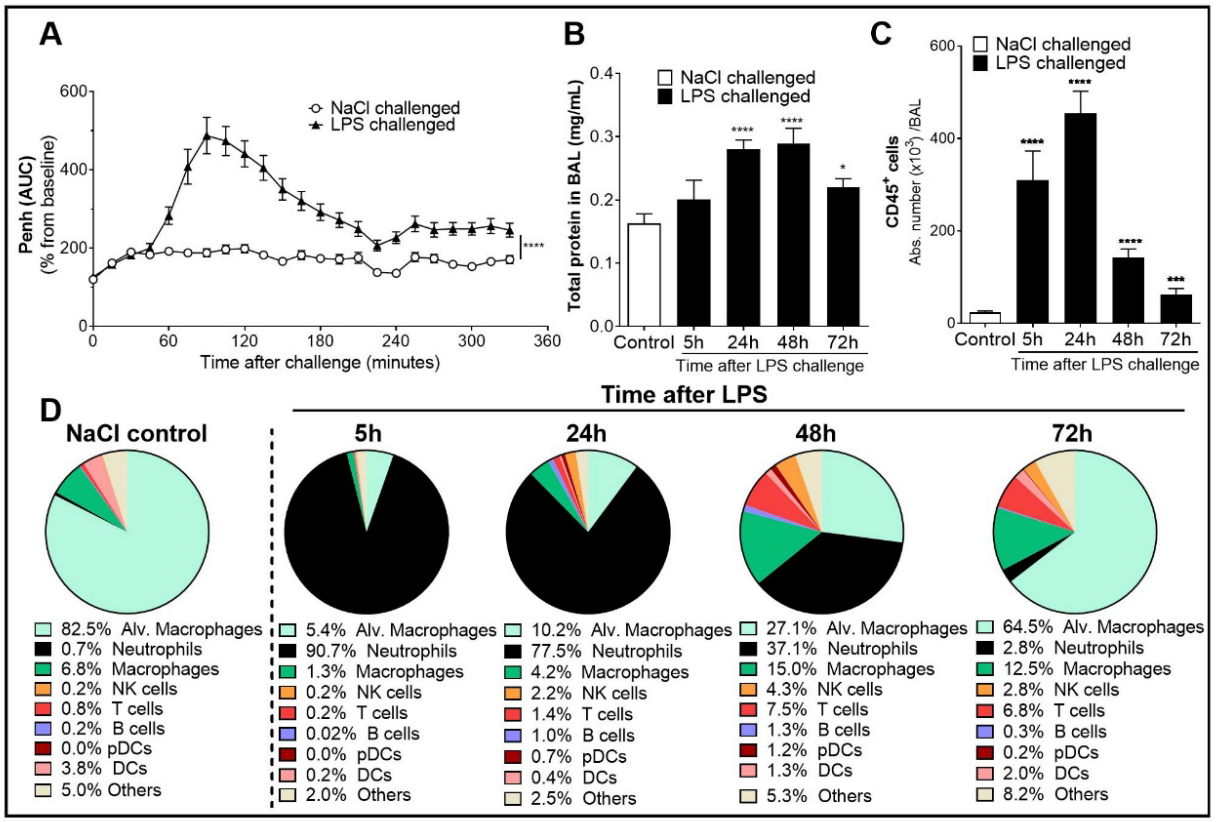

Figure 2: Kinetics of the expression of CXCR3/CXCR4 and its ligands in the bronchoalveolar lavage of LPS-challenged DBA/1 mice.

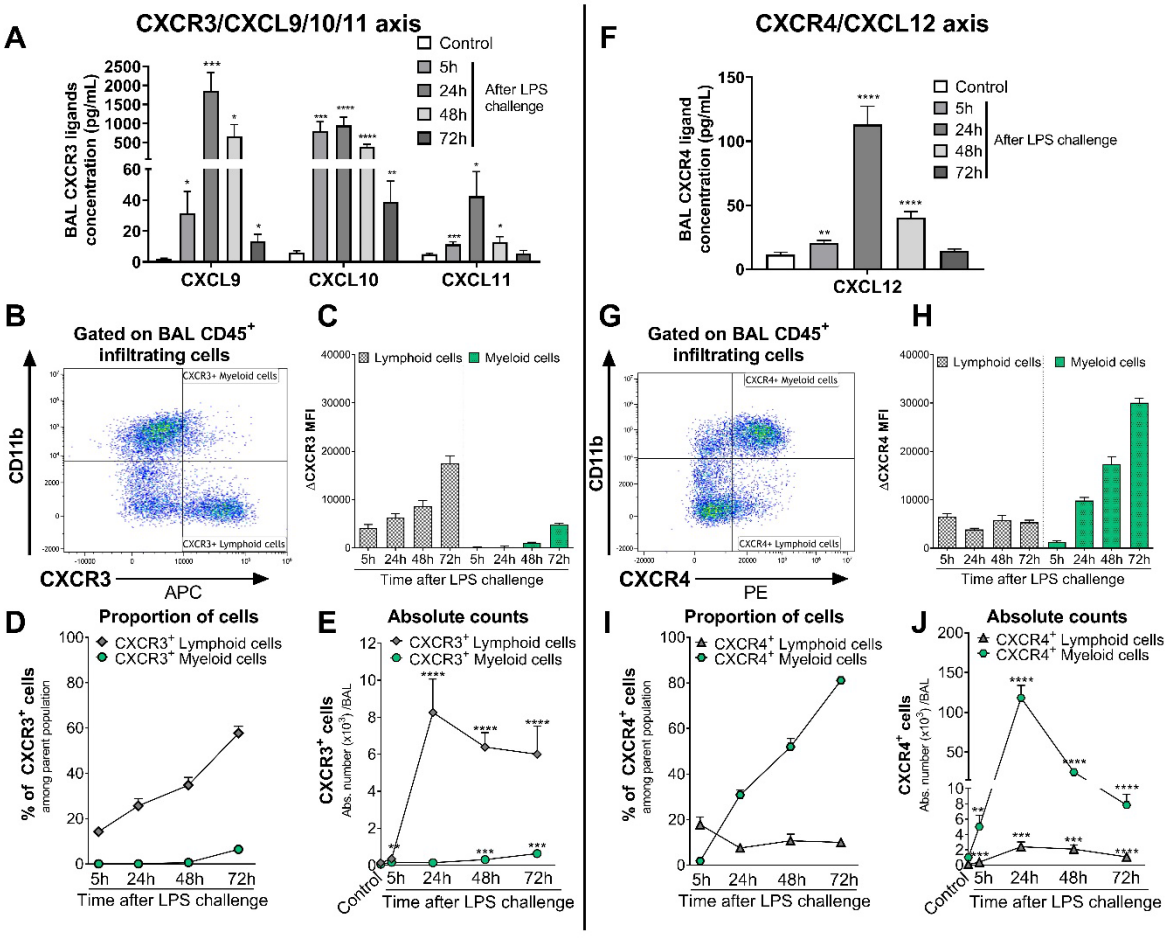

Figure 3: Antagonism of CXCR7 increases plasma CXCL11 and CXCL12 levels and decreases CXCR3$^+$ and CXCR4$^+$ BAL infiltrates post LPS challenge.

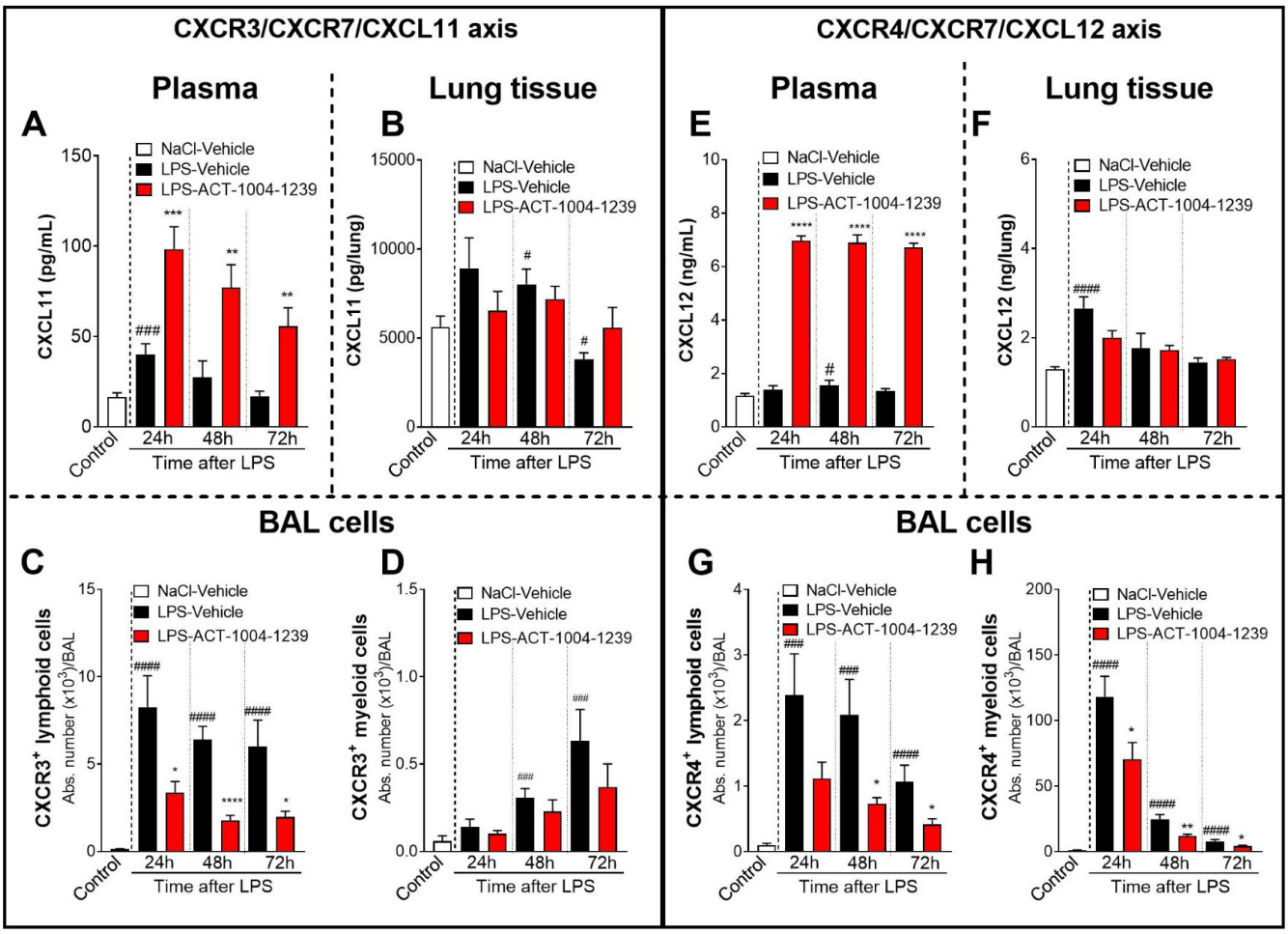

Figure 4: Treatment with ACT-1004-1239 dose-dependently increases plasma CXCL11 and CXCL12 levels and reduces BAL T cell and inflammatory macrophage infiltrates in the LPS-induced ALI/ARDS model.

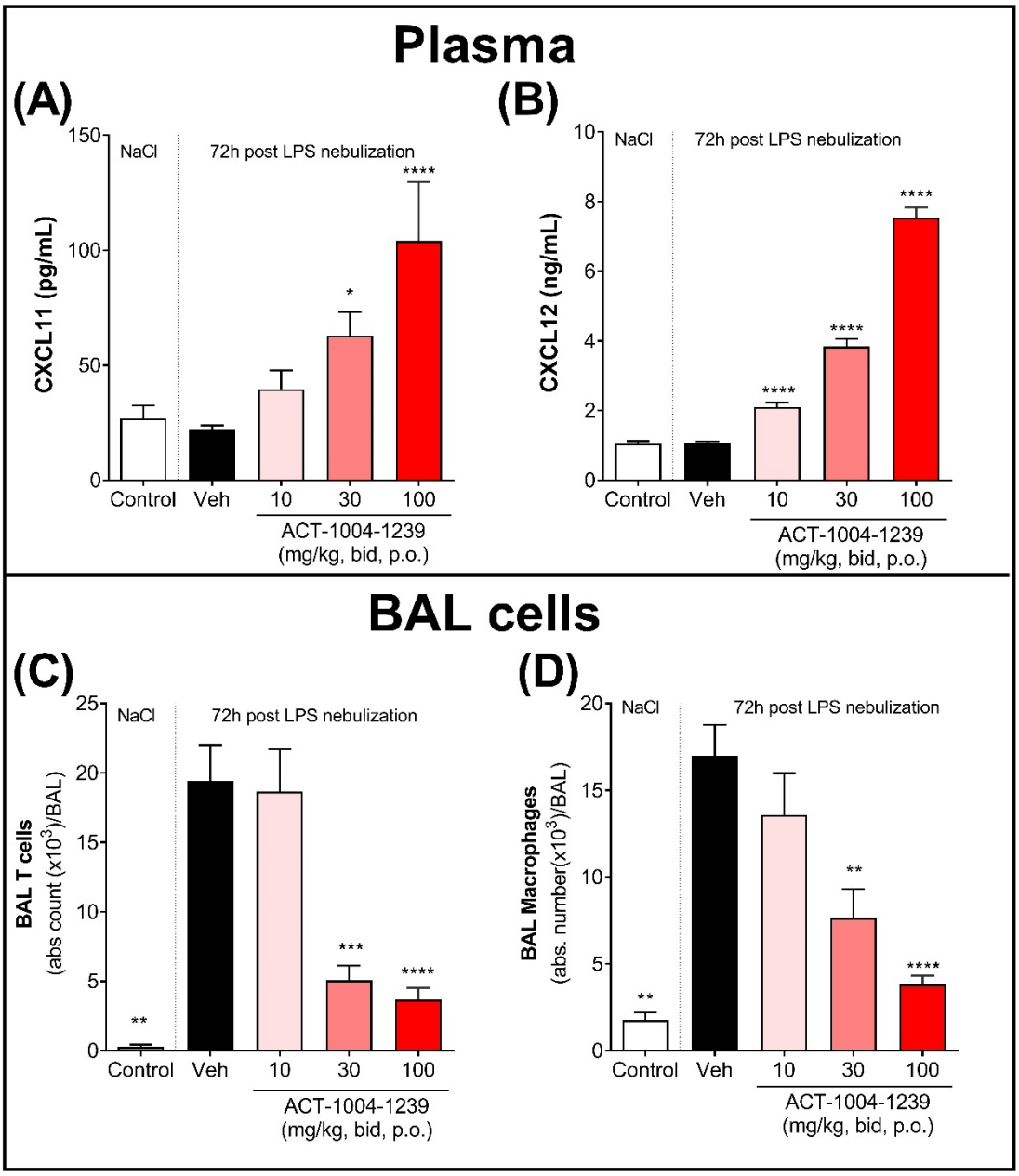

Figure 5: Antagonism of CXCR7 reduces LPS-induced ALI/ARDS.

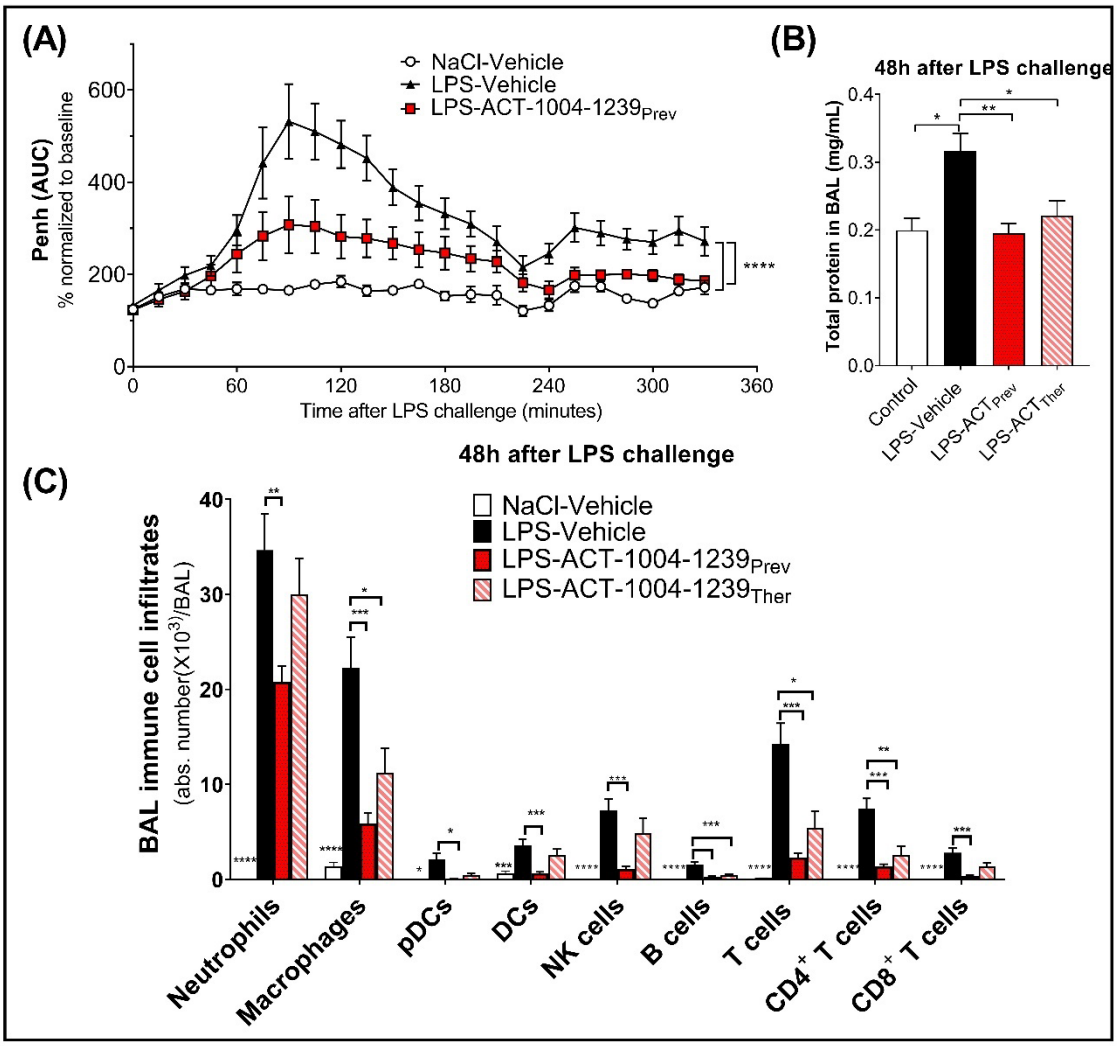

Figure 6: Summary of pathological role of CXCR7 and potential benefit of CXCR7 antagonism during ALI/ARDS.

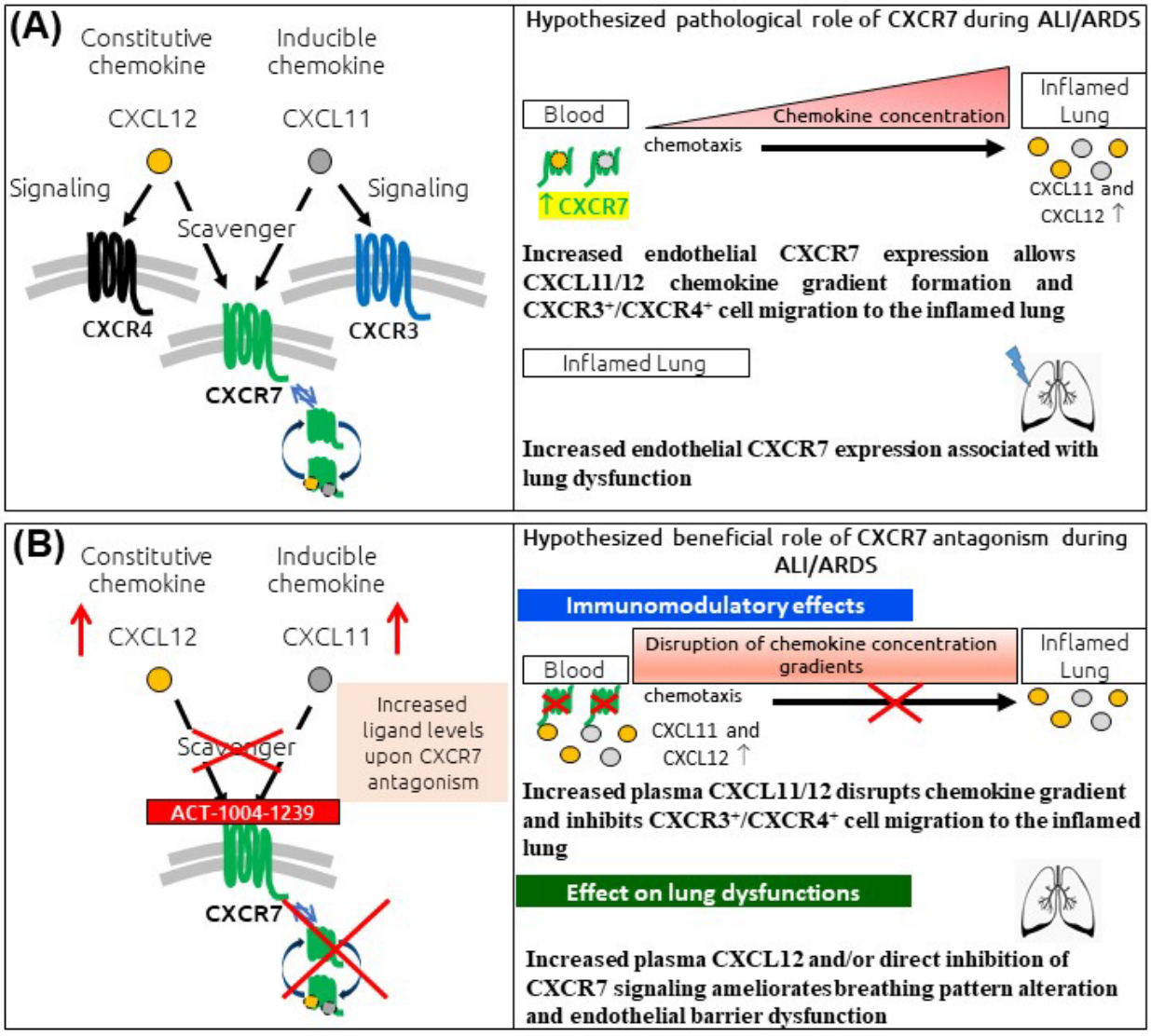

Supplementary materials

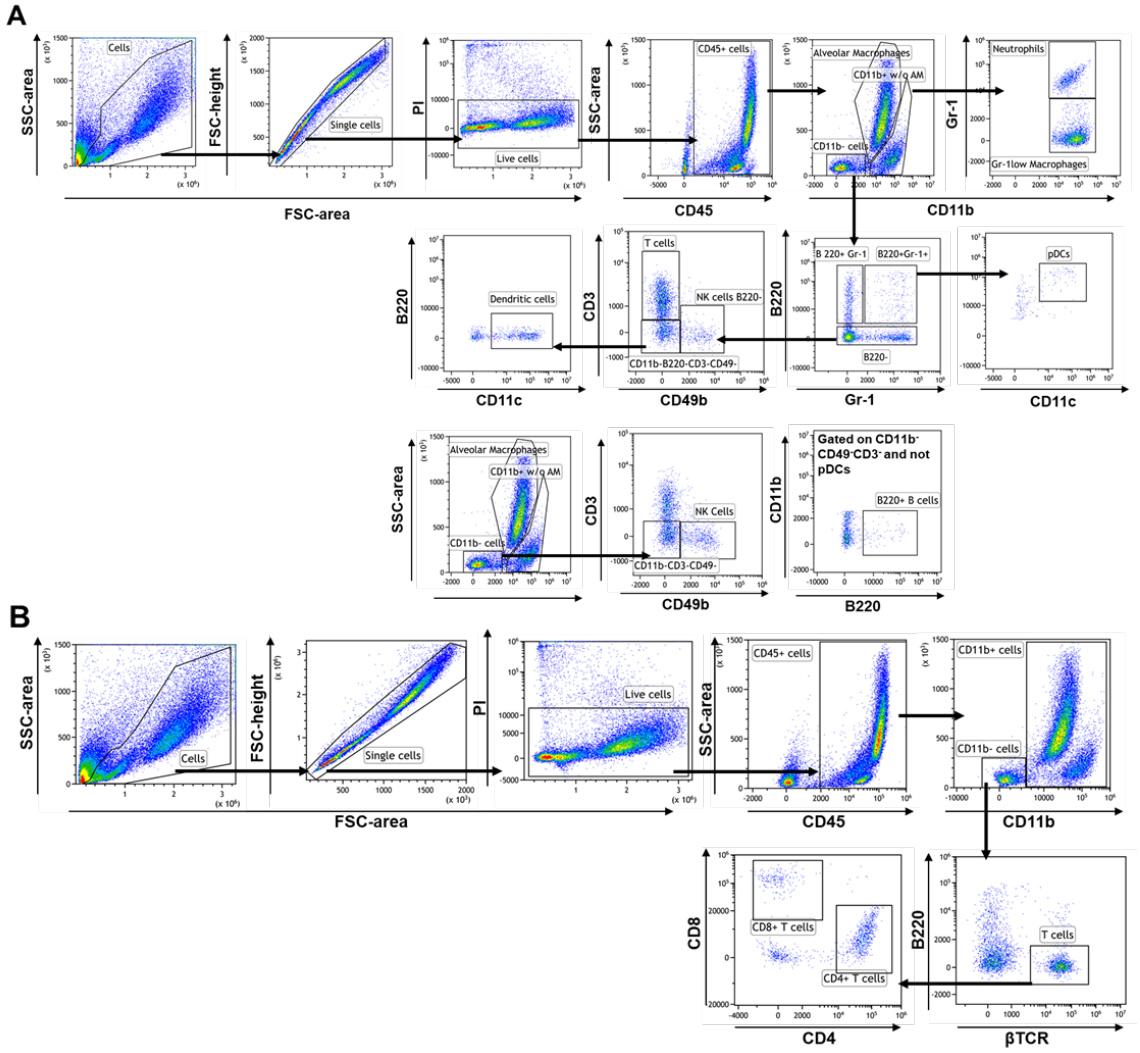

Figure S1. Gating strategy for bronchoalveolar lavage (BAL) cell immunophenotyping. Male DBA/1 mice were exposed to nebulized LPS. BAL samples were collected 5h, 24h, 48h and 72h post LPS challenge and analyzed using flow cytometry. The gating strategy depicts representative plots from vehicle-treated mice, 72h post LPS challenge. (A) After gating on the cell population based on forward scatter (FSC) vs. side scatter (SSC), the exclusion of doublets and dead cells, $CD45^+$ viable cells were defined against the SSC. Among $CD45^+$ cells, the following populations were gated: alveolar macrophages ($CD11b^{int}$, SSC^{high}), macrophages ($CD11b^+$, $Gr\text{-}1^{low}$), neutrophils ($CD11b^+$, $Gr\text{-}1^{high}$), plasmacytoid dendritic cells (pDCs) ($CD11b^-$, $Gr\text{-}1^{int}$, $B220^+$, $CD11c^+$), T cells ($CD11b^-$

, $B220^-$, $CD49b^-$, $CD3^+$), classical $CD11b^-$ dendritic cells (DCs) ($CD11b^-$, $B220^-$, $CD49b^-$, $CD3^-$, $CD11c^+$ cells), natural killer (NK) cells ($CD11b^-$, $CD3^-$, $CD49b^+$), and B cells ($CD11b^-$, $Gr\text{-}1^-$, $CD49b^-$, $CD3^-$, $B220^+$). (B) After gating on the cell population based on FSC vs. SSC, the exclusion of doublets and dead cells, $CD45^+$ viable cells were defined against the SSC. $CD45^+$ cells were then further gated on CD11b vs. SSC, and the $CD11b^-$ cells on B220 vs. βTCR to select βTCR^+B220^- T cells. Subpopulation of βTCR^+B220^- T cells were then further defined based on their CD8 vs. CD4 stain.

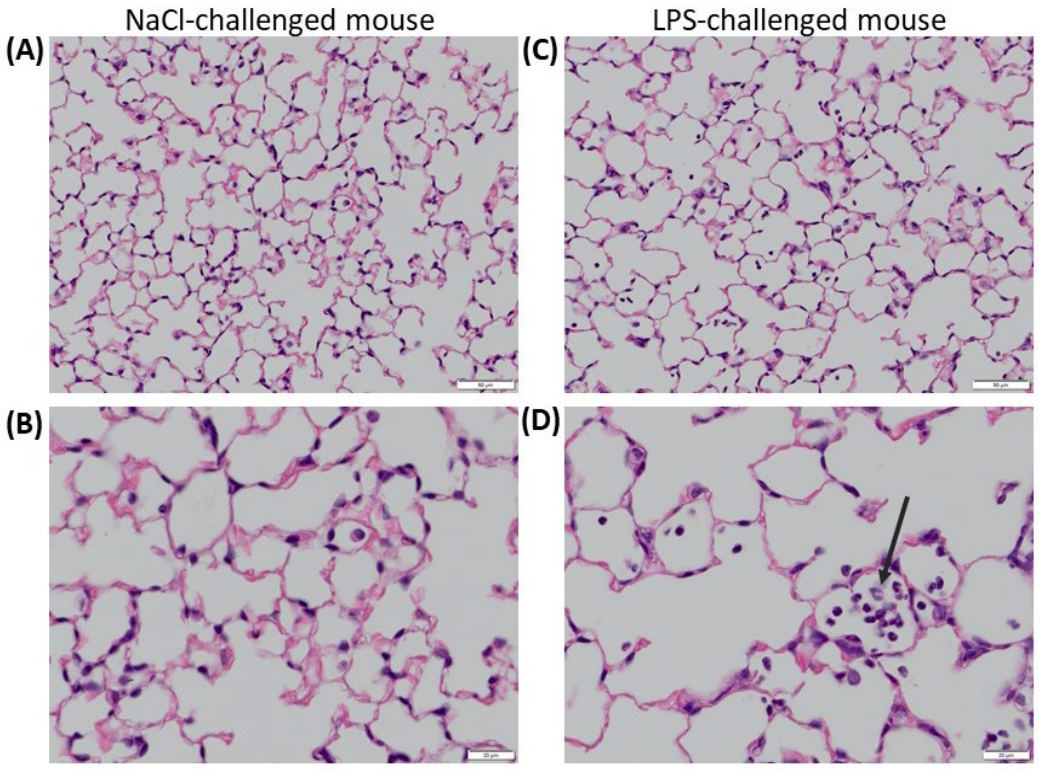

Figure S2: Representative pictures of lung tissue stained with hematoxylin & Eosin. Male DBA/1 mice were exposed to nebulized NaCL (control) or LPS. 24 hours following challenge, mice were euthanized with pentobarbital and lungs were collected as a whole, filled with 4% paraformaldehyde and then postfixed for 24h, dehydrated with alcohol, and embedded in paraffin wax. Lung paraffin sections of 2 µm were stained with hematoxylin-Eosin and assessed by a pathologist for evidence of inflammation. (A and B) 20x and 40x, respectively from a control mouse challenged with NaCl. (C and D) 20x and 40x, respectively from a mouse challenged with LPS. (scale bar, 20µm in B and D and 50µm inA and C) The arrow shows a neutrophil.

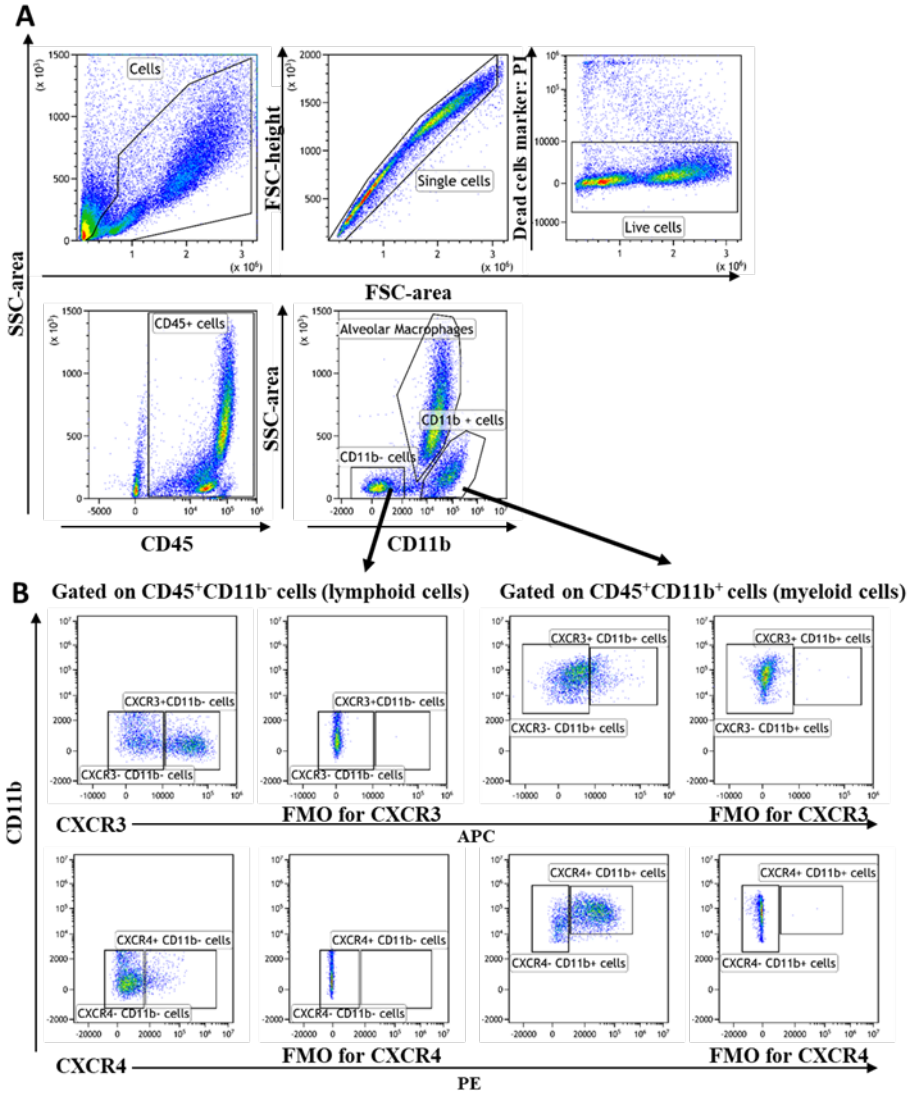

Fig. S3. Gating strategy for bronchoalveolar lavage (BAL) lymphoid and myeloid cell immunophenotyping. Male DBA/1 mice were exposed to nebulized LPS. BAL samples were collected 5h, 24h, 48h and 72h post LPS challenge and analyzed using flow cytometry. The gating strategy depicts representative plots from vehicle-treated mice, 72h post LPS challenge. (A) After gating on the cell population based on FSC vs. SSC, excluding doublets and dead cells, $CD45^+$ viable cells were defined against the SSC. Among $CD45^+$ cells, the following populations were gated: alveolar macrophages ($CD11b^{int}$, SSC^{high}), lymphoid cells ($CD11b^-$, SSC^{lo}), myeloid cells ($CD11b^+$, SSC^{lo}). (B) Gating strategy for $CXCR3^+$ and $CXCR4^+$

BAL lymphoid and myeloid cells based on the FMO control for CXCR3 and CXCR4, respectively.

3 Article II: Effect of ACT-1004-1239 in preclinical MS models

3.1 Preamble

Pharmacology studies are part of the preclinical development package needed to initiate FIH trials with a PCC compound (Introduction, section 2.2). Therefore, one of my main goals with ACT-1004-1239 was to demonstrate that this first-in-class ACKR3 antagonist exhibited the desired pharmacological activity to justify its development for the targeted MS indication.

Previous findings with the ACKR3 agonist, CCX771, suggested that ACKR3 might be a good target to both reduce inflammatory infiltrates and enhance myelin repair into the CNS (see Introduction, section 3.4). However, it remained unclear whether the observed beneficial effects were due to CCX771 agonistic activity on ACKR3 through β-arrestin recruitment or CCX771 functional antagonism induced by receptor desensitization (see Introduction, section 3.5).

To fulfill our objective, we assessed the efficacy of ACT-1004-1239 in several preclinical models reflecting relevant aspects of MS disease, including neuroinflammation and demyelination. Some models were established in my laboratory (EAE model) and others were ran in collaboration with contract research organizations (cuprizone model and *in vitro* co-culture assay) under my supervision.

In line with the literature, treatment with ACT-1004-1239 demonstrated both immunomodulatory and pro-myelinating therapeutic effects, that supported the preclinical development package allowing us to submit an IND to start a Phase I clinical trial in healthy volunteers.

3.2 Manuscript

ACT-1004-1239, a first-in-class CXCR7 antagonist with both immunomodulatory and pro-myelinating effects for the treatment of inflammatory demyelinating diseases

Laetitia Pouzol[1], Nadège Baumlin, Anna Sassi, Mélanie Tunis, Julia Marrie, Enrico Vezzali, Hervé Farine, Ulrich Mentzel, and Marianne M. Martinic

Affiliation: Idorsia Pharmaceuticals Ltd, Allschwil, Basel-Landschaft, Switzerland
[1]Correspondence to Laetitia Pouzol:
Idorsia Pharmaceuticals Ltd
Hegenheimermattweg 91
4123 Allschwil
Basel-Landschaft
Switzerland
E-Mail: laetitia.pouzol@idorsia.com
Telephone: +41-58-844 07 12

***FASEB Journal*, published online 20 February 2021, DOI: 10.1096/fj.202002465R**

Short Running Title:

Dual mode of action of ACT-1004-1239 in MS models

Non-standard abbreviations
Bid: twice daily
CFA: Complete Freund's Adjuvant
CNS: Central nervous system
CPZ: Cuprizone
CV-LFB: Cresyl-violet and Luxol fast blue
EAE: Experimental autoimmune encephalomyelitis
GPCR: G-protein-coupled receptors

IFA: Incomplete Freund's Adjuvant
i.p.: intraperitoneal
LFB-CV: Luxol fast blue-Cresyl Violet
MBP: Myelin basic protein
MdCs: Monocyte-derived cells
MOG: Myelin oligodendrocyte glycoprotein
MS: Multiple sclerosis
NfL: Neurofilament light chain
NK: Natural killer
OL: Oligodendrocyte
OPC: Oligodendrocyte precursor cell
PBS: phosphate buffer saline
pDC: Plasmacytoid dendritic cell
s.c.: subcutaneous
TSA: Tyramide Signal Amplification

ABSTRACT

Current strategies for the treatment of demyelinating diseases such as multiple sclerosis (MS) are based on anti-inflammatory or immunomodulatory drugs. Those drugs have the potential to reduce the frequency of new lesions but do not directly promote remyelination in the damaged central nervous system (CNS). Targeting CXCR7 (ACKR3) has been postulated as a potential therapeutic approach in demyelinating diseases, leading to both immunomodulation by reducing leukocyte infiltrates and promyelination by enhancing myelin repair. ACT-1004-1239 is a potent, selective, insurmountable, and orally available first-in-class CXCR7 receptor antagonist. The effect of ACT-1004-1239 was evaluated in the myelin oligodendrocyte glycoprotein (MOG)-induced experimental autoimmune encephalomyelitis (EAE) and the cuprizone-induced demyelination mouse models. In addition, ACT-1004-1239 was assessed in a rat oligodendrocyte precursor cell (OPC) differentiation assay *in vitro*. In the MOG-induced EAE model, ACT-1004-1239 treatment (10-100 mg/kg, twice daily, orally) showed a significant dose-dependent reduction in disease clinical scores, resulting in increased survival. At

the highest dose tested (100 mg/kg, twice daily), ACT-1004-1239 delayed disease onset and significantly reduced immune cell infiltrates into the CNS and plasma neurofilament light chain concentration. Treatment with ACT-1004-1239 dose-dependently increased plasma CXCL12 concentration, which correlated with a reduction of the cumulative disease score. Furthermore, in the cuprizone model, ACT-1004-1239 treatment significantly increased the number of mature myelinating oligodendrocytes and enhanced myelination *in vivo*. *In vitro,* ACT-1004-1239 promoted the maturation of OPCs into myelinating oligodendrocytes. These results provide evidence that ACT-1004-1239 both reduces neuroinflammation and enhances myelin repair substantiating the rationale to explore its therapeutic potential in a clinical setting.

Keywords:

CXCR7
Experimental autoimmune encephalomyelitis
Immunomodulation
Myelin repair
Demyelinating diseases

INTRODUCTION

Multiple sclerosis (MS) is a chronic autoimmune demyelinating disease of the central nervous system (CNS) that results in multiple neurological deficits. Pathologically, the disease is characterized by inflammation, blood-brain barrier increased permeability, gliosis, multifocal plaques of demyelination, and axonal loss[1]. Loss of myelin coupled with an inability to achieve remyelination leads to subsequent degeneration of axons and eventually neuronal loss which might underlie the neurological disability observed in patients[2]. Current MS treatment strategies are based on anti-inflammatory or immunomodulatory drugs that have the potential to reduce the number of newly evolving lesions. However, these therapies do not actively promote remyelination in the damaged CNS and are therefore much less effective in progressive stages of the disease[3,4,5]. In view of the complex pathogenesis of MS, a therapy that has both immunomodulatory and remyelinating properties could prove to be highly beneficial to patients.

Many chemokines and their receptors are dysregulated in active plaque lesions, blood, and cerebrospinal fluid in different stages of MS disease[6,7,8]. CXCR7, also referred to as ACKR3, is an atypical chemokine receptor which is expressed on endothelial cells and other non-lymphoid cells including mesenchymal cells, neurons, astrocytes, and oligodendrocyte precursor cells (OPCs)[9,10,11,12]. Unlike classical G-protein-coupled receptors (GPCRs), CXCR7 does not signal through G protein pathways, but rather functions predominantly as a scavenger receptor for a number of different ligands including the chemokines CXCL11 and CXCL12 as well as several opioid peptides[13]. Binding of its ligands leads to β-arrestin recruitment followed by internalization of the CXCR7-ligand complex[9,14] and ligand degradation[15]. Importantly, while CXCL11 and CXCL12 show a higher binding affinity to CXCR7[9,14], they also bind to and activate the signaling chemokine receptors CXCR3 and CXCR4, respectively. Both these receptors play an important role in the trafficking of immune cells and are heavily implicated in the pathology of a number of diseases including MS[7]. CXCR7 scavenging activity tightly regulates the extracellular levels of these chemokines, facilitating the establishment and the

maintenance of CXCL11 and CXCL12 chemokine concentration gradients, thereby indirectly influencing both CXCR3- and CXCR4-mediated functions[16,17,18].

Findings from studies in patients with MS and in preclinical settings suggest that CXCL12 expression at the perivascular space within plaque lesions plays a role in facilitating the infiltration of CXCR4-expressing leukocytes in the CNS[19,20,21]. Furthermore, in experimental autoimmune encephalomyelitis (EAE), a murine model of MS, the pathological increase and change in spatial distribution of CXCL12 has been associated with an increased expression of CXCR7 on endothelial cells triggering CXCL12 internalization[10]. Treatment with an agonist behaving as a functional CXCR7 antagonist prevented this pathological CXCL12 redistribution and resulted in reduced CNS inflammatory infiltrates and axonal damage[21,22].

Besides the role of CXCR7 in leukocyte migration, the CXCR7/CXCR4/CXCL12 axis also plays a role in the recruitment and maturation of OPCs which have been implicated in contributing to remyelination and neuroprotection in MS[23,24,25,26]. CXCR7 is expressed on oligodendroglial cells in human MS brains and, in vitro, CXCL12 has been shown to induce differentiation of human OPCs[11]. Similar to what is observed in humans, both CXCR4 and CXCR7 are also expressed on OPCs in mice[10]. The CXCR4/CXCL12 axis has been shown to promote the maturation of OPCs, leading to myelin repair after a CNS injury[24,27]. Importantly, CXCR7 expression is enhanced during demyelination in preclinical models of MS[10,25]. This points to a potentially detrimental role of CXCR7, which, by scavenging CXCL12 within the demyelinated area, inhibits CXCR4/CXCL12-mediated OPC proliferation and maturation, and ultimately remyelination. In preclinical studies, treatment with CCX771, a CXCR7 agonist, led to increased CXCL12 levels in the CNS and increased CXCR4/CXCL12-dependent OPC maturation, resulting in increased myelin content[25].

While the scavenging activity of the CXCR7 receptor is widely accepted, less consensus exists regarding the potential signaling capacity of CXCR7[28]. Since only CXCR7 agonists which recruit β-arrestin upon binding to the receptor have been used in preclinical MS models,[21,22,29,30] it remains unclear whether the observed

activity is due to their agonistic activity on CXCR7 through β-arrestin recruitment or their functional antagonism induced by receptor desensitization. To elucidate whether CXCR7 receptor antagonism was indeed responsible for both the prevention of leukocyte infiltration and increased myelination, ACT-1004-1239, a first-in-class, potent, selective, and insurmountable small molecule CXCR7 receptor antagonist was developed[31]and evaluated in the myelin oligodendrocyte glycoprotein (MOG)-induced experimental autoimmune encephalomyelitis (EAE) and cuprizone-induced demyelination mouse models. In addition, ACT-1004-1239 was assessed in an oligodendrocyte precursor cell (OPC) differentiation assay in vitro.

MATERIALS AND METHODS

Mice and treatment administration.

Female C57BL/6 mice were purchased from Janvier Laboratories (Le Genest-Saint-Isle, France). Male C57BL/6 mice were purchased from Charles River Laboratories (Cologne, Germany). All mice were group-housed in a light-controlled environment and used at 8-9 weeks of age after acclimation. Food and drinking water were available ad libitum.

ACT-1004-1239 was synthesized as previously described[31]. For in vivo studies, ACT-1004-1239 was formulated in 0.5% methylcellulose (Sigma-Aldrich, Schnelldorf, Germany), 0.5% Tween 80 (Sigma-Aldrich) in water. ACT-1004-1239 and vehicle (0.5% methylcellulose, 0.5% Tween-80 in water) were given orally twice a day (bid) at a volume of 5mL/kg at doses and time indicated in the figure legends.

Myelin oligodendrocyte glycoprotein (MOG)-induced EAE model

Under anesthesia with isoflurane, female C57BL/6 mice were immunized in the rear flanks by subcutaneous injection (s.c.) of 150µg MOG_{35-55} peptide (Biotrend Chemicals, Zurich, Switzerland) emulsified 1:1 in Complete Freund's Adjuvant (CFA) (Chondrex, Redmond, WA, USA) containing 4mg/mL Mycobacterium tuberculosis. On days 0 and 2 post-immunization, mice were injected intraperitoneally (i.p.) with

400 ng of pertussis toxin (List Biological Laboratories, Campbell, CA, USA). Vehicle or ACT-1004-1239 were given from day 0 after immunization.

Control mice were injected s.c. with phosphate buffer saline (PBS) emulsified 1:1 in incomplete Freund's Adjuvant (IFA) (Sigma-Aldrich) on day 0. On days 0 and 2, control mice were injected i.p. with PBS.

Clinical score assessment

Mice were scored daily for EAE disease evaluation as follows: 0= no symptoms, 0.5= end tail paralysis, 1= full tail paralysis, 1.5= one hind limb weakness, 2= bilateral partial hind limb paralysis, 2.5= unilateral complete hind limb paralysis, 2.75= score of 2.5 + unilateral partial hind limb paralysis, 3= complete bilateral hind limb paralysis, 3.25= 3 + unilateral partial forelimb paralysis, 3.5= 3 + unilateral complete forelimb paralysis, 4= complete paralysis (moribund) and, 5= death or euthanized. Mice were euthanized if they reached a score of 4, or if they had a score of 3.5 during 3 consecutive days, or a score of 3.25 during 5 consecutive days, or a score of 3 during 7 consecutive days. For each mouse found dead or euthanized, the clinical score of 5 was kept until the end of the study.

All animal EAE experiments were carried out in accordance with the Swiss animal protection law, under protocols approved by the Basel Cantonal Veterinary Office.

Flow cytometry of the CNS tissue

To evaluate immune-cell infiltration in the CNS, brain and spinal cord were harvested at the peak of the disease (16 or 17 days post-immunization) and prepared as neural single cell suspensions and analyzed by flow cytometry. Briefly, mice were euthanized with an overdose of pentobarbital (Esconarkon, Streuli Pharma SA, Uznach, Switzerland), perfused with saline, and spinal cord and right brain hemisphere were isolated and weighed. CNS tissue was homogenized and strained through a 100 mm nylon mesh (Corning, NY, USA). After centrifugation, CNS cell suspensions were separated by 37%/70% Percoll (GE Healthcare, Chicago, IL, USA) centrifugation as previously described[32]. CNS cells were stained with the

following surface monoclonal anti-mouse antibodies: B220 (BD Biosciences, Franklin Lakes, NJ, USA, Clone RA3-6B2), Gr-1 (Biolegend, San Diego, CA, USA, Clone 1RB6-8C5), CD11b (Biolegend, Clone M1/70), CD3 (Biolegend, Clone 17A2), CD45 (Biolegend, Clone 30-F11), CD11c (Biolegend, clone N418), CXCR4 (Invitrogen-Thermo Fisher Scientific, Waltham, MA, USA, Clone 2B11), CD49b (Biolegend, Clone DX5). Staining was performed on ice, in the dark, during 35 minutes after preincubation with a Fc receptor blocker (CD16/CD32, BD Biosciences). Dead cells were excluded based on their positive staining with propidium iodide (PI, CAS 25535-16-4, Sigma-Aldrich). Cell subsets were quantified among singlets/viable/$CD45^+$ cells (PI^-, $CD45^+$ cells): neutrophils ($CD11b^+$, $Gr\text{-}1^{high}$ cells), monocytes ($CD11b^+$, $Gr\text{-}1^{int}$ cells), microglia ($CD11b^+$, $Gr\text{-}1^{low}$, $CD45^{low}$ cells), monocyte-derived cells (MdCs) ($CD11b^+$, $Gr\text{-}1^{low}$, $CD45^{high}$ cells), B cells ($CD11b^-$, $Gr\text{-}1^-$, $B220^+$ cells), plasmacytoid dendritic cells (pDCs) ($CD11b^-$, $Gr\text{-}1^{int}$, $B220^+$, $CD11c^+$ cells), T cells ($CD11b^-$, $B220^-$, $CD49b^-$, $CD3^+$ cells), natural killer (NK) T cells ($CD11b^-$, $B220^-$, $CD49b^+$, $CD3^+$ cells), NK cells ($CD11b^-$, $B220^-$, $CD49b^+$, $CD3^-$ cells), and dendritic cells (DCs) ($CD11b^{-/low}$, $B220^-$, $CD49b^-$, $CD3^-$, $CD11c^+$ cells). The $CXCR4^+$ $CD45^+$cells were identified based on the fluorescence minus one (FMO) control for CXCR4. The gating strategy is illustrated in the supplementary figure 1A.

To detect the pathogenic TNF-α-, IFN-γ-, and IL-17-secreting $CD69^+$T cells, CNS cells were stimulated with MOG_{35-55} at 10 mg/mL final in the presence of GolgiPlug and GolgiStop (BD Biosciences) for 4h. After the stimulation, cells were incubated on ice with a Fc receptor blocker (CD16/CD32, BD Biosciences) and then stained with the following surface fluorochrome conjugated monoclonal anti-mouse antibodies: CD11b (Biolegend, Clone M1/70), CD19 (Biolegend, Clone 6D5), together with Acqua Dye live/dead dye (Invitrogen-Thermo Fisher Scientific). Staining was performed on ice, in the dark, for 20 minutes. Cells were then fixed and permeabilized using Cytofix/Cytoperm solution (BD Biosciences). The intracellular cytokine stain was carried out using the following antibodies diluted in permeabilization buffer (BD Biosciences): IL-17A (Biolegend, Clone TC11-18H10.1), CD3 (BioLegend, Clone 17A2), IFN-γ (Biolegend, Clone XMG1.2), TNF-a

(Biolegend, Clone MP6-XT22), CD69 (BD Biosciences, Clone H1.2F3). The gating strategy is illustrated in Supplementary figure 1B.

Flow cytometry was performed on a CytoFLEX flow cytometer (Beckman Coulter Life Sciences, Nyon, Switzerland) and analyzed using Kaluza analysis software version 2.1 (Beckman Coulter).

Cuprizone-induced demyelination model

Cuprizone (Sigma-Aldrich) was formulated as a homogeneous suspension alone or in combination with ACT-1004-1239, in 0.5% methylcellulose (Sigma), 0.5% Tween 80 (Sigma) in water. Cuprizone or combined cuprizone-ACT-1004-1239 suspensions were prepared freshly, daily, and protected from light. Male C57BL/6 mice were administrated orally, twice a day with vehicle or Cuprizone at 150 mg/kg for six weeks (300 mg/kg/day total). Co-treatment of cuprizone with ACT-1004-1239 (100 mg/kg, bid) was initiated either from the start of cuprizone treatment on day 0 (preventive setting) or after 3 weeks of cuprizone exposure (therapeutic setting). Tissue samples from the vehicle group (control) and cuprizone treatment groups were processed after 6 weeks of cuprizone exposure.

The in-life phase of this study was performed at Charles River Facility (Kuopio, Finland) and was carried out in accordance with the National Institute of Health guidelines for the care and use of laboratory animals and approved by the national animal board from Finland.

Histological analysis

Mice were euthanized with pentobarbital (Mebunat, Orion Pharma, Finland) after 6 weeks of cuprizone or vehicle exposure. After cardiac perfusion with 4% paraformaldehyde, brains were collected, post-fixed into 4% paraformaldehyde for 48 hours, dehydrated with alcohol and embedded in paraffin wax. Frontal brain coronal paraffin sections of 2 µm were stained with Cresyl-violet and Luxol fast blue (CV-LFB) for evidence of demyelination.

Immunohistochemistry

Paraffin Coronal brain sections (4 µm) were stained using Leica Bond RX (Leica Microsystems, Milton Keynes, UK) automated stainer with optimized staining protocols. Oligodendrocytes (OLs) were identified by Olig2 (Invitrogen, #P21954), OPCs by PDGFRa (R&D systems, Minneapolis, MN, USA, #AF1062) and mature OLs by GSTp (MBL, Woburn, MA, USA #312); astrocytes by GFAP (Dako, Agilent Santa Clara, CA, USA, #Z0334). Singleplex IHC using 3,3'-diaminobenzidine (DAB) detection (BOND Intense R Detection, Leica #DS9263) was used for GFAP staining. Multiplex IHC using Tyramide Signal Amplification (TSA) were applied for oligodendrocyte population characterization. 4 fluorophores were used: TSA Plus Cyanine 3.5. fluorescein, Cyanine 5.5 (Akoya Biosciences, Marlborough, MA, USA). Counterstain DAPI (Sigma, #D-9542).

Image acquisition and analysis

Slides were scanned using S60 Nanozoomer whole slide scanner (Hamamatsu Photonics, Solothurn, Switzerland). Images were acquired at 20x magnification for chromogenic staining and 40x for fluorescently labelled staining.

The images were uploaded onto the ORBIT image analysis platform (https://www.orbit.bio; Idorsia Pharmaceuticals Ltd, Allschwil, Switzerland) for quantification[33].

The corpus callosum was delineated manually as region of interest. Following tissue annotation, a classification model and cell segmentation were carried out for positive area percentage and cell count per mm2 analysis, respectively.

Quantification of plasma CXCL12 concentration

Blood was collected in EDTA-coated tubes (BD Microtainer) and centrifuged to prepare plasma. Concentrations of CXCL12 were measured in plasma using a commercial quantikine ELISA mouse CXCL12/SDF1α kit (R&D Systems) according to manufacturer's instructions.

Quantification of plasma Neurofilament light chain (NfL) concentration

Concentrations of NfL were measured in plasma samples using a customized Meso Scale Discovery assay as previously described34 with some modifications. Briefly, multi array 96-well small spot plate (Meso Scale Diagnostics, MSD, Rockville, Maryland, USA)) was coated with 1.25 mg/mL capture monoclonal antibody anti-NF-L 47:3 (Uman Diagnostics, Umea, Sweden) diluted in Carbonate-bicarbonate buffer (0.05 M, pH 9.6) and incubated overnight at 4°C. All following incubation steps were done on a plate shaker and were preceded by three wash steps with 250 µl per well of PBS-Tween 20 0.1% (Sigma-Aldrich). The wells were saturated with 100 mL of 3% milk in PBS and incubated for 1 hour at room temperature (RT). Dilutions of plasma samples (1/5 for MOG EAE mice and 1/2 for control mice in assay buffer (1% milk in PBS from Biorad, Hercules, CA, USA)) were added and the plate was incubated for 2 hours at RT. The detection biotinylated mAB 2:1 (Uman Diagnostics) was diluted at 500 ng/mL in assay buffer, added to the wells, and the plate was incubated 1 hour at RT. Then MSD SULFO-TAGTM labelled streptavidin (MSD) at 250 ng/mL was added and the plate was incubated 1 hour at RT. The electrochemiluminescence (ECL) read buffer (MSD) was added to each well and ECL was determined using the Mesoscale Sector Imager 600 plate reader (MSD). Plasma levels of NfL were interpolated from a standard curve obtained by serial dilutions of a stock solution of bovine NfL (Uman Diagnostics) from 10000 to 10 pg/mL in assay buffer.

Primary co-culture of rat OPCs and neurons

Primary mixed cultures of neurons and OPCs used in this study were differentiated from forebrains from E17 Wistar rat fetuses (Janvier Laboratories) as previously described35. All coculture experiments were performed by Neuro-Sys SAS (Gardanne, France) and were carried out in accordance with the National Institutes of Health Guide for the Care and Use of Laboratory Animals and followed current European Union regulations (Directive 2010/63/EU, Agreement number: A1301310). Viable cells were seeded in 96 well-plates (20'000 cells/well) pre-coated with poly-L-lysine (BD Falcon) and laminin (Sigma-Aldrich) in culture medium as described previously[35]. The plates were maintained at 37 °C in a humidified

incubator, in an atmosphere of air (95 %)-CO2 (5 %). The study was divided into 2 independent experiments (plate 1 and 2) using 2 different preparations of cells to assess maturation of OPCs. Cells were incubated with or without test compounds on day 1 of culture, one day following seeding, and treated up to day 30. Rat CXCL12a (Peprotech, Cranbury, NJ, USA) stimulation was carried out at concentrations of 0.1, 0.3, 1, 3, 10, 30, and 100 ng/mL in culture medium. ACT-1004-1239 was applied at concentrations of 1, 3, and 10mM. The CXCR4 antagonist AMD3100 (Sigma-Aldrich) was added at 3 mM[36]. In each experiment a non-treated control condition and one positive control condition, olesoxime at 300 nM (Sigma-Aldrich), was added to the 96-well plate. Half of the medium was exchanged every other day with fresh medium supplemented with test compounds. Six wells were seeded for each experimental condition.

Immunocytochemistry

On day 30 of co-culture, cell supernatants were collected and the cells were fixed, permeabilized, and stained as previously described[35]. Cells were stained with the following antibodies: Myelin basic protein (MBP, dilution:1/1000, NOVUS Biologicals, Centennial, CO, USA), secondary goat anti-mouse CF488 A (dilution: 1/800, Sigma-Aldrich), goat anti-rabbit CF568 (dilution: 1/400, Sigma-Aldrich). Cell nuclei were stained using a Hoechst solution (Sigma-Aldrich).

30 pictures per well (distributed to cover 80% of the surface of the well) were automatically acquired and analysed using ImageXpress (molecular devices) with 20x magnification, equipped with LED lamp (excitation 360/480/565 and emission 460/535/620). The results were expressed as the average number of cells per picture (n=30 pictures) per well (n=6 wells per experimental condition). The maturation of OPCs into myelinating OLs was estimated by counting the number of MBP positive cells per picture and per well. Some wells were excluded from the analysis as no signal was detected during the image acquisition process and, therefore, the number of wells per experimental condition varied from 4 to 6. For each condition, data were expressed relative to the mean of the non-treated control wells of the same plate, set to 100%.

CXCL12 quantification in the supernatant of the co-cultures

Concentrations of CXCL12 were measured in the supernatant of the co-cultures using a commercial quantikine ELISA mouse CXCL12/SDF1α kit (R&D Systems, Minneapolis, MN, USA) according to manufacturer's instructions with some modifications. Briefly, the standard curve was done with rat CXCL12α (Peprotech) starting at 0.39 ng/mL up to 50 ng/mL. All samples were tested undiluted.

Statistical analysis

All statistical analysis were performed using the Prism version 8.1.1 (GraphPad Software, San Diego, CA, USA) using the tests specified in the figure legends. Briefly, one or two-ways analysis of variance (ANOVA) or Kruskal-Wallis with a post hoc Dunnett's, Fisher's or Dunn's multiple comparisons tests were used as appropriate. Spearman correlation coefficient test and Log-rank Mantel-Cox test were used to assess correlations and survival data, respectively. Differences were considered significant at $p<0.05$.

RESULTS

ACT-1004-1239 treatment dose-dependently reduces MOG-EAE disease severity

The effect of ACT-1004-1239 was investigated in the monophasic MOG-induced EAE model. EAE was induced by immunization of female mice with MOG_{35-55}/CFA. ACT-1004-1239 (10, 30, and 100 mg/kg) or vehicle were administered orally twice daily starting on the same day as the MOG_{35-55}/CFA immunization. ACT-1004-1239 treatment dose-dependently reduced clinical disease scores which assessed the ascending paralysis over a period of 29 days (Figure 1A). The highest and intermediate doses tested (100 and 30 mg/kg, twice daily) significantly reduced the mean cumulative disease scores, representing the overall extent of the disease, compared to vehicle-treated mice (Figure 1B). The severe clinical signs observed in vehicle-treated mice resulted in the spontaneous death or euthanasia of 90% of the mice from day 24 after EAE induction until the end of the study (Figure 1C).

Treatment with ACT-1004-1239 resulted in a dose-dependent increase in survival rate, reaching 90% in the highest dosage group at the end of the study.

Dose-dependent increase in CXCL12 plasma concentration upon ACT-1004-1239 treatment correlates with overall reduction of disease score

Regulation of CXCL12 levels by CXCR7 has been proposed to be at least one of the mechanisms by which inhibition of CXCR7 could exert therapeutic effects[37]. Treatment with ACT-1004-1239 in the MOG-induced EAE model led to a significant dose-dependent increase in plasma CXCL12 concentration measured at the end of the study (Figure 2A). At the highest dose tested (100 mg/kg, twice daily), ACT-1004-1239 treatment induced a 7-fold mean CXCL12 plasma elevation relative to vehicle-treated EAE mice. This plasma CXCL12 increase, utilized as a surrogate for CXCR7 antagonism, significantly correlated with the reduction of the cumulative disease scores for the 29-days study period (Figure 2B). Only the highest oral dose of 100 mg/kg, twice daily, provided sufficient drug plasma exposure to sustain plasma CXCL12 increase in C57BL/6 mice at all times (data not shown) and was therefore used in all subsequent in vivo experiments.

ACT-1004-1239 treatment reduces infiltration of pathogenic cells in the CNS

Elevation of CXCL12 in the plasma has been shown to affect leukocyte migration in vivo[37,38]. The impact of ACT-1004-1239 treatment on CNS inflammation was therefore evaluated in the MOG-induced EAE model at the peak of disease. ACT-1004-1239-treated mice, compared to vehicle-treated mice, had a significantly lower clinical score (Figure 3A) that was associated with a significant decrease of immune cells in the CNS (Figure 3B). Specifically, ACT-1004-1239 treatment reduced the infiltration of neutrophils, monocytes, monocytes-derived cells (MdCs), plasmacytoid dendritic cells (pDCs), DCs, natural killer (NK) cells, NK T cells, B cells, and T cells (Figure 3B). Importantly, ACT-1004-1239 treatment also reduced the number of MOG_{35-55} peptide antigen-specific, TNF-α-, IFN-γ-, and IL-17-secreting T cells in the CNS (Figure 3C).

CXCR4 expression was detected on the cell surface of most CNS-infiltrating leukocytes, with highest surface expression on myeloid cells, specifically MdCs, monocytes, and neutrophils (Figure 4A-C). ACT-1004-1239-mediated plasma CXCL12 increase was associated with a nearly complete inhibition (98%) of $CXCR4^+$ leukocyte infiltration in the CNS (Figure 4D, E). Treatment with ACT-1004-1239 also tended to reduce CXCR4- leukocyte infiltration but without reaching statistical significance (Figure 4E).

Taken together, these data provide evidence for the immunomodulatory effect of ACT-1004-1239 in the MOG-induced EAE model in vivo.

ACT-1004-1239 treatment reduces neurofilament light chain, a biomarker for axonal injury

Axonal loss occurs very early in the MOG-EAE model and does not recover over time[39]. Neurofilament light chain (NfL) is an axonal structural protein that can be measured in the plasma as a biomarker of axonal damage and neuronal death. Recently, reduction of plasma NfL concentration has been associated with MS disease activity and MS progression[40,41]. The plasma NfL concentration was significantly increased in diseased EAE mice compared to non-immunized control mice at the peak of disease (Figure 5A). Treatment with ACT-1004-1239 significantly reduced NfL plasma concentrations (Figure 5A). NfL levels directly correlated with the clinical disease score at sacrifice ($r=0.94$, $p<0.0001$) (Figure 5B), making NfL a valuable plasma biomarker for measuring treatment efficacy also in this preclinical MS model.

ACT-1004-1239 treatment increases the number of mature oligodendrocytes and increases myelination in the cuprizone-induced demyelination model

The direct effect of ACT-1004-1239 on myelination was assessed in the cuprizone-induced non-immune-mediated demyelination model. Oral administration of cuprizone (150 mg/kg, twice daily) for 6 weeks induced significant demyelination in the corpus callosum (Figure 6A-C). Co-treatment with ACT-1004-1239 was initiated either from the start of cuprizone treatment from day 0 (preventive

setting) or after 3 weeks of cuprizone exposure, when demyelination had already started[42] (therapeutic setting) (Figure 6A). In both settings, treatment with ACT-1004-1239 resulted in a significant increase in myelination in the corpus callosum as assessed by LFB-CV-staining, compared with cuprizone alone (Figure 6B-C). While cuprizone leads to the death of mature OLs[43], treatment with ACT-1004-1239 in both regimens, significantly increased mature GSTp$^+$ OL numbers in the corpus callosum (Figure 6D, E). In parallel, preventive and therapeutic ACT-1004-1239 treatment led to a normalization of the cuprizone-induced increase in the proportion of OPCs (PDGFRα$^+$ Olig2$^+$ cells) among all oligodendrocytes (Figure 6D, F), indicating that ACT-1004-1239 treatment induced OPC maturation in the demyelinated corpus callosum. ACT-1004-1239 treatment did not affect cuprizone-induced astrogliosis (GFAP expression) (Figure 6D, G), suggesting that the co-administration of ACT-1004-1239 with cuprizone did not interfere with the cuprizone-mediated reactive astrogliosis.

CXCL12 promotes OPC differentiation in vitro

CXCL12 has been proposed as a critical regulator for OPC maturation and subsequent myelination within damaged CNS[25,24,44]. To confirm the pro-differentiating effect of CXCL12 on OPCs, primary cell co-cultures containing neurons and OPCs[35] were treated with recombinant CXCL12a at doses ranging from 0.1 to 100 ng/mL for 30 days. Olesoxime (300 nM), which has been shown to accelerate OL maturation and myelination in vitro and in vivo[45], was included as a positive assay control. As expected, olesoxime promoted maturation of OPCs into mature OLs, as shown by a significant increase in MBP-expressing cells after 30 days of treatment, (Figure 7A). In accordance with prior in vitro studies[46,47], addition of CXCL12a (1 to 30 ng/mL) dose-dependently increased maturation of OPCs into MBP$^+$ OLs as shown by an increase in MBP$^+$ cell counts. At 30 ng/mL, the effect was as pronounced as with the positive control olesoxime (Figure 7A). CXCL12a at 100 ng/mL led to an opposite effect with a significant decrease in the number of MBP$^+$ cells (Figure 7A).

By increasing CXCL12 levels, ACT-1004-1239 promotes OPC differentiation in vitro

To determine whether CXCR7 antagonism would affect OPC maturation, co-cultures were treated with ACT-1004-1239 at doses ranging from 1 to 10 µM for 30 days. Presence of ACT-1004-1239 in the treatment co-culture was associated with an elevation of CXCL12 concentration in the co-culture supernatant (Figure 7B). Starting at 3 µM, treatment with ACT-1004-1239 led to a significant increase in MBP+ cell counts (Figure 7C, D). These data suggest that CXCL12 is endogenously produced in this co-culture and that ACT-1004-1239, similar to the obtained in vivo data, inhibited the CXCL12 scavenging activity of CXCR7 (Figure 7B). To evaluate whether CXCR4/CXCL12 signaling was required for OPC maturation in the in vitro co-cultures, the CXCR4 antagonist AMD3100 (Plerixafor) 48 was applied to the co-culture. CXCR4 blockade significantly reduced MBP^+ cell counts (Figure 7C, D). These results are in line with previous in vivo data[24,44], confirming the requirement of CXCR4/CXCL12 signaling for proper OPC maturation. Of note, AMD3100 did not increase CXCL12 levels in the co-culture supernatant (Figure 7B), indicating that at this dose (3 µM), the CXCR4 antagonist did not interfere with CXCR7-mediated CXCL12 scavenging activity, confirming previous reports that showed that AMD3100 is an agonist for CXCR7 only at high concentrations (>10 µM)[49].

DISCUSSION

Multiple sclerosis is a complex disease, associated with CNS inflammation and extensive tissue damage. Current approved therapies for the treatment of demyelinating diseases such as MS reduce relapse rates, but do not initiate myelin repair nor prevent or reverse disability progression. In the present study, ACT-1004-1239, a first-in-class potent and selective CXCR7 antagonist[31], demonstrated a dual mechanism of action: on one hand, an immunomodulatory effect, through inhibition of immune cell infiltration into the brain and hence reduction of neuroinflammation and, on the other hand, a promyelinating effect, through enhancement of OPC maturation into myelinating OLs. In preclinical models of MS,

this dual mechanism of action led to a significant reduction in disease activity and enhanced myelination.

Identifying CXCR7 as a potential therapeutic target in demyelinating diseases, acting both on leukocyte infiltrates and on myelin repair, has been previously reported in the literature [21,50]. However, understanding of the complex role of CXCR7 in this context has been limited by the lack of small molecule antagonists that block β-arrestin recruitment upon CXCL11 and CXCL12 binding to CXCR7 in contrast to functional antagonists[51]. It remained unclear whether previous reported data obtained in preclinical MS models utilizing CCX771[21,25,] a small molecule CXCR7 agonist of the β-arrestin pathway[29], was due to its agonistic activity on CXCR7 and/or its functional antagonistic effect on CXCR7. Indeed, previous studies reported that following the recruitment of β-arrestin, CXCR7 induced activation of downstream cell signaling pathways in different cells, including glial cells[52,53,54] which could also contribute to the efficacy observed. Our study provides evidence that CXCR7 antagonism is solely responsible for the beneficial effects observed in our preclinical MS studies, and that previous observations made in similar models with CCX771 were probably due to a functional antagonistic effect via targeted cellular CXCR7 desensitization and not through agonistic signaling via CXCR7.

The EAE mouse model manifests several features of MS, including inflammation, demyelination, and neurodegeneration[55]. ACT-1004-1239 treatment dose-dependently reduced the overall clinical severity of mouse EAE. Furthermore, repeated administration of ACT-1004-1239 dose-dependently increased plasma CXCL12 levels in EAE mice by blocking CXCR7-mediated scavenging of CXCL12. ACT-1004-1239-mediated increase in plasma CXCL12 levels significantly correlated with reduced overall extent of EAE, supporting its measurement as a pharmacodynamic biomarker in clinical trials with CXCR7 antagonists[56]. Previous reports have shown that elevation in CXCL12 plasma levels correlated with an inhibition of leukocyte migration to the site of inflammation[37], 38. In line with these results, treatment with ACT-1004-1239 reduced CNS immune cell infiltrates including autoantigen-specific cytokine-secreting T cells. Compelling evidence has

previously highlighted the role of the CXCR4/CXCL12 axis in MS pathophysiology in regulating the recruitment of pathogenic cells into the human CNS[20,57,58]. Consistent with findings in human MS lesions[20, 57], CXCR4 was also expressed on the cell surface of CNS infiltrating leukocytes in EAE mice. Treatment with ACT-1004-1239 preferentially prevented $CXCR4^+$ leukocyte infiltration in the CNS, suggesting that by blocking CXCR7 and therefore increasing circulating CXCL12 levels, ACT-1004-1239 disrupted the CXCL12 chemokine concentration gradient between the blood and the CNS, responsible for the infiltration of $CXCR4^+$ leukocytes into the CNS during neuroinflammation. The overall reduction in CNS inflammation observed with ACT-1004-1239 was accompanied by a significant reduction of the plasma NfL concentration, a biomarker of disease progression in MS patients[40,41], providing evidence of axonal protection. Taken together, these data suggest that the CXCR7/CXCL12/CXCR4 axis plays a major role in the recruitment of inflammatory cells to the CNS and subsequent axonal damage in the MOG-EAE model. CXCR7 has also been reported to scavenge not only CXCL12 but also CXCL11[15] and ACT-1004-1239 has been demonstrated to inhibit CXCL11-mediated CXCR7 internalization in vitro[31]. An increase in plasma CXCL11 levels could therefore also be expected upon treatment with ACT-1004-1239 in vivo, reducing the CXCL11-mediated infiltration of $CXCR3^+$ immune cells into the CNS, thus potentially broadening the immunomodulatory effect of ACT-1004-1239 during neuroinflammation. Due to the absence of CXCL11 expression in C57BL/6 mice[59], the strain used for the MOG-EAE model, the role of the CXCR7/CXCL11/CXCR3 axis in this model could not be investigated. More studies in strains of mice expressing CXCL11 are needed to understand the immunomodulatory effect of ACT-1004-1239 in this context.

The repair of demyelinating lesions in MS is key to impacting disability progression. Despite the abundance of OPCs in the CNS[60], their maturation process is impaired as the pathology transitions into progressive MS[61,62]. Therefore, promoting OPC maturation into myelinating OLs and so enhancing remyelination is recognized as a promising therapeutic approach for demyelinating diseases. There are multiple lines of evidence pointing towards a protective function of CXCL12 in CNS

pathology[26,44]. Previous studies using CXCR7 gene deletion or small molecule CXCR7 agonists used as functional antagonists have shown that CXCR7 regulates CXCL12 levels in vivo, both in the bloodstream[37] and in tissues[16,25,63]. In the present study, ACT-1004-1239 also increased CXCL12 levels, raising the possibility that ACT-1004-1239 could promote myelination within the CNS. The cuprizone-induced demyelination model is a non-immune based animal model, where the primary demyelination is not mediated by the immune system[64]. Cuprizone induces the depletion of mature OLs leading to significant demyelination already 2 to 3 weeks after cuprizone exposure[42]. ACT-1004-1239 co-administrated with cuprizone either in a preventive setting (from day 0) or starting only after 3 weeks of cuprizone exposure, significantly reduced demyelination in the corpus callosum without affecting reactive astrogliosis. Both treatment regimens increased mature myelinating OLs while decreasing the cuprizone-induced increase in the proportion of OPCs within the OL population. These data suggest that ACT-1004-1239 treatment, by promoting OPC differentiation into mature myelinating OLs, increased the myelin content in cuprizone-treated mice. In line with our results, CCX771, used as a functional CXCR7 antagonist[29,30] in the cuprizone model, increased CXCL12 brain levels resulting in increased mature OLs and subsequent remyelination25. Importantly, activation of CXCR4/CXCL12 signaling was shown to promote OPC differentiation leading to myelin repair following CNS injury[24,27,47]. Pharmacological inhibition of CXCR4 as well as neutralization of CXCL12 resulted in detrimental OPC differentiation[25] and aggravated EAE disease[65]. In the present study, CXCL12 was able to dose-dependently promote differentiation of OPCs into myelinating OLs in rat OPC-neuron co-cultures. However, a high concentration of CXCL12 (100 ng/mL) in the co-culture gave the opposite effect and led to reduced mature OLs, suggesting that this high CXCL12 concentration triggers CXCR4 endocytosis and degradation as previously described[16]. Published data with the CXCR7 agonists CCX771 and CCX754, wrongly reported as CXCR7 antagonists, claimed that CXCL12-dependent OPC maturation both in rodent and human cells was not CXCR4- but CXCR7-dependent[11,66]. This statement is in contradiction with our data as blockade of CXCR7 with ACT-1004-1239 increased maturation of OPCs to myelinating OLs. A possible explanation to the results of Göttle and Kremer

could be that the reported studies were performed in the presence of both the CXCR7 agonist and high doses of exogenous CXCL12. It has been shown that CCX771 led to increased extracellular levels of CXCL12[63] and therefore the combination of exogenous CXCL12 plus CXCR7 agonist could result in the internalization and degradation of CXCR4 as mentioned above. Importantly, and in line with reported data[24,46], in our co-culture studies, the CXCR4 antagonist AMD3100 induced a significant reduction in mature OL numbers, confirming that CXCL12-induced maturation of OPCs in this rat co-culture was CXCR4-dependent. Taken together, our in vivo and in vitro findings suggest that antagonizing CXCR7 with ACT-1004-1239 promotes remyelination by increasing CXCL12 concentrations within the CNS, thus enhancing the CXCR4/CXCL12-mediated maturation of OPCs.

In conclusion, our results demonstrate that ACT-1004-1239, a first-in-class CXCR7 antagonist currently undergoing clinical trials (NCT03869320 and NCT04286750), is efficacious in two preclinical models of MS. ACT-1004-1239 blocks the infiltration of CXCR4-expressing leukocytes into the CNS and enhances CXCR4/CXCL12-mediated CNS myelin repair. This dual mechanism of action positions ACT-1004-1239 as a potential new therapy to target both neuroinflammation and remyelination in patients with demyelinating diseases.

Acknowledgements

We thank Idorsia's immunology, translational biomarker, DMPK, and preformulation and preclinical galenics groups for their continuous support with in vitro and in vivo experiments. We thank the staff of Charles River and Neuro-Sys, especially N. Callizot and A. Henriques for excellent technical work and discussion. We thank C. Gnerre, F. Lehembre, M. Murphy, M. Holdener, A. Zalewska, A. Boulay, M. Keller, P. Sidharta, D. Strasser and G. Schlecht-Louf for their careful review of the manuscript.

Conflict of interest Statement

The authors declared the following potential conflicts of interest with respect to the research, authorship, and/or publication of this article: all authors acknowledge

that the work was performed as employees of Idorsia Pharmaceuticals Ltd. The authors declare no other financial interests.

Author contributions

L. Pouzol was responsible for the conception, design and execution of the studies, data interpretation, and manuscript drafting; N. Baumlin, A. Sassi, M. Tunis J. Marrie, E. Vezzali, H. Farine carried out experiments and analyzed the data; U. Mentzel was involved in study concept and design. M. M. Martinic was involved in the conception, and design of the studies, data interpretation, and manuscript drafting. All authors helped to critically revise the intellectual content of the manuscript and approved the final submission.

References

1. Martin R, Sospedra M, Rosito M, Engelhardt B. Current multiple sclerosis treatments have improved our understanding of MS autoimmune pathogenesis. Eur J Immunol. 2016;46(9):2078-2090.

2. Motavaf M, Sadeghizadeh M, Javan M. Attempts to Overcome Remyelination Failure: Toward Opening New Therapeutic Avenues for Multiple Sclerosis. Cell Mol Neurobiol. 2017;37(8):1335-1348.

3. Kappos L, Radue EW, O'Connor P, et al. A placebo-controlled trial of oral fingolimod in relapsing multiple sclerosis. N Engl J Med. 2010;362(5):387-401.

4. Gold R, Kappos L, Arnold DL, et al. Placebo-controlled phase 3 study of oral BG-12 for relapsing multiple sclerosis. N Engl J Med. 2012;367(12):1098-1107.

5. Oh J, O'Connor PW. Teriflunomide in the treatment of multiple sclerosis: current evidence and future prospects. Ther Adv Neurol Disord. 2014;7(5):239-252.

6. Cheng W, Chen G. Chemokines and chemokine receptors in multiple sclerosis. Mediators Inflamm. 2014;2014:659206.

7. Sadeghian-Rizi T, Khanahmad H, Jahanian-Najafabadi A. Therapeutic Targeting of Chemokines and Chemokine Receptors in Multiple Sclerosis:

Opportunities and Challenges. CNS Neurol Disord Drug Targets. 2018;17(7):496-508.

8. Williams JL, Holman DW, Klein RS. Chemokines in the balance: maintenance of homeostasis and protection at CNS barriers. Front Cell Neurosci. 2014;8:154.

9. Burns JM, Summers BC, Wang Y, et al. A novel chemokine receptor for SDF-1 and I-TAC involved in cell survival, cell adhesion, and tumor development. J Exp Med. 2006;203(9):2201-2213.

10. Banisadr G, Podojil JR, Miller SD, Miller RJ. Pattern of CXCR7 Gene Expression in Mouse Brain Under Normal and Inflammatory Conditions. J Neuroimmune Pharmacol. 2016;11(1):26-35.

11. Kremer D, Cui QL, Gottle P, et al. CXCR7 Is Involved in Human Oligodendroglial Precursor Cell Maturation. PLoS One. 2016;11(1):e0146503.

12. Puchert M, Pelkner F, Stein G, et al. Astrocytic expression of the CXCL12 receptor, CXCR7/ACKR3 is a hallmark of the diseased, but not developing CNS. Mol Cell Neurosci. 2017;85:105-118.

13. Meyrath M, Szpakowska M, Zeiner J, et al. The atypical chemokine receptor ACKR3/CXCR7 is a broad-spectrum scavenger for opioid peptides. Nat Commun. 2020;11(1):3033.

14. Balabanian K, Lagane B, Infantino S, et al. The chemokine SDF-1/CXCL12 binds to and signals through the orphan receptor RDC1 in T lymphocytes. J Biol Chem. 2005;280(42):35760-35766.

15. Naumann U, Cameroni E, Pruenster M, et al. CXCR7 functions as a scavenger for CXCL12 and CXCL11. PLoS One. 2010;5(2):e9175.

16. Sanchez-Alcaniz JA, Haege S, Mueller W, et al. Cxcr7 controls neuronal migration by regulating chemokine responsiveness. Neuron. 2011;69(1):77-90.

17. Lewellis SW, Knaut H. Attractive guidance: how the chemokine SDF1/CXCL12 guides different cells to different locations. Semin Cell Dev Biol. 2012;23(3):333-340.

18. Quinn KE, Mackie DI, Caron KM. Emerging roles of atypical chemokine receptor 3 (ACKR3) in normal development and physiology. Cytokine. 2018;109:17-23.

19. McCandless EE, Wang Q, Woerner BM, Harper JM, Klein RS. CXCL12 limits inflammation by localizing mononuclear infiltrates to the perivascular space during experimental autoimmune encephalomyelitis. J Immunol. 2006;177(11):8053-8064.

20. McCandless EE, Piccio L, Woerner BM, et al. Pathological expression of CXCL12 at the blood-brain barrier correlates with severity of multiple sclerosis. Am J Pathol. 2008;172(3):799-808.

21. Cruz-Orengo L, Holman DW, Dorsey D, et al. CXCR7 influences leukocyte entry into the CNS parenchyma by controlling abluminal CXCL12 abundance during autoimmunity. J Exp Med. 2011;208(2):327-339.

22. Cruz-Orengo L, Chen YJ, Kim JH, Dorsey D, Song SK, Klein RS. CXCR7 antagonism prevents axonal injury during experimental autoimmune encephalomyelitis as revealed by in vivo axial diffusivity. J Neuroinflammation. 2011;8:170.

23. Carbajal KS, Schaumburg C, Strieter R, Kane J, Lane TE. Migration of engrafted neural stem cells is mediated by CXCL12 signaling through CXCR4 in a viral model of multiple sclerosis. Proc Natl Acad Sci U S A. 2010;107(24):11068-11073.

24. Patel JR, McCandless EE, Dorsey D, Klein RS. CXCR4 promotes differentiation of oligodendrocyte progenitors and remyelination. Proc Natl Acad Sci U S A. 2010;107(24):11062-11067.

25. Williams JL, Patel JR, Daniels BP, Klein RS. Targeting CXCR7/ACKR3 as a therapeutic strategy to promote remyelination in the adult central nervous system. J Exp Med. 2014;211(5):791-799.

26. Zilkha-Falb R, Kaushansky N, Kawakami N, Ben-Nun A. Post-CNS-inflammation expression of CXCL12 promotes the endogenous myelin/neuronal

repair capacity following spontaneous recovery from multiple sclerosis-like disease. J Neuroinflammation. 2016;13(1):7.

27. Carbajal KS, Miranda JL, Tsukamoto MR, Lane TE. CXCR4 signaling regulates remyelination by endogenous oligodendrocyte progenitor cells in a viral model of demyelination. Glia. 2011;59(12):1813-1821.

28. Wang C, Chen W, Shen J. CXCR7 Targeting and Its Major Disease Relevance. Front Pharmacol. 2018;9:641.

29. Zabel BA, Wang Y, Lewen S, et al. Elucidation of CXCR7-mediated signaling events and inhibition of CXCR4-mediated tumor cell transendothelial migration by CXCR7 ligands. J Immunol. 2009;183(5):3204-3211.

30. Menhaji-Klotz E, Ward J, Brown JA, et al. Discovery of Diphenylacetamides as CXCR7 Inhibitors with Novel β-Arrestin Antagonist Activity. ACS Medicinal Chemistry Letters. 2020.

31. Richard-Bildstein S, Aissaoui H, Pothier J, et al. Discovery of the Potent, Selective, Orally Available CXCR7 Antagonist ACT-1004-1239. J Med Chem. 2020;63(24):15864-15882.

32. Greter M, Heppner FL, Lemos MP, et al. Dendritic cells permit immune invasion of the CNS in an animal model of multiple sclerosis. Nat Med. 2005;11(3):328-334.

33. Stritt M, Stalder AK, Vezzali E. Orbit Image Analysis: An open-source whole slide image analysis tool. PLoS Comput Biol. 2020;16(2):e1007313.

34. Gaiottino J, Norgren N, Dobson R, et al. Increased neurofilament light chain blood levels in neurodegenerative neurological diseases. PLoS One. 2013;8(9):e75091.

35. Hauser J, Sultan S, Rytz A, Steiner P, Schneider N. A blend containing docosahexaenoic acid, arachidonic acid, vitamin B12, vitamin B9, iron and sphingomyelin promotes myelination in an in vitro model. Nutr Neurosci. 2019:1-15.

36. Fricker SP, Anastassov V, Cox J, et al. Characterization of the molecular pharmacology of AMD3100: a specific antagonist of the G-protein coupled chemokine receptor, CXCR4. Biochem Pharmacol. 2006;72(5):588-596.

37. Berahovich RD, Zabel BA, Lewen S, et al. Endothelial expression of CXCR7 and the regulation of systemic CXCL12 levels. Immunology. 2014;141(1):111-122.

38. O'Boyle G, Mellor P, Kirby JA, Ali S. Anti-inflammatory therapy by intravenous delivery of non-heparan sulfate-binding CXCL12. FASEB J. 2009;23(11):3906-3916.

39. Herrero-Herranz E, Pardo LA, Gold R, Linker RA. Pattern of axonal injury in murine myelin oligodendrocyte glycoprotein induced experimental autoimmune encephalomyelitis: implications for multiple sclerosis. Neurobiol Dis. 2008;30(2):162-173.

40. Kuhle J, Kropshofer H, Haering DA, et al. Blood neurofilament light chain as a biomarker of MS disease activity and treatment response. Neurology. 2019;92(10):e1007-e1015.

41. Jakimovski D, Zivadinov R, Ramanthan M, et al. Serum neurofilament light chain level associations with clinical and cognitive performance in multiple sclerosis: A longitudinal retrospective 5-year study. Mult Scler. 2019:1352458519881428.

42. Doan V, Kleindienst AM, McMahon EJ, Long BR, Matsushima GK, Taylor LC. Abbreviated exposure to cuprizone is sufficient to induce demyelination and oligodendrocyte loss. J Neurosci Res. 2013;91(3):363-373.

43. Mason JL, Toews A, Hostettler JD, et al. Oligodendrocytes and progenitors become progressively depleted within chronically demyelinated lesions. Am J Pathol. 2004;164(5):1673-1682.

44. Li Y, Tang G, Liu Y, et al. CXCL12 Gene Therapy Ameliorates Ischemia-Induced White Matter Injury in Mouse Brain. Stem Cells Transl Med. 2015;4(10):1122-1130.

45. Magalon K, Zimmer C, Cayre M, et al. Olesoxime accelerates myelination and promotes repair in models of demyelination. Ann Neurol. 2012;71(2):213-226.

46. Maysami S, Nguyen D, Zobel F, et al. Modulation of rat oligodendrocyte precursor cells by the chemokine CXCL12. Neuroreport. 2006;17(11):1187-1190.

47. Kadi L, Selvaraju R, de Lys P, Proudfoot AE, Wells TN, Boschert U. Differential effects of chemokines on oligodendrocyte precursor proliferation and myelin formation in vitro. J Neuroimmunol. 2006;174(1-2):133-146.

48. Hatse S, Princen K, Bridger G, De Clercq E, Schols D. Chemokine receptor inhibition by AMD3100 is strictly confined to CXCR4. FEBS Lett. 2002;527(1-3):255-262.

49. Kalatskaya I, Berchiche YA, Gravel S, Limberg BJ, Rosenbaum JS, Heveker N. AMD3100 is a CXCR7 ligand with allosteric agonist properties. Mol Pharmacol. 2009;75(5):1240-1247.

50. Chu T, Shields LBE, Zhang YP, Feng SQ, Shields CB, Cai J. CXCL12/CXCR4/CXCR7 Chemokine Axis in the Central Nervous System: Therapeutic Targets for Remyelination in Demyelinating Diseases. Neuroscientist. 2017;23(6):627-648.

51. Lounsbury N. Advances in CXCR7 Modulators. Pharmaceuticals (Basel). 2020;13(2).

52. Odemis V, Boosmann K, Heinen A, Kury P, Engele J. CXCR7 is an active component of SDF-1 signalling in astrocytes and Schwann cells. J Cell Sci. 2010;123(Pt 7):1081-1088.

53. Odemis V, Lipfert J, Kraft R, et al. The presumed atypical chemokine receptor CXCR7 signals through G(i/o) proteins in primary rodent astrocytes and human glioma cells. Glia. 2012;60(3):372-381.

54. Bao J, Zhu J, Luo S, Cheng Y, Zhou S. CXCR7 suppression modulates microglial chemotaxis to ameliorate experimentally-induced autoimmune encephalomyelitis. Biochem Biophys Res Commun. 2016;469(1):1-7.

55. Robinson AP, Harp CT, Noronha A, Miller SD. The experimental autoimmune encephalomyelitis (EAE) model of MS: utility for understanding disease pathophysiology and treatment. Handb Clin Neurol. 2014;122:173-189.

56. Huynh C, Henrich A, Strasser DS, et al. A multi-purpose first-in-human study with the novel CXCR7 antagonistACT-1004-1239 using CXCL12 plasma concentrations as target engagement biomarker. Clin Pharmacol Ther. 2021.

57. Moll NM, Cossoy MB, Fisher E, et al. Imaging correlates of leukocyte accumulation and CXCR4/CXCL12 in multiple sclerosis. Arch Neurol. 2009;66(1):44-53.

58. Galli E, Hartmann FJ, Schreiner B, et al. GM-CSF and CXCR4 define a T helper cell signature in multiple sclerosis. Nat Med. 2019;25(8):1290-1300.

59. Sierro F, Biben C, Martinez-Munoz L, et al. Disrupted cardiac development but normal hematopoiesis in mice deficient in the second CXCL12/SDF-1 receptor, CXCR7. Proc Natl Acad Sci U S A. 2007;104(37):14759-14764.

60. Kuhlmann T, Miron V, Cui Q, Wegner C, Antel J, Bruck W. Differentiation block of oligodendroglial progenitor cells as a cause for remyelination failure in chronic multiple sclerosis. Brain. 2008;131(Pt 7):1749-1758.

61. Kipp M, Victor M, Martino G, Franklin RJ. Endogeneous remyelination: findings in human studies. CNS Neurol Disord Drug Targets. 2012;11(5):598-609.

62. Chang A, Tourtellotte WW, Rudick R, Trapp BD. Premyelinating oligodendrocytes in chronic lesions of multiple sclerosis. N Engl J Med. 2002;346(3):165-173.

63. Luker KE, Lewin SA, Mihalko LA, et al. Scavenging of CXCL12 by CXCR7 promotes tumor growth and metastasis of CXCR4-positive breast cancer cells. Oncogene. 2012;31(45):4750-4758.

64. Gudi V, Gingele S, Skripuletz T, Stangel M. Glial response during cuprizone-induced de- and remyelination in the CNS: lessons learned. Front Cell Neurosci. 2014;8:73.

65. Meiron M, Zohar Y, Anunu R, Wildbaum G, Karin N. CXCL12 (SDF-1alpha) suppresses ongoing experimental autoimmune encephalomyelitis by selecting antigen-specific regulatory T cells. J Exp Med. 2008;205(11):2643-2655.

66. Gottle P, Kremer D, Jander S, et al. Activation of CXCR7 receptor promotes oligodendroglial cell maturation. Ann Neurol. 2010;68(6):915-924.

Figure Legends

Figure 1: ACT-1004-1239 treatment dose-dependently reduces disease severity in the MOG-induced EAE model. EAE was induced by immunization of female C57BL/6 mice with MOG_{35-55}/CFA on day 0. ACT-1004-1239 (10, 30, or 100 mg/kg) or vehicle was administered by oral gavage (p.o.), twice daily (bid), starting on day 0 after MOG/CFA immunization. (A) ACT-1004-1239 treatment dose-dependently reduced mean EAE clinical score. Scoring was performed daily by independent examiners. Results are expressed as mean + SEM. ****$p<0.0001$ compared to vehicle control by two-way ANOVA followed by Dunnett's multiple comparison test. (B) ACT-1004-1239 treatment dose-dependently reduced mean overall disease burden as assessed by cumulative disease scores, defined as the sum of the clinical scores for each mouse over the 29-days study. Results are expressed as mean + SEM (n=9-10 mice/group). *$p<0.05$, ****$p<0.0001$ compared to vehicle control group by Kruskal-Wallis followed by Dunn's multiple comparisons test. (C) ACT-1004-1239 treatment dose-dependently increased survival. **$p<0.01$, ***$p<0.001$ compared to vehicle control group using Log-rank Mantel-Cox test.

Figure 2: Dose-dependent increase in CXCL12 plasma concentration upon ACT-1004-1239 treatment correlates with overall reduction of disease score in the MOG-induced EAE model. EAE was induced by immunization of female C57BL/6 mice with MOG_{35-55}/CFA on Day 0. Vehicle or ACT-1004-1239 (10, 30, or 100 mg/kg) was given orally (p.o.), twice daily (bid), starting on Day 0 after MOG/CFA immunization. Plasma samples were prepared at sacrifice 2 ± 1.5 hours

after last dosing. (A) ACT-1004-1239 treatment dose-dependently increased CXCL12 plasma concentrations, expressed as mean + SEM (n=7-10 per group). ****p<0.0001 vs. vehicle-treated EAE mice, using one-way ANOVA followed by Dunnett's multiple comparisons test. (B) Correlation between the mean cumulative disease score (the sum of the daily clinical scores over the 29-days study for each mouse) and CXCL12 plasma concentration in individual animals treated with vehicle or ACT-1004-1239 (n=7-10 per group); Spearman correlation coefficient test.

Figure 3: ACT-1004-1239 treatment significantly reduces CNS inflammation, including MOG-specific cytokine-secreting CNS T cells during the acute phase of EAE.

EAE was induced by immunization of female C57BL/6 mice with MOG_{35-55}/CFA on Day 0. Negative control mice (control) were injected with PBS/IFA on Day 0 (n=7). Vehicle or ACT-1004-1239 (100 mg/kg, twice daily, bid) were given orally (p.o.), starting on Day 0 after MOG/CFA immunization (n=8/group). Animals were sacrificed at the peak of disease (16 or 17 days post-immunization). (A) ACT-1004-1239 treatment significantly reduced mean EAE clinical score measured at sacrifice. Scoring was performed daily by independent examiners. Results are expressed as mean + SEM; *** p<0.001 vs. vehicle-treated EAE mice by Mann-Whitney test. (B) Right brain hemisphere and spinal cord of each mouse were collected at the peak of disease, weighed, and processed as neural single cell suspensions for flow cytometry analysis. The gating strategy for all immune populations is illustrated in supplementary figure 1. ACT-1004-1239 treatment significantly reduced overall immune cells in the CNS ($CD45^+$ cells). Results are expressed as mean of the absolute number normalized to the weight of the collected CNS tissue + SEM. *p<0.05, **p<0.01, ***p<0.001 vs. vehicle-treated EAE mice using one-way ANOVA followed by Dunnett's multiple comparisons test. (C) ACT-1004-1239 treatment significantly reduced MOG-specific TNF-α^+, IFN-□$^+$, and IL-17^+ $CD69^+$ T cell counts. Numbers are expressed as mean of the absolute number normalized to the weight of the collected CNS tissue + SEM. **p<0.01, ***p<0.001 vs. vehicle-treated EAE mice using one-way ANOVA followed by Dunnett's multiple comparisons test.

Figure 4: ACT-1004-1239 treatment preferentially reduces the number of CXCR4-expressing leukocytes in the course of EAE. EAE was induced by immunization of female C57BL/6 mice with MOG_{35-55}/CFA on Day 0. Negative control mice (control) were injected with PBS/IFA on Day 0 (n=7). Vehicle or ACT-1004-1239 (ACT-1239, 100 mg/kg, twice daily, bid) were given orally, starting on Day 0 after MOG/CFA immunization (n=8/group). Right brain hemisphere and spinal cord of each mouse were collected, weighed, and processed as neural single cell suspensions for flow cytometry analysis. (A) Gating strategy for live CNS $CD45^+$ singlet cells, after exclusion of debris and doublets. (B) Differential expression of CXCR4 on $CD45^+$ cells (green) and monocyte-derived cells (MdCs) (pink) as compared to its respective fluorescence minus one (FMO) control for CXCR4 (purple and red). (C) In EAE mice, CXCR4 is expressed on the cell surface of most CNS-infiltrating leukocytes with highest expression on myeloid cells. Results are expressed as mean + SEM of the mean fluorescence intensity (MFI) obtained for each vehicle-treated EAE mouse (n=8) corrected by the MFI obtained in the FMO controls for CXCR4 in each specific cell population. The gating strategy for all immune populations is illustrated in supplementary figure 1. (D) Gating strategy for $CXCR4^+CD45^+$CNS cells based on the FMO control for CXCR4. (E) ACT-1004-1239 treatment significantly reduced CXCR4-expressing leukocytes in the CNS in EAE mice. **$p<0.01$ vs. vehicle-treated EAE mice using one-way ANOVA followed by Dunnett's multiple comparisons test.

Figure 5: ACT-1004-1239 treatment reduces plasma neurofilament light chain (NfL) concentration, a biomarker for axonal damage that correlates with clinical scores.
EAE was induced by immunization of female C57BL/6 mice with MOG_{35-55}/CFA on Day 0 (n=7). Negative control mice (control) were injected with PBS/IFA on Day 0. Vehicle or ACT-1004-1239 (100 mg/kg, twice daily) were given orally, starting on Day 0 after MOG/CFA immunization (n=8/group). Plasma samples were prepared at sacrifice at the peak of disease (day 16 or 17 after immunization). (A) ACT-1004-1239, treatment significantly reduced plasma NfL concentration. Values are

expressed as mean + SEM. ****p<0.0001 vs. vehicle-treated EAE mice using one-way ANOVA followed by Dunnett's multiple comparisons test. (B) Plasma NfL concentration significantly correlated with the clinical score at sacrifice for each mouse; Spearman correlation test.

Figure 6: Preventive and therapeutic ACT-1004-1239 treatment increases myelination in the cuprizone-induced demyelination model.

(A) Study design: Male C57BL/6 mice were orally administered with vehicle (control) or cuprizone (CPZ) (150 mg/kg, twice daily) for 6 weeks. ACT-1004-1239 (ACT) was given orally at 100 mg/kg, twice daily, co-administered with CPZ, either in a preventive mode (starting from Day 0; CPZ + ACT_{Prev}) or in a therapeutic mode (starting after 3 weeks of oral CPZ exposure; CPZ + ACT_{Ther}). (B) Preventive and therapeutic ACT-1004-1239 treatment significantly increased myelination. Quantitative analysis of myelinated areas in the corpus callosum after six weeks of treatment using image quantification software Orbit. Results are expressed as mean + SEM; n=7 to 8 mice in each group; *p<0.05, **p<0.001, ****p<0.0001 vs. CPZ group, using one-way ANOVA followed by uncorrected Fisher's test. C) Representative Luxol Fast Blue-Cresyl Violet (LFB-CV) images in the body of the corpus callosum of mice from each treatment group after six weeks of treatment. (D) Representative immunohistochemistry images on corpus callosum sections of mice after 6 weeks of treatment. Preventive and therapeutic ACT-1004-1239 treatment significantly increased the number of mature oligodendrocytes (GSTπ) (E) while maintaining the frequency of oligodendrocyte precursor cells (OPCs) (% $PDGFRa^+$ cells out of $Olig2^+$ cells) as seen in control animals (F). ACT-1004-1239 treatment did not impact astrogliosis (G). Quantitative analysis of GSTπ (E), Olig2 and PDGFR□ (F), and GFAP (G) was performed using Orbit software. Data are expressed as the mean number of cells normalized by the selected region of interest in mm^2 (GSTπ), the percentage of PDGFR□$^+$ cells among $Olig2^+$ cells, or the percentage of mean positive area (GFAP). All quantifications are expressed as mean + SEM; n= 5 to 8 mice in each group; *p<0.05, **p<0.01, ***p<0.001, ****p<0.0001 vs. CPZ group, using one-way ANOVA followed by uncorrected Fisher's test (scale bar, 410µm in C, 100µm in D).

Figure 7: CXCL12 and ACT-1004-1239 dose-dependently increase mature MBP$^+$ oligodendrocytes (OLs) in primary cell co-cultures of oligodendrocyte precursor cells (OPCs) and neurons. (A) Exogenously added CXCL12α dose-dependently increased MBP$^+$ OLs up to and including 30 ng/mL. Myelin basic protein (MBP) was quantified using ImageXpress software in rat OPC-neuron co-cultures treated for 30 days with CXCL12α at doses ranging from 0.1 to 100 ng/mL. Olesoxime (300nM) was used as a positive control. Results are expressed as the mean + SEM of the percentage of the medium control, which is set to 100% (n=4-6 wells/condition). For each well, 30 pictures were acquired and quantified. *p<0.05, **p<0.01, ****p<0.0001 vs. medium control using one-way ANOVA followed by Fisher's test. (B) CXCL12 was detected in the supernatant of OPC-neuron co-cultures in the presence of ACT-1004-1239 or exogenous CXCL12α but not AMD3100. CXCL12 concentrations were measured in the co-culture supernatant after 30 days of treatment and collected approximately 48h after the last medium change. No optical density (OD) values were detected for CXCL12 in the AMD3100 wells. Few OD values were detected in the Olesoxime wells but were below the OD measured in the smallest standard used (0.39 ng/mL). Results are expressed as the mean + SEM (n=12 wells/condition). **p<0.01, ***p<0.001, ****p<0.0001 vs. medium control using one-way ANOVA followed by Fisher's test. (C) ACT-1004-1239 increased MBP$^+$ OLs. MBP was quantified using ImageXpress software in rat OPC-neuron co-cultures treated for 30 days with ACT-1004-1239 at doses ranging from 1 to 10 µM. Olesoxime (300nM) and CXCL12α at 30 ng/mL were used as positive controls. AMD3100 (3µM), a CXCR4 antagonist, reduced the number of mature MBP$^+$ OLs. Results are expressed as the mean + SEM of the percentage of the medium control, which is set to 100% (n=4-6 wells/condition). *p<0.05, **p<0.01, ***p<0.001, ****p<0.0001 vs. medium control using one-way ANOVA followed by Fisher's test. (D) Representative images of the MBP immunostaining in OPC-neuron co-cultures treated with medium control, ACT-1004-1239 (10µM), CXCL12α (30ng/mL), AMD3100 (3µM), and Olesoxime (300nM). Scale bar: 100µm.

Figure 1: ACT-1004-1239 treatment dose-dependently reduces disease severity in the MOG-induced EAE model.

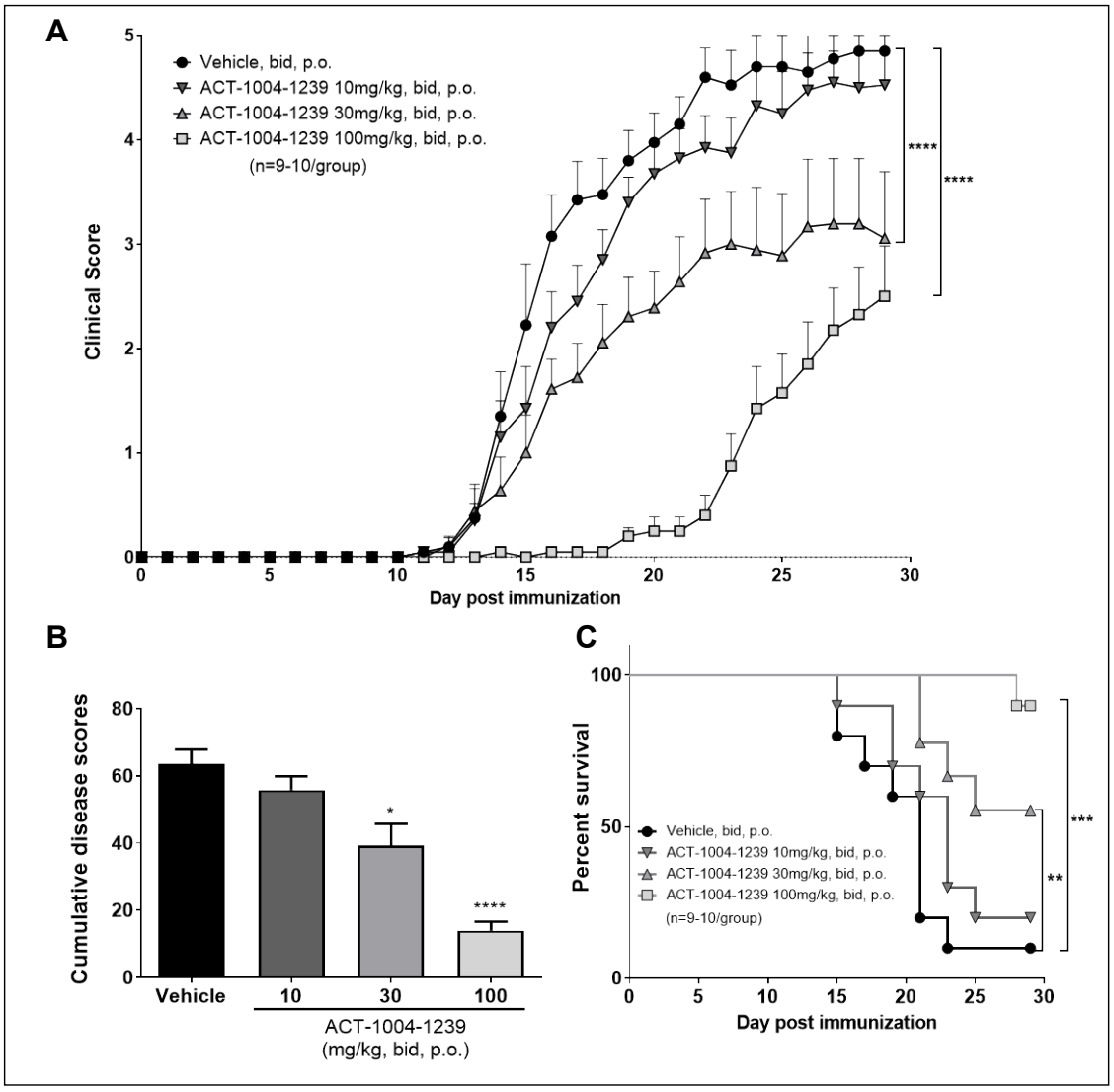

Figure 2: Dose-dependent increase in CXCL12 plasma concentration upon ACT-1004-1239 treatment correlates with overall reduction of disease score in the MOG-induced EAE model.

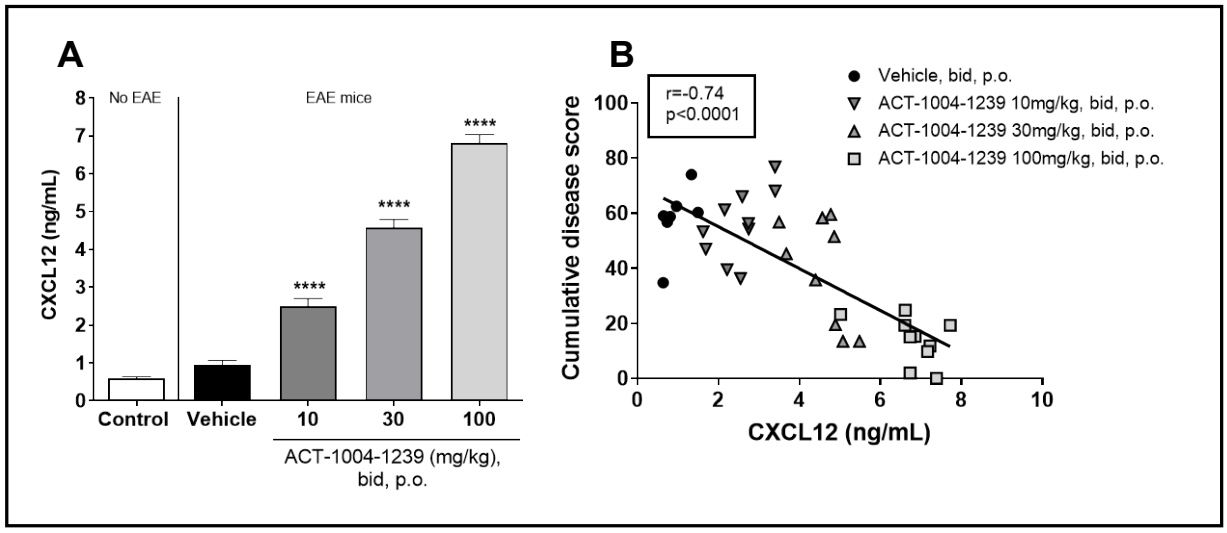

Figure 3: ACT-1004-1239 treatment significantly reduces CNS inflammation, including MOG-specific cytokine-secreting CNS T cells during the acute phase of EAE.

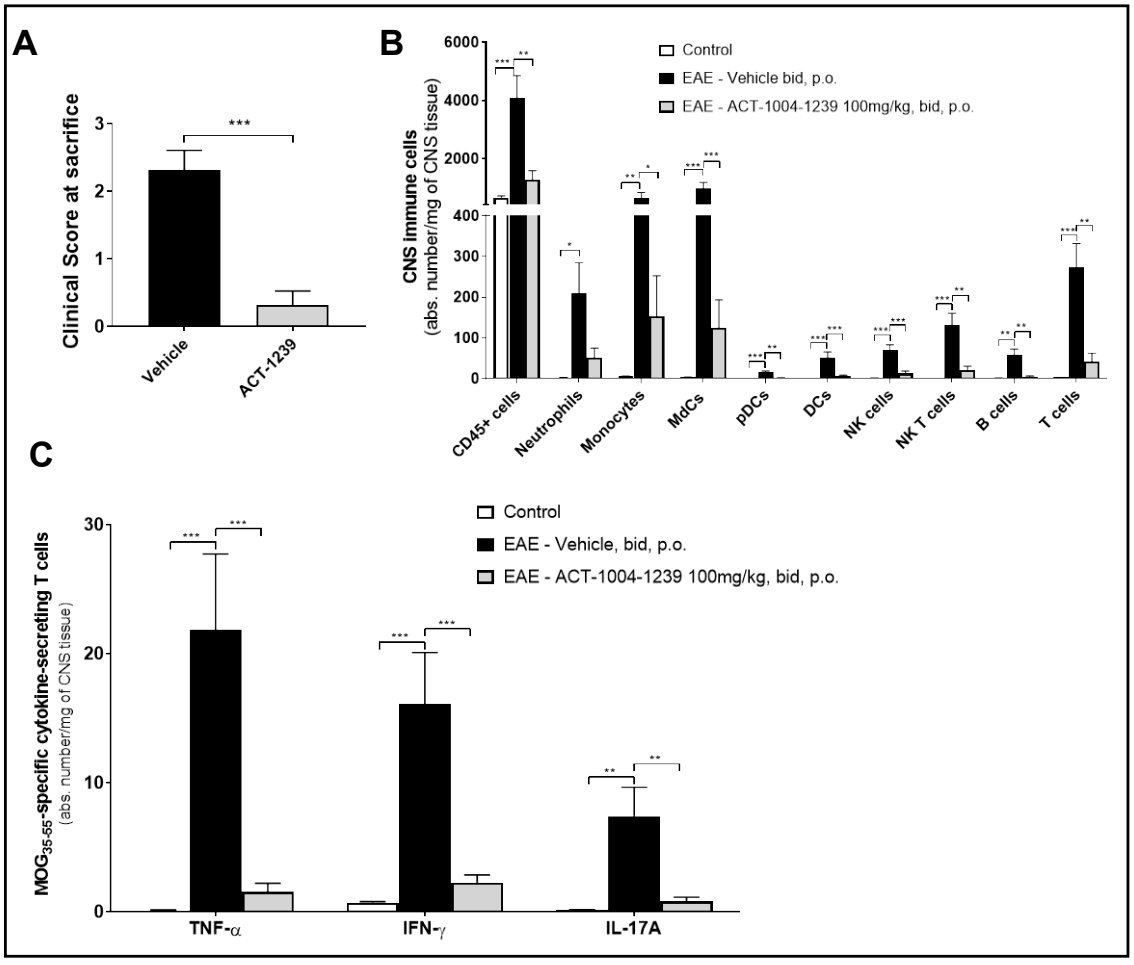

Figure 4: ACT-1004-1239 treatment preferentially reduces the number of CXCR4-expressing leukocytes in the course of EAE.

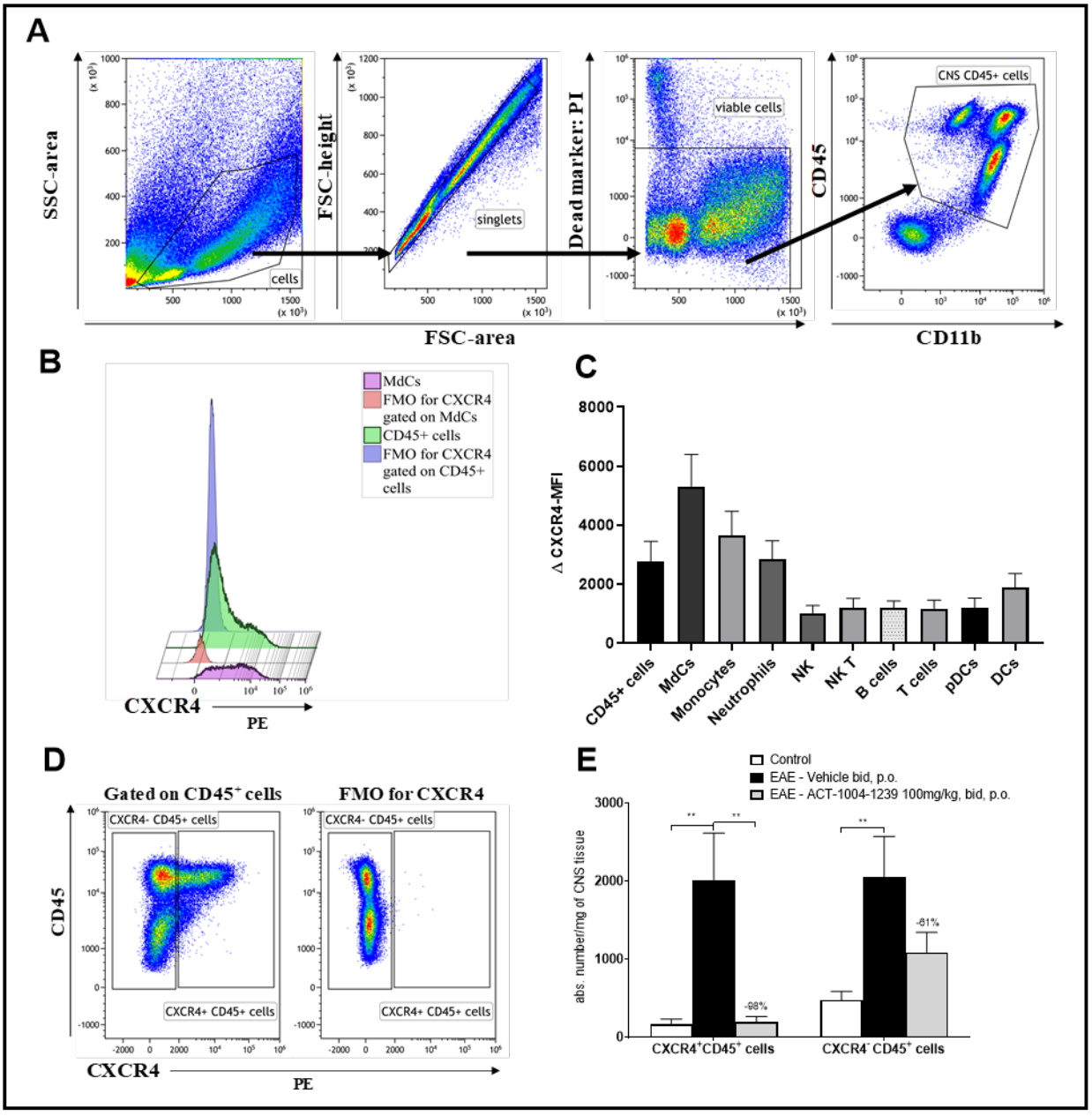

Figure 5: ACT-1004-1239 treatment reduces plasma neurofilament light chain (NfL) concentration, a biomarker for axonal damage that correlates with clinical scores.

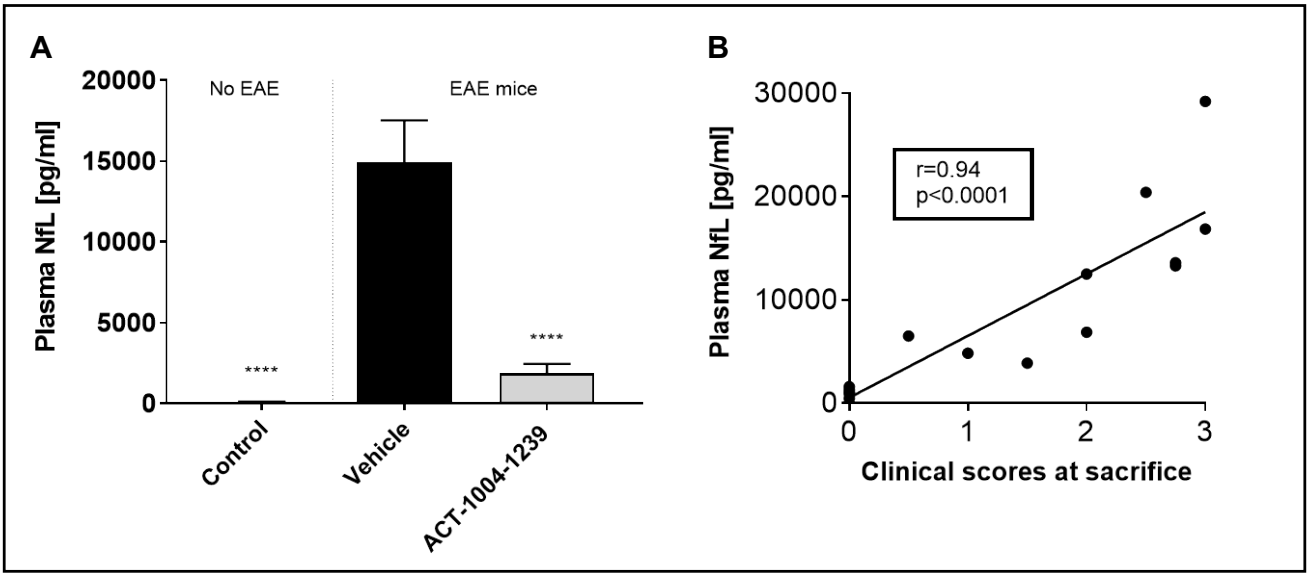

Figure 6: Preventive and therapeutic ACT-1004-1239 treatment increases myelination in the cuprizone-induced demyelination model.

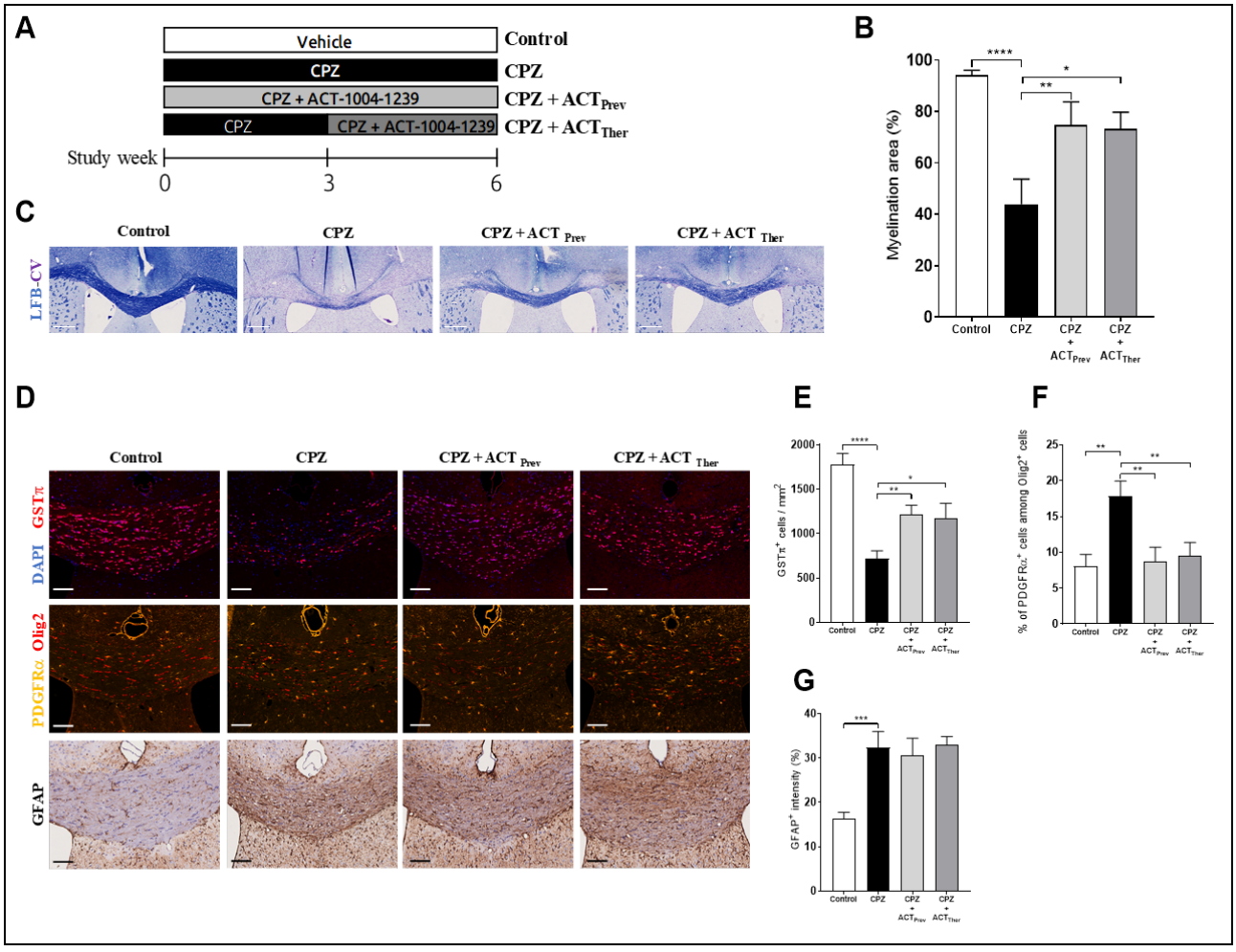

Figure 7: CXCL12 and ACT-1004-1239 dose-dependently increase mature MBP+ oligodendrocytes (OLs) in primary cell co-cultures of oligodendrocyte precursor cells (OPCs) and neurons.

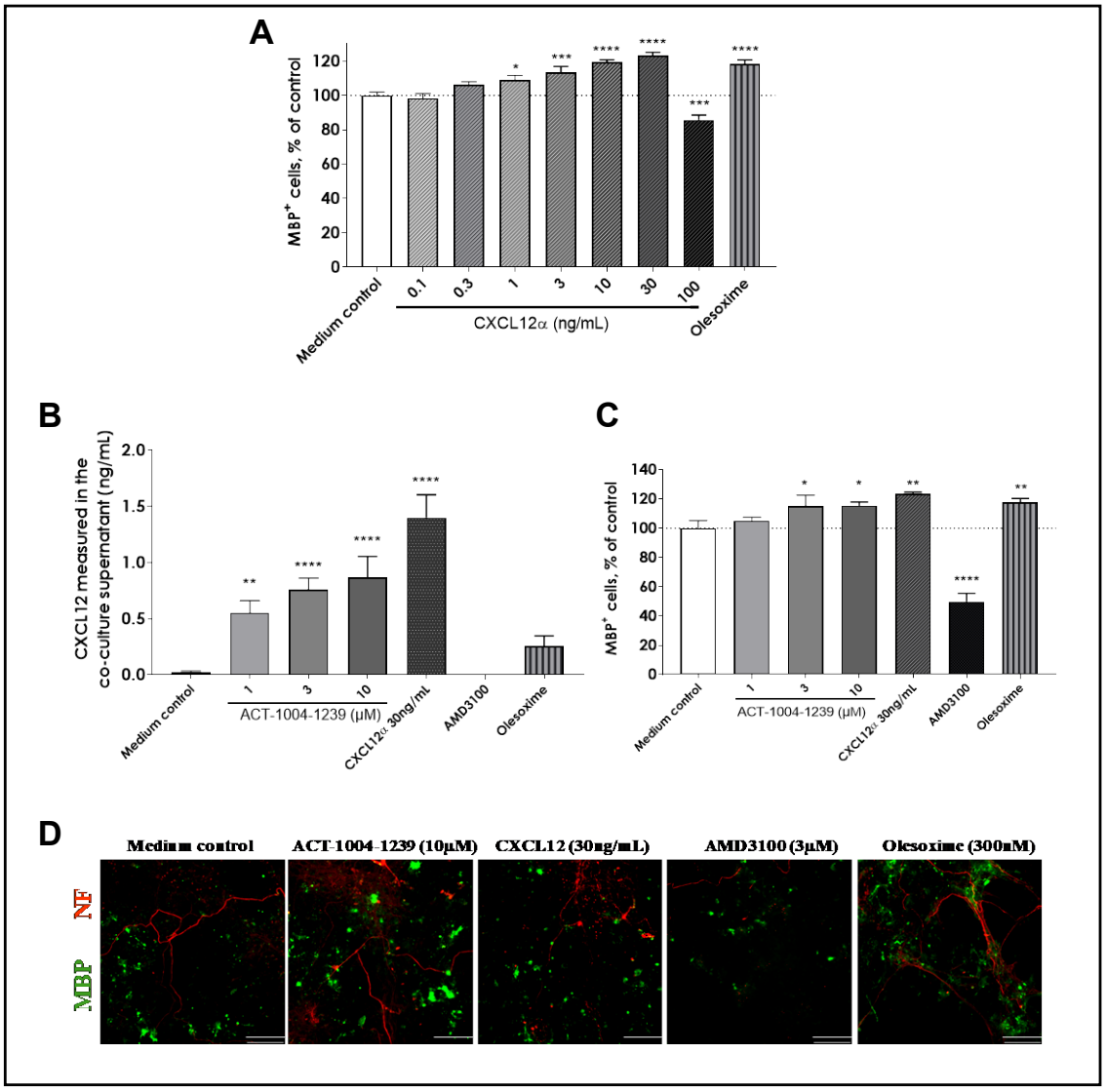

Supplementary materials

Supplementary Figure 1: Gating strategy for neural single cell suspensions from the brain and spinal cord of mice sacrificed at the peak of MOG-EAE disease.
EAE was induced by immunization of female C57BL/6 mice with MOG35-55/CFA on Day 0. Negative control mice (control) were injected with PBS/IFA on Day 0 (n=7). Vehicle or ACT-1004-1239 (100 mg/kg, twice daily, bid) were given orally (p.o.), starting on Day 0 after MOG/CFA immunization (n=8/group). Animals were sacrificed at the peak of disease (16 or 17 days post-immunization). Right brain hemisphere and spinal cord of each mouse were collected at the peak of disease, weighed, and processed as neural single cell suspensions for flow cytometry analysis. **(A)** After excluding doublets and dead cells, following $CD45^+$ singlets and viable cell subsets were defined: neutrophils ($CD11b^+$, $Gr\text{-}1^{high}$ cells), monocytes ($CD11b^+$, Gr-1int cells), microglia ($CD11b^+$, $Gr\text{-}1^{low}$, $CD45^{low}$ cells), monocyte-derived cells (MdCs) ($CD11b^+$, $Gr\text{-}1^{low}$, $CD45^{high}$ cells), B cells ($CD11b^-$, $Gr\text{-}1^-$, $B220^+$ cells), plasmacytoid dendritic cells (pDCs) ($CD11b^-$, $Gr\text{-}1^{int}$, $B220^+$, $CD11c^+$ cells), T cells ($CD11b^-$, $B220^-$, $CD49b^-$, $CD3^+$ cells), natural killer (NK) T cells ($CD11b^-$, $B220^-$, $CD49b^+$, $CD3^+$ cells), NK cells ($CD11b^-$, $B220^-$, $CD49b^+$, $CD3^-$ cells), and dendritic cells (DCs) ($CD11b^{-/low}$, $B220^-$, $CD49b^-$, $CD3^-$, $CD11c^+$ cells). **(B)** Gating strategy for intracellular cytokine stain of neural single cell suspensions. After exclusion of doublets, dead cells, and $CD11b^+/CD19^+$ cells, $CD3^+$ T cells were evaluated for CD69 and cytokine expression (TNF-α, IFN-γ, or IL-17A). Representative flow cytometry density plots show the percentage of $CD69^+TNF\text{-}\alpha^+$, $CD69^+$ IFN-γ^+, and $CD69^+IL\text{-}17A^+$ $CD3^+$ T cells. The gating strategies show representative plots from a vehicle-treated animal.

Supplementary Figure 1: Gating strategy for neural single cell suspensions from the brain and spinal cord of mice sacrificed at the peak of MOG-EAE disease.

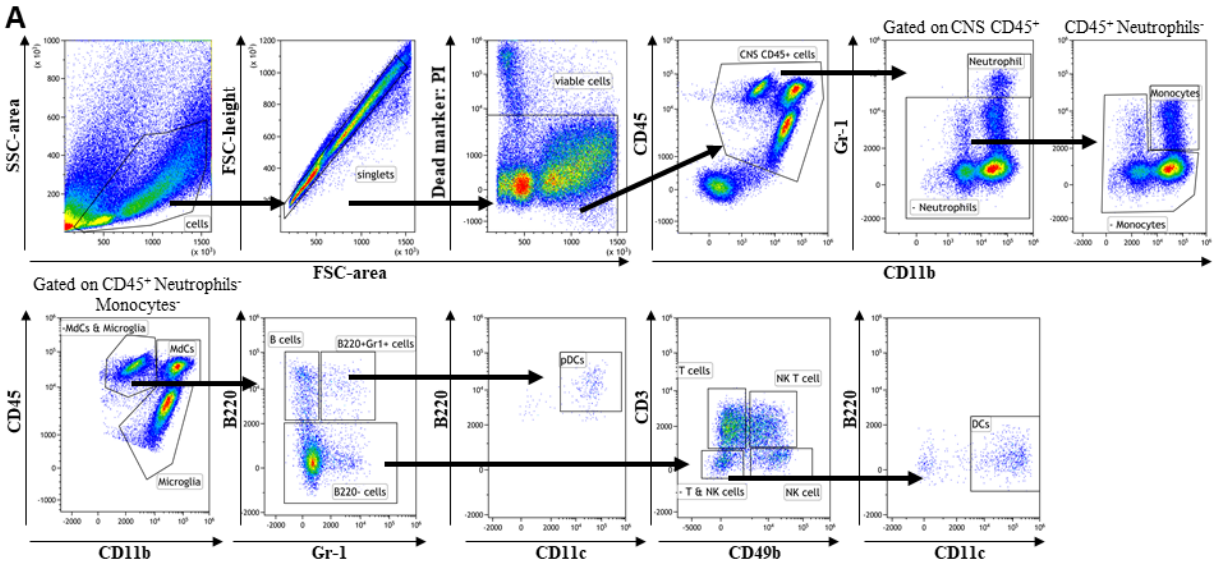

Supplementary Figure 1: Gating strategy for neural single cell suspensions from the brain and spinal cord of mice sacrificed at the peak of MOG-EAE disease.

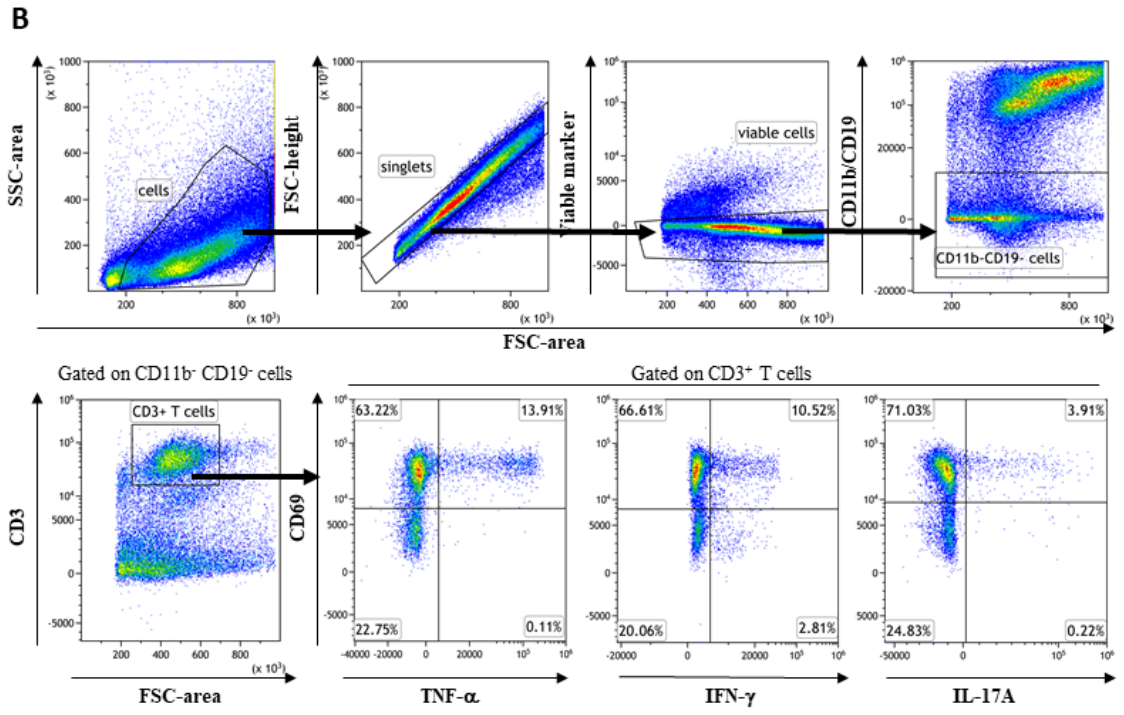

DISCUSSION AND PERSPECTIVES

1 Context of my PhD work

My PhD is carried out in the context of a validation of my experience, gained over a 13-year work experience in the pharmacology and immunology department within Idorsia Pharmaceuticals Ltd (previously Actelion Pharmaceuticals), a pharmaceutical company based in Switzerland, specialized in discovering, developing, and commercializing small molecule drugs for the treatment of different diseases. I have joined this company in 2009 and was hired as a research associate. In 2015, my work and expertise have been recognized with a position of "laboratory head/scientist", followed in 2019 by a position of "senior scientist". In this position, I am the research project leader in pharmacology for three different projects, including the ACKR3 project and I am the head of a laboratory with 4-5 research associates (see the folder "experience professionnelle de recherche").

The discovery and the development of a novel small molecule drug require the expertise of a multidisciplinary project team with various competences including pharmacologists. During the preclinical drug development process, multiple stages exist, which necessitate the efforts and cooperation between all team members (see Introduction section 2). In the context of the CXCR7/ACKR3 research project within Idorsia Pharmaceuticals Ltd, these interdisciplinary efforts culminated in the discovery and selection of ACT-1004-1239, a first-in-class, potent, selective, insurmountable, and orally available ACKR3 antagonist [202]. To our knowledge, ACT-1004-1239 is the first ACKR3 antagonist inhibiting the recruitment of β-arrestin to ACKR3 following CXCL11 and CXCL12 stimulation. Treatment with ACT-1004-1239 demonstrated proof-of-efficacy in a variety of animal disease models and the project has now reached the clinical development stage (NCT03869320 and NCT04286750).

As the preclinical pharmacologist leader of this research project, my main goal in this doctoral thesis was to generate pharmacological data to build a solid preclinical package which allowed us to submit regulatory documents to start human trials with ACT-1004-1239. After the establishment of a target engagement assay, aiming at characterizing the PK/PD relationship of ACT-1004-1239 in healthy mice using plasma CXCL12 as a PD biomarker [202,326], we assessed the efficacy of ACT-1004-1239 in murine disease models to further characterize its mechanism(s) of action and its therapeutic potential for the treatment of inflammatory demyelinating diseases, such as MS [327,328]. In this section, I will discuss the results we have obtained with ACT-1004-1239 in the context of drug development, together with the perspectives of clinical development of this compound, which has demonstrated a dual mechanism of action, leading to both the reduction of leukocyte migration to the site of inflammation, and a promyelinating effect.

2 CXCL11 and CXCL12 as PD biomarkers of target engagement

The study of drug effects *in vivo*, in an intact organism, is central in the process of preclinical drug development. Target engagement PD biomarkers are useful tools to prioritize drug candidates and to determine the dose or efficacious concentration of compound needed *in vivo* to fully engage the intended target. Target engagement biomarkers can also be used to understand the drug concentration needed to saturate the desired downstream effect. Characterization of the drug PK/PD biomarker relationship in the species that will be used to demonstrate efficacy can then be used to further design proper efficacy studies, giving indication on the appropriate dose schedule in animal disease models. In addition, PD biomarkers may be useful to show that a drug produces the expected pharmacologic response in humans. This information can guide the team to define the appropriate doses to be considered in trials to evaluate a clinical outcome.

One of my first objectives in the ACKR3 research project was to investigate the potential of ACKR3 antagonists *in vivo* and evaluate whether CXCL11 and/or CXCL12 plasma levels could be used as biomarkers of target engagement.

Our results demonstrated that ACT-1004-1239, after a single or repeated oral administration, dose- and time-dependently increased the CXCL12 plasma concentration in healthy mice, confirming the inhibition of the scavenging activity of ACKR3 *in vivo*. The observed CXCL12 elevation effect, compared to vehicle-treated mice, was rapid and sustained, suggesting that ACKR3 is constantly and rapidly degrading circulating CXCL12 under physiological conditions. These results were in line with previous reported data using ACKR3 agonists, such as CCX754 and CCX771, which demonstrated elevation of serum and plasma CXCL12, respectively, in mice [244,332]. Interestingly, while these compounds led to approximately a 2- to 4- fold increase, ACT-1004-1239 at the highest dose evaluated (100 mg/kg, twice daily), led to a 6- to 7-fold increase (Annex II, figure 1) which was closer to the effect observed in genetically *Ackr3* deficient mice [244].

This difference in the magnitude of the effect, that we could also confirm in experiments where we compared side by side an ACKR3 agonist versus an ACKR3 antagonist in the same strain of mice (data not shown), might indicate that functional antagonism induced by ACKR3 desensitization with ACKR3 agonists is less efficient to fully block the scavenging activity of the receptor. Indeed, Berahovich et al., have reported that increased CXCL12 plasma levels were seen only when CCX771 plasma concentrations were high enough to engage more than 90% of the ACKR3 molecules. In contrast, our data demonstrate that significant plasma CXCL12 increase was already observed after one single oral administration at the lowest dose tested of ACT-1004-1239 (1 mg/kg), showing that ACT-1004-1239 can reduce ACKR3 scavenging activity at low plasma concentrations close to the mouse IC_{50} of the drug [202]. This difference might be due to the constant recycling of ACKR3 between the membrane and the endosomal compartment [243], and might also relate to the intrinsic properties of the small molecules, such as their ability in crossing the cell membranes and target the intracellular pool of ACKR3. Evaluation of the functional differences between ACKR3 agonists and antagonists would be needed to better understand the currently debated mechanisms behind the functional interaction between ACKR3 and its ligands.

The duration of CXCL12 increase upon ACT-1004-1239 treatment was also dose-dependent. In line with PK data generated *in vitro* in rodents [202], ACT-1004-1239 was rapidly cleared *in vivo* in mice and consequently only the highest doses regimen evaluated (100 mg/kg in single dose or 100 mg/kg, twice daily for 3 days) were able to provide quantifiable drug plasma exposure, 24 hours after the last administration, that resulted in a sustained CXCL12 plasma levels increase. At this dose (100 mg/kg, twice daily), PK/PD modeling of the data indicated that CXCL12 elevation reached a plateau that was maintained over time, suggesting that the drug plasma concentrations reached were sufficient to fully block ACKR3 and its scavenging activity. This was in line with the measured compound plasma concentration at 24h, which was two times above the concentration expected to block at least 90% of the ACKR3 molecules based on the drug's potency in the mouse β-arrestin assay and plasma-protein-binding properties (data not shown).

However, the fact that plasma CXCL12 elevation reaches a plateau underpins the involvement of other CXCL12 elimination pathways than via ACKR3, such as posttranslational modifications, another scavenger receptor, or another to date unknown mechanism. The IC_{50} of ACT-1004-1239, defining the total plasma concentration of ACT-1004-1239 leading to a half maximal effect on CXCL12 increase, was estimated at 11.2 ng/mL, meaning 21nM. Considering the plasma protein binding of ACT-1004-1239 in mice (81%, data not shown), this value corresponds to 4 nM of plasma unbound fraction of ACT-1004-1239, which is very close to the *in vitro* IC_{50} of 2.3 nM determined in the mouse β-arrestin assay [202], confirming its high potency on the receptor *in vivo* and supporting the use of CXCL12 as a PD biomarker for target engagement in mice but also in humans.

In contrast, an increase in plasma CXCL11 concentration was observed only with the highest dose of ACT-1004-1239 at 100 mg/kg, administrated twice daily for 3 days in healthy mice. To our knowledge, this is the first time that a CXCL11 increase is observed *in vivo* upon ACKR3 antagonism treatment, confirming our previous *in vitro* data [202]. However, the fact that the CXCL11 increase was more variable than that of CXCL12 and only seen after the treatment with a high dose of ACT-1004-1239, may be explained by a), the IFN-inducible nature of CXCL11 (see Introduction, section 3.2.2.2), which is hardly detectable under physiological conditions in the plasma, and b), the lower affinity of ACKR3 for CXCL11 compared to CXCL12, suggesting that cells expressing low endogenous ACKR3 such as under physiological conditions, would efficiently scavenge CXCL12 but not CXCL11 [333].

Taken together, these data suggest that while CXCL12 is a valuable primary PD biomarker for target engagement under physiological conditions, CXCL11 might be considered as an additional PD biomarker under inflammatory conditions.

3 Consequences of ACKR3 antagonism on immune cell migration to the sites of inflammation

3.1 Role of ACKR3 in migration of immune cells to the inflamed lungs in a preclinical ALI model

One of the objectives I had during the lead optimization phase of the ACKR3 project was to select, develop, and characterize a target-relevant proof-of-mechanism model to assess efficacious concentrations of the lead ACKR3 antagonists to further help the identification of the best drug candidate. Selecting the appropriate animal models to establish relationship between drug potency, dose, plasma and/or tissue exposure and efficacy on a given mechanism, is a strategically important decision and requires good characterization of the experimental model and the drug PK/PD in the specie used.

To fulfill this objective, we have selected and characterized a murine ALI model induced by inhalation of nebulized LPS in DBA/1 mice. This strain of mice was previously used in our *in vivo* ACKR3 target engagement assay and expresses both ACKR3 chemokine ligands. In addition, both CXCL11 and CXCL12 gradients had been involved in the recruitment of immune cells to different lung compartments during acute pulmonary inflammation induced by lipopolysaccharide (LPS) in mice [329,330]. The ALI mouse model was characterized over time for the main features of ALI, including inflammatory cell recruitment to the bronchoalveolar space and the release of CXCR3/CXCR4/ACKR3 chemokine ligands in different compartments. Consistent with findings from human patients and mouse models of ALI [330,334,335], CXCR3 and CXCR4 chemokine ligands were elevated in the BAL of LPS-challenged mice. This increase was associated with increased BAL $CXCR3^+$ and $CXCR4^+$ leukocyte infiltrates, which have been suggested to exert a damaging effect in the lung [330,336]. We also observed that CXCR4 was mainly expressed on myeloid cells while CXCR3 was mainly expressed on lymphoid cells infiltrated into the BAL, suggesting a non-redundant role for these two chemokine receptors in the recruitment of cells towards the site of inflammation. In addition, the expression of

CXCR3 on lymphoid cells and CXCR4 on myeloid cells steadily increased over time following LPS-induced lung injury, suggesting their involvement in the recruitment and/or prolonged retention of immune cells during ALI.

The mechanism leading to directed cell migration to the site of inflammation is tightly regulated. While molecular mechanisms have not been fully elucidated, a clear consensus that cells use spatial and possibly temporal sensing of fluctuations in chemoattractant concentrations to guide their long-distance directional movement has emerged. The expression of ACKR3 on leukocytes has been debated both in mice and humans [337]. In contrast, its CXCL12 scavenging activity on endothelial cells has been shown to enable CXCR4-dependent cell migration from the blood to inflamed tissue by regulating CXCL12 plasma concentration and the subsequent formation of the CXCL12 concentrations gradients [244,246,338]. Consistent with this mechanism, antagonizing ACKR3 with ACT-1004-1239 led to a dose-dependent increase in plasma CXCL12 which was associated with a dose-dependent decrease of LPS-induced leukocytes infiltrates in the BAL. At all the time points investigated following LPS challenge, ACT-1004-1239, at the highest evaluated dose (100 mg/kg, twice daily), significantly increased CXCL12 plasma concentrations and reduced $CXCR4^+$ leukocytes infiltrates in the BAL. These results on cell migration inhibition were in line with previous findings demonstrating the anti-inflammatory effect of the ACKR3 agonist, CCX771, which reduced migration of neutrophils into the BAL, in a similar murine ALI model [339]. Our study, using an ACKR3 antagonist, provides evidence that the effect observed on neutrophil migration with CCX771 in ALI, is likely due to its functional antagonistic activity rather than its agonistic effect on ACKR3.

Previous studies assessing the effect of CCX771 in ALI were performed in C57BL/6 mice, which do not express CXCL11 [339,340]. Consequently, the role of ACKR3 on the CXCL11/CXCR3 axis *in vivo* could not be investigated. Our results provide the first demonstration that, under inflammatory conditions, as is the case in LPS-challenged mice, blocking ACKR3 with ACT-1004-1239 dose-dependently increases CXCL11 plasma concentration. This ACT-1004-1239-induced plasma

CXCL11 increase was also observed consistently at all the time points investigated following LPS challenge, supporting its use as a PD biomarker for target engagement under inflammatory conditions. This effect was associated with a significant reduction in $CXCR3^+$ lymphoid cell infiltrates in the BAL, suggesting that ACKR3 not only modulates the CXCR4-dependent cell migration but also the CXCR3-dependent cell migration by regulating both CXCL12 and CXCL11 plasma concentrations under inflammatory conditions.

We observed that best efficacy on cell migration was achieved at the dose of ACT-1004-1239 (100 mg/kg, twice daily) that always maintained CXCL12 concentrations close to the plateau in the target engagement assay, suggesting that disruption of the chemokine gradients works best when ACKR3 is fully blocked over time. This mechanism of action resulted in a broad immunomodulatory effect of ACT-1004-1239, which was consistently demonstrated both in a preventive and therapeutic setting. In addition, ACT-1004-1239 demonstrated efficacy on several key pathological features of ALI, such as breathing dysfunctions and alteration in the alveolar capillary barrier. These findings are discussed in more details in the article I [327].

Thanks to this proof-of-mechanism model, we determined the efficacious concentrations of ACT-1004-1239 needed to reduce cell migration in a disease model and hence, established key relationships between PK/PD and efficacy. In the context of drug development, these data together with toxicology data helped us to determine the therapeutic index for each ACKR3 antagonist evaluated in this proof-of-mechanism model (data not shown) and allowed us to identify ACT-1004-1239 as the best drug candidate to move forward into clinical development.

3.2 Role of ACKR3 in migration of immune cell to the CNS in a preclinical MS model

My last goal was to assess the potential of ACT-1004-1239 for the treatment of different key pathological features of MS, including neuroinflammation.

The MOG-induced EAE model manifests several features of MS, including neuroinflammation (see Introduction, section 2.3.1). Our results demonstrated that ACT-1004-1239 treatment dose-dependently reduced the EAE disease severity and subsequent mortality. These results were in line with previous efficacy data obtained in similar EAE models using the ACKR3 agonist, CCX771 [288], suggesting that like in the ALI model, the beneficial roles of this compound were due to its functional antagonism rather than its agonistic effect.

In line with our previous observations in the ALI model, ACT-1004-1239 treatment dose-dependently increased plasma CXCL12 concentrations in EAE mice which significantly correlated with a reduced overall extent of clinical EAE disease. Interestingly, the CXCL12 levels reached following treatment with ACT-1004-1239 were similar to the levels obtained in healthy mice and in the two disease models (ALI, MOG-EAE), suggesting that this PD biomarker is robust and does not fluctuate depending on the inflammatory environment, supporting its use as PD biomarker in clinical trials. Again, best efficacy on clinical EAE disease was obtained at the dose of ACT-104-1239 (100 mg/kg, twice daily) that maintained enough drug concentration at trough to fully block ACKR3 based on the target engagement assay described above (see Discussion and perspectives, section 2). At this dose, ACT-1004-1239 treatment significantly reduced infiltration of immune cells into the CNS of EAE mice, including MOG-specific pathogenic secreting T cells, which was associated with a reduced clinical score. This overall reduction in neuroinflammation was associated with a significant decrease in plasma NFL concentration, providing evidence for axonal protection (see Introduction, section 1.9.1). Consistent with findings in human MS lesions, most of the CNS-infiltrating leukocytes expressed CXCR4 on the cell surface and in line with what was already observed in our ALI model, highest expression was found on myeloid cells [45,297,300]. Treatment with ACT-1004-1239 completely resulted in the paucity of $CXCR4^+$ infiltrates in the CNS, consistent with its hypothesized mechanism of action, namely the disruption of the CXCL12 gradient along which $CXCR4^+$ leukocytes migrate from the blood to the sites of inflammation, such as the CNS in EAE.

Previous findings from studies, both in patients with MS and in EAE mice, reported that a change in the spatial CXCL12 distribution at the perivascular space within the lesions was associated with increased infiltration of $CXCR4^+$ leukocytes in the CNS (see Introduction, section 3.4.1) [297]. In our study, while we demonstrated decreased $CXCR4^+$ leukocyte infiltrates in the CNS, we did not perform immunohistochemistry to assess the localization of CXCL12 expression at the BBB nor did we evaluate whether ACT-1004-1239 would restore the expected abluminal expression of CXCL12. This should be considered in future studies with this compound. In addition, this model was conducted in C57BL/6 mice; thus, we could not investigate the effect of ACT-1004-1239 on the CXCL11/CXCR3 axis in EAE. However, my laboratory has already conducted several experiments in the PLP-induced EAE model in SJL mice which express both chemokine ligands. The results obtained are in line with the published efficacy results in the MOG EAE model and will be the subject of a new article. In addition, some of these results were already presented at the ACTRIMS and AAN 2021 and are available as Annex III.

Taken together, these data confirmed that ACKR3 plays a major role in the recruitment of inflammatory cells to the CNS and subsequent tissue damage leading to paralysis in EAE mice.

3.3 Concluding remarks

The evaluation of a candidate drug in a variety of animal disease models and the measurement of different biological and clinical endpoints increases confidence in the mechanistic understanding of heretofore unprecedented targets. In addition, it may help the research project team to identify both the most relevant and broadest clinical indications where a drug might show efficacy. Using both the ALI and EAE models, we demonstrated the dose-dependent efficacy of ACT-1004-1239 treatment on the reduction of cell recruitment to the sites of inflammation, supporting its development in inflammatory diseases, such as in neuroinflammation. Best effect on cell migration was achieved when the plasma concentration of ACT-1004-1239 at trough was high enough to fully block ACKR3 and thus maintain the maximal elevation of the plasma PD biomarker CXCL12.

4 Consequences of ACKR3 antagonism on demyelination

Demyelination and neurodegeneration are key hallmarks of all forms of MS. Despite the approval of new DMTs for the treatment of patients with MS, there is currently no drug approved to repair the damaged CNS. The promotion of regeneration of the myelin sheath has emerged as one of the most promising strategies to halt progression of the disease in patients with MS. Targeting ACKR3 has been proposed as a valuable target to enhance differentiation of OPCs into myelinating OLs, resulting in remyelination [290]. However, conflicting data have been published and it remained unclear whether the beneficial effects observed with CCX771 in demyelinating models come from its agonistic activity on ACKR3 or its functional antagonism [88,89].

4.1 Role of ACKR3 in myelination

One of my goals was to assess the potential therapeutic effect of ACT-1004-1239 on demyelination in an animal model where the primary demyelination is not mediated by the immune system, to avoid interference with the anti-inflammatory properties of ACT-1004-1239. We used the cuprizone-induced demyelination model that we introduced in Introduction, section 2.3.2. Our results demonstrated that ACT-1004-1239 co-administrated with cuprizone either in a preventive setting or starting after 3 weeks of cuprizone exposure, significantly reduced cuprizone-induced demyelination in the corpus callosum. In this model, apoptosis of mature OLs starts already during the first week of cuprizone exposure and leads to the activation, migration, and proliferation of glial cells, including astrocytes [233]. Treatment with ACT-1004-1239 in both settings did not affect reactive astrogliosis, suggesting that ACT-1004-1239 co-administration did not prevent cuprizone-induced apoptosis of mature OLs and subsequent astrogliosis. However, co-treatment with ACT-1004-1239 in both settings increased mature myelinating OLs while decreasing the cuprizone-induced increase in the proportion of OPCs within the OL population in the corpus callosum. These data suggest that, while the

environment is toxic for mature OLs due to cuprizone exposure, ACT-1004-1239 treatment promotes the differentiation of OPCs into mature myelinating OLs and subsequent myelination in cuprizone-treated mice. In line with our results, in the same model, the ACKR3 agonist, CCX771, was also shown to increase mature OLs within the demyelinated area and to increase myelination [290], suggesting that the beneficial effect was due to its functional antagonism rather than to its agonistic activity. In line with this hypothesis, the observed myelinating effect was associated with an increase in CXCL12 protein within the demyelinated area and was abrogated by treatment with a CXCR4 antagonist, suggesting that CCX771-induced differentiation of OPCs into myelinating OPCs happens through an indirect CXCL12-driven agonistic effect on CXCR4 [290]. In our study presented in Article II, we observed the increase in myelination upon ACT-1004-1239 treatment but did not assess CXCL12 levels in the brains of mice. However, recent studies conducted in my laboratory could demonstrate that ACT-1004-1239 treatment increased CXCL12 protein levels in the mouse CNS, confirming previous results with CCX771. These results were partially presented in a poster presented at two international congresses: ACTRIMS and AAN 2021 (Annex III). Next steps will be to link this increase in myelination with a functional effect such as an effect in a behavioral test or a direct assessment of the conduction properties.

4.2 Role of ACKR3 in the differentiation of OPCs into myelinating OLs

Based on the above-mentioned results, we hypothesized that the beneficial effect of ACT-1004-1239 on myelination in the cuprizone model was indirect, through modulation of the CXCL12/CXCR4 axis on OPCs.

First, in rat OPC-neuron co-culture experiments performed by Neuro-Sys, we assessed the effect of recombinant rat CXCL12 on the differentiation of OPCs. In line with previous reports, CXCL12 dose-dependently promoted the differentiation of OPCs into myelinating OLs *in vitro* [88,89]. However, at high concentration (100 ng/mL), CXCL12 gave the opposite effect and led to a reduction of mature OLs, suggesting that this high CXCL12 concentration triggers CXCR4 endocytosis

and degradation, as previously described [283]. In line with this observation, and with previous studies [75,290,313], the CXCR4 antagonist AMD3100 induced a significant reduction in mature OL numbers, confirming that CXCL12-induced maturation of OPCs in this rat co-culture was CXCR4-dependent. Importantly, blockade of ACKR3 with ACT-1004-1239 dose-dependently increased maturation of OPCs to myelinating OLs. This effect was associated with a dose-dependent elevation of CXCL12 concentration in the co-culture supernatant, demonstrating target engagement in this CNS co-culture *in vitro* and confirming the hypothesis that the beneficial effect of ACT-1004-1239 on OPCs differentiation might be through modulation of the CXCL12/CXCR4 axis on OPCs. Interestingly, the highest concentration of ACT-1004-1239 (10mM) led to a CXCL12 concentration in the co-culture supernatant that was lower than when exogenous CXCL12 (30 ng/mL) was added to the co-cultures. These data suggest that ACKR3 antagonism might not lead to a high enough CXCL12 increase that triggers CXCR4 endocytosis and degradation. The pro-differentiation effect observed upon ACT-1004-1239 treatment in this co-culture was in contradiction with published data with the ACKR3 agonists CCX771 and CCX754, wrongly reported as ACKR3 antagonists, that claimed that CXCL12-dependent OPC maturation both in rodent and human cells was not CXCR4- but ACKR3-dependent [88,89]. These conflicting results could be explained by the fact that these studies were performed in the presence of both the ACKR3 agonist and high doses of exogenous CXCL12. As CCX771 is known to reduce the scavenging activity of ACKR3 and consequently increases extracellular levels of CXCL12 [244,290], the combination of exogenous CXCL12 plus CCX771 could have resulted in such a high concentration of CXCL12 in the culture, leading to the internalization and degradation of CXCR4.

Taken together, our *in vitro* findings suggest that antagonizing ACKR3 with ACT-1004-1239 promotes differentiation of OPCs into myelinating OLs by increasing CXCL12 concentrations in the co-culture, thus, enhancing the CXCR4/CXCL12-mediated maturation of OPCs.

4.3 Concluding remarks

Our findings suggest that antagonizing ACKR3 with ACT-1004-1239 promotes differentiation of OPCs into myelinating OLs and subsequent myelination, supporting its development for the treatment of demyelinating diseases. However, whether improved remyelination can indeed attenuate axonal loss and subsequent disability accumulation in patients with MS is still a key question that needs to be addressed in clinical trials. However, there are many challenges to effectively translate pharmacological strategies that target remyelination into clinical reality. Such challenges include developing new imaging approaches to be able to monitor myelin status in patients, selecting the most appropriate target population of patients with MS, and determining the most effective timing to administrate the pro-myelinating drug.

5 Perspectives with ACT-1004-1239

5.1 ACKR3: the tip of the iceberg

Recently, ACKR3 has been reported as a scavenger receptor for opioid peptides *in vitro* [286], including the subfamily of dynorphins which binds KOR, an opioid receptor which has been proposed to enhance the proliferation and differentiation of OPCs, and subsequent remyelination *in vivo* (see Introduction, section 3.4.3). The functional relevance of this effect mediated by ACKR3 scavenging activity *in vivo* has not been reported yet. Next step will be to assess the effect of ACT-1004-1239 treatment on opioid peptide levels *in vivo* and to understand its functional effect such as the contribution of this opioid axis in the observed remyelinating effect or in pain. Indeed, pain is a common symptom in patients with MS, reported in up to 75% of the patients [341]. However, pain is poorly managed and therefore is a high unmet need for patients with MS. ACKR3 by scavenging opioid peptides, might also play a detrimental role in pain, which might be improved with ACT-1004-1239 treatment.

As mentioned in the introduction, section 3.4.2, binding of CXCL11 and CXCL12 to ACKR3 reduced gap junctional intercellular communication in astrocytes trough Cx43 internalization [310], which could contribute to the pathological role of ACKR3 in MS. Therefore, future studies will assess whether ACT-1004-1239 treatment could restore the Cx43-dependent gap junction-mediated communication between astrocytes and OLs *in vivo* and may thus also contribute to the beneficial effect observed with this compound in the cuprizone and EAE models.

5.2 Clinical development of ACT-1004-1239

Despite the crucial role of chemokines in immune function and brain homeostasis, only two drugs targeting chemokine receptors have been developed and reached clinical approval in very specific indications: stem cell mobilization for the CXCR4 antagonist plerixafor, and HIV-1 infection for the CCR5 antagonist maraviroc. Most of the evidence explaining the failures of previous chemokine receptor antagonists in the clinic point towards an insufficient dosing of chemokine receptor antagonists *in vivo* [342].

Our preclinical findings have demonstrated that CXCL12 could be used as a PD biomarker of target engagement that could guide the selection of the dose of ACT-1004-1239 to get maximal efficacy in animal disease models. In line with our results in healthy mice, and with our PK predictions [202], ACT-1004-1239 dose-dependently increased CXCL12 plasma concentrations in healthy humans, reaching a plateau at doses ≥ 100 mg ACT-1004-1239, once daily [326]. Therefore, in contrast to most of the previous chemokine receptor antagonists investigated in clinical trials, ACT-1004-1239 has a PD biomarker of target engagement, which can guide us for optimal dose selection during clinical development.

In addition, previous failures with chemokine receptor antagonists might have also occurred due to the redundancy of the target. Therefore, targeting several chemokine receptors has been proposed as an innovative way to overcome redundancy issues and generate effective therapeutics. Our results demonstrated that ACT-1004-1239, by targeting ACKR3, increased both CXCL11 and CXCL12 and thus indirectly modulated CXCR3- and CXCR4-mediated signaling in animal

disease models. In addition, as described above, ACKR3 might also scavenge opioid peptides and have potentially other direct functions such as a direct effect on gap junctions, suggesting that ACKR3 is an interesting therapeutic target that can interact with multiple targets at once. Of note, multiple doses of ACT-1004-1239 for 7 days once daily were well tolerated in healthy volunteers, supporting further clinical development of ACT-1004-1239 in patients [326].

CONCLUSION

To summarize, I have contributed to the discovery, selection, and preclinical development of ACT-1004-1239, a potent, selective, and orally available ACKR3 antagonist, currently undergoing clinical trials. We have provided evidence on the essential role of ACKR3 in inflammatory demyelinating diseases, such as MS. Blocking the 'scavenging' activity of ACKR3 with an antagonist, such as ACT-1004-1239, is expected to have both an immunomodulatory and promyelinating effect [Figure 23]. Specifically, ACT-1004-1239 is expected to 1) increase the concentrations of CXCL11 and CXCL12 in the circulation leading to the disruption of these chemokine gradients (immunomodulatory effect) required for the directional migration of CXCR3- and CXCR4-positive cells, known to play a pathological role in inflammatory diseases, and 2) increase the CXCL12 concentration within the demyelinated area and thereby activate CXCR4-mediated OPC maturation, resulting in increased myelin content (promyelinating effect). In summary, our data underscore the clinical potential of ACT-1004-1239, reducing the inflammation and improving myelination in patients with inflammatory demyelinating diseases.

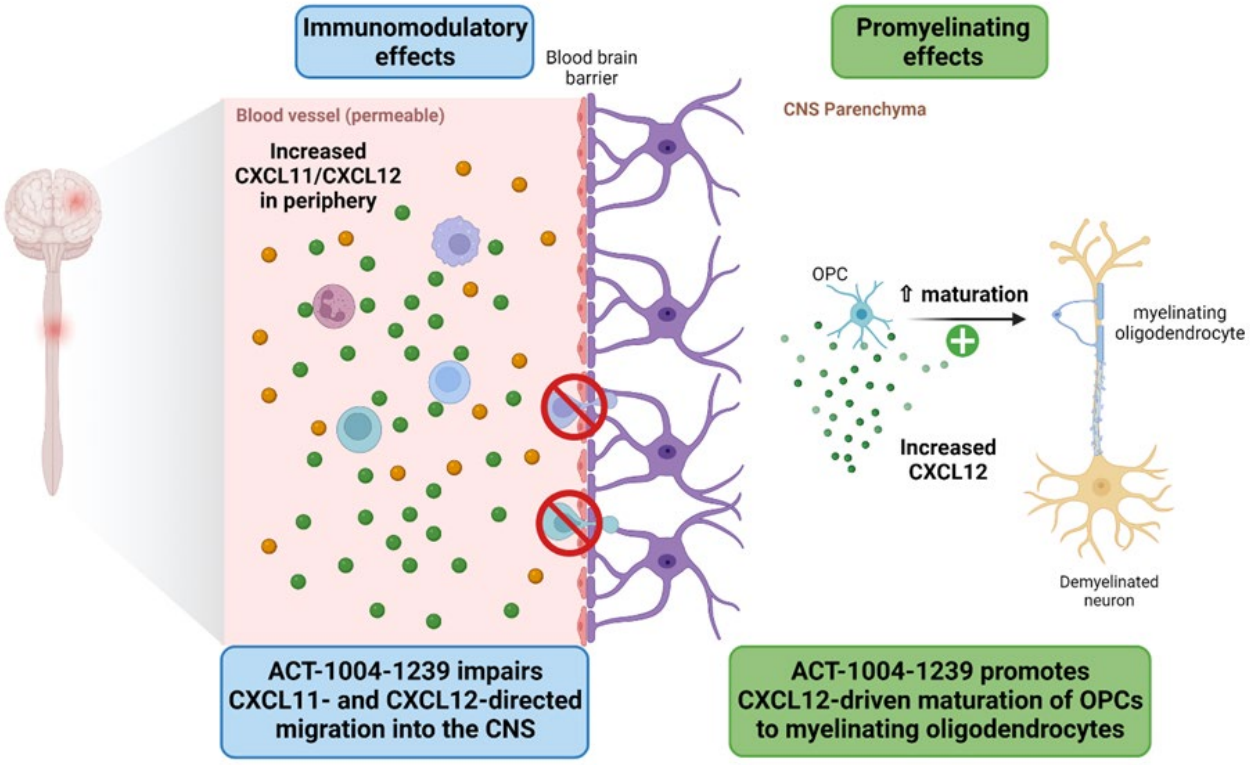

Figure 23: Potential therapeutic effects of ACT-1004-1239 for the treatment of MS.

BIBLIOGRAPHY

1. Zalc B. One hundred and fifty years ago Charcot reported multiple sclerosis as a new neurological disease. *Brain*. 2018;141(12):3482-3488.
2. Popescu BF, Pirko I, Lucchinetti CF. Pathology of multiple sclerosis: where do we stand? *Continuum (Minneap Minn)*. 2013;19(4 Multiple Sclerosis):901-921.
3. Walton C, King R, Rechtman L, et al. Rising prevalence of multiple sclerosis worldwide: Insights from the Atlas of MS, third edition. *Mult Scler*. 2020;26(14):1816-1821.
4. Leray E, Moreau T, Fromont A, Edan G. Epidemiology of multiple sclerosis. *Rev Neurol (Paris)*. 2016;172(1):3-13.
5. Belbasis L, Bellou V, Evangelou E, Ioannidis JP, Tzoulaki I. Environmental risk factors and multiple sclerosis: an umbrella review of systematic reviews and meta-analyses. *Lancet Neurol*. 2015;14(3):263-273.
6. Bjornevik K, Cortese M, Healy BC, et al. Longitudinal analysis reveals high prevalence of Epstein-Barr virus associated with multiple sclerosis. *Science*. 2022;375(6578):296-301.
7. Ascherio A, Munger KL, White R, et al. Vitamin D as an early predictor of multiple sclerosis activity and progression. *JAMA Neurol*. 2014;71(3):306-314.
8. Sintzel MB, Rametta M, Reder AT. Vitamin D and Multiple Sclerosis: A Comprehensive Review. *Neurol Ther*. 2018;7(1):59-85.
9. Sadovnick AD, Baird PA. The familial nature of multiple sclerosis: age-corrected empiric recurrence risks for children and siblings of patients. *Neurology*. 1988;38(6):990-991.
10. Fagnani C, Neale MC, Nistico L, et al. Twin studies in multiple sclerosis: A meta-estimation of heritability and environmentality. *Mult Scler*. 2015;21(11):1404-1413.
11. Bertrams J, Kuwert E, Liedtke U. HL-A antigens and multiple sclerosis. *Tissue Antigens*. 1972;2(5):405-408.
12. Isobe N, Keshavan A, Gourraud PA, et al. Association of HLA Genetic Risk Burden With Disease Phenotypes in Multiple Sclerosis. *JAMA Neurol*. 2016;73(7):795-802.

13. Parnell GP, Booth DR. The Multiple Sclerosis (MS) Genetic Risk Factors Indicate both Acquired and Innate Immune Cell Subsets Contribute to MS Pathogenesis and Identify Novel Therapeutic Opportunities. *Front Immunol*. 2017;8:425.
14. Baranzini SE, Oksenberg JR. The Genetics of Multiple Sclerosis: From 0 to 200 in 50 Years. *Trends Genet*. 2017;33(12):960-970.
15. Lublin FD, Reingold SC, Cohen JA, et al. Defining the clinical course of multiple sclerosis: the 2013 revisions. *Neurology*. 2014;83(3):278-286.
16. Dendrou CA, Fugger L, Friese MA. Immunopathology of multiple sclerosis. *Nat Rev Immunol*. 2015;15(9):545-558.
17. Klineova S, Lublin FD. Clinical Course of Multiple Sclerosis. *Cold Spring Harb Perspect Med*. 2018;8(9).
18. Eshaghi A, Prados F, Brownlee WJ, et al. Deep gray matter volume loss drives disability worsening in multiple sclerosis. *Ann Neurol*. 2018;83(2):210-222.
19. Kister I, Bacon TE, Chamot E, et al. Natural history of multiple sclerosis symptoms. *Int J MS Care*. 2013;15(3):146-158.
20. Fox RJ, Bacon TE, Chamot E, et al. Prevalence of multiple sclerosis symptoms across lifespan: data from the NARCOMS Registry. *Neurodegener Dis Manag*. 2015;5(6 Suppl):3-10.
21. Society NMS. Symptoms & Diagnosis. https://www.nationalmssociety.org/Symptoms-Diagnosis/Diagnosing-MS. Published 2021. Accessed.
22. Ghasemi N, Razavi S, Nikzad E. Multiple Sclerosis: Pathogenesis, Symptoms, Diagnoses and Cell-Based Therapy. *Cell J*. 2017;19(1):1-10.
23. Rovira A, Wattjes MP, Tintore M, et al. Evidence-based guidelines: MAGNIMS consensus guidelines on the use of MRI in multiple sclerosis-clinical implementation in the diagnostic process. *Nat Rev Neurol*. 2015;11(8):471-482.
24. Fisniku LK, Brex PA, Altmann DR, et al. Disability and T2 MRI lesions: a 20-year follow-up of patients with relapse onset of multiple sclerosis. *Brain*. 2008;131(Pt 3):808-817.
25. Trip SA, Miller DH. Imaging in multiple sclerosis. *Journal of Neurology, Neurosurgery & Psychiatry*. 2005;76(suppl 3):iii11.
26. Frischer JM, Bramow S, Dal-Bianco A, et al. The relation between inflammation and neurodegeneration in multiple sclerosis brains. *Brain*. 2009;132(Pt 5):1175-1189.

27. Jin JM, Bai P, He W, et al. Gender Differences in Patients With COVID-19: Focus on Severity and Mortality. *Front Public Health*. 2020;8:152.
28. Chang HC, Huang PH, Syu FS, et al. Critical involvement of atypical chemokine receptor CXCR7 in allergic airway inflammation. *Immunology*. 2017.
29. Yong HYF, Yong VW. Mechanism-based criteria to improve therapeutic outcomes in progressive multiple sclerosis. *Nature Reviews Neurology*. 2021.
30. Lucchinetti C, Bruck W, Parisi J, Scheithauer B, Rodriguez M, Lassmann H. Heterogeneity of multiple sclerosis lesions: implications for the pathogenesis of demyelination. *Ann Neurol*. 2000;47(6):707-717.
31. Frischer JM, Weigand SD, Guo Y, et al. Clinical and pathological insights into the dynamic nature of the white matter multiple sclerosis plaque. *Ann Neurol*. 2015;78(5):710-721.
32. Elliott C, Wolinsky JS, Hauser SL, et al. Slowly expanding/evolving lesions as a magnetic resonance imaging marker of chronic active multiple sclerosis lesions. *Mult Scler*. 2019;25(14):1915-1925.
33. Luchetti S, Fransen NL, van Eden CG, Ramaglia V, Mason M, Huitinga I. Progressive multiple sclerosis patients show substantial lesion activity that correlates with clinical disease severity and sex: a retrospective autopsy cohort analysis. *Acta Neuropathol*. 2018;135(4):511-528.
34. Guerrero BL, Sicotte NL. Microglia in Multiple Sclerosis: Friend or Foe? *Frontiers in Immunology*. 2020;11(374).
35. Wu GF, Alvarez E. The immunopathophysiology of multiple sclerosis. *Neurol Clin*. 2011;29(2):257-278.
36. Salvetti M, Giovannoni G, Aloisi F. Epstein-Barr virus and multiple sclerosis. *Curr Opin Neurol*. 2009;22(3):201-206.
37. Brucklacher-Waldert V, Stuerner K, Kolster M, Wolthausen J, Tolosa E. Phenotypical and functional characterization of T helper 17 cells in multiple sclerosis. *Brain*. 2009;132(Pt 12):3329-3341.
38. Kaskow BJ, Baecher-Allan C. Effector T Cells in Multiple Sclerosis. *Cold Spring Harb Perspect Med*. 2018;8(4).
39. Panitch HS, Hirsch RL, Haley AS, Johnson KP. Exacerbations of multiple sclerosis in patients treated with gamma interferon. *Lancet*. 1987;1(8538):893-895.

40. Havrdova E, Belova A, Goloborodko A, et al. Activity of secukinumab, an anti-IL-17A antibody, on brain lesions in RRMS: results from a randomized, proof-of-concept study. *J Neurol*. 2016;263(7):1287-1295.
41. van Langelaar J, Rijvers L, Smolders J, van Luijn MM. B and T Cells Driving Multiple Sclerosis: Identity, Mechanisms and Potential Triggers. *Front Immunol*. 2020;11:760.
42. Rasouli J, Ciric B, Imitola J, et al. Expression of GM-CSF in T Cells Is Increased in Multiple Sclerosis and Suppressed by IFN-beta Therapy. *J Immunol*. 2015;194(11):5085-5093.
43. Carrieri PB, Provitera V, De Rosa T, Tartaglia G, Gorga F, Perrella O. Profile of cerebrospinal fluid and serum cytokines in patients with relapsing-remitting multiple sclerosis: a correlation with clinical activity. *Immunopharmacol Immunotoxicol*. 1998;20(3):373-382.
44. Fleetwood AJ, Cook AD, Hamilton JA. Functions of granulocyte-macrophage colony-stimulating factor. *Crit Rev Immunol*. 2005;25(5):405-428.
45. Galli E, Hartmann FJ, Schreiner B, et al. GM-CSF and CXCR4 define a T helper cell signature in multiple sclerosis. *Nat Med*. 2019;25(8):1290-1300.
46. Bitsch A, Schuchardt J, Bunkowski S, Kuhlmann T, Bruck W. Acute axonal injury in multiple sclerosis. Correlation with demyelination and inflammation. *Brain*. 2000;123 (Pt 6):1174-1183.
47. Eikelenboom MJ, Killestein J, Izeboud T, et al. Chemokine receptor expression on T cells is related to new lesion development in multiple sclerosis. *J Neuroimmunol*. 2002;133(1-2):225-232.
48. Denic A, Wootla B, Rodriguez M. CD8(+) T cells in multiple sclerosis. *Expert opinion on therapeutic targets*. 2013;17(9):1053-1066.
49. Willing A, Leach OA, Ufer F, et al. CD8(+) MAIT cells infiltrate into the CNS and alterations in their blood frequencies correlate with IL-18 serum levels in multiple sclerosis. *Eur J Immunol*. 2014;44(10):3119-3128.
50. Romano M, Fanelli G, Albany CJ, Giganti G, Lombardi G. Past, Present, and Future of Regulatory T Cell Therapy in Transplantation and Autoimmunity. *Frontiers in Immunology*. 2019;10(43).
51. Kimura K. Regulatory T cells in multiple sclerosis. *Clinical and Experimental Neuroimmunology*. 2020;11(3):148-155.
52. Correale J, Villa A. Isolation and characterization of CD8+ regulatory T cells in multiple sclerosis. *J Neuroimmunol*. 2008;195(1-2):121-134.

53. Sumida T, Lincoln MR, Ukeje CM, et al. Activated β-catenin in Foxp3(+) regulatory T cells links inflammatory environments to autoimmunity. *Nat Immunol*. 2018;19(12):1391-1402.
54. Meiron M, Zohar Y, Anunu R, Wildbaum G, Karin N. CXCL12 (SDF-1alpha) suppresses ongoing experimental autoimmune encephalomyelitis by selecting antigen-specific regulatory T cells. *J Exp Med*. 2008;205(11):2643-2655.
55. Kinnunen T, Chamberlain N, Morbach H, et al. Specific peripheral B cell tolerance defects in patients with multiple sclerosis. *J Clin Invest*. 2013;123(6):2737-2741.
56. Hausser-Kinzel S, Weber MS. The Role of B Cells and Antibodies in Multiple Sclerosis, Neuromyelitis Optica, and Related Disorders. *Front Immunol*. 2019;10:201.
57. Badihian S, Shaygannejad V, Soleimani P, et al. Decreased serum levels of interleukin-35 among multiple sclerosis patients may be related to disease progression. *J Biol Regul Homeost Agents*. 2018;32(5):1249-1253.
58. Wei Y, Chang H, Feng H, Li X, Zhang X, Yin L. Low Serum Interleukin-10 Is an Independent Predictive Factor for the Risk of Second Event in Clinically Isolated Syndromes. *Frontiers in Neurology*. 2019;10(604).
59. Baker D, Marta M, Pryce G, Giovannoni G, Schmierer K. Memory B Cells are Major Targets for Effective Immunotherapy in Relapsing Multiple Sclerosis. *EBioMedicine*. 2017;16:41-50.
60. Ifergan I, Miller SD. Potential for Targeting Myeloid Cells in Controlling CNS Inflammation. *Frontiers in Immunology*. 2020;11(2446).
61. Mishra MK, Yong VW. Myeloid cells - targets of medication in multiple sclerosis. *Nat Rev Neurol*. 2016;12(9):539-551.
62. Miron VE, Boyd A, Zhao JW, et al. M2 microglia and macrophages drive oligodendrocyte differentiation during CNS remyelination. *Nat Neurosci*. 2013;16(9):1211-1218.
63. Butovsky O, Ziv Y, Schwartz A, et al. Microglia activated by IL-4 or IFN-gamma differentially induce neurogenesis and oligodendrogenesis from adult stem/progenitor cells. *Mol Cell Neurosci*. 2006;31(1):149-160.
64. Kouwenhoven M, Teleshova N, Ozenci V, Press R, Link H. Monocytes in multiple sclerosis: phenotype and cytokine profile. *J Neuroimmunol*. 2001;112(1-2):197-205.

65. Chuluundorj D, Harding SA, Abernethy D, La Flamme AC. Expansion and preferential activation of the CD14(+)CD16(+) monocyte subset during multiple sclerosis. *Immunol Cell Biol*. 2014;92(6):509-517.
66. van Noort JM, van den Elsen PJ, van Horssen J, Geurts JJ, van der Valk P, Amor S. Preactive multiple sclerosis lesions offer novel clues for neuroprotective therapeutic strategies. *CNS Neurol Disord Drug Targets*. 2011;10(1):68-81.
67. Politis M, Giannetti P, Su P, et al. Increased PK11195 PET binding in the cortex of patients with MS correlates with disability. *Neurology*. 2012;79(6):523-530.
68. Voss EV, Skuljec J, Gudi V, et al. Characterisation of microglia during de- and remyelination: can they create a repair promoting environment? *Neurobiol Dis*. 2012;45(1):519-528.
69. International Multiple Sclerosis Genetics C. Multiple sclerosis genomic map implicates peripheral immune cells and microglia in susceptibility. *Science*. 2019;365(6460).
70. Ponath G, Park C, Pitt D. The Role of Astrocytes in Multiple Sclerosis. *Front Immunol*. 2018;9:217.
71. Masaki K. Early disruption of glial communication via connexin gap junction in multiple sclerosis, Balo's disease and neuromyelitis optica. *Neuropathology*. 2015;35(5):469-480.
72. Ponath G, Ramanan S, Mubarak M, et al. Myelin phagocytosis by astrocytes after myelin damage promotes lesion pathology. *Brain*. 2017;140(2):399-413.
73. Michel L, Touil H, Pikor NB, Gommerman JL, Prat A, Bar-Or A. B Cells in the Multiple Sclerosis Central Nervous System: Trafficking and Contribution to CNS-Compartmentalized Inflammation. *Front Immunol*. 2015;6:636.
74. Back SA, Tuohy TM, Chen H, et al. Hyaluronan accumulates in demyelinated lesions and inhibits oligodendrocyte progenitor maturation. *Nat Med*. 2005;11(9):966-972.
75. Patel JR, Williams JL, Muccigrosso MM, et al. Astrocyte TNFR2 is required for CXCL12-mediated regulation of oligodendrocyte progenitor proliferation and differentiation within the adult CNS. *Acta Neuropathol*. 2012;124(6):847-860.

76. Plemel JR, Liu W-Q, Yong VW. Remyelination therapies: a new direction and challenge in multiple sclerosis. *Nature Reviews Drug Discovery*. 2017;16(9):617-634.
77. Nave KA, Werner HB. Myelination of the nervous system: mechanisms and functions. *Annu Rev Cell Dev Biol*. 2014;30:503-533.
78. Craner MJ, Newcombe J, Black JA, Hartle C, Cuzner ML, Waxman SG. Molecular changes in neurons in multiple sclerosis: altered axonal expression of Nav1.2 and Nav1.6 sodium channels and Na+/Ca2+ exchanger. *Proc Natl Acad Sci U S A*. 2004;101(21):8168-8173.
79. Nikic I, Merkler D, Sorbara C, et al. A reversible form of axon damage in experimental autoimmune encephalomyelitis and multiple sclerosis. *Nat Med*. 2011;17(4):495-499.
80. Barcelos IP, Troxell RM, Graves JS. Mitochondrial Dysfunction and Multiple Sclerosis. *Biology (Basel)*. 2019;8(2).
81. Bjartmar C, Kidd G, Mork S, Rudick R, Trapp BD. Neurological disability correlates with spinal cord axonal loss and reduced N-acetyl aspartate in chronic multiple sclerosis patients. *Ann Neurol*. 2000;48(6):893-901.
82. Bergles DE, Richardson WD. Oligodendrocyte Development and Plasticity. *Cold Spring Harb Perspect Biol*. 2015;8(2):a020453.
83. Hughes EG, Kang SH, Fukaya M, Bergles DE. Oligodendrocyte progenitors balance growth with self-repulsion to achieve homeostasis in the adult brain. *Nat Neurosci*. 2013;16(6):668-676.
84. Yeung MS, Zdunek S, Bergmann O, et al. Dynamics of oligodendrocyte generation and myelination in the human brain. *Cell*. 2014;159(4):766-774.
85. Munzel EJ, Williams A. Promoting remyelination in multiple sclerosis-recent advances. *Drugs*. 2013;73(18):2017-2029.
86. Williamson JM, Lyons DA. Myelin Dynamics Throughout Life: An Ever-Changing Landscape? *Frontiers in Cellular Neuroscience*. 2018;12(424).
87. Carbajal KS, Miranda JL, Tsukamoto MR, Lane TE. CXCR4 signaling regulates remyelination by endogenous oligodendrocyte progenitor cells in a viral model of demyelination. *Glia*. 2011;59(12):1813-1821.
88. Kremer D, Cui QL, Gottle P, et al. CXCR7 Is Involved in Human Oligodendroglial Precursor Cell Maturation. *PLoS One*. 2016;11(1):e0146503.
89. Gottle P, Kremer D, Jander S, et al. Activation of CXCR7 receptor promotes oligodendroglial cell maturation. *Ann Neurol*. 2010;68(6):915-924.

90. Osso LA, Rankin KA, Chan JR. Experience-dependent myelination following stress is mediated by the neuropeptide dynorphin. *Neuron*. 2021;109(22):3619-3632 e3615.
91. VonDran MW, Singh H, Honeywell JZ, Dreyfus CF. Levels of BDNF impact oligodendrocyte lineage cells following a cuprizone lesion. *J Neurosci*. 2011;31(40):14182-14190.
92. Wilkins A, Chandran S, Compston A. A role for oligodendrocyte-derived IGF-1 in trophic support of cortical neurons. *Glia*. 2001;36(1):48-57.
93. Piaton G, Aigrot M-S, Williams A, et al. Class 3 semaphorins influence oligodendrocyte precursor recruitment and remyelination in adult central nervous system. *Brain*. 2011;134(4):1156-1167.
94. Yuelling LW, Waggener CT, Afshari FS, Lister JA, Fuss B. Autotaxin/ENPP2 regulates oligodendrocyte differentiation in vivo in the developing zebrafish hindbrain. *Glia*. 2012;60(10):1605-1618.
95. Mi S, Hu B, Hahm K, et al. LINGO-1 antagonist promotes spinal cord remyelination and axonal integrity in MOG-induced experimental autoimmune encephalomyelitis. *Nat Med*. 2007;13(10):1228-1233.
96. Lampron A, Larochelle A, Laflamme N, et al. Inefficient clearance of myelin debris by microglia impairs remyelinating processes. *J Exp Med*. 2015;212(4):481-495.
97. Biname F, Pham-Van LD, Spenle C, et al. Disruption of Sema3A/Plexin-A1 inhibitory signalling in oligodendrocytes as a therapeutic strategy to promote remyelination. *EMBO Mol Med*. 2019;11(11):e10378.
98. Stoffels JMJ, de Jonge JC, Stancic M, et al. Fibronectin aggregation in multiple sclerosis lesions impairs remyelination. *Brain*. 2013;136(1):116-131.
99. Saraswat D, Shayya HJ, Polanco JJ, et al. Overcoming the inhibitory microenvironment surrounding oligodendrocyte progenitor cells following experimental demyelination. *Nature Communications*. 2021;12(1):1923.
100. Franklin RJM, Frisen J, Lyons DA. Revisiting remyelination: Towards a consensus on the regeneration of CNS myelin. *Semin Cell Dev Biol*. 2021;116:3-9.
101. Duncan ID, Brower A, Kondo Y, Curlee JF, Jr., Schultz RD. Extensive remyelination of the CNS leads to functional recovery. *Proc Natl Acad Sci U S A*. 2009;106(16):6832-6836.

102. Mei F, Lehmann-Horn K, Shen YA, et al. Accelerated remyelination during inflammatory demyelination prevents axonal loss and improves functional recovery. *Elife*. 2016;5.
103. Kornek B, Storch MK, Weissert R, et al. Multiple sclerosis and chronic autoimmune encephalomyelitis: a comparative quantitative study of axonal injury in active, inactive, and remyelinated lesions. *Am J Pathol*. 2000;157(1):267-276.
104. Bodini B, Veronese M, Garcia-Lorenzo D, et al. Dynamic Imaging of Individual Remyelination Profiles in Multiple Sclerosis. *Ann Neurol*. 2016;79(5):726-738.
105. Coman I, Aigrot MS, Seilhean D, et al. Nodal, paranodal and juxtaparanodal axonal proteins during demyelination and remyelination in multiple sclerosis. *Brain*. 2006;129(Pt 12):3186-3195.
106. Zambonin JL, Zhao C, Ohno N, et al. Increased mitochondrial content in remyelinated axons: implications for multiple sclerosis. *Brain*. 2011;134(Pt 7):1901-1913.
107. Patrikios P, Stadelmann C, Kutzelnigg A, et al. Remyelination is extensive in a subset of multiple sclerosis patients. *Brain*. 2006;129(Pt 12):3165-3172.
108. Gruchot J, Weyers V, Gottle P, et al. The Molecular Basis for Remyelination Failure in Multiple Sclerosis. *Cells*. 2019;8(8).
109. Foerster S, Hill MFE, Franklin RJM. Diversity in the oligodendrocyte lineage: Plasticity or heterogeneity? *Glia*. 2019;67(10):1797-1805.
110. Jäkel S, Agirre E, Mendanha Falcão A, et al. Altered human oligodendrocyte heterogeneity in multiple sclerosis. *Nature*. 2019;566(7745):543-547.
111. Duncan ID, Radcliff AB, Heidari M, Kidd G, August BK, Wierenga LA. The adult oligodendrocyte can participate in remyelination. *Proc Natl Acad Sci U S A*. 2018;115(50):E11807-E11816.
112. Yeung MSY, Djelloul M, Steiner E, et al. Dynamics of oligodendrocyte generation in multiple sclerosis. *Nature*. 2019;566(7745):538-542.
113. Kuhlmann T, Miron V, Cui Q, Wegner C, Antel J, Bruck W. Differentiation block of oligodendroglial progenitor cells as a cause for remyelination failure in chronic multiple sclerosis. *Brain*. 2008;131(Pt 7):1749-1758.
114. Boyd A, Zhang H, Williams A. Insufficient OPC migration into demyelinated lesions is a cause of poor remyelination in MS and mouse models. *Acta Neuropathol*. 2013;125(6):841-859.

115. Chang A, Tourtellotte WW, Rudick R, Trapp BD. Premyelinating oligodendrocytes in chronic lesions of multiple sclerosis. *N Engl J Med*. 2002;346(3):165-173.
116. Goldschmidt T, Antel J, Konig FB, Bruck W, Kuhlmann T. Remyelination capacity of the MS brain decreases with disease chronicity. *Neurology*. 2009;72(22):1914-1921.
117. Ruckh JM, Zhao JW, Shadrach JL, et al. Rejuvenation of regeneration in the aging central nervous system. *Cell Stem Cell*. 2012;10(1):96-103.
118. McGinley MP, Goldschmidt CH, Rae-Grant AD. Diagnosis and Treatment of Multiple Sclerosis: A Review. *JAMA*. 2021;325(8):765-779.
119. Plosker GL. Interferon-beta-1b: a review of its use in multiple sclerosis. *CNS Drugs*. 2011;25(1):67-88.
120. Dhib-Jalbut S, Marks S. Interferon-beta mechanisms of action in multiple sclerosis. *Neurology*. 2010;74 Suppl 1:S17-24.
121. Leary SM, Miller DH, Stevenson VL, Brex PA, Chard DT, Thompson AJ. Interferon beta-1a in primary progressive MS: an exploratory, randomized, controlled trial. *Neurology*. 2003;60(1):44-51.
122. Panitch H, Miller A, Paty D, Weinshenker B, North American Study Group on Interferon beta-1b in Secondary Progressive MS. Interferon beta-1b in secondary progressive MS: results from a 3-year controlled study. *Neurology*. 2004;63(10):1788-1795.
123. Racke MK, Lovett-Racke AE, Karandikar NJ. The mechanism of action of glatiramer acetate treatment in multiple sclerosis. *Neurology*. 2010;74 Suppl 1:S25-30.
124. Johnson KP, Brooks BR, Cohen JA, et al. Copolymer 1 reduces relapse rate and improves disability in relapsing-remitting multiple sclerosis: results of a phase III multicenter, double-blind placebo-controlled trial. The Copolymer 1 Multiple Sclerosis Study Group. *Neurology*. 1995;45(7):1268-1276.
125. Subei AM, Cohen JA. Sphingosine 1-phosphate receptor modulators in multiple sclerosis. *CNS Drugs*. 2015;29(7):565-575.
126. Chun J, Hartung HP. Mechanism of action of oral fingolimod (FTY720) in multiple sclerosis. *Clin Neuropharmacol*. 2010;33(2):91-101.
127. Brinkmann V, Billich A, Baumruker T, et al. Fingolimod (FTY720): discovery and development of an oral drug to treat multiple sclerosis. *Nat Rev Drug Discov*. 2010;9(11):883-897.

128. Pinschewer DD, Ochsenbein AF, Odermatt B, Brinkmann V, Hengartner H, Zinkernagel RM. FTY720 immunosuppression impairs effector T cell peripheral homing without affecting induction, expansion, and memory. *J Immunol*. 2000;164(11):5761-5770.
129. Choi JW, Gardell SE, Herr DR, et al. FTY720 (fingolimod) efficacy in an animal model of multiple sclerosis requires astrocyte sphingosine 1-phosphate receptor 1 (S1P1) modulation. *Proc Natl Acad Sci U S A*. 2011;108(2):751-756.
130. Pitteri M, Magliozzi R, Bajrami A, Camera V, Calabrese M. Potential neuroprotective effect of Fingolimod in multiple sclerosis and its association with clinical variables. *Expert Opin Pharmacother*. 2018;19(4):387-395.
131. Kappos L, Radue EW, O'Connor P, et al. A placebo-controlled trial of oral fingolimod in relapsing multiple sclerosis. *N Engl J Med*. 2010;362(5):387-401.
132. Lublin F, Miller DH, Freedman MS, et al. Oral fingolimod in primary progressive multiple sclerosis (INFORMS): a phase 3, randomised, double-blind, placebo-controlled trial. *Lancet*. 2016;387(10023):1075-1084.
133. McGinley MP, Cohen JA. Sphingosine 1-phosphate receptor modulators in multiple sclerosis and other conditions. *Lancet*. 2021;398(10306):1184-1194.
134. Kappos L, Bar-Or A, Cree BAC, et al. Siponimod versus placebo in secondary progressive multiple sclerosis (EXPAND): a double-blind, randomised, phase 3 study. *Lancet*. 2018;391(10127):1263-1273.
135. Osiri M, Shea B, Robinson V, et al. Leflunomide for the treatment of rheumatoid arthritis: a systematic review and metaanalysis. *J Rheumatol*. 2003;30(6):1182-1190.
136. Bruneau JM, Yea CM, Spinella-Jaegle S, et al. Purification of human dihydro-orotate dehydrogenase and its inhibition by A77 1726, the active metabolite of leflunomide. *Biochem J*. 1998;336 (Pt 2):299-303.
137. Fox RI, Herrmann ML, Frangou CG, et al. Mechanism of action for leflunomide in rheumatoid arthritis. *Clin Immunol*. 1999;93(3):198-208.
138. Ruckemann K, Fairbanks LD, Carrey EA, et al. Leflunomide inhibits pyrimidine de novo synthesis in mitogen-stimulated T-lymphocytes from healthy humans. *J Biol Chem*. 1998;273(34):21682-21691.
139. Zeyda M, Poglitsch M, Geyeregger R, et al. Disruption of the interaction of T cells with antigen-presenting cells by the active leflunomide metabolite

teriflunomide: involvement of impaired integrin activation and immunologic synapse formation. *Arthritis Rheum*. 2005;52(9):2730-2739.

140. Li L, Liu J, Delohery T, Zhang D, Arendt C, Jones C. The effects of teriflunomide on lymphocyte subpopulations in human peripheral blood mononuclear cells in vitro. *J Neuroimmunol*. 2013;265(1-2):82-90.
141. Korn T, Magnus T, Toyka K, Jung S. Modulation of effector cell functions in experimental autoimmune encephalomyelitis by leflunomide--mechanisms independent of pyrimidine depletion. *J Leukoc Biol*. 2004;76(5):950-960.
142. Vermersch P, Czlonkowska A, Grimaldi LM, et al. Teriflunomide versus subcutaneous interferon beta-1a in patients with relapsing multiple sclerosis: a randomised, controlled phase 3 trial. *Mult Scler*. 2014;20(6):705-716.
143. Gold R, Kappos L, Arnold DL, et al. Placebo-controlled phase 3 study of oral BG-12 for relapsing multiple sclerosis. *N Engl J Med*. 2012;367(12):1098-1107.
144. Schweckendiek W. [Treatment of psoriasis vulgaris]. *Med Monatsschr*. 1959;13(2):103-104.
145. Albrecht P, Bouchachia I, Goebels N, et al. Effects of dimethyl fumarate on neuroprotection and immunomodulation. *J Neuroinflammation*. 2012;9:163.
146. Dibbert S, Clement B, Skak-Nielsen T, Mrowietz U, Rostami-Yazdi M. Detection of fumarate-glutathione adducts in the portal vein blood of rats: evidence for rapid dimethylfumarate metabolism. *Arch Dermatol Res*. 2013;305(5):447-451.
147. Linker RA, Lee DH, Ryan S, et al. Fumaric acid esters exert neuroprotective effects in neuroinflammation via activation of the Nrf2 antioxidant pathway. *Brain*. 2011;134(Pt 3):678-692.
148. Scannevin RH, Chollate S, Jung MY, et al. Fumarates promote cytoprotection of central nervous system cells against oxidative stress via the nuclear factor (erythroid-derived 2)-like 2 pathway. *J Pharmacol Exp Ther*. 2012;341(1):274-284.
149. Nguyen T, Sherratt PJ, Pickett CB. Regulatory mechanisms controlling gene expression mediated by the antioxidant response element. *Annu Rev Pharmacol Toxicol*. 2003;43:233-260.
150. Lin SX, Lisi L, Dello Russo C, et al. The anti-inflammatory effects of dimethyl fumarate in astrocytes involve glutathione and haem oxygenase-1. *ASN Neuro*. 2011;3(2).

151. Wierinckx A, Breve J, Mercier D, Schultzberg M, Drukarch B, Van Dam AM. Detoxication enzyme inducers modify cytokine production in rat mixed glial cells. *J Neuroimmunol*. 2005;166(1-2):132-143.
152. Hanson J, Gille A, Zwykiel S, et al. Nicotinic acid- and monomethyl fumarate-induced flushing involves GPR109A expressed by keratinocytes and COX-2-dependent prostanoid formation in mice. *J Clin Invest*. 2010;120(8):2910-2919.
153. Tang H, Lu JY, Zheng X, Yang Y, Reagan JD. The psoriasis drug monomethylfumarate is a potent nicotinic acid receptor agonist. *Biochem Biophys Res Commun*. 2008;375(4):562-565.
154. Parodi B, Rossi S, Morando S, et al. Fumarates modulate microglia activation through a novel HCAR2 signaling pathway and rescue synaptic dysregulation in inflamed CNS. *Acta Neuropathol*. 2015;130(2):279-295.
155. Chen H, Assmann JC, Krenz A, et al. Hydroxycarboxylic acid receptor 2 mediates dimethyl fumarate's protective effect in EAE. *J Clin Invest*. 2014.
156. Gerdes S, Shakery K, Mrowietz U. Dimethylfumarate inhibits nuclear binding of nuclear factor kappaB but not of nuclear factor of activated T cells and CCAAT/enhancer binding protein beta in activated human T cells. *Br J Dermatol*. 2007;156(5):838-842.
157. Treumer F, Zhu K, Glaser R, Mrowietz U. Dimethylfumarate is a potent inducer of apoptosis in human T cells. *J Invest Dermatol*. 2003;121(6):1383-1388.
158. Loewe R, Holnthoner W, Groger M, et al. Dimethylfumarate inhibits TNF-induced nuclear entry of NF-kappa B/p65 in human endothelial cells. *J Immunol*. 2002;168(9):4781-4787.
159. Gillard GO, Collette B, Anderson J, et al. DMF, but not other fumarates, inhibits NF-kappaB activity in vitro in an Nrf2-independent manner. *J Neuroimmunol*. 2015;283:74-85.
160. Litjens NH, Rademaker M, Ravensbergen B, et al. Monomethylfumarate affects polarization of monocyte-derived dendritic cells resulting in down-regulated Th1 lymphocyte responses. *Eur J Immunol*. 2004;34(2):565-575.
161. de Jong R, Bezemer AC, Zomerdijk TP, van de Pouw-Kraan T, Ottenhoff TH, Nibbering PH. Selective stimulation of T helper 2 cytokine responses by the anti-psoriasis agent monomethylfumarate. *Eur J Immunol*. 1996;26(9):2067-2074.

162. Ghoreschi K, Bruck J, Kellerer C, et al. Fumarates improve psoriasis and multiple sclerosis by inducing type II dendritic cells. *J Exp Med*. 2011;208(11):2291-2303.
163. Tahvili S, Zandieh B, Amirghofran Z. The effect of dimethyl fumarate on gene expression and the level of cytokines related to different T helper cell subsets in peripheral blood mononuclear cells of patients with psoriasis. *Int J Dermatol*. 2015;54(7):e254-260.
164. Kornberg MD, Bhargava P, Kim PM, et al. Dimethyl fumarate targets GAPDH and aerobic glycolysis to modulate immunity. *Science*. 2018;360(6387):449-453.
165. Giovannoni G, Comi G, Cook S, et al. A placebo-controlled trial of oral cladribine for relapsing multiple sclerosis. *N Engl J Med*. 2010;362(5):416-426.
166. Cook S, Vermersch P, Comi G, et al. Safety and tolerability of cladribine tablets in multiple sclerosis: the CLARITY (CLAdRIbine Tablets treating multiple sclerosis orallY) study. *Mult Scler*. 2011;17(5):578-593.
167. Leist TP, Weissert R. Cladribine: mode of action and implications for treatment of multiple sclerosis. *Clin Neuropharmacol*. 2011;34(1):28-35.
168. Laugel B, Borlat F, Galibert L, et al. Cladribine inhibits cytokine secretion by T cells independently of deoxycytidine kinase activity. *J Neuroimmunol*. 2011;240-241:52-57.
169. Kraus SH, Luessi F, Trinschek B, et al. Cladribine exerts an immunomodulatory effect on human and murine dendritic cells. *Int Immunopharmacol*. 2014;18(2):347-357.
170. Polman CH, O'Connor PW, Havrdova E, et al. A randomized, placebo-controlled trial of natalizumab for relapsing multiple sclerosis. *N Engl J Med*. 2006;354(9):899-910.
171. Kapoor R, Ho PR, Campbell N, et al. Effect of natalizumab on disease progression in secondary progressive multiple sclerosis (ASCEND): a phase 3, randomised, double-blind, placebo-controlled trial with an open-label extension. *Lancet Neurol*. 2018;17(5):405-415.
172. Brandstadter R, Katz Sand I. The use of natalizumab for multiple sclerosis. *Neuropsychiatr Dis Treat*. 2017;13:1691-1702.
173. Biogen. Highlights of prescribing information: Tysabri (natalizumab) injection, for intravenous use. . https://www.tysabri.com/content/dam/commercial/tysabri/pat/en_us/pdf/t

ysabri_prescribing_information.pdf. Published Revised 06/2020. Accessed October 31, 2021.

174. Thomas K, Eisele J, Rodriguez-Leal FA, Hainke U, Ziemssen T. Acute effects of alemtuzumab infusion in patients with active relapsing-remitting MS. *Neurol Neuroimmunol Neuroinflamm*. 2016;3(3):e228.
175. Wiendl H, Kieseier B. Multiple sclerosis: reprogramming the immune repertoire with alemtuzumab in MS. *Nat Rev Neurol*. 2013;9(3):125-126.
176. Cohen JA, Coles AJ, Arnold DL, et al. Alemtuzumab versus interferon beta 1a as first-line treatment for patients with relapsing-remitting multiple sclerosis: a randomised controlled phase 3 trial. *Lancet*. 2012;380(9856):1819-1828.
177. Coles AJ, Twyman CL, Arnold DL, et al. Alemtuzumab for patients with relapsing multiple sclerosis after disease-modifying therapy: a randomised controlled phase 3 trial. *Lancet*. 2012;380(9856):1829-1839.
178. Agency EM. Measures to minimise risk of serious side effects of multiple sclerosis medicine Lemtrada. https://www.ema.europa.eu/en/documents/referral/lemtrada-article-20-procedure-measures-minimise-risk-serious-side-effects-multiple-sclerosis_en-0.pdf. Published 2020. Updated 16 January 2020. Accessed 31 October 2021, 2021.
179. Mulero P, Midaglia L, Montalban X. Ocrelizumab: a new milestone in multiple sclerosis therapy. *Ther Adv Neurol Disord*. 2018;11:1756286418773025.
180. Gingele S, Jacobus TL, Konen FF, et al. Ocrelizumab Depletes CD20(+) T Cells in Multiple Sclerosis Patients. *Cells*. 2018;8(1).
181. Hauser SL, Bar-Or A, Comi G, et al. Ocrelizumab versus Interferon Beta-1a in Relapsing Multiple Sclerosis. *N Engl J Med*. 2017;376(3):221-234.
182. Montalban X, Hauser SL, Kappos L, et al. Ocrelizumab versus Placebo in Primary Progressive Multiple Sclerosis. *N Engl J Med*. 2017;376(3):209-220.
183. Mayer L, Kappos L, Racke MK, et al. Ocrelizumab infusion experience in patients with relapsing and primary progressive multiple sclerosis: Results from the phase 3 randomized OPERA I, OPERA II, and ORATORIO studies. *Mult Scler Relat Disord*. 2019;30:236-243.
184. Berkovich R. Treatment of acute relapses in multiple sclerosis. *Neurotherapeutics*. 2013;10(1):97-105.

185. Valet M, Quoilin M, Lejeune T, et al. Effects of Fampridine in People with Multiple Sclerosis: A Systematic Review and Meta-analysis. *CNS Drugs*. 2019;33(11):1087-1099.
186. Ziemssen T, Akgün K, Brück W. Molecular biomarkers in multiple sclerosis. *Journal of Neuroinflammation*. 2019;16(1):272.
187. Kuhle J, Disanto G, Dobson R, et al. Conversion from clinically isolated syndrome to multiple sclerosis: A large multicentre study. *Mult Scler*. 2015;21(8):1013-1024.
188. Kuhle J, Kropshofer H, Haering DA, et al. Blood neurofilament light chain as a biomarker of MS disease activity and treatment response. *Neurology*. 2019;92(10):e1007-e1015.
189. Kappos L, D'Souza M, Lechner-Scott J, Lienert C. On the origin of Neurostatus. *Mult Scler Relat Disord*. 2015;4(3):182-185.
190. Pardo G, Coates S, Okuda DT. Outcome measures assisting treatment optimization in multiple sclerosis. *Journal of Neurology*. 2021.
191. Skeen MB. Changing Paradigms and Unmet Needs in Multiple Sclerosis: The Role of Clinical Neurophysiology. *J Clin Neurophysiol*. 2021;38(3):162-165.
192. Mehr SR, Zimmerman MP. Reviewing the Unmet Needs of Patients with Multiple Sclerosis. *Am Health Drug Benefits*. 2015;8(8):426-431.
193. Costello K, Kennedy P, Scanzillo J. Recognizing nonadherence in patients with multiple sclerosis and maintaining treatment adherence in the long term. *Medscape J Med*. 2008;10(9):225.
194. Ng R. *Drugs: From Discovery to Approval, 3rd Edition*. Third edition ed2015.
195. Dowden H, Munro J. Trends in clinical success rates and therapeutic focus. *Nat Rev Drug Discov*. 2019;18(7):495-496.
196. Hauser AS, Attwood MM, Rask-Andersen M, Schiöth HB, Gloriam DE. Trends in GPCR drug discovery: new agents, targets and indications. *Nature Reviews Drug Discovery*. 2017;16(12):829-842.
197. Gashaw I, Ellinghaus P, Sommer A, Asadullah K. What makes a good drug target? *Drug Discovery Today*. 2012;17:S24-S30.
198. Mei F, Fancy SPJ, Shen YA, et al. Micropillar arrays as a high-throughput screening platform for therapeutics in multiple sclerosis. *Nat Med*. 2014;20(8):954-960.
199. Hughes JP, Rees S, Kalindjian SB, Philpott KL. Principles of early drug discovery. *Br J Pharmacol*. 2011;162(6):1239-1249.

200. Moore K, Rees S. Cell-based versus isolated target screening: how lucky do you feel? *J Biomol Screen*. 2001;6(2):69-74.
201. Fox S, Wang H, Sopchak L, Khoury R. High throughput screening: early successes indicate a promising future. *J Biomol Screen*. 2001;6(3):137-140.
202. Richard-Bildstein S AH, Pothier J, Schäfer G, Gnerre C, Lindenberg E, Lehembre F, Pouzol L, Guerry P. Discovery of the potent, selective, orally available CXCR7 antagonist ACT-1004-1239. *J Med Chem*. 2020.
203. Strovel J, Sittampalam S, Coussens NP, et al. Early Drug Discovery and Development Guidelines: For Academic Researchers, Collaborators, and Start-up Companies. In: Markossian S, Grossman A, Brimacombe K, et al., eds. *Assay Guidance Manual*. Bethesda (MD)2004.
204. Draft FDA Guidance for Industry. In Vitro Metabolism- and Transporter-Mediated Drug-Drug Interaction Studies. https://www.fda.gov/files/drugs/published/In-Vitro-Metabolism--and-Transporter--Mediated-Drug-Drug-Interaction-Studies-Guidance-for-Industry.pdf. Published October 2017. Accessed.
205. ICH Safety Guidelines S7B. The Non-Clinical Evaluation of the Potential for Delayed Ventricular Repolarization (QT Interval Prolongation) by Human Pharmaceuticals. https://www.ich.org/page/safety-guidelines. Published 2005, May 12. Accessed.
206. ICH S7A. Safety pharmacology studies for human pharmaceuticals https://www.ich.org/page/safety-guidelines. Published 2000, November 8. Accessed.
207. Haute Autorité de Santé. Ponvory (ponésimod). https://www.has-sante.fr/jcms/p_3284793/fr/ponvory-ponesimod. Published 2021, sept 7. Accessed.
208. Strasser DS, Froidevaux S, Sippel V, et al. Preclinical to clinical translation of cenerimod, a novel S1P₁ receptor modulator, in systemic lupus erythematosus. *RMD Open*. 2020;6(2):e001261.
209. ICH M3(R2). Guidance of nonclinical safety studies for the conduct of human clinical trials and marketing authorization for pharmaceuticals. https://www.ich.org/page/ich-guidelines. Published 2009, June 11. Accessed.
210. Shen J, Swift B, Mamelok R, Pine S, Sinclair J, Attar M. Design and Conduct Considerations for First-in-Human Trials. *Clin Transl Sci*. 2019;12(1):6-19.

211. Muller PY, Milton MN. The determination and interpretation of the therapeutic index in drug development. *Nature Reviews Drug Discovery*. 2012;11(10):751-761.
212. Collis MG. What is the future role of pharmacologists in the pharmaceutical industry? *Trends in Pharmacological Sciences*. 2006;27(3):126-129.
213. Lassmann H, Bradl M. Multiple sclerosis: experimental models and reality. *Acta Neuropathol*. 2017;133(2):223-244.
214. Stuart G, Krikorian KS. The Neuro-Paralytic Accidents of Anti-Rabies Treatment. *Annals of Tropical Medicine & Parasitology*. 1928;22(3):327-377.
215. Olitsky PK, Yager RH. Experimental disseminated encephalomyelitis in white mice. *J Exp Med*. 1949;90(3):213-224.
216. Robinson AP, Harp CT, Noronha A, Miller SD. The experimental autoimmune encephalomyelitis (EAE) model of MS: utility for understanding disease pathophysiology and treatment. *Handb Clin Neurol*. 2014;122:173-189.
217. Miller SD, Karpus WJ. Experimental autoimmune encephalomyelitis in the mouse. *Curr Protoc Immunol*. 2007;Chapter 15:Unit 15 11.
218. Bittner S, Afzali AM, Wiendl H, Meuth SG. Myelin oligodendrocyte glycoprotein (MOG35-55) induced experimental autoimmune encephalomyelitis (EAE) in C57BL/6 mice. *J Vis Exp*. 2014(86).
219. Oliver AR, Lyon GM, Ruddle NH. Rat and human myelin oligodendrocyte glycoproteins induce experimental autoimmune encephalomyelitis by different mechanisms in C57BL/6 mice. *J Immunol*. 2003;171(1):462-468.
220. Weber MS, Prod'homme T, Patarroyo JC, et al. B-cell activation influences T-cell polarization and outcome of anti-CD20 B-cell depletion in central nervous system autoimmunity. *Ann Neurol*. 2010;68(3):369-383.
221. Hausler D, Hausser-Kinzel S, Feldmann L, et al. Functional characterization of reappearing B cells after anti-CD20 treatment of CNS autoimmune disease. *Proc Natl Acad Sci U S A*. 2018;115(39):9773-9778.
222. Ignatius Arokia Doss PM, Roy A-P, Wang A, Anderson AC, Rangachari M. The Non-Obese Diabetic Mouse Strain as a Model to Study CD8+ T Cell Function in Relapsing and Progressive Multiple Sclerosis. *Frontiers in Immunology*. 2015;6(541).
223. Kipp M, Nyamoya S, Hochstrasser T, Amor S. Multiple sclerosis animal models: a clinical and histopathological perspective. *Brain Pathol*. 2017;27(2):123-137.

224. Stefferl A, Brehm U, Storch M, et al. Myelin oligodendrocyte glycoprotein induces experimental autoimmune encephalomyelitis in the "resistant" Brown Norway rat: disease susceptibility is determined by MHC and MHC-linked effects on the B cell response. *J Immunol*. 1999;163(1):40-49.
225. Pitarokoili K, Ambrosius B, Gold R. Lewis Rat Model of Experimental Autoimmune Encephalomyelitis. *Curr Protoc Neurosci*. 2017;81:9 61 61-69 61 20.
226. Kap YS, Laman JD, t Hart BA. Experimental autoimmune encephalomyelitis in the common marmoset, a bridge between rodent EAE and multiple sclerosis for immunotherapy development. *J Neuroimmune Pharmacol*. 2010;5(2):220-230.
227. Bjelobaba I, Begovic-Kupresanin V, Pekovic S, Lavrnja I. Animal models of multiple sclerosis: Focus on experimental autoimmune encephalomyelitis. *J Neurosci Res*. 2018;96(6):1021-1042.
228. 't Hart BA, Luchicchi A, Schenk GJ, Killestein J, Geurts JJG. Multiple sclerosis and drug discovery: A work of translation. *EBioMedicine*. 2021;68:103392.
229. Peterson RE, Bollier ME. Spectrophotometric Determination of Serum Copper with Biscyclohexanoneoxalyldihydrazone. *Analytical Chemistry*. 1955;27(7):1195-1197.
230. Carlton WW. Response of mice to the chelating agents sodium diethyldithiocarbamate, α-benzoinoxime, and biscyclohexanone oxaldihydrazone. *Toxicology and Applied Pharmacology*. 1966;8(3):512-521.
231. Blakemore WF. Observations on oligodendrocyte degeneration, the resolution of status spongiosus and remyelination in cuprizone intoxication in mice. *Journal of Neurocytology*. 1972;1(4):413-426.
232. Blakemore WF. Remyelination of the superior cerebellar peduncle in the mouse following demyelination induced by feeding cuprizone. *Journal of the Neurological Sciences*. 1973;20(1):73-83.
233. Gudi V, Moharregh-Khiabani D, Skripuletz T, et al. Regional differences between grey and white matter in cuprizone induced demyelination. *Brain Research*. 2009;1283:127-138.
234. Gudi V, Gingele S, Skripuletz T, Stangel M. Glial response during cuprizone-induced de- and remyelination in the CNS: lessons learned. *Front Cell Neurosci*. 2014;8:73.

235. Mason JL, Toews A, Hostettler JD, et al. Oligodendrocytes and progenitors become progressively depleted within chronically demyelinated lesions. *Am J Pathol*. 2004;164(5):1673-1682.
236. Hiremath MM, Chen VS, Suzuki K, Ting JPY, Matsushima GK. MHC class II exacerbates demyelination in vivo independently of T cells. *Journal of Neuroimmunology*. 2008;203(1):23-32.
237. Murphy PM. 10 - Chemokines and Chemokine Receptors. In: Rich RR, Fleisher TA, Shearer WT, Schroeder HW, Frew AJ, Weyand CM, eds. *Clinical Immunology (Fifth Edition)*. London: Elsevier; 2019:157-170.e151.
238. Hughes CE, Nibbs RJB. A guide to chemokines and their receptors. *FEBS J*. 2018;285(16):2944-2971.
239. Bachelerie F, Graham GJ, Locati M, et al. New nomenclature for atypical chemokine receptors. *Nat Immunol*. 2014;15(3):207-208.
240. Burns JM, Summers BC, Wang Y, et al. A novel chemokine receptor for SDF-1 and I-TAC involved in cell survival, cell adhesion, and tumor development. *J Exp Med*. 2006;203(9):2201-2213.
241. Balabanian K, Lagane B, Infantino S, et al. The chemokine SDF-1/CXCL12 binds to and signals through the orphan receptor RDC1 in T lymphocytes. *J Biol Chem*. 2005;280(42):35760-35766.
242. Szpakowska M, Nevins AM, Meyrath M, et al. Different contributions of chemokine N-terminal features attest to a different ligand binding mode and a bias towards activation of ACKR3/CXCR7 compared with CXCR4 and CXCR3. *Br J Pharmacol*. 2018;175(9):1419-1438.
243. Naumann U, Cameroni E, Pruenster M, et al. CXCR7 functions as a scavenger for CXCL12 and CXCL11. *PLoS One*. 2010;5(2):e9175.
244. Berahovich RD, Zabel BA, Lewen S, et al. Endothelial expression of CXCR7 and the regulation of systemic CXCL12 levels. *Immunology*. 2014;141(1):111-122.
245. Saaber F, Schütz D, Miess E, et al. ACKR3 Regulation of Neuronal Migration Requires ACKR3 Phosphorylation, but Not β-Arrestin. *Cell Reports*. 2019;26(6):1473-1488.e1479.
246. Lewellis SW, Knaut H. Attractive guidance: how the chemokine SDF1/CXCL12 guides different cells to different locations. *Semin Cell Dev Biol*. 2012;23(3):333-340.

247. Dambly-Chaudiere C, Cubedo N, Ghysen A. Control of cell migration in the development of the posterior lateral line: antagonistic interactions between the chemokine receptors CXCR4 and CXCR7/RDC1. *BMC Dev Biol*. 2007;7:23.
248. Rajagopal S, Kim J, Ahn S, et al. Beta-arrestin- but not G protein-mediated signaling by the "decoy" receptor CXCR7. *Proc Natl Acad Sci U S A*. 2010;107(2):628-632.
249. Kumar R, Tripathi V, Ahmad M, et al. CXCR7 mediated Gialpha independent activation of ERK and Akt promotes cell survival and chemotaxis in T cells. *Cell Immunol*. 2012;272(2):230-241.
250. Koenen J, Bachelerie F, Balabanian K, Schlecht-Louf G, Gallego C. Atypical Chemokine Receptor 3 (ACKR3): A Comprehensive Overview of its Expression and Potential Roles in the Immune System. *Mol Pharmacol*. 2019;96(6):809-818.
251. Levoye A, Balabanian K, Baleux F, Bachelerie F, Lagane B. CXCR7 heterodimerizes with CXCR4 and regulates CXCL12-mediated G protein signaling. *Blood*. 2009;113(24):6085-6093.
252. Sierro F, Biben C, Martinez-Munoz L, et al. Disrupted cardiac development but normal hematopoiesis in mice deficient in the second CXCL12/SDF-1 receptor, CXCR7. *Proc Natl Acad Sci U S A*. 2007;104(37):14759-14764.
253. Berahovich RD, Penfold ME, Schall TJ. Nonspecific CXCR7 antibodies. *Immunol Lett*. 2010;133(2):112-114.
254. Liu L, Chen J-X, Zhang X-W, et al. Chemokine receptor 7 overexpression promotes mesenchymal stem cell migration and proliferation via secreting Chemokine ligand 12. *Scientific Reports*. 2018;8(1):204.
255. Hattermann K, Held-Feindt J, Lucius R, et al. The chemokine receptor CXCR7 is highly expressed in human glioma cells and mediates antiapoptotic effects. *Cancer Res*. 2010;70(8):3299-3308.
256. Puchert M, Pelkner F, Stein G, et al. Astrocytic expression of the CXCL12 receptor, CXCR7/ACKR3 is a hallmark of the diseased, but not developing CNS. *Mol Cell Neurosci*. 2017;85:105-118.
257. Lipfert J, Odemis V, Wagner DC, Boltze J, Engele J. CXCR4 and CXCR7 form a functional receptor unit for SDF-1/CXCL12 in primary rodent microglia. *Neuropathol Appl Neurobiol*. 2013;39(6):667-680.
258. Shimizu S, Brown M, Sengupta R, Penfold ME, Meucci O. CXCR7 protein expression in human adult brain and differentiated neurons. *PLoS One*. 2011;6(5):e20680.

259. Ma W, Liu Y, Ellison N, Shen J. Induction of C-X-C chemokine receptor type 7 (CXCR7) switches stromal cell-derived factor-1 (SDF-1) signaling and phagocytic activity in macrophages linked to atherosclerosis. *J Biol Chem*. 2013;288(22):15481-15494.
260. Chatterjee M, von Ungern-Sternberg SN, Seizer P, et al. Platelet-derived CXCL12 regulates monocyte function, survival, differentiation into macrophages and foam cells through differential involvement of CXCR4-CXCR7. *Cell Death Dis*. 2015;6:e1989.
261. Atlas THP. ACKR3: RNA single cell type specificity. https://www.proteinatlas.org/ENSG00000144476-ACKR3/single+cell+type. Published version 21.0. Accessed 2021.
262. Karlsson M, Zhang C, Mear L, et al. A single-cell type transcriptomics map of human tissues. *Sci Adv*. 2021;7(31).
263. Sanchez-Martin L, Sanchez-Mateos P, Cabanas C. CXCR7 impact on CXCL12 biology and disease. *Trends Mol Med*. 2013;19(1):12-22.
264. Karin N. The multiple faces of CXCL12 (SDF-1alpha) in the regulation of immunity during health and disease. *J Leukoc Biol*. 2010;88(3):463-473.
265. Ma Q, Jones D, Borghesani PR, et al. Impaired B-lymphopoiesis, myelopoiesis, and derailed cerebellar neuron migration in CXCR4- and SDF-1-deficient mice. *Proc Natl Acad Sci U S A*. 1998;95(16):9448-9453.
266. Yu L, Cecil J, Peng SB, et al. Identification and expression of novel isoforms of human stromal cell-derived factor 1. *Gene*. 2006;374:174-179.
267. Janowski M. Functional diversity of SDF-1 splicing variants. *Cell Adh Migr*. 2009;3(3):243-249.
268. Handel TM, Johnson Z, Crown SE, Lau EK, Proudfoot AE. Regulation of protein function by glycosaminoglycans--as exemplified by chemokines. *Annu Rev Biochem*. 2005;74:385-410.
269. Sadir R, Imberty A, Baleux F, Lortat-Jacob H. Heparan sulfate/heparin oligosaccharides protect stromal cell-derived factor-1 (SDF-1)/CXCL12 against proteolysis induced by CD26/dipeptidyl peptidase IV. *J Biol Chem*. 2004;279(42):43854-43860.
270. Janssens R, Struyf S, Proost P. The unique structural and functional features of CXCL12. *Cellular & molecular immunology*. 2018;15(4):299-311.
271. Metzemaekers M, Vanheule V, Janssens R, Struyf S, Proost P. Overview of the Mechanisms that May Contribute to the Non-Redundant Activities of

Interferon-Inducible CXC Chemokine Receptor 3 Ligands. *Frontiers in Immunology*. 2018;8(1970).

272. Cole KE, Strick CA, Paradis TJ, et al. Interferon-inducible T cell alpha chemoattractant (I-TAC): a novel non-ELR CXC chemokine with potent activity on activated T cells through selective high affinity binding to CXCR3. *J Exp Med*. 1998;187(12):2009-2021.
273. Zohar Y, Wildbaum G, Novak R, et al. CXCL11-dependent induction of FOXP3-negative regulatory T cells suppresses autoimmune encephalomyelitis. *J Clin Invest*. 2014;124(5):2009-2022.
274. Torraca V, Cui C, Boland R, et al. The CXCR3-CXCL11 signaling axis mediates macrophage recruitment and dissemination of mycobacterial infection. *Dis Model Mech*. 2015;8(3):253-269.
275. Widney DP, Xia Y-R, Lusis AJ, Smith JB. The Murine Chemokine CXCL11 (IFN-Inducible T Cell α Chemoattractant) Is an IFN-γ- and Lipopolysaccharide-Inducible Glucocorticoid-Attenuated Response Gene Expressed in Lung and Other Tissues During Endotoxemia. *The Journal of Immunology*. 2000;164(12):6322-6331.
276. Severin IC, Gaudry J-P, Johnson Z, et al. Characterization of the Chemokine CXCL11-Heparin Interaction Suggests Two Different Affinities for Glycosaminoglycans*. *Journal of Biological Chemistry*. 2010;285(23):17713-17724.
277. Metzemaekers M, Mortier A, Janssens R, et al. Glycosaminoglycans Regulate CXCR3 Ligands at Distinct Levels: Protection against Processing by Dipeptidyl Peptidase IV/CD26 and Interference with Receptor Signaling. *International Journal of Molecular Sciences*. 2017;18(7):1513.
278. Van Raemdonck K, Van den Steen PE, Liekens S, Van Damme J, Struyf S. CXCR3 ligands in disease and therapy. *Cytokine & Growth Factor Reviews*. 2015;26(3):311-327.
279. Lasagni L, Francalanci M, Annunziato F, et al. An Alternatively Spliced Variant of CXCR3 Mediates the Inhibition of Endothelial Cell Growth Induced by IP-10, Mig, and I-TAC, and Acts as Functional Receptor for Platelet Factor 4. *Journal of Experimental Medicine*. 2003;197(11):1537-1549.
280. Ehlert JE, Addison CA, Burdick MD, Kunkel SL, Strieter RM. Identification and Partial Characterization of a Variant of Human CXCR3 Generated by Posttranscriptional Exon Skipping. *The Journal of Immunology*. 2004;173(10):6234-6240.

281. Berchiche YA, Sakmar TP. CXC Chemokine Receptor 3 Alternative Splice Variants Selectively Activate Different Signaling Pathways. *Molecular Pharmacology*. 2016;90(4):483-495.
282. Gerrits H, van Ingen Schenau DS, Bakker NE, et al. Early postnatal lethality and cardiovascular defects in CXCR7-deficient mice. *Genesis*. 2008;46(5):235-245.
283. Sanchez-Alcaniz JA, Haege S, Mueller W, et al. Cxcr7 controls neuronal migration by regulating chemokine responsiveness. *Neuron*. 2011;69(1):77-90.
284. Wang Y, Li G, Stanco A, et al. CXCR4 and CXCR7 Have Distinct Functions in Regulating Interneuron Migration. *Neuron*. 2011;69(1):61-76.
285. Abe P, Mueller W, Schutz D, et al. CXCR7 prevents excessive CXCL12-mediated downregulation of CXCR4 in migrating cortical interneurons. *Development*. 2014;141(9):1857-1863.
286. Meyrath M, Szpakowska M, Zeiner J, et al. The atypical chemokine receptor ACKR3/CXCR7 is a broad-spectrum scavenger for opioid peptides. *Nat Commun*. 2020;11(1):3033.
287. Veenstra M, Williams DW, Calderon TM, Anastos K, Morgello S, Berman JW. Frontline Science: CXCR7 mediates CD14(+)CD16(+) monocyte transmigration across the blood brain barrier: a potential therapeutic target for NeuroAIDS. *J Leukoc Biol*. 2017;102(5):1173-1185.
288. Cruz-Orengo L, Holman DW, Dorsey D, et al. CXCR7 influences leukocyte entry into the CNS parenchyma by controlling abluminal CXCL12 abundance during autoimmunity. *J Exp Med*. 2011;208(2):327-339.
289. Carbajal KS, Schaumburg C, Strieter R, Kane J, Lane TE. Migration of engrafted neural stem cells is mediated by CXCL12 signaling through CXCR4 in a viral model of multiple sclerosis. *Proc Natl Acad Sci U S A*. 2010;107(24):11068-11073.
290. Williams JL, Patel JR, Daniels BP, Klein RS. Targeting CXCR7/ACKR3 as a therapeutic strategy to promote remyelination in the adult central nervous system. *J Exp Med*. 2014;211(5):791-799.
291. Salvi V, Sozio F, Sozzani S, Del Prete A. Role of Atypical Chemokine Receptors in Microglial Activation and Polarization. *Frontiers in Aging Neuroscience*. 2017;9(148).
292. Chu T, Shields LBE, Zhang YP, Feng SQ, Shields CB, Cai J. CXCL12/CXCR4/CXCR7 Chemokine Axis in the Central Nervous System:

Therapeutic Targets for Remyelination in Demyelinating Diseases. *Neuroscientist*. 2017;23(6):627-648.

293. Calderon TM, Eugenin EA, Lopez L, et al. A role for CXCL12 (SDF-1α) in the pathogenesis of multiple sclerosis: Regulation of CXCL12 expression in astrocytes by soluble myelin basic protein. *Journal of Neuroimmunology*. 2006;177(1):27-39.
294. Zilkha-Falb R, Kaushansky N, Kawakami N, Ben-Nun A. Post-CNS-inflammation expression of CXCL12 promotes the endogenous myelin/neuronal repair capacity following spontaneous recovery from multiple sclerosis-like disease. *J Neuroinflammation*. 2016;13(1):7.
295. Banisadr G, Podojil JR, Miller SD, Miller RJ. Pattern of CXCR7 Gene Expression in Mouse Brain Under Normal and Inflammatory Conditions. *J Neuroimmune Pharmacol*. 2016;11(1):26-35.
296. McCandless EE, Wang Q, Woerner BM, Harper JM, Klein RS. CXCL12 limits inflammation by localizing mononuclear infiltrates to the perivascular space during experimental autoimmune encephalomyelitis. *J Immunol*. 2006;177(11):8053-8064.
297. McCandless EE, Piccio L, Woerner BM, et al. Pathological expression of CXCL12 at the blood-brain barrier correlates with severity of multiple sclerosis. *Am J Pathol*. 2008;172(3):799-808.
298. Ambrosini E, Remoli ME, Giacomini E, et al. Astrocytes produce dendritic cell-attracting chemokines in vitro and in multiple sclerosis lesions. *J Neuropathol Exp Neurol*. 2005;64(8):706-715.
299. Krumbholz M, Theil D, Cepok S, et al. Chemokines in multiple sclerosis: CXCL12 and CXCL13 up-regulation is differentially linked to CNS immune cell recruitment. *Brain*. 2005;129(1):200-211.
300. Moll NM, Cossoy MB, Fisher E, et al. Imaging correlates of leukocyte accumulation and CXCR4/CXCL12 in multiple sclerosis. *Arch Neurol*. 2009;66(1):44-53.
301. Constantin G, Majeed M, Giagulli C, et al. Chemokines trigger immediate beta2 integrin affinity and mobility changes: differential regulation and roles in lymphocyte arrest under flow. *Immunity*. 2000;13(6):759-769.
302. Hartmann TN, Grabovsky V, Pasvolsky R, et al. A crosstalk between intracellular CXCR7 and CXCR4 involved in rapid CXCL12-triggered integrin activation but not in chemokine-triggered motility of human T lymphocytes and CD34+ cells. *J Leukoc Biol*. 2008;84(4):1130-1140.

303. Cruz-Orengo L, Chen YJ, Kim JH, Dorsey D, Song SK, Klein RS. CXCR7 antagonism prevents axonal injury during experimental autoimmune encephalomyelitis as revealed by in vivo axial diffusivity. *J Neuroinflammation*. 2011;8:170.
304. Bao J, Zhu J, Luo S, Cheng Y, Zhou S. CXCR7 suppression modulates microglial chemotaxis to ameliorate experimentally-induced autoimmune encephalomyelitis. *Biochem Biophys Res Commun*. 2016;469(1):1-7.
305. Man S, Tucky B, Cotleur A, Drazba J, Takeshita Y, Ransohoff RM. CXCL12-induced monocyte-endothelial interactions promote lymphocyte transmigration across an in vitro blood-brain barrier. *Sci Transl Med*. 2012;4(119):119ra114.
306. Ma W, Liu Y, Wang C, Zhang L, Crocker L, Shen J. Atorvastatin inhibits CXCR7 induction to reduce macrophage migration. *Biochem Pharmacol*. 2014;89(1):99-108.
307. Zhao D, Zhu Z, Li D, Xu R, Wang T, Liu K. Pioglitazone Suppresses CXCR7 Expression To Inhibit Human Macrophage Chemotaxis through Peroxisome Proliferator-Activated Receptor gamma. *Biochemistry*. 2015;54(45):6806-6814.
308. Ottum PA, Arellano G, Reyes LI, Iruretagoyena M, Naves R. Opposing Roles of Interferon-Gamma on Cells of the Central Nervous System in Autoimmune Neuroinflammation. *Frontiers in Immunology*. 2015;6(539).
309. Williams JL, Manivasagam S, Smith BC, et al. Astrocyte-T cell crosstalk regulates region-specific neuroinflammation. *Glia*. 2020;68(7):1361-1374.
310. Fumagalli A, Heuninck J, Pizzoccaro A, et al. The atypical chemokine receptor 3 interacts with Connexin 43 inhibiting astrocytic gap junctional intercellular communication. *Nature Communications*. 2020;11(1):4855.
311. Li Y, Tang G, Liu Y, et al. CXCL12 Gene Therapy Ameliorates Ischemia-Induced White Matter Injury in Mouse Brain. *Stem Cells Transl Med*. 2015;4(10):1122-1130.
312. Kadi L, Selvaraju R, de Lys P, Proudfoot AE, Wells TN, Boschert U. Differential effects of chemokines on oligodendrocyte precursor proliferation and myelin formation in vitro. *J Neuroimmunol*. 2006;174(1-2):133-146.
313. Patel JR, McCandless EE, Dorsey D, Klein RS. CXCR4 promotes differentiation of oligodendrocyte progenitors and remyelination. *Proc Natl Acad Sci U S A*. 2010;107(24):11062-11067.

314. Tian Y, Yin H, Deng X, Tang B, Ren X, Jiang T. CXCL12 induces migration of oligodendrocyte precursor cells through the CXCR4activated MEK/ERK and PI3K/AKT pathways. *Mol Med Rep*. 2018;18(5):4374-4380.
315. Mei F, Mayoral SR, Nobuta H, et al. Identification of the Kappa-Opioid Receptor as a Therapeutic Target for Oligodendrocyte Remyelination. *The Journal of Neuroscience*. 2016;36(30):7925-7935.
316. Osso LA, Rankin KA, Chan JR. Experience-dependent myelination following stress is mediated by the neuropeptide dynorphin. *Neuron*. 2021;109(22):3619-3632.e3615.
317. Peng H, Zhang H, Zhu H. Blocking CXCR7-mediated adipose tissue macrophages chemotaxis attenuates insulin resistance and inflammation in obesity. *Biochem Biophys Res Commun*. 2016;479(4):649-655.
318. Salazar N, Carlson JC, Huang K, et al. A Chimeric Antibody against ACKR3/CXCR7 in Combination with TMZ Activates Immune Responses and Extends Survival in Mouse GBM Models. *Mol Ther*. 2018;26(5):1354-1365.
319. Dong BC, Li MX, Wang XY, et al. Effects of CXCR7-neutralizing antibody on neurogenesis in the hippocampal dentate gyrus and cognitive function in the chronic phase of cerebral ischemia. *Neural Regen Res*. 2020;15(6):1079-1085.
320. Lounsbury N. Advances in CXCR7 Modulators. *Pharmaceuticals (Basel)*. 2020;13(2).
321. Zabel BA, Wang Y, Lewen S, et al. Elucidation of CXCR7-mediated signaling events and inhibition of CXCR4-mediated tumor cell transendothelial migration by CXCR7 ligands. *J Immunol*. 2009;183(5):3204-3211.
322. Luker KE, Gupta M, Luker GD. Imaging chemokine receptor dimerization with firefly luciferase complementation. *FASEB J*. 2009;23(3):823-834.
323. Kolodziej A, Schulz S, Guyon A, et al. Tonic Activation of CXC Chemokine Receptor 4 in Immature Granule Cells Supports Neurogenesis in the Adult Dentate Gyrus. *The Journal of Neuroscience*. 2008;28(17):4488-4500.
324. Menhaji-Klotz E, Ward J, Brown JA, et al. Discovery of Diphenylacetamides as CXCR7 Inhibitors with Novel β-Arrestin Antagonist Activity. *ACS Medicinal Chemistry Letters*. 2020.
325. Aissaoui H. GP, Lehembre F., Pothier J., Pouzol L., Richard-Bildstein S., Yuan S., Inventor. Piperidine CXCR7 receptor modulators. International Patent Application. WO/2018/019929A1. 01 February 2018, 2018.

326. Huynh C, Brussee JM, Pouzol L, et al. Target engagement of the first-in-class CXCR7 antagonist ACT-1004-1239 following multiple-dose administration in mice and humans. *Biomed Pharmacother*. 2021;144:112363.
327. Pouzol L, Sassi A, Baumlin N, et al. CXCR7 Antagonism Reduces Acute Lung Injury Pathogenesis. *Front Pharmacol*. 2021;12:748740.
328. Pouzol L, Baumlin N, Sassi A, et al. ACT-1004-1239, a first-in-class CXCR7 antagonist with both immunomodulatory and promyelinating effects for the treatment of inflammatory demyelinating diseases. *FASEB J*. 2021;35(3):e21431.
329. Pouzol L, Inventor. Combination of a CXCR7 antagonist with an S1P1 receptor modulator. International Patent Application. WO 2021/084068A1. May 06 2021, 2021.
330. Petty JM, Sueblinvong V, Lenox CC, et al. Pulmonary stromal-derived factor-1 expression and effect on neutrophil recruitment during acute lung injury. *J Immunol*. 2007;178(12):8148-8157.
331. Porter JC, Falzon M, Hall A. Polarized localization of epithelial CXCL11 in chronic obstructive pulmonary disease and mechanisms of T cell egression. *J Immunol*. 2008;180(3):1866-1877.
332. Wang H, Beaty N, Chen S, et al. The CXCR7 chemokine receptor promotes B-cell retention in the splenic marginal zone and serves as a sink for CXCL12. *Blood*. 2012;119(2):465-468.
333. Benredjem B, Girard M, Rhainds D, St.-Onge G, Heveker N. Mutational Analysis of Atypical Chemokine Receptor 3 (ACKR3/CXCR7) Interaction with Its Chemokine Ligands CXCL11 and CXCL12*. *Journal of Biological Chemistry*. 2017;292(1):31-42.
334. Costello CM, McCullagh B, Howell K, et al. A role for the CXCL12 receptor, CXCR7, in the pathogenesis of human pulmonary vascular disease. *Eur Respir J*. 2012;39(6):1415-1424.
335. Ichikawa A, Kuba K, Morita M, et al. CXCL10-CXCR3 enhances the development of neutrophil-mediated fulminant lung injury of viral and nonviral origin. *Am J Respir Crit Care Med*. 2013;187(1):65-77.
336. Kelsen SG, Aksoy MO, Georgy M, et al. Lymphoid follicle cells in chronic obstructive pulmonary disease overexpress the chemokine receptor CXCR3. *Am J Respir Crit Care Med*. 2009;179(9):799-805.
337. Berahovich RD, Zabel BA, Penfold ME, et al. CXCR7 protein is not expressed on human or mouse leukocytes. *J Immunol*. 2010;185(9):5130-5139.

338. Koch C, Engele J. Functions of the CXCL12 Receptor ACKR3/CXCR7—What Has Been Perceived and What Has Been Overlooked. *Molecular Pharmacology*. 2020;98(5):577-585.
339. Ngamsri KC, Muller A, Bosmuller H, Gamper-Tsigaras J, Reutershan J, Konrad FM. The Pivotal Role of CXCR7 in Stabilization of the Pulmonary Epithelial Barrier in Acute Pulmonary Inflammation. *J Immunol*. 2017;198(6):2403-2413.
340. Konrad FM, Meichssner N, Bury A, Ngamsri KC, Reutershan J. Inhibition of SDF-1 receptors CXCR4 and CXCR7 attenuates acute pulmonary inflammation via the adenosine A2B-receptor on blood cells. *Cell Death Dis*. 2017;8(5):e2832.
341. Solaro C, Trabucco E, Messmer Uccelli M. Pain and multiple sclerosis: pathophysiology and treatment. *Curr Neurol Neurosci Rep*. 2013;13(1):320.
342. Schall TJ, Proudfoot AE. Overcoming hurdles in developing successful drugs targeting chemokine receptors. *Nat Rev Immunol*. 2011;11(5):355-363.

ANNEX

1 Annex 1

Richard-Bildstein S AH, Pothier J, Schäfer G, Gnerre C, Lindenberg E, Lehembre F, Pouzol L, Guerry P. Discovery of the potent, selective, orally available CXCR7 antagonist ACT-1004-1239. *J Med Chem*. 2020.

2 Annex 2

Huynh C, Brussee JM, Pouzol L, et al. Target engagement of the first-in-class CXCR7 antagonist ACT-1004-1239 following multiple-dose administration in mice and humans. *Biomed Pharmacother*. 2021;144:112363.

3 Annex 3

Pouzol L. TM, Baumlin N., Sassi A., Marrie J., Vezzali E., Gnerre C., Strasser D. S., Mentzel U., Martinic M. M. P150: CXCR7 Antagonism with ACT-1004-1239 Reduces Neuroinflammation and Accelerates Remyelination in Murine Demyelinating Models _ ACTRIMS Forum 2021 – Poster Presentations. Multiple Sclerosis Journal 2021 **27**(1_suppl):15-122.

université PARIS-SACLAY
ÉCOLE DOCTORALE
Innovation thérapeutique
du fondamental à l'appliqué
(ITFA)

Titre : Développement préclinique d'ACT-1004-1239, un antagoniste puissant et sélectif du récepteur CXCR7/ACKR3 pour le traitement de la sclérose en plaques.

Mots clés : ACKR3/CXCR7, CXCR3 et CXCR4, CXCL12 et CXCL11, Sclérose en plaques, remyélinisation, immunomodulation

Résumé : La sclérose en plaques (SEP) est une maladie auto-immune chronique qui affecte le système nerveux central (SNC) et qui est caractérisée par une inflammation, une démyélinisation et une dégénérescence axonale. Des avancées considérables ont été réalisées ces dernières années et les traitements actuels permettent de réduire le nombre de poussées et permettent d'améliorer la qualité de vie des patients. Cependant, ces nouveaux traitements n'empêchent pas la progression de la maladie et aucun traitement ne répare les gaines de myéline endommagées.

Le développement d'un médicament est un processus complexe nécessitant une approche pluridisciplinaire, incluant la pharmacologie. Avant de pouvoir tester une molécule candidate chez l'être humain, un médicament doit passer par le développement préclinique. Cette première étape débute avec l'identification et la validation d'une cible thérapeutique, puis l'identification et l'optimisation de molécules candidates. Dans ce processus, les données visant à étudier la pharmacocinétique (PK), la pharmacodynamique (PD), le mécanisme d'action et l'efficacité de la molécule au sein d'organismes animaux vivants sont essentielles et sont nécessaires à la constitution du dossier réglementaire permettant d'entrer chez l'Homme.

Le récepteur atypique des chimiokines ACKR3 (précédemment nommé CXCR7) a été proposé comme étant une cible thérapeutique potentielle pour le traitement de la SEP. Cependant aucun antagoniste au récepteur ACKR3 inhibant le recrutement de β-arrestine, n'a été testé dans des modèles animaux.

Cette thèse de doctorat décrit la découverte et le développement préclinique, d'un point de vue pharmacologique, d'ACT-1004-1239, le premier antagoniste au récepteur ACKR3, puissant, sélectif et insurmontable qui peut être donné par voie orale. ACKR3 est un récepteur atypique qui lie les chimiokines CXCL11 et CXCL12 et qui les dégradent. Après avoir caractérisé les propriétés PK/PD d'ACT-1004-1239, en mesurant l'augmentation de CXCL12 dans le plasma comme PD biomarqueur, le mécanisme d'action de l'antagoniste a été évalué dans un modèle d'inflammation du poumon. Ces expériences ont mis en évidence le rôle d'ACKR3 dans la migration des cellules immunitaires vers le site de l'inflammation, supportant l'hypothèse qu'ACKR3 contribue à la mise en place de gradients de migration en modulant la concentration de ses ligands. Enfin, le principal but de ce travail de thèse est d'évaluer l'efficacité d'ACT-1004-1239 dans des modèles animaux de la SEP, notamment les modèles d'encéphalomyélite auto-immune expérimentale et de démyélinisation induite par l'ingestion de cuprizone chez la souris. Ces résultats ont confirmé l'effet immunomodulateur d'ACT-1004-1239 sur l'infiltration des cellules inflammatoires dans le SNC. De plus, ACT-1004-1239 a permis d'augmenter le nombre d'oligodendrocytes matures produisant de la myéline à la fois *in vitro* et *in vivo*.

Les résultats exposés dans cette thèse démontrent qu'antagoniser le récepteur ACKR3 avec ACT-1004-1239 réduit à la fois la neuro-inflammation et améliore la myélinisation, ce qui supporte le développement clinique de ce composé pour le traitement des patients ayant une SEP.

Title : Preclinical development of ACT-1004-1239, a potent and selective CXCR7/ACKR3 antagonist in multiple sclerosis treatment.

Keywords : ACKR3/CXCR7, CXCR3 and CXCR4 chemokine receptors, CXCL12 and CXCL11 chemokine ligands, Multiple sclerosis, Remyelination, Immunomodulation

Abstract : Multiple sclerosis (MS) is a chronic autoimmune disease of the central nervous system involving inflammation, demyelination, and axonal degeneration. Remarkable advances have been achieved in drug development with the approval of several disease-modifying therapies able to reduce the number of relapses. However, halting the progression of the disease is still an unmet need and there is currently no drug approved to repair the damaged myelin.

Developing a new drug is a complex effort involving various fields, including pharmacology. Preclinical drug development of small molecules encompasses the different activities needed to bring a compound from drug discovery to initiation of human clinical trials. Preclinical drug development starts with the identification and validation of a good drug target, followed by the identification and optimization of the best compound candidates. In this complex process, the study of drug-effects *in vivo* in appropriate animal models is central. Targeting ACKR3 – also known as CXCR7, an atypical chemokine receptor – has been postulated as a potential therapeutic approach in MS by reducing neuroinflammation and promoting remyelination. However, so far, no ACKR3 antagonist inhibiting β-arrestin signaling has been identified nor investigated *in vivo* in animal disease models.

This doctoral thesis describes the pharmacological preclinical development of ACT-1004-1239, a potent, selective, insurmountable, and orally available first-in-class ACKR3 antagonist.

ACKR3 has been described as a scavenger receptor for its chemokine ligands, namely CXCL11 and CXCL12. After the characterization of the pharmacokinetic/pharmacodynamic (PK/PD) properties of ACT-1004-1239, with the measurement of plasma CXCL12 as PD biomarker, its immunomodulatory properties were evaluated in a proof of mechanism model of acute lung injury in mice. These results demonstrated the pivotal role of ACKR3 on immune cell infiltration to sites of inflammation. The current hypothesis is that ACKR3, by scavenging its ligands, enables the formation of CXCL11 and CXCL12 concentration gradients from the blood to the site of inflammation and hence immune cell migration to inflamed tissue. Furthermore, the efficacy of ACT-1004-1239 was assessed in preclinical MS models such as the experimental autoimmune encephalomyelitis and the cuprizone-induced demyelination mouse models. These studies confirmed the immunomodulatory effect of ACT-1004-1239 on the migration of immune cells to the CNS. In addition, both *in vitro* and *in vivo*, ACT-1004-1239 increased the number of mature myelinating oligodendrocytes and enhanced myelination in the cuprizone model.

These results provide evidence that ACT-1004-1239 both reduces neuroinflammation and enhances remyelination, underscoring the clinical potential of ACT-1004-1239 for the treatment of patients with multiple sclerosis.